



final report

Project code: B.FLT.0356

Prepared by: M R Redding^a, P Shorten^d, S Weidemann^c, F Phillips^b,
C Pratt^a, J Devereaux^a, R Lewis^a, T Naylor^b, T Kearton^a, J Hill^a
^aAgri-Science Queensland, Department of Agriculture and Fisheries, PO Box 102
Toowoomba, Queensland, Australia;
^bThe Centre for Atmospheric Chemistry, School of Chemistry, University of
Wollongong, Northfields Ave Wollongong, New South Wales, Australia;
^cFSA Consulting, Clifford St. Toowoomba, Queensland, Australia;
^dAgResearch, Hamilton, New Zealand

Date published: 10 April 2015

PUBLISHED BY
Meat and Livestock Australia Limited
PO Box 1961
NORTH SYDNEY NSW 2059

Greenhouse gas emissions from intensive beef manure management

Meat & Livestock Australia acknowledges the matching funds provided by the Australian Government to support the research and development detailed in this publication.

This publication is published by Meat & Livestock Australia Limited ABN 39 081 678 364 (MLA). Care is taken to ensure the accuracy of the information contained in this publication. However MLA cannot accept responsibility for the accuracy or completeness of the information or opinions contained in the publication. You should make your own enquiries before making decisions concerning your interests. Reproduction in whole or in part of this publication is prohibited without prior written consent of MLA.

Abstract

Emissions of GHG's from manure management at Australian feedlots are uncertain, and inventory estimates are largely unverified. There is a lack of understanding of the factors that control emission in Australian manure management systems, where conditions of climate and practices differ greatly from the overseas (often non-feedlot) sources of the data on which the inventory is based.

Despite this uncertainty, inventory estimates account for nitrous oxide emissions from feedlot manure management as the second largest Australian agricultural manure management emission source.

Where these manure emissions are significant, decreasing them may constitute a simple opportunity for emission mitigation. Failure to act in this regard presents the very real risk of missing the 'low hanging fruit' in the rush towards a meaningful response to climate change. To this end, we established the major emissions from each manure management system element in relation to the whole.

The key finding was that aggregate emissions from pen manure, compacted stockpiles, and composting were far less than the inventory protocols suggest. Volatilisation of ammonia from the operation is likely substantially higher, though the study suggests there is reason to question the way these values are used to calculate indirect nitrous oxide emissions.

Federal legislation in this area is probably still in flux. However, the results of these studies enable fairer attribution of emission costs to the industry overall, and will decrease any future undue burden associated with those industry emissions on individual producers. There is also scope for the advances in management responsive to enable reward of improved management practices.

Executive summary

1 Why the work was done

Emissions of greenhouse gas (GHG) from manure management systems at Australian feedlots are uncertain, and GHG inventory estimates are largely unverified. The factors that control emissions in Australian manure management systems are not well understood; climatic conditions and manure management practices differ greatly from the overseas (often non-feedlot) sources of emissions data on which the inventory is based. Data from other sectors that might improve beef feedlot emission estimates are also lacking. Most of Australasia's key livestock manure management GHG emission profiles are either questionable or are unsubstantiated by region-specific research.

Despite this uncertainty, inventory estimates attribute nitrous oxide emissions from feedlot manure management as the second-largest Australian agricultural manure management emission source.

Where these manure emissions are significant, decreasing them may constitute a simple opportunity for emission mitigation compared with the more difficult-to-implement and long-term strategies that currently dominate agricultural GHG mitigation research. At an international level, there is a critical need to carefully reassess GHG emission profiles, particularly if such reassessments have not been made since the original compilation of inventories. Failure to do this presents the very real risk of missing the 'low hanging fruit' in the rush towards a meaningful response to climate change. To this end, quantifying emissions from each manure management system element in relation to the whole will enable emission mitigation. A good understanding of the processes and life cycle will also minimise the potential for decreases at one point leading to greater emissions at another point in the lifecycle.

2 What was achieved

Pen manure emission measurements

Validated emission measurement techniques for accurate emission measurements from pen manure were not available. A new technique was developed, carefully validated, and the technique published in a major, high-impact international journal.

The emissions that we observed at a northern and southern feedlot were much lower than standard inventory calculations.

- Mean measured pen N₂O emissions were 0.496 $\mu\text{g m}^{-2} \text{s}^{-1}$ (0.292 to 0.800 $\mu\text{g m}^{-2} \text{s}^{-1}$) and 0.00469 $\mu\text{g m}^{-2} \text{s}^{-1}$ (0.00132 to 0.0128 $\mu\text{g m}^{-2} \text{s}^{-1}$) for the northern and southern feedlots (range indicates 95 % confidence interval). Standard inventory calculations estimate much larger emissions: 2.6 $\mu\text{g m}^{-2} \text{s}^{-1}$ (stockpile plus pen manure emissions; Environment, 2013) and 3.0 kg N₂O head⁻¹ year⁻¹ (IPCC, 2006).
- Mean measured emission of CH₄ was 0.273 $\mu\text{g m}^{-2} \text{s}^{-1}$ (0.189 to 0.385 $\mu\text{g m}^{-2} \text{s}^{-1}$) for the northern feedlot and 4.55 $\mu\text{g m}^{-2} \text{s}^{-1}$ (2.99 to 6.72 $\mu\text{g m}^{-2} \text{s}^{-1}$) for the southern feedlot. Using Australian GHG Inventory values gives an emission rate of 1.24 kg CH₄ head⁻¹ year⁻¹ and 4.14 kg CH₄ head⁻¹ year⁻¹ for the southern and northern feedlots (the southern feedlot's climate is classified as 'temperate' whereas the northern feedlot's climate is 'warm'; Environment, 2014). By comparison, using the most recent Intergovernmental Panel on Climate Change parameters (where the climate of both feedlots would be regarded as 'temperate') gives a CH₄ emission rate of 1.9 kg head⁻¹ year⁻¹ (IPCC, 2006).

In the course of conducting the pen manure emission measurements, a limited number of measurements were collected from bare soil in a recently cleaned pen. These measurements suggest that emissions from these soils at this location were higher than emissions from the manures themselves. This is almost certainly related to the very high nitrate concentrations measured in this soil.

In order to ensure that this study effectively influences Australian inventory protocols these results have been submitted to a major international journal, and the manuscript is now accepted and available on-line (Redding et al., 2015).

A management-responsive and region-specific pen manure emission calculation protocol

Gaseous emissions from pen manure are largely controlled by manure temperature and moisture (emission peaking at 20 % dry basis moisture content). Strong relationships were not evident between N₂O emission and masses or concentrations of either NO₃⁻ or total N. This is significant as the standard inventory calculation protocols predict N₂O emissions using the mass of nitrogen excreted by the animal.

In essence, the inventory protocol approach was not supported by the data.

Emission was more closely related to the area of manure-covered pens than the total mass of manure or the manure N content. Management that results in altered manure covered area, or altered moisture content relative to the peak emission moisture range, will alter emissions.

The team developed and validated a physical process-based model of the effect of air temperature, solar radiation and time of day on manure temperature. A physical process-based model was also formulated to characterise the effect of rainfall, evapo-transpiration and drainage on manure moisture.

Using this model methane emissions at the northern feedlot were predicted to be 0.40 kg CH₄ head⁻¹ year⁻¹, substantially less than the standard protocol calculated values for manure emission: 4.14 and 1.9 kg CH₄ head⁻¹ year⁻¹ (Australian and IPCC). Nitrous oxide emissions at the northern feedlot were predicted to be 0.31 kg N₂O head⁻¹ year⁻¹. Standard inventory calculation approaches produce larger estimates of emission: 2.6 and 3.0 kg N₂O head⁻¹ year⁻¹. These differences could be partly related to regional conditions and climates; however, the inventory calculation protocols are reliant on a relationship between emission magnitude and total excreted N that was not supported by our study.

In order to ensure that this study effectively impacts Australian inventory protocols these results have been submitted to a major international journal, and the manuscript is now in its first review (Shorten and Redding, In Press).

This study developed a simple model to enable region-specific estimation of emissions under Australian conditions, by using the moisture, temperature and emission components. The research team assisted FSA Consulting to prepare a regionalised tabulation of results using this model in a report commissioned by the Federal Department of Environment (Wiedemann, 2014).

Preliminary work was also conducted toward developing a protocol that better calculates ammonia volatilisation from the pen area and deposition to the surrounding land – both on strong physical basis and on the basis of a new rule of thumb emission value. This study has been prepared as a manuscript for submission to an international journal.

Ammonia volatilisation and deposition

At intensive livestock enterprises, excreted N is vulnerable to volatilisation, and subsequently may form a source of indirect nitrous oxide (N₂O) emissions. We completed simultaneous measurements of volatilisation and deposition of N at a beef feedlot semi-continuously over a 5-month period.

Total ammonia volatilised amounted to 210 tonnes of NH³-N (110 g animal⁻¹ day⁻¹), suggesting that the inventory volatilisation factor (30% of excreted N) probably underestimates volatilisation in this case. The observed volatilisation represents about 60% of the inventory calculated N excretion.

Deposition within 600 m of the pen boundary represented only 1.7 to 3.2 % of total volatilised NH₄⁺-N, between 3.6 to 6.7 tonnes of N. Beyond this distance deposition approached background rates.

Using the inventory emission factor for deposited N, ammonia volatilization and subsequent indirect emission of N₂O-N probably represents around 0.012 kg N₂O-N/(kg of N excreted). This estimate assumes 5% infrastructure area within 600 m of the feedlot with no effective N uptake by plants, 0.01 kg N₂O-N/(kg of N deposited on cultivated land), and 0.6 kg of NH₄⁺-N volatilised/(kg of N excreted).

The deposition of N to the wider landscape (measured to be 96.8% of volatilised N) could be considered a manageable fertiliser application with low embodied transport and manufacturing emissions. Where re-deposition coincides with the nutrient uptake of any growing vegetation, these applications are unlikely to remain resident for long, meaning there would be little accumulation potential under these circumstances.

It is notable that the benefit from this “manageable fertiliser application with low embodied transport and manufacturing emissions” currently accrues to the third party land-holder, but the inventory imposition is applied to the originator. The data collected for this project, and further research may inform discussion around this issue which could account for a large proportion of emissions attributable to indirect emissions.

A mitigation approach was described involving careful nutrient management at the boundaries of beef feedlots which would likely achieve a small decrease in N₂O emissions. This mitigation would only affect the small proportion of volatilised N deposited close to the boundary of the feedlot (measured to be 3.2 % of volatilised N).

While it is possible to mitigate ammonia volatilisation from the pen, the successful development of a Carbon Farming Initiative method is dependent on also demonstrating that final manure application to land (outside the scope of this project) results in decreased emissions relative to the indirect N₂O emissions related to volatilisation. This is the subject of current University of Melbourne research where the team have had success decreasing volatilisation from pen surface by using lignite. The key to success will therefore lie in identifying if emissions following land application can be decreased. The DAF team has had recent success decreasing N₂O emission from soil applied beef manure (National Agricultural Manure Management Project). If the University of Melbourne approach is not successful, a collaboration with the DAF team using technology developed for the National Agricultural Manure Management Project is likely succeed. Testing this in the DAF laboratory would be a very economical way to guide decisions on potential further work.

A detailed investigation of indirect emissions

In the landscape surrounding a feedlot, volatilised ammonia may be re-deposited, not only increasing the fertility of soils, but also presenting a risk of subsequent conversion and loss as an indirect N₂O emission.

To close the gap between inventory calculations and the real processes involved, we conducted a study to investigate the relationship between N₂O emissions, low magnitude NH₄⁺ deposition (0 to 30 kg N ha⁻¹) and soil moisture content in two soils using in-vessel incubations.

Our results showed that soil N availability controls indirect N₂O emissions. This outcome challenges the IPCC approach which predicts indirect emissions from atmospheric N deposition. Our management-responsive clay soil emission model suggests a range of scenarios that would result in decreased emission, potentially providing an incentive for improved management.

Emissions from an ideal agricultural soil (vertisol, a clay soil) peaked ($< 0.002 \mu\text{g N [g soil]}^{-1} \text{ min}^{-1}$) from 85 to 93 % WFPS (water filled pore space; in this case very close to saturation with water), increasing to a plateau as remaining mineral-N increased. A process-based mathematical model was well suited to the clay soil data where all mineral-N was assumed to be nitrified ($R^2 = 90\%$).

Peak N₂O emissions for a sandy soil were much lower ($< 5 \times 10^{-5} \mu\text{g N [g soil]}^{-1} \text{ min}^{-1}$) and occurred at about 60 % WFPS (much dryer than was observed for the clay soil), with an indistinct relationship with increasing resident mineral N due to the low rate of nitrification in that soil.

It was observed that for the clay soil, significant N₂O emission did not occur where mineral-N was $< 70 \text{ mg (kg of soil)}^{-1}$.

Composting and stockpiling

The two studies described in this report are the first studies to measure feedlot manure emissions during composting and compacted stockpiles. Both studies were conducted at a scale equivalent to a small commercial operation, using common commercial techniques.

Composting emissions greatly exceed those from compacted stockpiling (54 x), largely due to the effect of aeration and turning on nitrous oxide emissions. This suggests that stockpiling is a more effective mitigation practice than composting.

The results suggest that the following changes to inventory values are warranted for temperate locations:

- A CH₄ conversion factor for compacted stockpiling of 0.14 % of initially excreted VS rather than the 4% currently recommended (IPCC, 2006).
- A N₂O emission factor of 0.02% of initially excreted N rather than the current 0.5% (IPCC, 2006).
- An NH₃ volatilisation factor of about 2 % of the initially excreted N rather than the current inventory value of 45% (IPCC, 2006).
- A conservative CH₄ conversion factor for active windrow composting of 0.003 % of initial VS rather than the 1 % of initial VS currently recommended (IPCC, 2006).

An integrated view of the emission picture

A gate-to-gate life cycle assessment (LCA) was conducted to investigate impacts of the grain finishing stage for cattle in seven feedlots in eastern Australia. Three market related feeding periods were investigated: short-fed domestic market (55-80 days on feed), mid-fed export (108-164 days on feed) and long-fed export (>300 days on feed). Impacts were reported per kilogram of live weight gain.

Mean greenhouse gas emissions ranged from 4.0 to 7.8 kg CO₂-e/kg live weight gain (excluding land use and direct land use change emissions). Emissions were dominated by

enteric methane and contributions from the production, transport and milling of feed inputs. Linear regression analysis showed that the feed conversion ratio was able to explain >86% of the variation in greenhouse gas intensity and energy demand.

Relative contributions to total manure management emissions (46 to 68 kg co₂ eq/ 100 kg live weight gain; northern and southern feedlots respectively; reverting to the 0.01 N₂O-/kg to land application and indirect emission factor; all units kg co₂ eq/ 100 kg live weight gain) given the assumptions were: pen and stockpile manure 22.5 and 10.2; indirect emission 27 and 4.5; pond 22.5 and 10.2; land application 6 and 4.4. Given the current inventory assumptions the corresponding manure management emission 146.7 and 183.4 kg co₂ eq/ 100 kg live weight gain, with the difference dominantly due to the revised emission estimates for the pen and stockpile made possible by this research project.

Some of the emission factors associated with these calculations were beyond the scope of the current project to investigate. Notable among these were the emission factors for indirect emission and land application of manure. Data collected from soils surrounding the northern feedlot suggest that values available for the LCA analysis may be inappropriate. Current uncertainty around the appropriateness of the emission factors related to indirect nitrous oxide emission factors, and the emission factor associated with land application of manure are not likely to raise overall emission manure management emissions to the previous estimated values unless they are multiples higher than their current inventory value (0.01 2O-N / kg N). A small additional study would likely resolve this uncertainty. Less conclusive data may also flow from several known concurrent research projects where this may be a peripheral observation.

Towards an index of site suitability for manure-carbon retention

This study sought to determine the importance of site selection in maximising the carbon sequestration potential of pen manure carbon. Moreover, we specifically tested whether the greatest carbon retention would be achieved with soils that have previously lost the most carbon (i.e., degraded soils).

We found that site selection was very important with regard to maximising carbon retention. However, degraded sites did not consistently retain greater amounts of carbon. In practice selection of sites presumed to be degraded is not likely to provide high levels of carbon retention for manure end users, without some additional technological advance.

Approximate retention of applied manure carbon ranged from 30 to 60 %, with significant differences between soils. Addition of manure carbon had a detrimental effect on pre-existent soil organic carbon in only one of the 12 soils studied.

3 When and how industry can benefit from the work

Within the project, effort has been made to engage with the federal regulator and departments (Department of Environment and Department of Agriculture) to ensure uptake of the proposed new greenhouse gas inventory values. These discussions were conducted prior to the deadline for consideration of new data to be considered for a revision of the National Greenhouse Gas Inventory protocols. It is hoped that these studies, publications, and discussions will assist uptake of this quality science, and have an impact on next year's version of the inventory.

This will result in significantly lower emissions being attributed to the industry, as manure management emissions are estimated to be a fraction of those calculated in the current inventory protocols.

4 Who can benefit from the results

Federal legislation in this area appears to change with each new government. However, the results of these studies enable fairer attribution of emission costs to the industry overall, and will decrease any future undue burden associated with those industry emissions on individual producers. There is also scope for the advances in management responsive inventories to enable reward of improved management practices. In turn, the supply chain will also benefit, and ultimately the consumer.

Table of contents

1	Background.....	14
1.1	Summary	14
1.2	Introduction.....	14
1.3	Deficiencies in inventory emission estimates for beef feedlots	15
1.3.1	Direct emissions from manure management.....	16
1.3.2	Indirect emissions and ammonia deposition.....	16
1.3.3	Variation in stock numbers.....	17
1.3.4	Manure harvesting and stockpile practices	17
1.4	GHG mitigation options and implications for this project.....	18
1.4.1	Mitigation options.....	18
1.4.2	Policy implications of inaccurate estimates: considerations in striving for best returns on research investment.....	18
1.5	Implications for project objectives	19
2	Determining surface fluxes in a multi-source environment (<i>Redding et al., 2013</i>).....	20
2.1	Summary	20
2.2	Introduction.....	20
2.3	Materials and methods.....	22
2.3.1	Theory of fabric-covered large chamber.....	23
2.3.2	Construction and operation of the emission source.....	24
2.3.3	Application of the bLS technique.....	25
2.3.4	Design and operation of the large chamber	26
2.3.5	Comparison of bLS versus large chamber	28
2.3.6	Statistics	28
2.4	Results and discussion	28
2.4.1	Tracer gas recovery, rejection criteria and bLS.....	28
2.4.2	Model fit and discussion of large chamber characteristics.....	29
2.4.3	Large chamber versus bLS.....	31
2.5	Conclusion.....	36
3	Pen emission measurements suggest the need for a revision of greenhouse gas inventory calculations (<i>Redding et al., 2015</i>).....	37
3.1	Summary	37
3.2	Introduction.....	38
3.3	Materials and methods.....	39

3.3.1	Site selection	39
3.3.2	Site instrumentation	42
3.3.3	Selection of emission sampling times	42
3.3.4	Application of the large-chamber technique	42
3.3.5	Statistics	44
3.4	Materials and methods.....	44
3.4.1	Field measurement of pen manure emissions.....	44
3.4.2	Parameter relationships	46
3.4.3	Estimating annual emissions.....	49
3.4.4	Emissions from bare pen soils	51
3.5	Conclusion	52
4	From control factors to an emission protocol (based on shorten and Redding, in Press)..	53
4.1	Summary	53
4.2	Introduction	53
4.3	Materials and methods.....	54
4.3.1	Modelling data set.....	54
4.3.2	Emission process modelling.....	55
4.3.3	Temperature process modelling.....	58
4.3.4	Moisture process modelling	59
4.3.5	Statistics	60
4.4	Results and discussion	60
4.4.1	Emission modelling.....	60
4.4.2	Manure temperature modelling	63
4.4.3	Manure moisture modelling.....	64
4.4.4	Model prediction at the southern feedlot	65
4.4.5	Estimated annual emissions	66
4.4.6	Implications.....	67
4.5	Conclusion	67
5	Processes controlling emission of nitrous oxide suggest a flaw in the current inventory approach (Redding et al., review).....	68
5.1	Summary	68
5.2	Introduction	68
5.3	Materials and methods.....	69
5.3.1	Soil samples	69
5.3.2	Gas sampling and analysis apparatus	70

5.3.3	Experimental design	71
5.3.4	Emission modelling	72
5.3.5	Field validation	74
5.3.6	Statistics	75
5.4	Results and discussion	76
5.4.1	Toward an indirect emission factor algorithm	78
5.4.2	Clay soil field validation	81
5.4.3	Implications	82
5.5	Conclusion	84
6	The extent of ammonia volatilisation and deposition to the landscape (manuscript prepared for submission)	85
6.1	Summary	85
6.2	Introduction	85
6.3	Materials and methods	87
6.3.1	Site selection	87
6.3.2	Site instrumentation and calculated manure condition	87
6.3.3	Ammonia sampling and measurement	87
6.3.4	Deposition traps	89
6.3.5	Emission modelling	89
6.3.6	Deposition modelling	91
6.3.7	Statistical analysis	91
6.4	Results and discussion	92
6.4.1	Ammonia volatilisation	92
6.4.2	Nitrogen deposition	98
6.4.3	Implications	101
6.5	A mitigation management for indirect emissions	105
6.5.1	A small opportunity	105
6.5.2	Improved proximal nutrient management a small mitigation opportunity	106
6.5.3	A potentially larger opportunity with a major caveat	109
6.6	Conclusion	110
7	Compacted stockpile and composting emissions (manuscript to be prepared)	111
7.1	Summary	111
7.2	Introduction	111
7.3	Materials and methods	112
7.3.1	Location, stockpile, and composting	112
7.3.2	Windtrax layout, instrumentation and on-line analysis	112

7.4	Validation of ammonia measurements	113
7.4.1	Data rejection criteria	114
7.4.2	Statistics	114
7.5	Results and discussion	115
7.5.1	Stockpile measurements.....	115
7.5.1.1	Methane and nitrous oxide	115
7.5.1.2	Ammonia volatilisation.....	119
7.5.2	Compost emissions.....	121
7.5.3	Mitigation options	124
7.6	Conclusion	124
8	Resource use and environmental impacts from grain finishing beef cattle in Australia feedlots: a gate-to-gate life cycle assessment (closely based on manuscript to be submitted)	126
8.1	Summary	126
8.2	Introduction	127
8.3	Materials and methods.....	128
8.3.1	Goal and scope.....	128
8.3.2	Description of the case-study feedlots	128
8.3.3	Life cycle inventory	128
8.3.4	Fresh water consumption.....	131
8.3.5	Land occupation	132
8.3.6	Livestock and manure greenhouse gas emissions.....	133
8.3.7	Greenhouse gas emissions – feedlot operations and feed inputs.....	137
8.3.8	Handling co-production	137
8.3.9	Data analysis	137
8.4	Results.....	137
8.4.1	Fresh water consumption and stress weighted water use	137
8.4.2	Land Occupation.....	138
8.4.3	Energy demand	139
8.4.4	Greenhouse gas emissions – gate-to-gate.....	139
8.4.5	Greenhouse gas emissions – livestock and manure management sources .	140
8.5	Discussion	143
8.5.1	Resource use.....	143
8.5.2	Greenhouse gas emissions.....	144
8.5.3	Sensitivity to emission factors for GHG prediction.....	144
8.6	Conclusions	145

9	Identifying target soils for manure carbon sequestration (manuscript to be prepared)	146
9.1	Summary	146
9.2	Introduction	146
9.3	Materials and methods.....	147
9.4	Results and discussion	149
9.5	Conclusion	155
10	References.....	156

1 Background

1.1 Summary

According to Greenhouse Gas (GHG) Inventory estimates, nitrous oxide emissions from feedlot manure management is reported to be the second largest Australian agricultural manure management emission source, with methane emissions from this source being considerably less. Emissions of GHG's from manure management at Australian feedlots are uncertain, and inventory estimates are largely unverified. There is a lack of understanding of the factors that control emission in Australian manure management systems, where conditions of climate and practices differ greatly from the overseas (often non-feedlot) sources of the data on which the inventory is based.

Indeed, more generally, most of Australasia's key livestock manure management GHG emission profiles are either questionable or are unsubstantiated by region specific research. Where these manure emissions are significant, decreasing them may constitute a simple opportunity for emission mitigation compared with the more difficult-to-implement and long-term strategies that currently dominate agricultural GHG mitigation research. At an international level, our review highlights the critical need to carefully reassess GHG emission profiles, particularly if such assessments have not been made since the compilation of original inventories. Failure to act in this regard presents the very real risk of missing the 'low hanging fruit' in the rush towards a meaningful response to climate change. To this end, quantifying emissions from each manure management system element in relation to the whole will enable emission mitigation. Process and system knowledge will also minimise the potential for decreases at one point leading to greater emissions at another point in the lifecycle.

1.2 Introduction

Agriculture represents 5 - 15% of Australia's export revenues (NZGovt, 2013). This economic powerhouse is also a source of the greenhouse gases (GHGs) nitrous oxide (N_2O) and methane (CH_4). There are three main sources of agricultural GHGs in Australia and New Zealand (NZ): 1) enteric CH_4 , 2) soil N_2O and 3) manure management CH_4 and N_2O . Most of the agricultural emissions occur as enteric CH_4 and soil N_2O . According to GHG Inventory calculations for Australian agriculture, the annual emissions of enteric CH_4 , soil N_2O and manure management CH_4 and N_2O amount to approximately 55 Mt, 12 Mt and 4 Mt of CO_2 -e, respectively in Australia (Environment, 2014).

The causes, magnitude, and mitigation potential of enteric CH_4 and soil N_2O emissions are now well understood for Australia, and overseas (de Klein et al., 2001; Dalal et al., 2003; Saggar et al., 2004; Eckard et al., 2010; Cottle et al., 2011). By contrast, agricultural manure management emission estimates have not been verified by a rigorous review of the available literature since they were developed more than 15 years ago.

A review of manure management GHG emissions in Australia is therefore needed to assess the accuracy of the nation's GHG inventories for this category, for three reasons. First, it will allow for an evaluation of current inventory estimates. There is reason to expect some degree of inaccuracy. In NZ, Chung et al. (2013) demonstrated that CH_4 emissions from dairy effluent are potentially underestimated by 400%, and Hill (2012) showed that CH_4 emissions from pig effluent are being overestimated by a factor of about 200%. These inaccuracies were caused by the inappropriate adoption of international default factors as well as the omission of key emission sources by NZ's GHG Inventory. The studies by Hill (2012) and Chung et al. (2013) revealed that a GHG emission profile within a nation's inventory can shift from minor to major, or vice versa, upon clarification of emission factors

and management practices. Second, a review of manure management GHG emissions is timely because these emissions are point sources. Thus, mitigation options for these gases are more amenable to development and implementation than for diffuse, non-point CH₄ and soil N₂O emissions which occur at the paddock-scale.

Upon critically assessing manure management GHG emission estimates in Australia it is also possible to examine whether appropriate weighting is currently given to mitigating these emissions. This is a third reason why a review of this subject is important. Hence we evaluate: 1) manure management GHG emission estimates in Australia by comparing inventory emission factors with published country-specific data, where available; 2) mitigation options for emissions from this sector focusing on barriers to and drivers for uptake; and 3) whether funded research into agricultural GHG mitigation is currently balanced to achieve greatest effect.

1.3 Deficiencies in inventory emission estimates for beef feedlots

Figure 1 shows emission profiles for Australia's and NZ's main manure management GHG sources, based on inventory data. In this review, we use Australia's definition of 'manure management' which encompasses CH₄ and direct and secondary N₂O emissions from all manure management systems as well as CH₄ emissions from pasture-deposited livestock manure. Global warming potentials (GWP) of 21 and 310 were used to convert CH₄ and N₂O emissions, respectively, to units of CO₂-e. These GWPs are adopted by the most recent versions (Environment, 2014) of the Australian GHG Inventory.

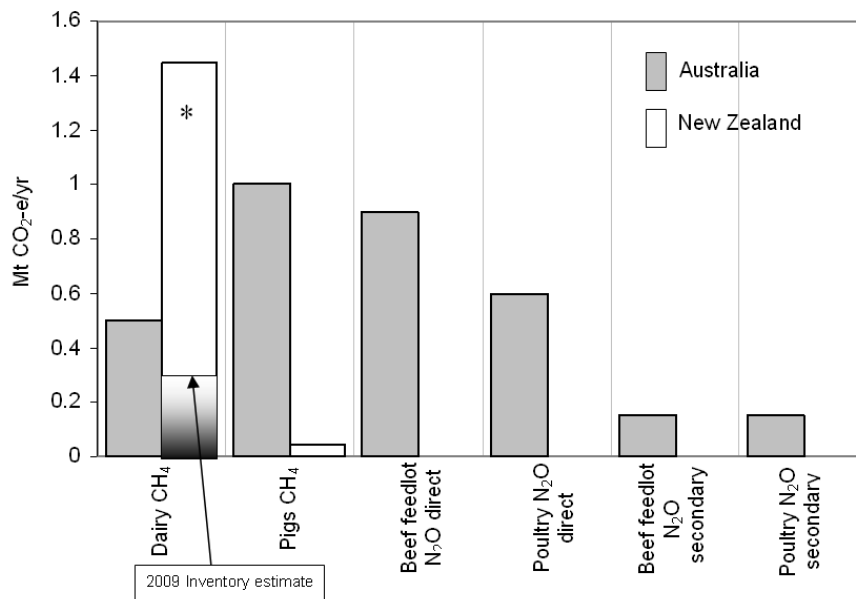


Figure 1.1. Inventory estimates for Australia and New Zealand (Pratt et al., 2014). *Estimate based on Chung et al. (2013), which applies the IPCC protocol (Intergovernmental Panel on Climate Change, 2006).

Feedlots are commonly used for finishing beef cattle from pastures and croplands in Australia. The Australian GHG Inventory reports that about 5% of Australia's beef cattle population (25-30 million: (MLA, 2013)) is on feed at any time (i.e., 1.17 million cattle) and that approximately 0.95 Mt of CO₂-eq/yr as direct N₂O is emitted from these feedlots (Fig. 1.1); almost one third of total 'manure management' emissions.

1.3.1 Direct emissions from manure management

The direct N₂O emission factor (0.02 kg N₂O/kg N excreted) represents the average outcome from complex biological mechanisms depending on ecological and environmental conditions, and was derived from IPCC expert judgement and research. The key study, Külling et al. (2003), was conducted using Swiss dairy cattle, not beef cattle. Moreover, the key processes affecting the N₂O emission factor, which include moisture (Montes et al., 2013), manure physical parameters (Chadwick, 2005) and temperature (Dobbie and Smith, 2001a), are likely very different in Switzerland than Australia.

For example, emissions from the manure in Külling et al.'s (2003) study were assessed at 20°C. By contrast, temperatures on Australian beef feedlot surfaces of 45°C are common (Redding et al., 2015) and can reach temperatures substantially higher. Manure on feedlot surfaces is often cracked and moisture content varies considerably from the surface to the base, in contrast with the manure assessed by Külling et al. (2003) which was a wet slurry. It appears likely that this study's validity for Australian feedlot conditions is therefore compromised.

Few published studies have verified the appropriateness of the above emission factors for Australia and no publications were identified reporting direct N₂O emissions from beef feedlots in the country. Two studies conducted in the USA documented direct N₂O measurements from beef cattle feedlots. Rahman et al. (2013), using a wind tunnel, reported an N₂O emission rate of 4.67 kg CO₂-eq (kg live weight)⁻¹ yr⁻¹ at a North Dakota feedlot, over four seasons. This rate is more than three times higher than the Australian GHG Inventory emission estimate (1.53 kg CO₂-eq (kg live weight)⁻¹ yr⁻¹). By contrast, Borhan et al. (2011), using flux chambers, reported 0.13 kg CO₂-eq (kg live weight)⁻¹ yr⁻¹ (as direct N₂O emissions) from a Texan beef feedlot over summer. The variability between these field measurements may have been due to differences in management practices, environmental conditions or measurement techniques. Rochette and Eriksen-Hamel (2008) noted that N₂O measurements determined using chambers can yield highly variable results from site to site, and the techniques used can influence the measured emission rate. Nonetheless, the emission fluxes reported from the two studies were not only markedly different from each other (30x difference); they also differed considerably from the Australian GHG Inventory estimate (3x and 12x difference). This highlights the need for actual field measurements of direct N₂O emissions from beef feedlots in Australia. A single field study, conducted over a sufficiently long period, could be used to develop a more appropriate emission factor than currently adopted for Australia. Without such measurements it is difficult to ascertain the appropriateness of the default emission factors currently used by the inventory. Consequently, the estimate of direct N₂O emissions from Australian beef feedlots given in Fig. 1.1 remains unverified.

1.3.2 Indirect emissions and ammonia deposition

In simple terms, indirect emissions of N₂O can occur from the deposition of NH₃ derived from the feedlot on the surrounding land, and subsequent conversion and emission as N₂O.

Indirect N₂O emissions from beef feedlots in Australia have also been estimated using IPCC default factors from the 1995 Second Assessment Report. The NH₃ volatilisation factor (0.3 kg NH₃-N (kg N excreted)⁻¹) used in Australia's GHG Inventory is sourced from publications by Hutchings et al. (2001), who focused on Denmark's gas inventory, and Rotz (2004), in their review on farm N management. Two Australian studies measured NH₃ emissions from beef feedlots: Denmead et al. (2008) reported 66 g NH₃-N/kg live weight.yr⁻¹, while Loh et al. (2008a) documented an average 108 g NH₃-N (kg live weight)⁻¹ yr⁻¹. Both studies used feedlots from Victoria and Queensland and employed open-path micrometeorological techniques to measure emissions. The NH₃ fluxes reported are higher than the national

GHG inventory estimate of $48 \text{ g NH}_3\text{-N (kg live weight)}^{-1} \text{ yr}^{-1}$, which suggests that a nationally relevant NH_3 volatilisation rate is more likely in the range of 0.4 to $0.7 \text{ kg NH}_3\text{-N (kg N excreted)}^{-1}$. Further process work would be required to confirm this.

The indirect N_2O emission factor ($0.01 \text{ kg N}_2\text{O-N (NH}_3\text{-N)}^{-1}$), adopted by the Australian government from the IPCC, uses several northern hemisphere studies based entirely on assumptions of N deposition (Butterbach-Bahl et al., 1997; Brumme et al., 1999; Corre et al., 1999; Denier van der Gon and Bleeker, 2005). Butterbach-Bahl et al. (1997) and Brumme et al. (1999) determined secondary N_2O emissions from German native forests, though atmospheric N deposition rates were assumed. Corre et al. (1999) did the same for various land-use types in Canada while Denier van der Gon and Bleeker (2005) determined secondary N_2O emission factors for the Netherlands based on literature estimates of N deposition rates. Actual N deposition rates were not measured in any of these investigations. Moreover, the studies did not specifically examine the conversion of ammonia-deposited N to N_2O from manure applications. Hence, as is the case with the direct N_2O emission factors, the relevance of secondary N_2O emission factors to agricultural systems in Australia is questionable.

1.3.3 Variation in stock numbers

In addition to unverified N_2O emission factors, there is uncertainty regarding Australia's beef feedlot population. The Inventory's estimate of 1.17 million for 2011 differs from other sources: Muir et al. (2011) noted that about 680,000 cattle are on Australia's feedlots at any time, while the industry itself reported a feedlot population of 788,000 in June 2011 (ALFA, 2013). These variations can affect Australia's beef feedlot manure GHG emission estimate by up to 100%. Thus, it is crucial that the inventory adopts the most accurate population estimate, which should be that given by the industry.

1.3.4 Manure harvesting and stockpile practices

Another important consideration in estimating beef feedlot manure GHG emissions is the practice of stockpiling (Fig. 1.1). An early publication indicated that manure from feedlots can be cleaned-out regularly (< 1 week) or as infrequently as < 6 months (Dantzman et al., 1983). This is probably no longer the case, though there is certainly a variation from weeks to months in cleaning frequency and manure may be mounded (in pen), stockpiled or composted before being applied to agricultural land. If feedlot manure is frequently removed and land applied, the pen-attributed (and stockpile-attributed, since these are not currently separated in the Australian inventory) GHG emissions will be low. However, emissions from the manure once it is applied to land may be high and will contribute to agricultural soils emissions ($12 \text{ Mt CO}_2\text{-eq yr}^{-1}$ for Australia). If manure is stockpiled or composted for a prolonged period, it could emit significant quantities of N_2O , NH_3 and CH_4 under suitable environmental conditions. For example, Pattey et al. (2005) demonstrated that GHG (N_2O and CH_4 combined) emissions from poorly-managed beef manure compost can be 7 times greater than from the same manure in well-aerated composting piles; although additional secondary N_2O emissions through NH_3 volatilisation would need to be considered.

Emissions from stockpiled or composted manure are not separately quantified in the Australian GHG Inventory. Moreover, as no published field-measured emissions from manure stockpiling exist it is difficult to ascertain whether these storage systems are significant GHG sources. Work is needed to elucidate GHG emissions from stockpiled and composted beef feedlot manure in Australia.

1.4 GHG mitigation options and implications for this project

1.4.1 Mitigation options

Direct and indirect N₂O emissions from beef feedlots and poultry sheds are the major sources of feedlot 'manure management' GHG emissions in Australia. Strategies to mitigate these emissions may be implemented at the farm-management level. For example, de Klein et al. (2001) suggested tightening the supply of manure N to crops as a way to restrict direct and secondary N₂O emissions. Reducing the amount of N excreted from livestock through dietary modifications has some potential to decrease gaseous emissions. A number of researchers have shown that a decrease in excreted N decreases ammonia emissions which would likely lead to decreased secondary N₂O emissions (Canh et al., 1998; Hayes et al., 2004). However, research is needed to conclusively demonstrate a link between decreased N excretion rates and lower direct N₂O emissions. In terms of technical mitigation options, the nitrification inhibitor dicyandiamide (DCD) has been shown to reduce pastoral N₂O emissions by approximately 25% in NZ (Monaghan et al., 2013) and could conceivably be applied to mitigate feedlot direct N₂O emissions. However, effectiveness of these types of inhibitors is hampered by breakdown processes at the higher temperatures experienced in Australia. Recently, concerns have also emerged regarding the detection of DCD in animal products (milk, rather than meat) and its effects on animal and human health are unknown.

For industries where effluent ponds receive reliable regular loadings of volatile solids, these inputs represent a significant proportion of total manure production, and mitigating methane emissions via biogas production can have a major emission mitigation impact (Pratt et al., 2014). However, only a small proportion of total manure volatile solids enters the ponds of beef feedlots, and these inputs are irregular (caused by rainfall).

Options to reduce emissions of NH₃ (the precursor to secondary N₂O) from feed pads and poultry sheds include the use of sorbing materials or acidifiers which could be incorporated into the manure management systems through direct application to pens or stockpiles or by adding to the animals' feed. Such materials have been shown to be effective in preliminary trials for the manures from meat-chicken production (Redding, 2011, 2013). Varel et al. (1999) showed that urease inhibitors can reduce NH₃ emissions from feedlot cattle waste. It is also conceivable that appropriate management of vegetation around intensive farming systems (such as beef feedlots and poultry sheds) could reduce indirect N₂O emissions via tighter cycling of NH₃ which is volatilised from manures.

Nonetheless, it should be borne in mind that discussing the wider potential strategies to mitigate N₂O from Australian beef feedlots and poultry farms is premature given:

- a. The uncertain emission estimates for these sources.
- b. Lack of understanding of the factors that control emission.
- c. Deficiencies in the understanding of the manure management life-cycle. Any system change is likely to influence emissions from other components of the manure management system.

1.4.2 Policy implications of inaccurate estimates: considerations in striving for best returns on research investment

Currently, no technologies are being widely deployed to mitigate 'manure management' GHG emissions in Australia or NZ. However, in terms of the 'state-of-readiness' of the technologies involved, it appears that most enteric mitigation options are far from developed to the stage of being adopted (Eckard et al., 2010). They comment that rumen manipulation technologies require much more research as vaccine-use is controversial and enzymes have yet to show any sustained positive results. Most enteric mitigation strategies have not been

tested in long-term experiments and, thus, require extensive future research (Patra, 2012). Although the magnitude of the costs associated with enteric mitigation technologies is not yet known, it is likely that they will be significant. Eckard et al. (2010) stated that it will be many years before practical and commercially viable technologies are ready for use on farms.

There is a need to develop accurate emission profiles as a prerequisite to balancing GHG mitigation research efforts to best effect (Pratt et al., 2014). In this respect, it is crucial to verify N₂O emission estimates from beef feedlots in Australia because, based on current data, we simply don't know if these are significant agricultural GHG sources.

1.5 Implications for project objectives

Several conclusions are evident from this literature review. Emissions of GHG' from manure management at Australian feedlots are not quantified, and inventory estimates are largely unverified. There is a lack of understanding of the factors that control emission in Australian manure management systems, where conditions of climate and practices differ greatly from the overseas (often non-feedlot) sources of the data on which the inventory is based. The study of the feedlot manure management system would benefit from a holistic approach, and Life Cycle Analysis (LCA) is likely to provide a useful tool to direct mitigation efforts.

Accordingly, the initial objectives of this project are appropriate relative to these requirements:

1. Provide accurate measurements of Australian feedlot manure emissions under different management methods for input to the National Greenhouse Gas Inventory, carbon footprint and LCA calculations.
2. Develop and extend manure management options that maximise the value of manure and decrease GHG emissions.
3. Develop management options that extend the mean residence time of manure-carbon in soils, thereby maximising the potential carbon offsets achievable through sequestration of this carbon and promoting the value of manure as a fertiliser.
4. Develop a management responsive estimation protocol to replace the current National Greenhouse Gas Inventory that recognises and rewards industry for emissions mitigation successes.

Additionally, this review highlights the uncertainty with regard to indirect emissions related to ammonia volatilisation and deposition. These aspects were not initially specifically included in the original project schedule (the more detailed implementation of the project supporting the above objectives). However, in response to the observed need in this area, substantial study was also directed at evaluating NH₃ volatilisation, deposition, and indirect emission.

2 Determining surface fluxes in a multi-source environment (*Redding et al., 2013*)

M.R. Redding^{*a}, R. Lewis^a, J. Waller^b, F. Phillips^c, and D. Griffith^c

^a Agri-Science Queensland, Department of Agriculture and Fisheries, PO Box 102 Toowoomba, Queensland, Australia; ^b AgResearch New Zealand, Ruakura, Hamilton, New Zealand; ^c The Centre for Atmospheric Chemistry, School of Chemistry, University of Wollongong, Northfields Ave., Wollongong, New South Wales, Australia

2.1 Summary

Measurement of individual emission sources (e.g. animals or pen manure) within intensive livestock enterprises is necessary to test emission calculation protocols and to identify targets for decreased emissions. This was a substantial challenge, as no existing methods were available for providing absolute emissions measurements from a single source co-located with a large number of other sources.

In this study a vented, fabric-covered large chamber (4.5 x 4.5 m, 1.5 m high) in combination with on-line analysis (nitrous oxide [N₂O] and methane [CH₄] via Fourier Transform Infra Red spectroscopy; 1 analysis min⁻¹) was tested as a means to isolate and measure emissions from beef feedlot pen-manure sources. A mathematical method was also developed to allow the interpretation of the data collected, taking into account surrounding air concentrations and air exchange between the chamber and the surrounding air. Alternating manure source emission measurements using the large chamber and the backward Lagrangian stochastic technique (5 month period; bLS validated via tracer gas release, recovery 94 to 104 %) produced comparable N₂O and CH₄ emission values (no significant difference $P < 0.05$). Greater precision of individual measurements was achieved via the large chamber than for the bLS (mean \pm standard error of variance components: bLS half hour measurements, 99.5 \pm 325 $\mu\text{g CH}_4 \text{ s}^{-1}$, 9.26 \pm 20.6 $\mu\text{g N}_2\text{O s}^{-1}$; large chamber measurements, 99.6 \pm 64.2 $\mu\text{g CH}_4 \text{ s}^{-1}$, 8.18 \pm 0.3 $\mu\text{g N}_2\text{O s}^{-1}$).

Through this work we have established the credibility of our approach, and shown that the large chamber design is suitable for measurement of emissions from manure on pen surfaces, isolating these emissions from surrounding emission sources.

Abbreviations: *A*, area of surface enclosed by a chamber; bLS, backward Lagrangian stochastic; *C*, gas concentration in a chamber; *C_b*, background air concentration during a chamber measurement; *C_{min}*, concentration of air in the chamber when initially closed; *F*, volumetric emission flux; IHF, integrated horizontal flux; *t*, time; *V*, chamber volume; *v_{exch}*, rate of exchange of air from inside with air from outside.

2.2 Introduction

Accurate techniques to measure emissions from greenhouse gas sources have been vigorously sought as concern over the effect of these gases on climate has increased. This is especially true for the measurement of greenhouse gas emissions from intensive livestock production, where it can be difficult to discriminate between multiple on-farm sources, which are often closely associated spatially.

Denmead (1979) discussed the advantages and disadvantages of two approaches to measure what they termed “very low flux density” emissions of gas species, particularly N₂O (at emissions < 940 ng N₂O m⁻² s⁻¹): 1) micrometeorological, and 2) chamber techniques. The relative advantages and disadvantages of the methods were significant. Two of these

may be simply stated: chambers (where an area of an emission source is enclosed within a vessel or impermeable canopy) tend to modify emissions while micrometeorological approaches suffer from poorer detection limits (Denmead, 2008).

Most recent measurements of emissions from beef feedlots rely on a significant advance in micrometeorological monitoring of gaseous emissions, namely the development of the backward Lagrangian stochastic (bLS) emission measurement technique (Flesch et al., 1995, 2004; Wilson et al., 2001). This micrometeorological technique operates at a scale appropriate for livestock emission sources such as ponds (Wilson et al., 2001), feedlot pens of cattle (McGinn et al., 2007, 2008; Loh et al., 2008a), waste composting or stockpiling areas (Sommer et al., 2004a), and land application of livestock wastes (Sanz et al., 2010), and is used for complex shaped emission sources (Flesch and Wilson, 2005). A wide range of validation studies has been published, reporting close to 100 % recovery and average within-study standard deviations of around 21 % (Harper et al., 2010). Importantly, this open-air technique retains the advantage of micro-meteorological techniques: it does not significantly influence the emission source. In addition to these advantages, comparisons between bLS and integrated horizontal flux (IHF, Denmead, 1983) measures suggest the two techniques can produce comparable results (Sommer et al., 2004a; Flesch and Wilson, 2005).

The bLS technique is well-suited to investigations of emissions over multi-week periods, rather than short-duration, precise measurements. Stringent acceptance criteria are often applied to the data collected. Consequently, many data points (each point is often a 15-min average) are rejected due to inappropriate wind x site interactions or wind direction (Flesch et al., 2005, 2007; Loh et al., 2008). The proportion of data rejected can be high, with 42% of observations being rejected in one published study (Gao et al., 2009). Individual bLS data points are also highly variable (McBain and Desjardins, 2005) with several potential sources of error (Flesch and Wilson, 2005). Standard deviations of individual measurements of 30% of the mean (Gao et al., 2009) or greater (Loh et al., 2008) are normal. In contrast, measurements with chambers are limited to periods of less than 40 min due to the potential for alteration of emission conditions (Rochette and Eriksen-Hamel, 2008). Moreover, short-duration, precise measurements with negligible data rejection suit some situations better than the conditions required by bLS (e.g., tracking emission process transitions over a period of several days or less).

The bLS technique is well suited to measure the emission rate of a single, isolated source area, but less suited to distinguish between spatially associated sources of gaseous emissions. As research begins to focus on strategies to decrease emissions from feedlot production a method to discriminate various on-farm emission sources is needed.

Chambers appear to be a simple solution to the problem of the separation of feedlot pen surface CH₄ emissions from nearby animal enteric emissions. Chamber techniques remain in wide use for the measurement of emissions in other applications (Rochette and Eriksen-Hamel, 2008; Butterbach-Bahl et al., 2011). While steady-state chambers (where a gas flow is maintained through the chamber to an analyser) were used for few published measurements (e.g. Denmead, 1979), most (at least for N₂O) were conducted using non-steady-state, non-flow-through chambers (Conen and Smith, 1998; Bouwman et al., 2002). A more recent review and examination of this type of chamber (Rochette and Eriksen-Hamel, 2008) recommended a range of measures to ensure inaccuracies are minimised. These recommendations highlight the need to minimise the influence of the chamber method on source emission rates due to factors including: alterations in air pressure, temperature, decreases in the diffusion gradient from the source to the air above, and physical disturbance of the emission source.

Increasing chamber size may have advantages. The greater area-to-circumference ratio of a large chamber compared to a smaller chamber potentially results in decreased error caused

by poor chamber sealing with the emission surface (Rochette and Eriksen-Hamel, 2008). The area of the large chamber will likely encompass greater spatial variability than achieved with a small chamber. Both of these factors would be significant advantages in many field deployments to uneven highly variable surfaces, such as the pen surfaces of commercial beef feedlots. Where a large chamber has a greater volume than a conventional chamber this would also result in a slower rise in the concentration of emitted gas in the internal volume and less disturbance of the concentration gradient, diffusion conditions, temperature and humidity. All of these factors can influence the measured emissions (Rochette and Eriksen-Hamel, 2008).

Setup and removal of a single, well-designed large chamber rather than a large number of small chambers (enclosing an equivalent area) is likely to save time and will restrict animal access to a smaller area of pen surface. This translates to decreased alteration of animal influence on the emission source and less interruption of normal commercial feedlot activities.

Due to the acceptance of bLS as a preferred method of measurement of emissions from feedlots, it is appropriate that bLS techniques be used as a benchmark against which to compare methods to isolate feedlot enterprise emission sources. One study compared micrometeorological (IHF) and chamber (area of 0.01815 m² with a 0.0024 m³ headspace, 12 chambers used concurrently) measurements of CH₄, CO₂ (carbon dioxide), and N₂O emissions from a beef manure stockpile (Sommer et al., 2004a). Results of the two techniques were not comparable. The difference was attributed to the strong influence of convective flow in the stockpile, and the very spatially heterogeneous emission pattern. Comparisons between manure source measurements conducted via bLS and chambers have not been attempted.

This paper describes the design of a large (20 m² emission area) chamber, with some similarities to that described by Galle et al. (1994), though the structure, procedures, circumference to enclosed area ratio, and analysis approach differ (e.g., we use a closed path analyser rather than an open path unit). The technique was developed for the specific purpose of measuring emissions from the spatially heterogeneous manure-packed surfaces of beef feedlot pens, while minimising setup and removal times to minimise disturbance of animal activities. The target was to develop a method that enabled manure emissions to be separated from enteric emissions, as well as encompassing a wide spatial variability more efficiently than smaller chambers (e.g., Sommer et al. 2004a). Moreover, pen manure emission data are lacking from the literature, apart from a small-chamber study at low temperatures (10°C; Boadi et al., 2004). Wider applications are likely where multiple emission sources are spatially associated or where instantaneous precise measurements are required. To test the technique, CH₄ and N₂O emissions from a feedlot pen surface were measured using the large chamber and compared with measurements obtained using a bLS technique. We hypothesised that where the design and use of this large chamber incorporates recent recommendations for the use of non-steady-state, non-flow-through chambers, the results obtained with such chambers do not differ from results collected via a bLS procedure (validated via tracer gas release), and moreover, individual chamber observations will be more precise than individual half-hour interval bLS measurements.

2.3 Materials and methods

The methods described here are centred around establishing the design of a large potentially leaky chamber (due to permeation of the fabric cover or imperfect sealing against the emission surface) and the theory behind using it to measure CH₄ and N₂O emissions, and establishing whether measurements collected with this device are likely to be consistent with those collected using the bLS method for feedlot pen surfaces.

In overview, the study entailed: using tracer gas releases to validate a bLS technique centred around a closed path analyser and two sampling manifolds (five intakes each); establishing a manure-based emission source; arranging two sampling manifolds (five intakes each) to collect N_2O , CH_4 (Figure 2.1) and establish emissions via bLS; periodically covering the source with the large chamber to conduct chamber emission measurements.

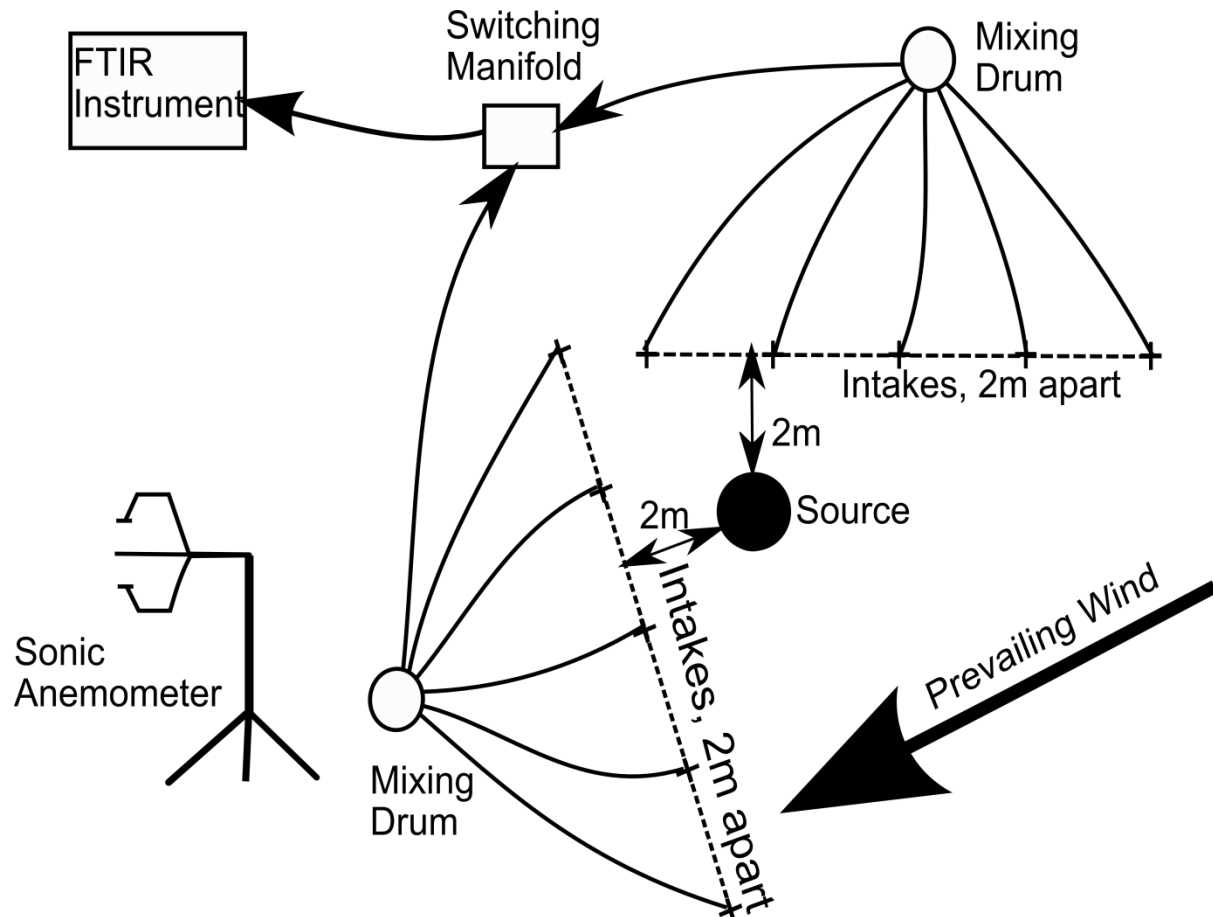


Figure 2.1. The layout used to conduct the Backward Lagrangian Stochastic measurements of emissions, with analysis by Fourier Transform Infra-Red spectroscopy, switching between two sets of 5 intakes.

2.3.1 Theory of fabric-covered large chamber

Where the exchange of air between the inside and outside of the chamber is negligible (and pressure constant), and the change in concentration (C , defined as $[\text{m}^3 \text{ analyte gas}] \text{m}^{-3}$) with time (t , s) is given by:

$$\frac{dC}{dt} = \frac{AF}{V} \quad [1]$$

where A is the area of surface enclosed (m^2), F is the flux ($[\text{m}^3 \text{ analyte gas}] \text{m}^{-2} \text{s}^{-1}$), and V is the volume of the chamber (m^3).

Solving for C at a given time, where the volume outflow due to expansion out the vent is a negligible loss of the analyte (C_b is the background air concentration, [m^3 analyte gas] m^{-3}):

$$C = \frac{AF}{V}t + C_b. \quad [2]$$

Our chamber design is fabric covered, with a skirt weighted against the emission surface as a seal. This configuration may be more permeable than conventional chambers. Given the above assumptions, if there is significant exchange of air from within the chamber with air from outside, the following differential equation (developed from eq. [1]) will represent the concentration behaviour in the large chamber (Meyer et al., 2001):

$$\frac{dC}{dt} = \frac{AF + v_{exch}(C_b - C)}{V} \quad [3]$$

where v_{exch} is the rate of exchange of air from inside with air from outside (volume time⁻¹). Solving for the concentration at a given time, and assuming the initial concentration is C_b gives:

$$C = \frac{AF}{v_{exch}}(1 - e^{-\frac{v_{exch} \times t}{V}}) + C_b \quad [4]$$

For small t (initial rise rate), or small/zero leak rate v_{exch} , the initial slope is AF/V , and with constant C_b and emission rate the concentration will rise to an asymptote with $AF/v_{exch} + C_b$.

Where the commencing concentration is not the same as the mean background concentration during the measurement period (C_b), but C_{min} at $t=0$:

$$C = \frac{AF}{v_{exch}}(1 - e^{-\frac{v_{exch} \times t}{V}}) + (C_{min} - C_b)e^{-\frac{v_{exch} \times t}{V}} + C_b \quad [5]$$

This equation can be applied even under conditions where v_{exch} approaches zero, by making use of the limit of the first term in eq. [5]:

$$\lim_{v_{exch} \rightarrow 0} \left[\frac{AF}{v_{exch}}(1 - e^{-\frac{v_{exch} \times t}{V}}) \right] = \frac{AF \times t}{V} \quad [6]$$

2.3.2 Construction and operation of the emission source

A 1 m diameter sharpened stainless steel cylindrical ring (95 mm high) was hammered 75 mm into the soil. The internal soil was excavated (75 mm deep), and the pit lined and sealed with polyethylene sheeting (at the source position displayed in Fig. 2.1). An aluminium disk (995 mm diameter, 2 mm thick) was placed at the base of the pit. The heating cables from four aquarium heaters were glued to the upper side of this aluminium disk in inter-leaved spirals (Dupla Inc.; 2 x Duplaflex model 750, 200 W; 2 x Dupla Therm Set model 250, 100 W). The pit was then packed with manure collected from a beef feedlot pen. A wooden ram was used to compact the manure in place during the filling process in order to simulate the manure condition encountered in the field (bulk density of $\approx 0.8 \text{ t m}^{-3}$).

Conditions applied to the manure ensured that where emission substrate was available, high microbial activity was favoured by moderately high temperature and moist conditions.

Manure temperature was maintained at $45\pm 2^\circ\text{C}$ (Novus Temperature PID Controller, N480D, used to switch the aquarium heaters) based on temperature readings collected at the centre of the manure profile (three Pt 100 Resistance Temperature Detectors). Moisture content was maintained at approximately field capacity via tri-weekly checks and water additions.

Four times throughout the trial, the manure in the source was replaced with manure recently collected from a feedlot pen. Replacement of the depleted emission substrate also allowed emission fluxes to be altered by increasing the manure depth. Manure depths ranged from 75 to 250 mm, representing depths encountered on pen surfaces and manure mounding in pens at Australian feedlots.

2.3.3 Application of the bLS technique

The bLS technique was applied in a manner that reflected the principles of the technique (Flesch and Wilson, 2005); however, there was some divergence from the scale and approach of recent studies (McGinn et al., 2006, 2008; Loh et al., 2008a). This was unavoidable, as our study was a comparison between bLS and large-chamber techniques.

Open-path instruments are more commonly used for bLS measurements; however, in our study the same closed-path Fourier Transform Infra-Red (FTIR) spectrometer used for the large chamber measurements was used in conjunction with the Windtrax model (Crenna et al., 2008) which applied the micrometeorological calculations using the half-hourly gas analyses, half-hourly wind statistics, and experimental layout. The line-averaging allowed with open-path instruments was achieved (Fig. 2.1) by using two lines of 5 inlets. Each set of 5 equal-flow (0.240 L min^{-1}) inlets was connected to a 20.7 L mixing drum (mixing achieved with a fan inside each drum; 40 mm diameter, 12 V, 0.08 A, brushless direct current motors; run at 6 V); then a single gas intake line led to the manifold responsible for automatically switching between the two sets of 5 inlets every 5 minutes.

The 5 inlets of the line-averaging air intakes were set at the sampling height (0.40 m) defining 5 points along a straight line at equal spacing (2 m). The Windtrax model represents line-averaging by defining multiple intakes along a single line, and consequently the model representation accurately described the sampling layout.

The use of mixing drums in combination with eq. [5] allowed continuous averaging of intake concentrations over the half-hour bLS period, despite the FTIR instrument switching sequentially between the two intakes at 5-minute intervals. Flow through the mixing drums was maintained at 1.2 L min^{-1} via two mass flow controllers (Alicat Scientific, USA, model MC).

Sample inlets were placed in close proximity to the source, with a minimum distance to the lines of intakes of 2 m (Fig. 2.1). This reflects the short fetch across the source ($< 1\text{ m}$) and the need to locate the sample intakes at a relatively high concentration point within the emission plume.

A 3D sonic anemometer (CSAT 3D, Campbell Scientific, USA) was placed in a position that, under the prevailing wind conditions, was downwind of the sample collection lines (Fig. 2.1), 7 m from the centre of the emission source, and centred 0.7 m above the ground. The Windtrax model uses the wind direction from the sonic anemometer to select which set of 5 inlets will provide the background concentration.

The scale of application of the bLS technique applied here was substantially smaller than that conventionally employed (compare Fig. 2.1 versus studies covering hundreds of metres similar to that of Loh et al., 2008), necessitating short fetches, gas sampling close to the ground, and characterisation of air turbulence closer to the ground surface (measured via the sonic anemometer) than normally is the case for applications of the bLS technique.

Additionally, turbulent eddy size decreases with height above the ground (Baum et al., 2008). Where measurements are conducted close to the ground surface it is desirable to use sonic anemometers with smaller path lengths in order to catch the high-frequency eddies. Commercially available sonic anemometers, such as that used here, have a path length of 0.1 m.

For this reason the method was validated against known releases of CH₄ and N₂O (via mass flow controller, Alicat Scientific, USA, model MC), in the same configuration and at the same location as the temperature-controlled manure emission measurements. These releases included: **Release 1**, 6230 µg CH₄ s⁻¹ measured over 44 half-hour periods (tracer gas 66.5±3.3% CH₄ by volume in a CO₂ balance, mean ± 95% confidence interval); **Release 2**, 15.1 µg N₂O s⁻¹ measured over 23 half-hour periods (tracer gas 108±4 ppm N₂O by volume in an air balance); and finally, **Release 3**, 8511 µg CH₄ s⁻¹ measured over 10 half-hour periods (tracer gas 68.3±1.0% CH₄ by volume in a CO₂ balance). These tracer gases were released from the source area (no manure present) via a 4-outlet diffuser.

Standard rejection criteria (Flesch et al., 2005, 2007; Loh et al., 2008) were applied: where the friction velocity (u_*) fell below 0.15 m s⁻¹, where the Obukhov length (L) was between +10 and -10 m, and where the estimated roughness height exceeded the sampler height. Data with inappropriate wind directions for the intake layout were removed from the data set, which generally removed Windtrax-calculated emission estimates with high standard deviations.

2.3.4 Design and operation of the large chamber

An impermeable fabric (Canvacon from Synthesis Fabrics Pty Ltd, a polyethylene coated fabric, <http://www.synthesisfabrics.com/>) was used to make a cover for a domestic steel-framed folding gazebo (OZtrail Pty Ltd, 4.5 x 4.5 m; height adjustable to 0.5 m or 1.5 m, all validation measurements conducted at 1.5 m height), forming the basis for the large chamber illustrated in Fig. 2.2. The cover included a skirt that spread across the emitting surface to a width of 0.30 m, allowing it to be weighted down (Fig. 2.2; weighted width of about 0.12 m).



Figure 2.2. The fabric covered large chamber is based around a modified commercial gazebo (4.5 x 4.5 x 1.5 m high) covered with a polyethylene-coated fabric.

A “sleeve” was stitched and sealed into a hole 0.35 m from the centre of one upper edge of the cover, and a vent tube installed in the sleeve and secured with duct tape. Calculations conducted using the recommended approach to designing chamber vent tubes (Hutchinson and Mosier, 1981; Rochette and Eriksen-Hamel, 2008) suggest that a vent tube of about 2 m length and 0.117 m internal diameter would suit the internal volume of the chamber and allow transmission of ambient pressure fluctuations from the external environment to the enclosed space for wind speeds of up to 4 m s^{-1} . We obtained commercial PVC pipe with an internal diameter of 0.120 m and a total length of 2.2 m. The additional length allowed us to ensure the external outlet to the vent tube was close to the surface of the ground, where wind speeds are lower than the air above. This measure was instituted to prevent unrepresentative pressure fluctuations due to wind passing across the outlet of other vent designs (Conen and Smith, 1998). In order to confirm that the vent configuration was effective, differential pressure between the chamber volume and outside air was logged (spot measurements at 6-second intervals) before, after, and throughout each period of chamber closure (pressure transducer, Setra Systems, Model 264, $\pm 25 \text{ Pa}$ measurement range).

The 1.5 m height of the chamber greatly exceeds the recommendation of $\geq 0.4 \text{ m}$ chamber height (Rochette and Eriksen-Hamel, 2008). Since the chamber was deployed to measure a manure source rather than the designed soil emission source (Rochette and Eriksen-Hamel, 2008), greater N_2O emission rates and significant CH_4 emission were anticipated. Improved headspace mixing was achieved via four fans located within the chamber volume (0.075 m diameter, 12 V, 0.2 A, brushless direct current motors; run at 6 V).

Sampling with the large chamber was conducted by moving the modified gazebo to the measurement site, expanding its folding frame, fitting the cover, and weighting down the skirt. The chamber was then insulated as recommended (Rochette and Eriksen-Hamel, 2008), in this case with foil-backed foam-rubber insulation. Internal air temperature was monitored via three PT100 sensors (Element 14 Pty Ltd).

Air from within the chamber was sampled continuously (1.2 L min^{-1} total flow from four inlets located within the upper third of the chamber volume; all gas volumes standardised to 101.33 kPa and 25°C ; mass flow controller Alicat Scientific, USA, model MC) via tubing and analysed by closed path Fourier Transform Infra-Red Spectrometry (FTIR); prototype instrument constructed by the University of Wollongong (Griffith et al., 2012; Hammer et al., 2012) for CH_4 and N_2O (and limited CO_2 analyses) at 1-min intervals, and the analysed air then returned to the chamber. Air sampling and analysis commenced before chamber closure, and ended after chamber opening. The 10 sample values immediately after chamber closure were used to calculate emissions. However, the chamber remained closed for an additional 15 to 20 min during which a tracer gas was released in order to measure the exchange of air between the enclosed volume and external air. This exchange reflects the effectiveness of the seal against the emission surface and leakage through the cover. During each sampling, a controlled input of 3.00 to $12.0 \mu\text{g N}_2\text{O s}^{-1}$ of tracer gas (tracer gas $100 \pm 4 \text{ ppm N}_2\text{O}$ by volume in an air balance) was conducted for 10 min following completion of each chamber measurement period.

The chamber was operated under conditions that provided variable quality of the seal with the ground surface due to varied surface pugging by cattle under different manure moisture conditions.

The N_2O emission data were fitted with Eq. [5] using an algorithm (R Development Core Team, 2014) that simultaneously fitted both for the initial 10 data points (one line segment where the emission is responsible for the slope), and the tracer gas release data (a second line segment where the emission + known tracer gas release combined to produce the slope of the concentration rise). This allowed greater confidence in the estimated value of V_{exch} .

The fit was regarded as satisfactory where $R^2 > 95\%$; the residuals were evenly distributed; and emission standard errors of less than 5% of the emission prediction were achieved.

Subsequently, the value of v_{exch} determined for the N_2O tracer release was used in the methane analysis for the source-only emission period (Eq. [5]).

2.3.5 Comparison of bLS versus large chamber

The comparison was conducted by alternating bLS (detailed layout Fig. 2.1) and large-chamber measurements of the temperature-controlled emission source. While a regular pattern was followed in the main, this schedule was modified to accommodate heavy rainfall, storms, and breakdowns. The experiment collected 53 large-chamber readings of the source and 221 half-hour bLS measurements over a period of 5 months. Each week, replicated large-chamber measurements were conducted over the soil adjacent to the heated emission source. These small soil emission values (CH_4 and N_2O) were used in emission calculations. Large-chamber deployments enclosed both the source and a portion of the surrounding soil, so manure source emissions were determined by subtracting soil emissions from the chamber measurement on the basis of relative enclosed emission area. For the bLS technique, if the soil emissions were significant they could be assigned as an emission source of known magnitude to the surrounding soil area extending well beyond the area enclosed within the sampling inlets (Fig. 2.1).

2.3.6 Statistics

Concentration models for the large-chamber data were fitted by non-linear regression using R (nlm procedure in R, R Development Core Team, 2014). The 30-minute flux bLS estimates versus individual large-chamber estimates were analysed using the REML directive of GenStat (VSN International, 2012) with date and time of sample as a random effect and the 'method' (chamber versus bLS) as the fixed effect. The analysis of the untransformed data scale was verified by analysing the rank transformed data (Conover and Iman, 1981).

2.4 Results and discussion

2.4.1 Tracer gas recovery, rejection criteria and bLS

The bLS technique employed using a closed path analyser returned close to complete recoveries of the tracer gas releases (Fig. 2.3), under wind conditions that encompassed the range of conditions encountered during the latter experimentation (Obukhov values, L , ranging from -8 to -988; u_* ranged from 0.06 to 0.55 $m\ s^{-1}$), and with an identical experimental layout. The initial tracer gas release (CH_4 ; **Release 1**) produced very few data values that fell within the acceptance criteria (4 half-hour estimates out of 44), due to adverse wind conditions. Significantly, the recovery of values meeting the u_* and L acceptance criteria (recovery $94 \pm 18\%$, mean \pm standard deviation % of the methane released, $n=4$) did not differ appreciably from the recovery calculated from all values (recovery $98.7 \pm 20\%$, $n=40$). **Release 2** (N_2O) was more successful, due to more favourable wind conditions (though friction velocities, u_* , averaged only 0.30 $m\ s^{-1}$), achieving $104 \pm 77\%$ recovery. Only 6 of the 23 values were rejected based on L (2 values), and Windtrax prediction standard deviations ($> 45\%$ of the predicted emission value; 4 values). Wind statistics for all periods during **Release 3** fell within the acceptance criteria, achieving $104 \pm 33\%$ analytical CH_4 recovery ($n=10$), with higher u_* contributing to a lower standard deviation (mean value of 0.5 ms^{-1}).

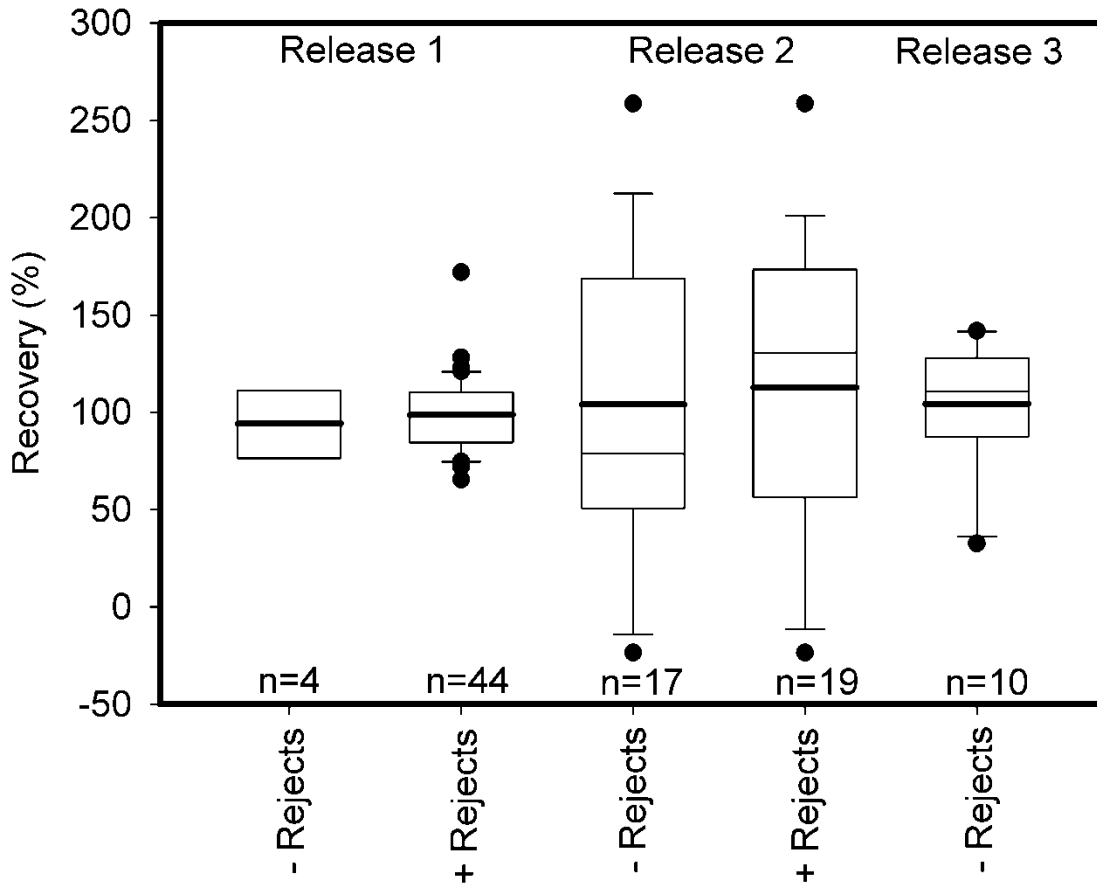


Figure 2.3. Box plots of recoveries for the trace gas releases analysed by the backward Lagrangian stochastic procedure (Release 1, CH₄; Release 2, N₂O; and Release 3, CH₄). The acceptance criteria based on friction velocity (u_*) and Obukhov length (L) had little influence on the result. The heavy central line indicates the mean, while the nearby (or superimposed) lighter line represents the median.

At the small spatial scale of bLS operation in this study the rejection criteria made little difference to the recovery data, as suggested by the lack of strong differences between the variances displayed with and without rejected values (Fig. 2.3). However, application of the rejection criteria to the emission estimates from the manure source decreased the variance of the bLS data. For CH₄, the rejection criteria decreased the standard deviation of the emission residuals (compared to the three-day means) from 101 to 49 $\mu\text{g s}^{-1}$, and for N₂O from 15 to 13 $\mu\text{g s}^{-1}$.

2.4.2 Model fit and discussion of large chamber characteristics

In many cases, the concentration rise of N₂O and CH₄ within the chamber indicated that a good seal was achieved with the ground surface and little leakage occurred through the fabric ($v_{exch} \approx 0 \text{ m}^3 \text{ s}^{-1}$). However, significant air exchange was observed during some deployments. Fig. 2.4 illustrates one example where the chamber was deployed to an irregular surface, with eq. [5] fitted. The concentration rise associated with N₂O emission (Fig. 2.4a; N₂O emission rate 2.75 $\mu\text{g N}_2\text{O s}^{-1}$), and that associated with the release of the tracer gas (tracer gas release, 11.8 $\mu\text{g N}_2\text{O s}^{-1}$) were well characterised via non-linear regression fitting both slope sections simultaneously ($R^2 = 0.998$). The estimate of v_{exch} (0.125 $\text{m}^3 \text{ s}^{-1}$) determined during each nitrous oxide measurement allowed Eq. [5] to fit other

analysed gasses, including CH₄ and CO₂ (e.g., Fig. 2.4b, 11.0 mg CO₂ s⁻¹; R² = 0.999). Under the full range of conditions, Eq. [5] represented the observed concentration behaviour well.

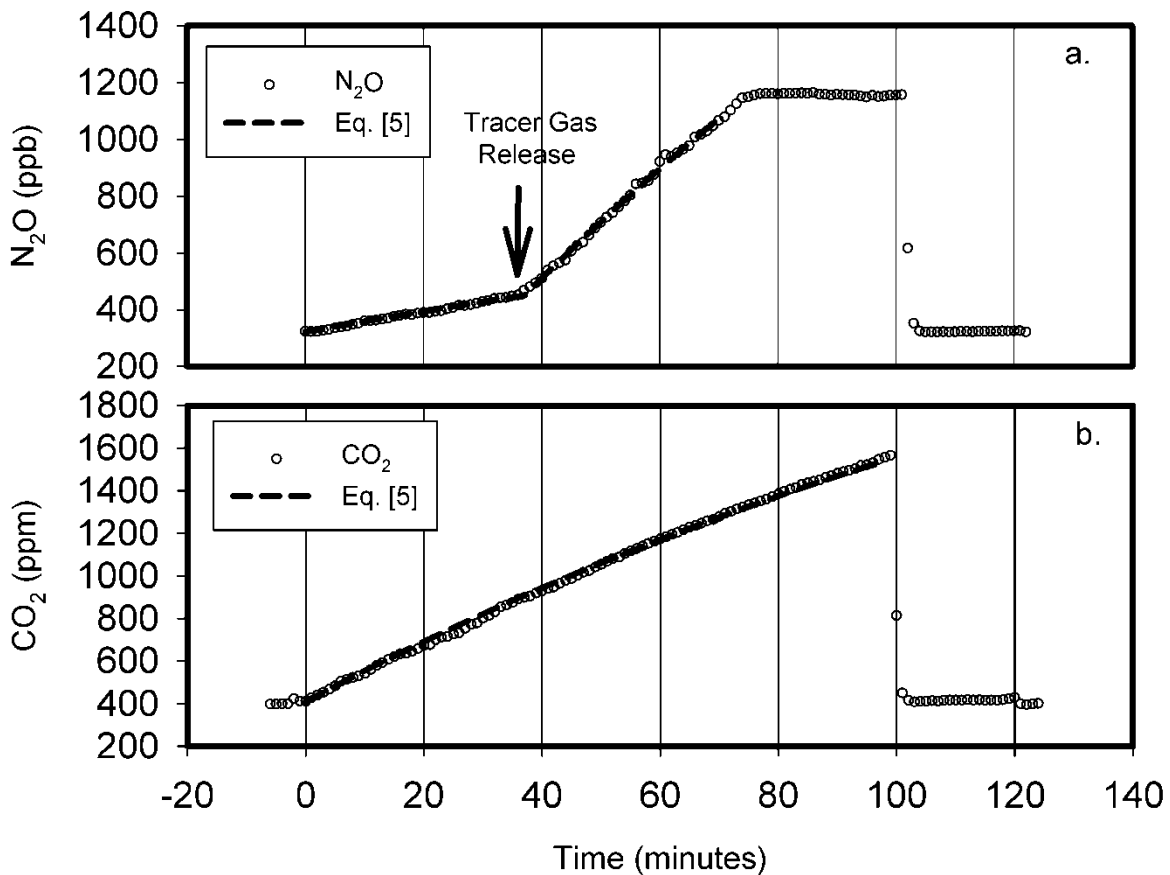


Figure 2.4. An example plot of the non-linear model fit (eq. [5]) to the chamber concentration data where there was substantial air exchange between the internal volume of the large chamber and external air. Panel a) shows the N₂O concentration rise associated with an emission of $2.75 \pm 0.06 \mu\text{g N}_2\text{O s}^{-1}$, and the release of the tracer. Panel b) shows the CO₂ concentration rise ($11.0 \pm 0.02 \text{ mg CO}_2 \text{ s}^{-1}$) calculated using an air exchange (v_{exch}) of $0.125 \pm 0.009 \text{ m}^3 \text{ min}^{-1}$ as determined from the N₂O data.

The chamber characteristics combined with gentle headspace mixing and continuous on-line analysis provided smooth data series (Fig. 2.4), proving appropriate under the experimental conditions. Where emission rates are smaller than we encountered, a shorter chamber may suit conditions better.

A recent review of chamber methods suggests that chambers deployed to soil surfaces should ideally be inserted into the surface to prevent accumulating emissions diffusing out of the chamber (Rochette and Eriksen-Hamel, 2008). For nitrous oxide, the recommended depth of insertion (Hutchinson and Livingston, 2001) was $> 0.12 \text{ m}$ where soil had 30% air-filled pore space. Insertion of chambers into a measurement surface also disturbs the surface and alters emission conditions, and often requires a lengthy settling time before emissions resume their normal behaviour. In applications where measurements are conducted in a livestock pen, anything left on the pen surface is a potential risk to stock and may well be damaged. Rather than inserting the chamber edge or a fixed base into the pen, the approach applied here was to seal the chamber skirt against the surface – to a width of about 0.12 m. It is noted that for field deployments this causes some degree of ambiguity

over the emission collection area, however, this only represents about a 5% increase in the collection area (if 50% of this additional covered area collects in the chamber volume). This 0.12m width was weighted down with sand-filled lay-flat polyethylene coated fabric hose. Additionally, the chamber area/perimeter ratio of the large chamber was 1.125 m. This is more than 10 times the recommended minimum (Healy et al., 1996), greatly decreasing the impact of chamber seal effects.

The combination of the chamber design and sealing technique proved capable of providing a good seal with the surface for many deployments ($v_{exch} \approx 0 \text{ m}^3 \text{ s}^{-1}$). Where difficult conditions were encountered, e.g. an irregular ground surface, significant air exchange was efficiently dealt with via eq. [5], preserving the value of measurements under these conditions. Whether v_{exch} was significant or not, disturbance of the pen surface during measurements was minimal.

Deployment of the large chamber did not greatly disturb the temperature and pressure conditions applied to the emission surface, or the compacted manure surface. Differential pressure measurements suggest that during each measurement period (during the first 15 min after large chamber closure), pressure within the large chamber is not significantly different than the external pressure (pressure differential $0.83 \pm 3.8 \text{ Pa}$, $n=1240$), and does not differ from measurements conducted prior to large-chamber closure ($0.52 \pm 3.2 \text{ Pa}$; $n=407$). Changes in air temperature within the large chamber after closure were small, averaging $< 2.5 \pm 1.0^\circ\text{C}$ increase within the initial 15 min. Ambient wind speeds during measurement ranged from 0 to 4 m s^{-1} , a range of values that falls within the design specification of the vent (Hutchinson and Mosier, 1981).

2.4.3 Large chamber versus bLS

Comparisons of the emissions determined using the two techniques indicates no difference between them ($P < 0.05$; using the REML directive of GenStat; VSN International, 2012). This result was the same irrespective of whether the restrictions on u^* and L were invoked or not. This is supported by Figs. 2.5 and 2.6, where data for both CH_4 and N_2O showed that the large-chamber measurements track bLS values over time. Fig. 2.7 plots CH_4 measurements using the large chamber versus bLS and also suggests that moving averages calculated over a three-day period for both techniques are comparable – though individual 30-minute flux values were used in the statistical analysis to avoid selection of arbitrary periods of averaging. The variance of the bLS values tended to be larger than those of the large-chamber measurements (based on mean \pm standard error of variance components: bLS half-hour measurements, $99.5 \pm 325 \mu\text{g CH}_4 \text{ s}^{-1}$, $9.26 \pm 20.6 \mu\text{g N}_2\text{O s}^{-1}$; large chamber measurements, $99.6 \pm 64.2 \mu\text{g CH}_4 \text{ s}^{-1}$, $8.18 \pm 0.3 \mu\text{g N}_2\text{O s}^{-1}$; Figs. 2.5 and 2.6). The standard deviations of the large chamber values are small relative to the mean and may closely reflect the real changes in emission rates throughout each three-day period. In contrast, quite large single-interval uncertainties are common for bLS (Harper et al., 2010), and standard deviations on averaged emissions can be a large proportion of the mean (McGinn et al., 2008). This sort of variability is also evident in the bLS data collected here, and has previously been attributed to uncertainties in the bLS model, uncertainty in the idealized representation of the wind, and noise in concentration observations (Harper et al., 2010). The impacts of these effects are minimised via averaging. As part of the overall spread of our values, some negative emissions were calculated. Consumption of N_2O has been reported in other studies (Blackmer and Bremner, 1976; Chapuis-Lardy et al., 2007). Additionally, negative errors have been attributed to sensitivity of the algebraic system solved by the bLS model to input parameter uncertainty (Crenna et al., 2008). Negative emission estimates may result from erroneous background calculations, due to variable wind direction during the half-hour averaging period or gas analysis sensor noise. These effects are likely to be exacerbated at the lower gas emission rates. The concentration differences between inlets during our study were sometimes less than 1 ppb V. Standard deviations on

comparable measurements with this Fourier Transform Infra-Red spectrometer are around 0.19 ppb V, suggesting that the N₂O emissions were determined at close to the limit of the precision of the instrument.

Under these circumstances it is appropriate to retain negative emissions in order to avoid artificially biasing the mean concentration value, since both analysis noise-related low values and high values are possible. In contrast, the chamber technique was able to operate at these emission rates without additional error as gas emissions are concentrated in the enclosed chamber volume.

Throughout the experiment, measured emissions from the surrounding soil were uniformly small, averaging 0.02 % of chamber CH₄ emissions and 0.1 % of chamber N₂O emissions for the manure source.

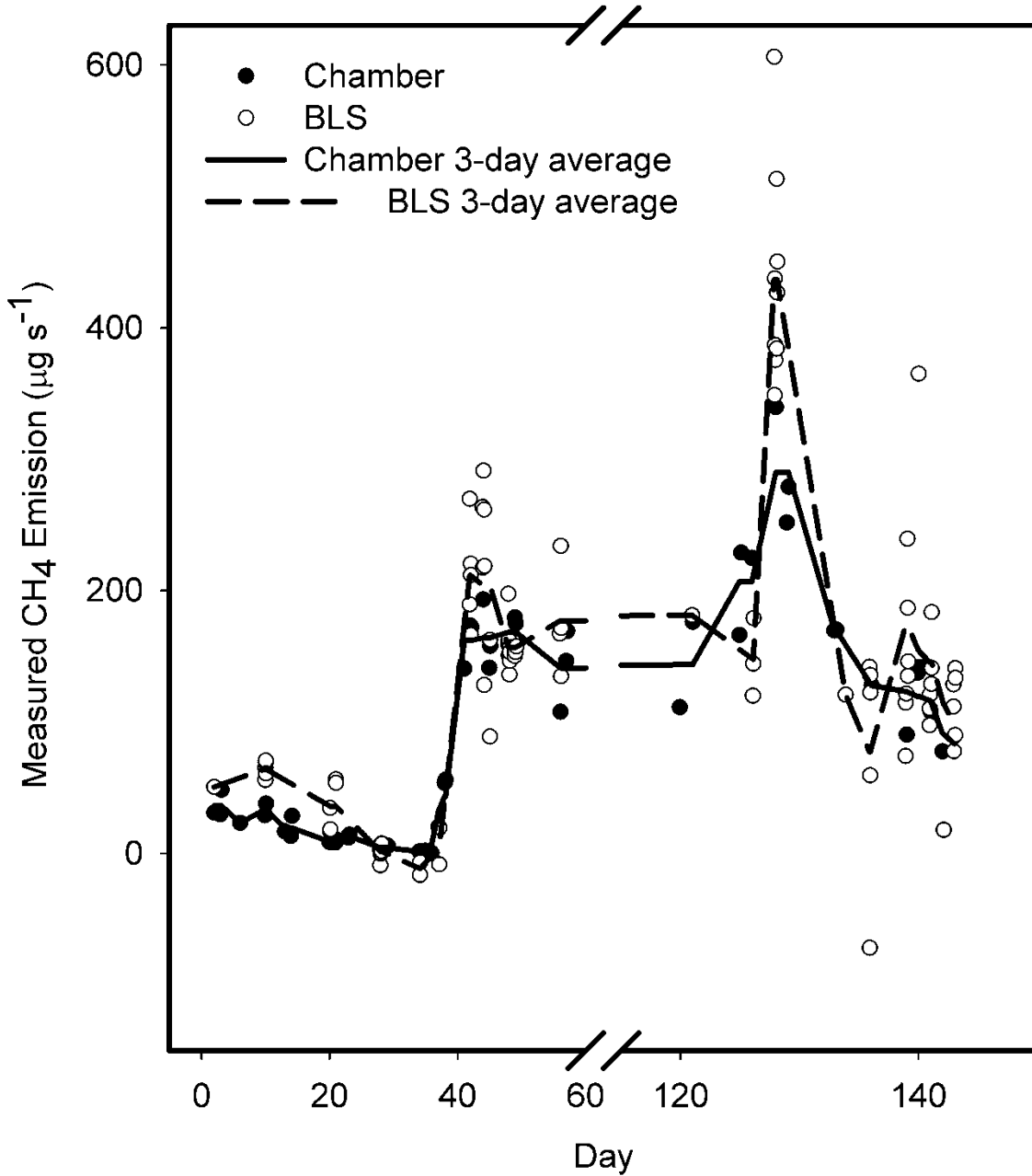


Figure 2.5. Measured CH₄ emissions versus time for data collected using the large chamber and the backward Lagrangian stochastic technique (bLS 30-minute flux values; restricted to data meeting acceptance criteria).

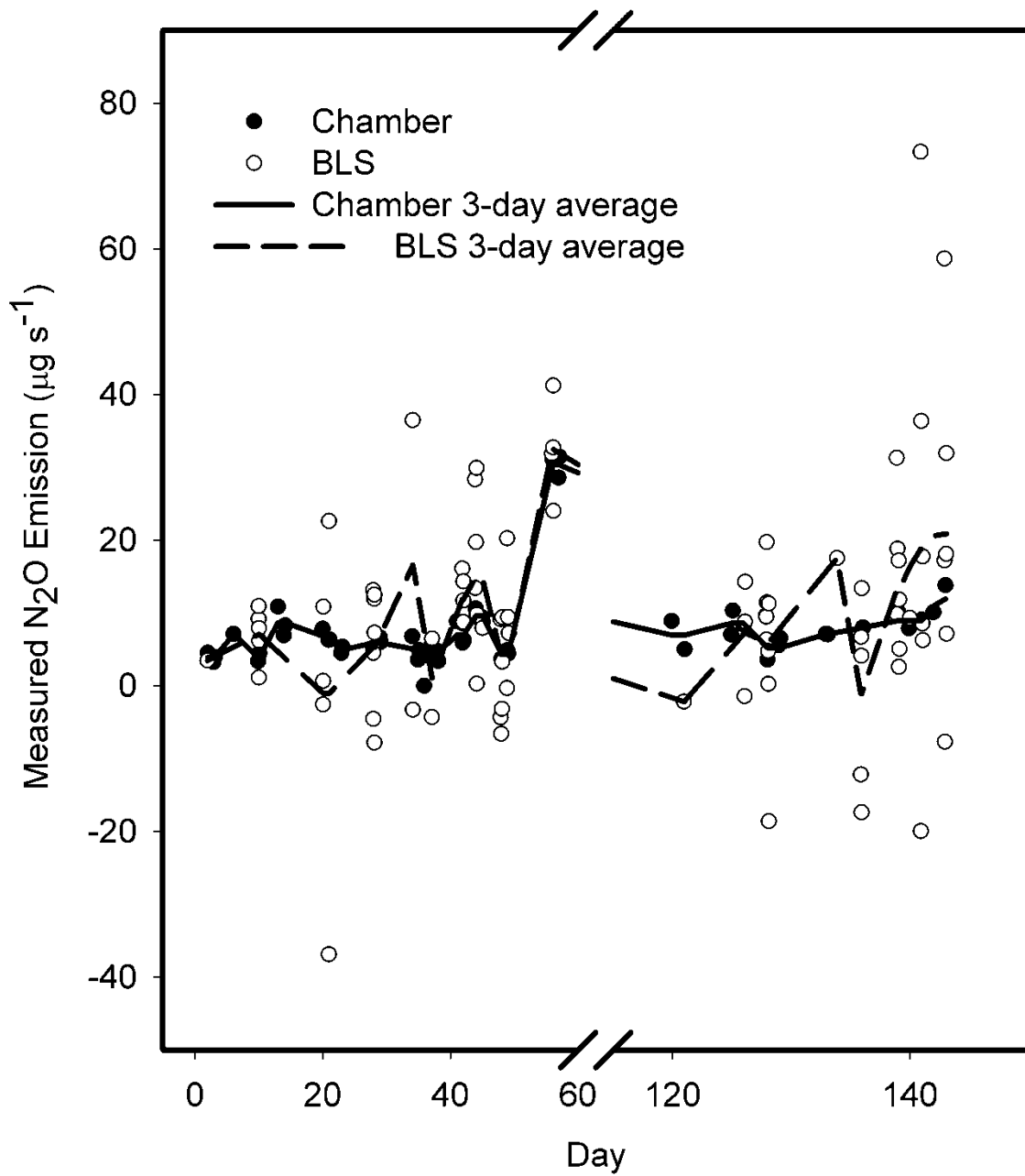


Figure 2.6. Measured N₂O emissions versus time for data collected using the large chamber and the backward Lagrangian stochastic technique (bLS 30-minute flux values; restricted to data meeting acceptance criteria).

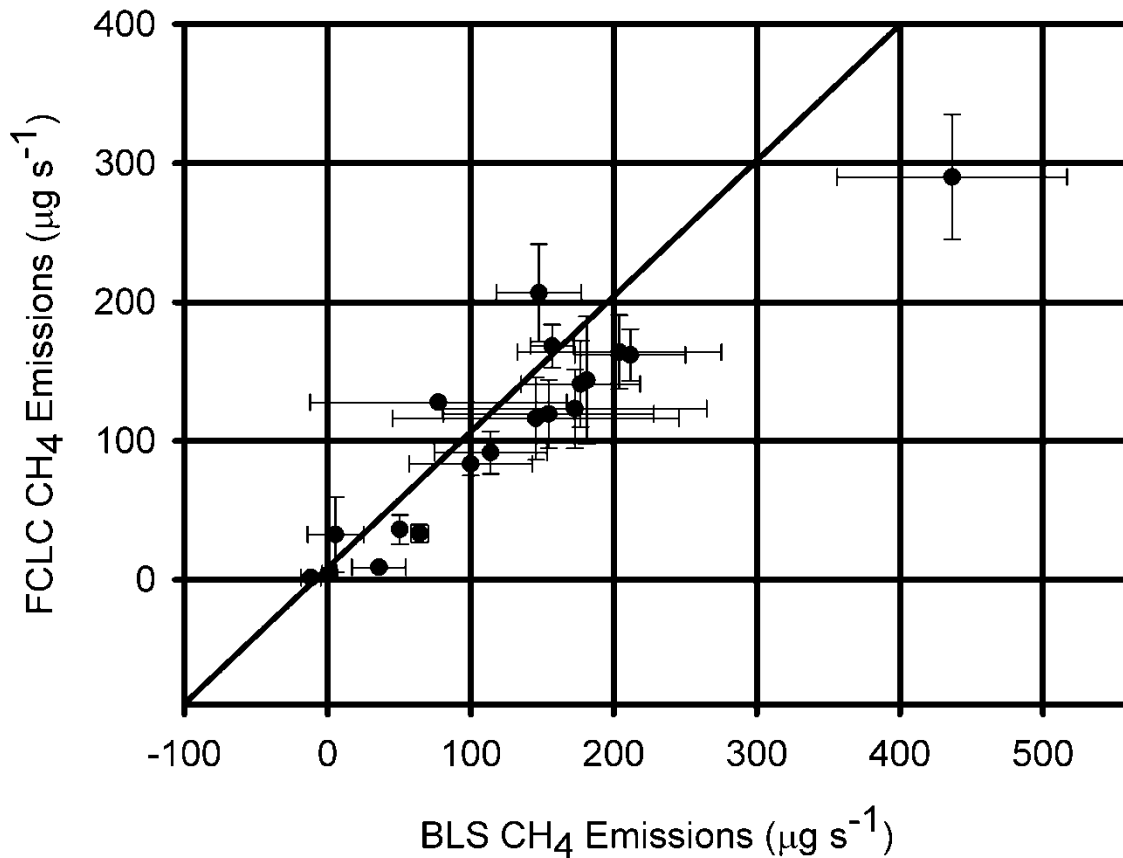


Figure 2.7. Large-chamber CH₄ emission measurements (three-day moving averages) versus backward Lagrangian stochastic measurements (bLS; three-day moving averages). The 1:1 line is plotted for reference and the error bars represent the standard deviations of the three-day averages.

We conclude that both techniques were mutually consistent, while the large-chamber measurements were more precise than the bLS measurements for a single measurement period. The application of the bLS technique was validated via tracer gas releases and recoveries, and the large chamber measurements of the temperature-controlled manure did not differ significantly from those determined via bLS ($P < 0.05$). While data rejection based on published criteria (Flesch et al., 2005, 2007; Loh et al., 2008) is common with bLS, an experienced team will generally collect useful data each time they deploy the large chamber.

The two techniques, however, are not interchangeable. The large chamber is designed to allow measurements from an emitting surface, separating this surface from surrounding or animal emissions. Like any other chamber techniques, flux detection limits can be lower than those achievable with the same instrument via bLS due to the concentration of gas emissions within the chamber volume.

The large-chamber method is more labour intensive than the bLS technique. Each large-chamber measurement requires the frame and cover to be deployed to the measurement site, and during operation requires constant monitoring. Consequently, 24-hour, multi-week monitoring by large chamber is less attractive than by bLS.

However, the large chamber method provides a technique that can be used in parallel with bLS to isolate surface emissions from surrounding emission sources, with the two methods

producing mutually consistent results. For the specific example of feedlot studies where animals cannot be completely removed from the pen, our results suggest that the large chamber can be used to determine the component of bLS-measured total emissions that can be attributed to the pen manure (excluding enteric emissions).

The values reported in this chapter are no substitute for measurement at real feedlot enterprises. The core temperature applied to the manure is within the range of conditions we have measured on the surface of manure in feedlot pens (4 to 65°C), as is the moisture content. However, maintenance of moisture content at field capacity, and maintenance of a steady high temperature without diurnal variation may have favoured emissions (up to 7 $\mu\text{g CH}_4 [\text{kg manure}]^{-1} \text{s}^{-1}$; up to 0.5 $\mu\text{g N}_2\text{O} [\text{kg manure}]^{-1} \text{s}^{-1}$) that are comparable or higher than those described for beef manure emissions in vessels (< 4 $\mu\text{g CH}_4 \text{kg}^{-1} \text{s}^{-1}$; < 0.12 $\mu\text{g N}_2\text{O kg}^{-1} \text{s}^{-1}$) (Pattey et al., 2005). Measurements of emissions from pen manure, for comparable temperatures, are not available in the literature (e.g., < 10°C; Boadi, et al., 2004). A subsequent publication will report the results of the application of the large-chamber method to measurement of emissions from pen manure surfaces at commercial feedlots.

2.5 Conclusion

The large chamber in combination with on-line analysis (1 analysis min^{-1}) produced comparable results to the bLS technique for manure emissions of N_2O and CH_4 (no significant difference, $P < 0.05$), with greater precision of individual measurements (bLS, $99.5 \pm 325 \mu\text{g CH}_4 \text{s}^{-1}$, $9.26 \pm 20.6 \mu\text{g N}_2\text{O s}^{-1}$; large chamber, $99.6 \pm 64.2 \mu\text{g CH}_4 \text{s}^{-1}$, $8.18 \pm 0.3 \mu\text{g N}_2\text{O s}^{-1}$). The technique is suitable for measurement of emissions from manure on pen surfaces, isolating these emissions from surrounding emissions sources. The large area (20.2 m^2) and height (1.5 m) of this chamber provides advantages over smaller, lower chambers, with regard to: a) the greater spatial variability encompassed with a single measurement, b) slower concentration rise in the large chamber volume, and c) a larger ratio of chamber area to circumference. Where air exchange between the chamber and external air was small, a linear equation fit data well. Under conditions of greater exchange (e.g., due to poor sealing of the skirt with the surface), an ordinary differential equation where the slope of concentration rise was dependent on emission, air exchange (chamber air loss and ambient air entry), and standard gas release rate (for air exchange measurement) allowed data to be fitted with high confidence.

3 Pen emission measurements suggest the need for a revision of greenhouse gas inventory calculations (Redding et al., 2015)

M.R. Redding^{*a}, J. Devereux^a, F. Phillips^b, R. Lewis^a, T. Naylor^b, T. Kearton^a, C., J. Hill^a, S. Wiedemann^c

^a Agri-Science Queensland, Department of Agriculture and Fisheries, PO Box 102, Toowoomba, Queensland, Australia; ^b The Centre for Atmospheric Chemistry, School of Chemistry, University of Wollongong, Northfields Ave Wollongong, New South Wales, Australia. ^c FSA Consulting, Clifford St, Toowoomba, Queensland, Australia

3.1 Summary

Few data exist on emissions directly from the pen manure at beef feedlots. Despite this lack, international and Australian inventories attempt to account for these emissions using a range of assumptions.

This study addresses the lack of data using the chamber technique validated in Chapter 1 (Redding et al., 2013) to isolate nitrous oxide (N₂O) and methane (CH₄) emissions from pen manure at two Australian commercial beef feedlots (42 northern and 51 southern feedlot measurements), and relates these emissions to a range of potential emission control factors. By investigating these factors, we sought to not only measure emissions but to understand emission processes sufficiently to provide advice as to how to mitigate emission and the potential effects of future changes to management practices.

These emission control factors included masses and concentrations of volatile solids (VS), nitrate (NO₃⁻), total nitrogen (N), ammonia (NH₄⁺), organic carbon (OC); and also additional factors such as total manure mass, cattle numbers, manure pack depth and density, temperature, and moisture content.

Mean measured pen N₂O emissions were 0.496 µg m⁻² s⁻¹ (upper and lower 95 % confidence interval 0.292 to 0.800 µg m⁻² s⁻¹) and 0.00469 µg m⁻² s⁻¹ (0.00132 to 0.0128 µg m⁻² s⁻¹) for the northern and southern feedlots (range indicates 95 % confidence interval).

Mean measured emission of CH₄ was 0.273 µg m⁻² s⁻¹ (0.189 to 0.385 µg m⁻² s⁻¹) for the northern feedlot and 4.55 µg m⁻² s⁻¹ (2.99 to 6.72 µg m⁻² s⁻¹) for the southern feedlot.

Nitrous oxide emission increased with density, pH, temperature, and manure mass, while negative relationships were evident with moisture and OC. Strong relationships were not evident between N₂O emission and masses or concentrations of either NO₃⁻ or total N. This is significant as many standard inventory calculation protocols predict N₂O emissions using the mass of nitrogen excreted by the animal.

In the course of conducting the pen manure emission measurements, a limited number of measurements were collected from bare soil in a recently cleaned pen. These measurements suggest that emissions from these soils at this location were higher than most emissions from the manures themselves, and under wetter conditions may greatly exceed manure emissions. This is almost certainly related to the very high nitrate concentrations measured in this soil. Further emission measurements from the infrastructure areas and cleaned pens would be required to fully quantify this contribution.

3.2 Introduction

A range of field methane emissions measurements from pens of feedlot cattle have been published (e.g. Harper et al., 1999; Loh et al., 2008a; McGinn et al., 2008; van Haarlem et al., 2008), especially since the development of the backward Lagrangian stochastic measurement technique (bLS; Flesch et al., 1995), and the Windtrax model that aids application of this technique (Crenna et al., 2008). These measurements have assisted the development of appropriate policy globally and allowed for the fine tuning of various greenhouse gas inventory calculation protocols (e.g. Intergovernmental Panel on Climate Change, 2006; Environment, 2014).

However, micrometeorological measurement from occupied pens measures aggregate methane emission from both enteric sources and the manure on the pen surface. The separated magnitudes of these two types of emission sources cannot normally be reported.

Measurement of N₂O emissions originating from the manure and pen surface are also largely lacking from the literature (Pratt et al., 2014), except for low temperature conditions (< 10°C, Boadi et al., 2004) or other production systems (Leytem et al., 2011). The IPCC (2006) provides a feedlot pen (classified as 'dry lot') emission factor for nitrous oxide based on expert judgement and Külling et al. (2003), which is the global benchmark for developing greenhouse gas inventories. Külling et al. (2003) investigated short-term emissions from farm yard manure from dairy cows (90% faeces, 10% urine and straw) in laboratory conditions in an attempt to simulate typical European housing conditions. The relevance of this study to dry packed manure pens elsewhere in the world (including Australia) is limited by differences in temperature and moisture, the ratio of urine and faeces, the addition of straw to the material and the duration of the trial. Moreover, the Külling et al. (2003) study sought to measure total N and trace gas losses from dairy cattle under different diets, and did not seek to establish a causal relationship between nitrogen mass and emissions – though the IPCC (2006) calculation protocol takes this approach. Similarly, a laboratory study was completed using mixtures of feedlot pen manure and soil measuring CH₄ and N₂O, seeking to replicate the manure soil mixtures observed under pen surface conditions in a restricted temperature range (18-22°C) (Miller and Berry, 2005).

Chamber techniques, both dynamic and static, have often been applied to measure emissions from soils (reviewed by Rochette and Eriksen-Hamel, 2008). They have also allowed studies investigating greenhouse gas emissions from manure surfaces (e.g. Texas Panhandle, flow-through flux chamber, Borhan et al., 2011; or using a flow-through steady-state chamber or wind tunnel, North Dakota, Rahman et al., 2013).

The use of chambers to provide emission values for emitting surfaces has raised questions. A wide-ranging review of soil N₂O emission measurements with chambers suggested a range of measures are required to minimise errors (Rochette and Eriksen-Hamel, 2008). In essence, there is a need to minimise the influence of the chamber on the factors that control emission. For example, the influence of the chamber on the temperature of the emission surface, the air pressure acting on it, and the concentration of emissions in the volume of air in the chamber. Similar concerns apply to some chamber greenhouse gas emission measurements from manure surfaces. This risk was acknowledged in one study of the quantification of pollutant emissions at concentrated animal feeding operations (Borhan et al., 2011). Another study suggested that the wind tunnels they use can duplicate the wind speeds of the surrounding ambient conditions (Rahman et al., 2013), but did not address the other recognised problems with chamber measurements. While these studies undoubtedly contributed valuable information in an area where little is available, neither fully addressed the issue of the absolute accuracy of the emission measurements obtained.

However, some progress has been made in finding solutions to the problems identified for chamber measurements (e.g. mitigating approaches proposed by Rochette and Eriksen-Hamel, 2008). A recent validation study has demonstrated that a large (20 m²) vented non-flow-through non-steady-state chamber can produce results that are consistent with bLS-measured emissions from the same source (Redding et al., 2013). The validation of this technique versus bLS measurements allows measurement of manure-sourced emissions from the feedpad, with established consistency with the body of published bLS data.

Emissions fluxes from beef feedlot pen manure are not well established in the literature, nor are the processes well understood. Given the lack of available data and the background of previous studies we sought to investigate two hypotheses: 1) that the IPCC emission calculation techniques (IPCC, 2006) for manure management in these systems are representative of actual emissions; and 2) that the factors controlling emission are consistent with IPCC calculation approaches. Our N₂O emission measurements did not closely align with calculated emissions nor did the process relationships observed in this study support the predictive rationale applied (IPCC, 2006). It does appear that some readily measured manure parameters may explain a large proportion of the variability in field manure emissions.

3.3 Materials and methods

3.3.1 Site selection

Measurements were conducted at two Australian feedlots. The northern feedlot was located on the Darling Downs in Queensland, a location with an average summer-dominated rainfall of 634 mm, and an annual average temperature of 25°C. All 44 measurements were collected from four locations within a single pen. These locations (Fig. 3.1) were selected to be representative of the range of manure depths, moistures, and feed wastage content (related to proximity to the feed bunkers). One of the sites received partial or full shade from approximately 10:00 to 14:00 each day.

The southern feedlot was located in the central northern part of the Riverina region of New South Wales. Average annual rainfall for the area is 530 mm with more rain falling in the spring-summer months than in autumn-winter months. Average annual temperature is 22°C. Again, all 54 measurements were conducted within the same pen, from one of three zones (Fig. 3.2): zone 1, the third of the feed pad close to the feed bunker, zone 2 the shaded mid area of the pen, and zone 3 the remaining pen area furthest from the feed bunker.

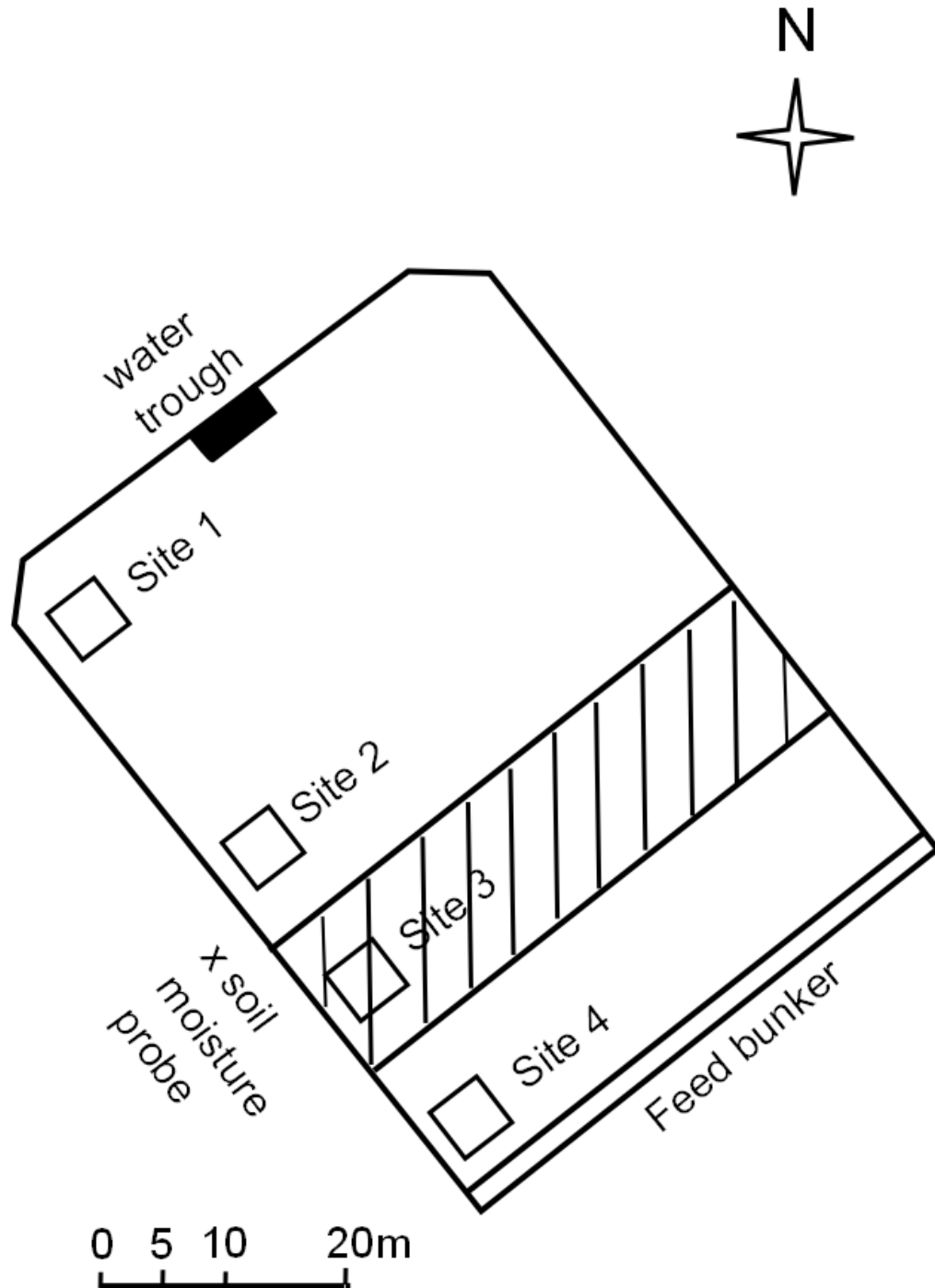


Figure 3.1. Northern feedlot pen and emission measurement site layout, showing standardised locations of field measurements. Site selection was constrained by animal management considerations, and was therefore restricted to one side of the pen.

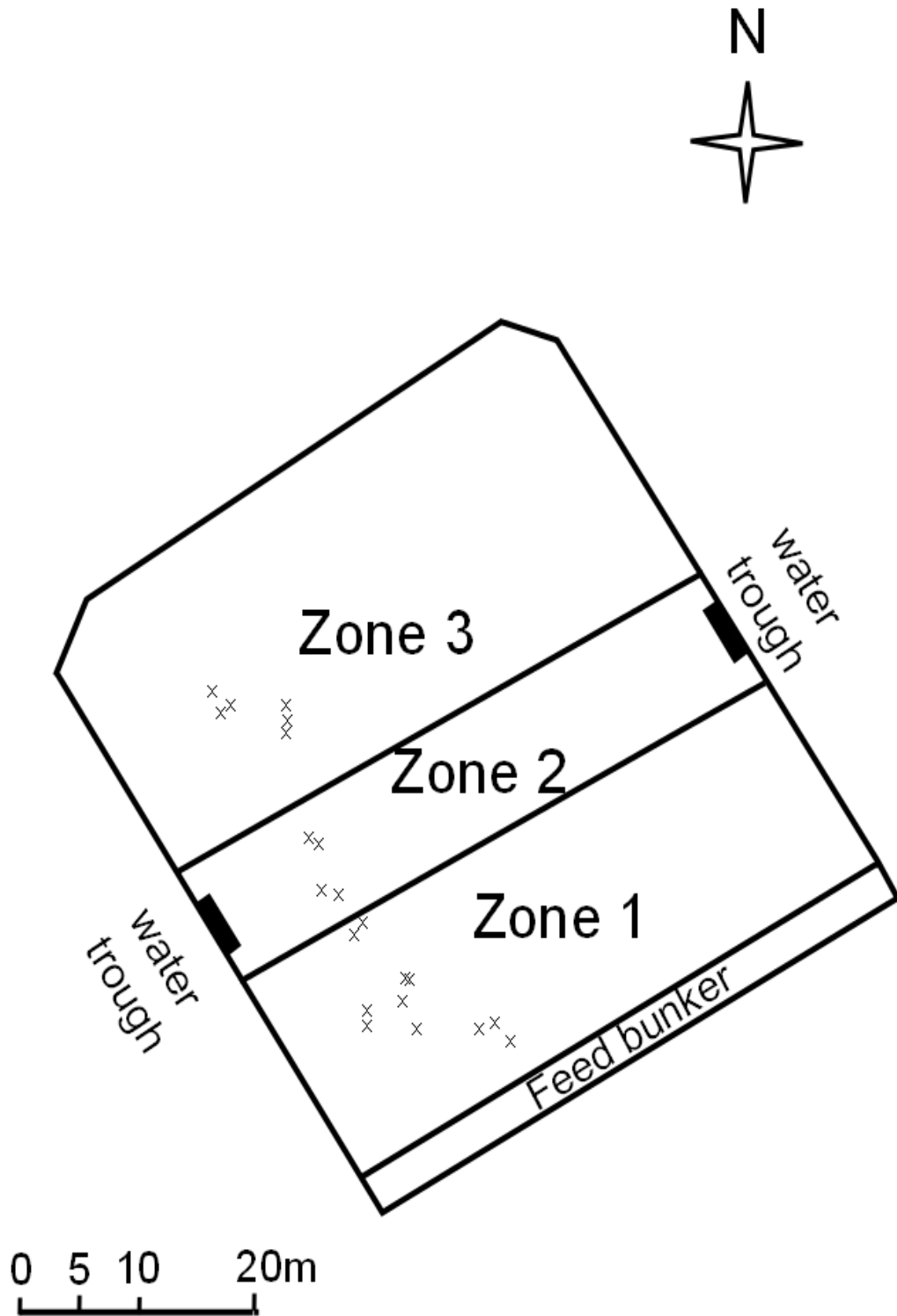


Figure 3.2. Southern feedlot pen and emission measurement site layout. Sample points, marked by “x”, are selected to be representative of the area close to the feed bunker (zone 1), the shaded area (zone 2), or the remaining area (zone 3). Site selection was constrained by animal management considerations, and was therefore restricted to one side of the pen.

3.3.2 Site instrumentation

The northern feedlot was instrumented throughout the 18-month chamber measurement collection period, and 4 months subsequently. While it was desirable to have 22 months of direct, continuous measurements of pen manure characteristics, it was found that any instrumentation installed on the pen surface (or even buried under it) attracted the attention of cattle and was soon destroyed. A suite of instrumentation was established that did not require any presence on the feedpad. Logged data (22 months) included rainfall collected adjacent to the pen (Hydrological Services model TB3/0.2 rain gauge connected to a Data Flow Systems Pty Ltd, Odyssey Rain Gauge Logger), manure surface temperature via infrared probe directed at the pen surface from outside the pen fence (Calex PC151LT-0 logged via a datataker DT 500 data logger), and soil moisture adjacent to the pen (location Fig. 3.1; via three Delta-t ThetaProbe, installed horizontally at a depth of 50 mm in re-packed vertosol soil; these probes function over a restricted salinity range, 50 to 500 mS m⁻¹, that also precludes use in manures).

Soil moisture probes were calibrated with cores collected through the manure profile within the pen (four to six replicates at each measurement site; Fig. 3.1). These cores were collected on 16 occasions and individually analysed (292 cores) to allow comparison of the adjacent soil and pen manure moisture contents, providing a regression relationship based on:

$$M_m = m M_s + c \quad [1]$$

where M_m is the manure moisture (g g⁻¹) and M_s is the soil moisture (g g⁻¹), and m and c are linear regression parameters.

During chamber deployments additional instrumentation was employed. The pen surface temperature was monitored via 6 sensors inserted at 5 mm depth (Microchip MCP9701A temperature sensors; three inside and three outside the chamber), air temperature via a shielded temperature sensor (Vaisala HMP45c), and atmospheric pressure via a barometer (Vaisala CS106; all logged by Campbell CR3000 data logger).

Instrumentation at the southern feedlot was restricted to the period during chamber measurements. A similar array of instruments as described for the period during chamber measurements for the northern feedlot was applied (6 temperature sensors inserted at 5 mm depth, air temperature via a shielded temperature sensor, rainfall measurement, and atmospheric pressure).

3.3.3 Selection of emission sampling times

For the northern feedlot sampling dates and times were selected to be as representative as possible of the full range of moisture contents, temperatures, and manure depths observed at the feedlot throughout the period from June 2011 to December 2012. A total of 44 measurements were conducted on this basis, 11 from each site.

Due to the remote location of the southern feedlot relative to the research team's headquarters, measurements were conducted from 15th to 24th February 2011 and 15th June to 1st of August 2011 to encompass a range of temperature and manure moisture conditions.

3.3.4 Application of the large-chamber technique

A full description and validation of the large-chamber technique has been published elsewhere (Redding et al., 2013). In brief, the chamber, consisting of an impermeable fabric-covered frame (4.5 x 4.5 m; height adjustable to 0.5 m or 1.5 m), was established over each measurement site. The skirt of the cover was weighed down across the emitting surface to a

width of 300 mm to form a seal. The fabric cover provides a sleeve into which a vent tube was installed in the fabric cover to allow the chamber volume to equalize with ambient pressure. Improved headspace mixing was achieved via four fans located irregularly within the chamber volume (75 mm diameter, 12 V, 0.2 A, brushless direct current motors; run at 6 V).

After establishing the chamber at a measurement site, it was then insulated with foil-backed foam-rubber. Internal air temperature was monitored via three sensors (Microchip MCP9701A).

Air from within the chamber was sampled continuously (1.2 L min^{-1} ; all gas volumes standardised to 101.33 kPa and 298.15°K; mass flow controller Alicat Scientific, USA, model MC) and analysed by closed path Fourier Transform Infra Red Spectrometry (FTIR; prototype instrument constructed by the University of Wollongong and subsequently marketed as a Spectronus Trace Gas and Isotope Analyser, <http://www.ecotech.com.au/>; Griffith et al., 2012; Hammer et al., 2012) for CO_2 , CH_4 , and N_2O at 1-min intervals. The analysed air was returned to the chamber. In order to assist determination of the exchange of air between the enclosed volume and external air, tracer gas releases were conducted for each chamber deployment (Redding et al., 2013). This tracer release was completed via a controlled gas input (tracer gas 100 ± 4 ppm N_2O by volume in an air balance) for 10 min following completion of each chamber measurement period. The exact rate of N_2O release was selected to greatly exceed native emission and allow precise calculations (as described fully in Redding et al., 2013; the range of values selected, 3.00 to $12.0 \mu\text{g N}_2\text{O s}^{-1}$).

The N_2O emission data were fitted with the following equation using an algorithm (R Development Core Team, 2014) that simultaneously fitted both for the initial 10 data points (one line segment where the emission is responsible for the slope), and the tracer gas release data (a second line segment where the emission + known tracer gas release combined to produce the slope of the concentration rise):

$$C = \frac{AF}{V_{exch}} (1 - e^{-\frac{V_{exch}t}{V}}) + (C_{min} - C_b) e^{-\frac{V_{exch}t}{V}} + C_b \quad [2]$$

where C is the concentration (defined as mass of analyte gas [total volume] $^{-1}$), A is the area of surface enclosed, F is the flux (mass of analyte gas area $^{-1}$ time $^{-1}$), V is the volume of the chamber, C_b is the background air concentration (volume analyte gas volume $^{-1}$), t is time (minutes), V_{exch} is the rate of exchange of air from inside with air from outside (volume time $^{-1}$), and C_{min} is the commencing concentration at $t=0$, allowing it to differ from mean background concentration during the measurement period (C_b).

Subsequently, the value of V_{exch} determined for the N_2O tracer release was used in the CH_4 analysis for the native emission period (Eq [2]).

Immediately after each chamber measurement was conducted at the northern feedlot, 20 cores, 75 mm diameter, were collected: five from each side, just outside the perimeter of the square chamber site. Sampling within the chamber site was avoided, to minimise site disturbance. The core sampler was driven into the pen surface with a slide-hammer until the upper surface of the underlying sediment had been penetrated. Depth from the manure surface to the sediment surface was recorded at four points on the circumference of each core hole (4 x 20 depth measurements). The following physical and chemical analyses were also applied: manure moisture contents were determined by oven drying at 65°C, and reported as dry basis % (method 2540 G; Greenberg et al., 1992); NH_4^+ nitrogen and $\text{NO}_3^- + \text{NO}_2^-$ nitrogen were extracted with 2 M KCl and analysed via steam distillation (method 7C1; Rayment and Lyons, 2010); total N content of the manures was estimated via Kjeldahl digestion (method 7A2a; Rayment and Lyons, 2010); organic carbon was determined via

dichromate oxidation (Walkley and Black, 1934); electrical conductivity (EC) was determined in a 1:5 dry manure to deionised water ratio, as was pH (methods 3A1 and 4A1; Rayment and Lyons, 2010). Manure density was calculated from the mass of dry manure extracted from the core sampler volume. The number of cattle in the pen at the time of measurement was obtained from pen records.

A decreased set of chamber-associated data was collected for the southern feedlot, incorporating manure depth, moisture content, and temperature of the manure during chamber measurements.

3.3.5 Statistics

Concentration models for the large-chamber data were fitted by non-linear regression using R (nlm procedure in R, R Development Core Team, 2014). Summary statistics, analysis of variance, confidence intervals, and t-tests were also conducted using R. Probability distributions were fitted to data using the `fitdist` function of R's `fitdistrplus` package, and the Kolmogorov-Smirnov Test was applied to determine if sample distributions differed significantly. Boxplots were plotted with “notches” designed to represent an approximate confidence interval of the median value of the distribution (Chambers et al., 1983) using R.

3.4 Materials and methods

3.4.1 Field measurement of pen manure emissions

Pen manure CH₄ emissions were 0.273 µg m⁻² s⁻¹ (95% confidence interval, CI : 0.189 to 0.385 µg m⁻² s⁻¹) and 4.55 µg m⁻² s⁻¹ (CI: 2.99 to 6.72 µg m⁻² s⁻¹) for the northern and southern feedlots, based on data transformed to a normal distribution (Fig. 3.3). Emissions of N₂O were much greater at the northern feedlot (0.496 µg N₂O m⁻² s⁻¹; CI: 0.292 to 0.800 µg m⁻² s⁻¹) than at the southern feedlot (0.00469 µg N₂O m⁻² s⁻¹; CI: 0.00132 to 0.0128 µg N₂O m⁻² s⁻¹; Fig. 3.4).

Every one of the northern feedlot measurements was associated with a tracer gas release to calculate chamber characteristics (Redding et al., 2013), and the release of known quantities of N₂O as a tracer also served to ensure data processing accuracy. One in four of the southern feedlot measurements also included a tracer gas release assessment.

These direct mean values are representative of the systems involved, only to the extent to which the selected sample times are representative of the conditions encountered at the sites year round. The large-chamber method is well suited to instantaneous measurements and the separation of manure emissions from those eventuating from surrounding sources (e.g. the ponds or enteric CH₄ from the cattle; Redding et al., 2013).

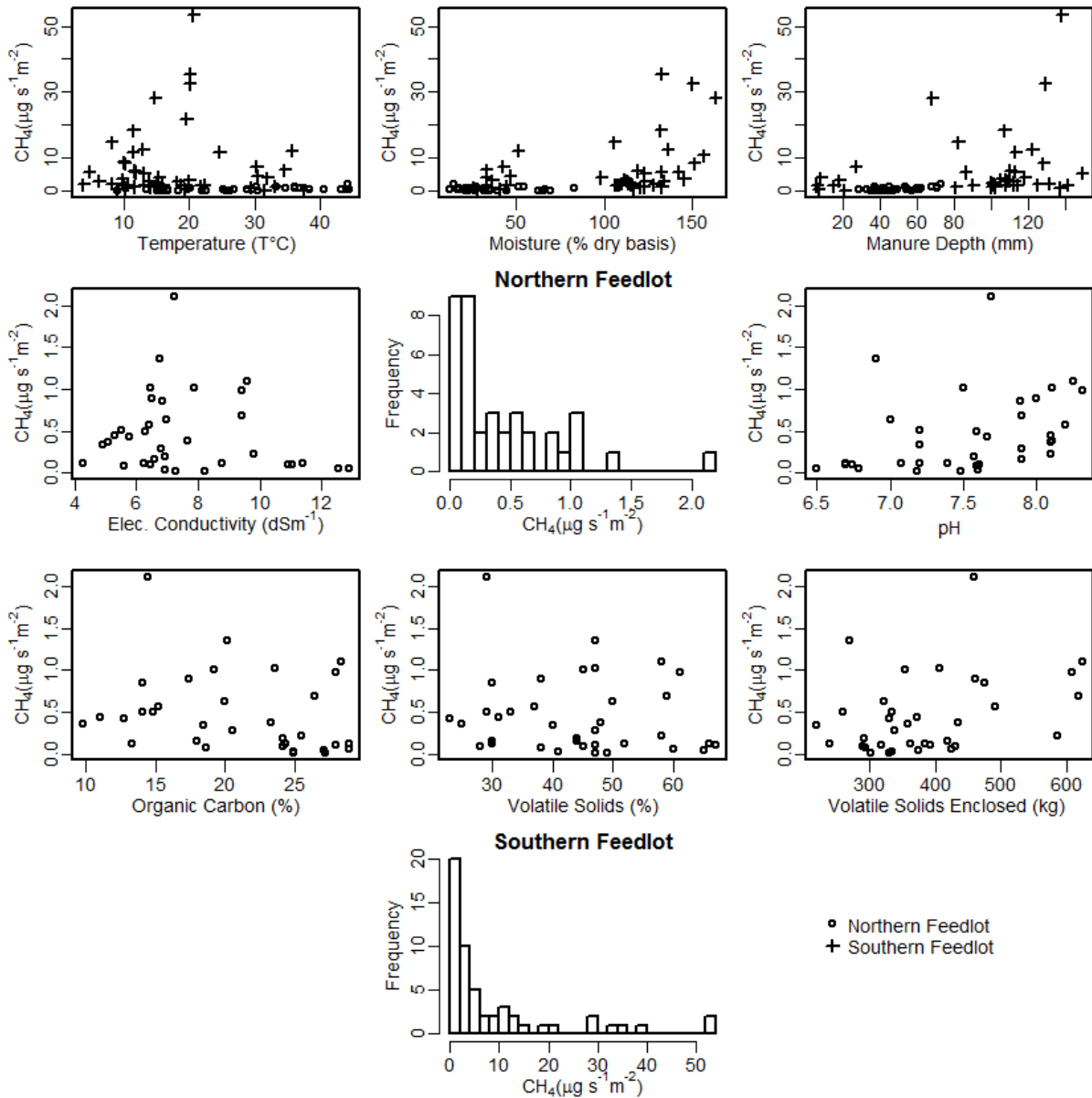


Figure 3.3. Methane emissions from pen manure *in situ* at the two feedlots, plotted versus several key process parameters. Similar to the nitrous oxide data, clear relationships were observed for some, while others revealed little.

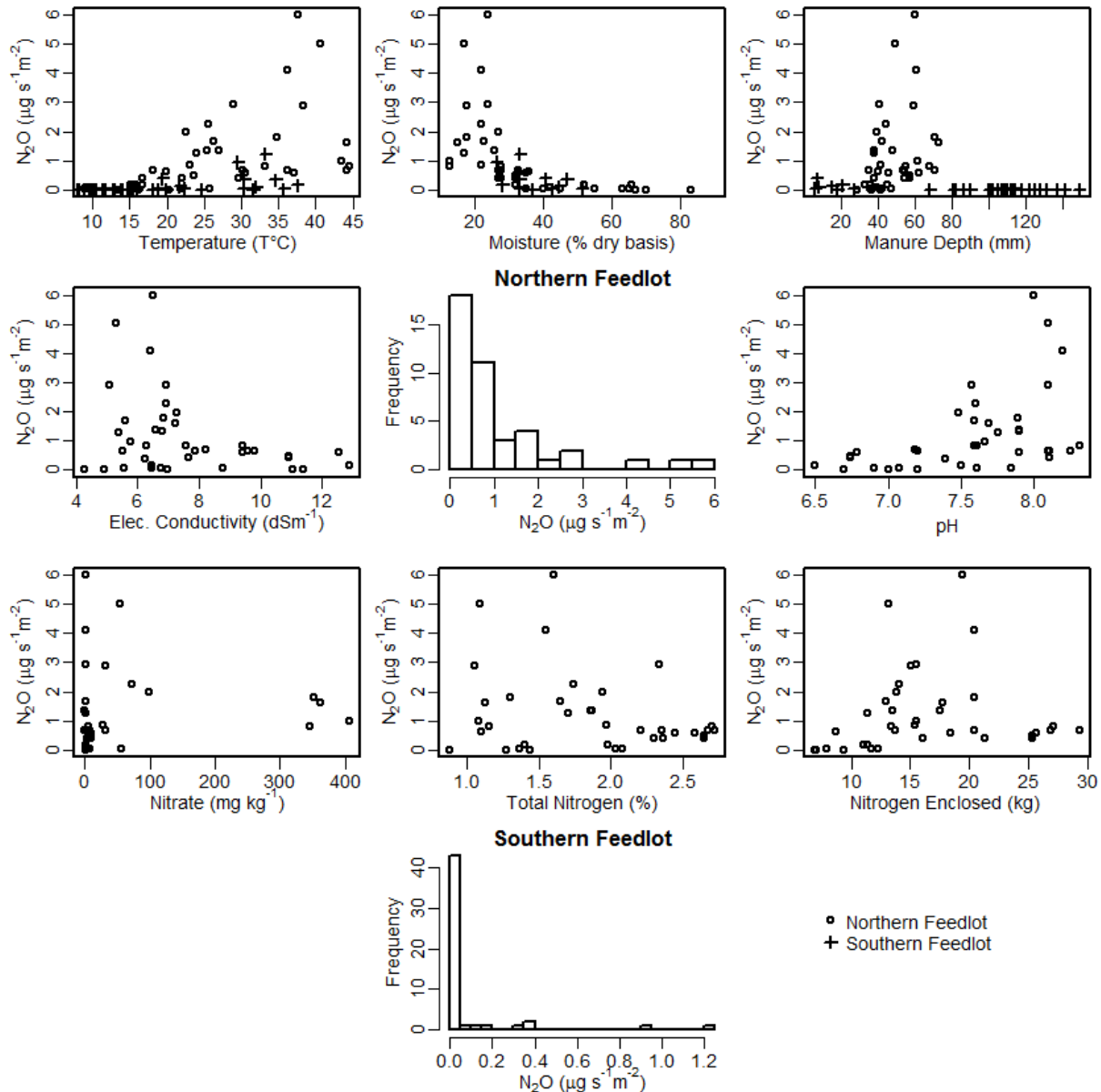


Figure 3.4. Nitrous oxide emissions from pen manure in situ at the two feedlots, plotted versus several key process parameters. Clear relationships were observed for some, while others revealed little.

3.4.2 Parameter relationships

The strong differences between the emissions from the two feedlots probably reflect the striking differences in temperature and the manure moisture conditions encountered (Figs. 3.3 and 3.4). Relatively strong correlations were evident for N₂O emissions and these two parameters (correlation coefficient > 0.5 for temperature and negative < -0.5 for moisture, Figs. 3.5 and 3.6). Emission of CH₄ was moderately related to temperature at the northern feedlot (correlation coefficient 0.37) and to manure moisture at the southern feedlot (correlation coefficient 0.37). While northern feedlot measurements were conducted year-round, southern feedlot measurements were conducted in two concentrated campaigns – one of which was conducted during a period of substantial rainfall (about 55 mm), and both at relatively low temperatures compared to the northern feedlot.

It is possible that the pen cleaning frequency at the northern feedlot (3 to 4 months) and the southern feedlot (about 2 months) may also have caused some emission differences between feedlots, and could be reflected in VS data. A comprehensive data set of VS data was collected for the northern feedlot, but no matching set collected for the southern feedlot. However, for the northern feedlot these relationships were weak: the correlation between VS and N₂O emission was weakly negative (correlation coefficient, -0.14; Fig. 3.5), and between VS and CH₄ emission was not notable (correlation coefficient, -0.06; Fig. 3.5).

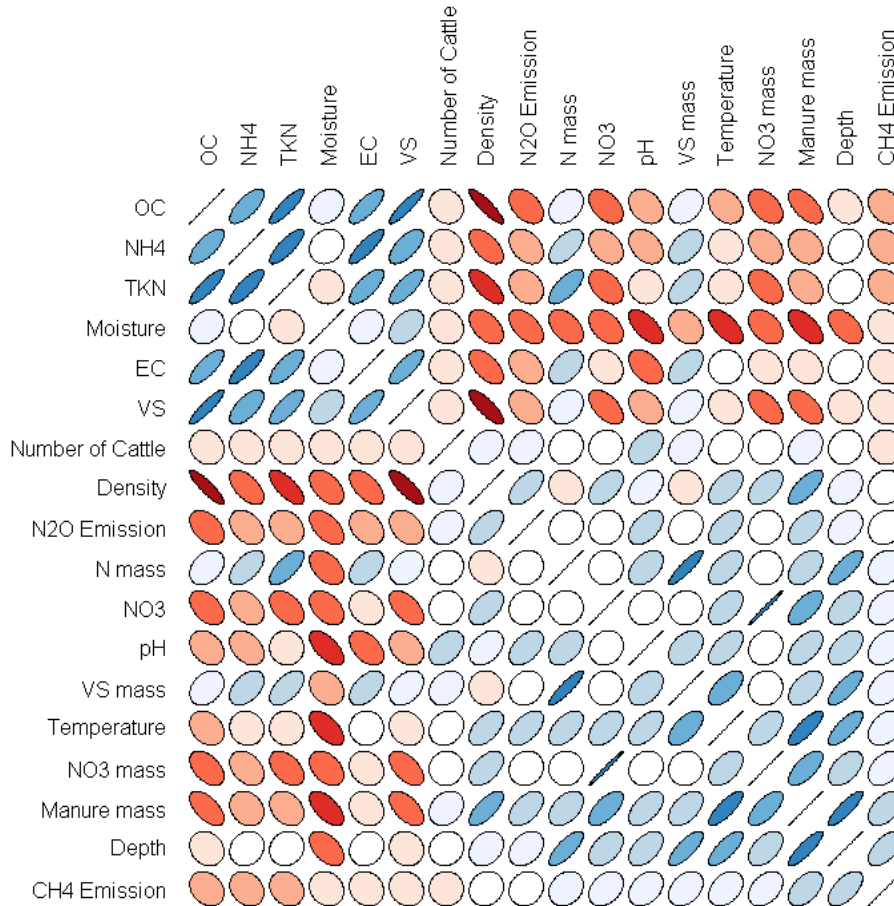


Figure 3.5. Correlation between measured northern feedlot variables. The more linear an ellipse appears, the greater the correlation, with slope representing the sign of the correlation. For reference, the relationship between N₂O emission and moisture is a correlation of -0.35 , while that between VS and OC has a correlation coefficient of 0.91.

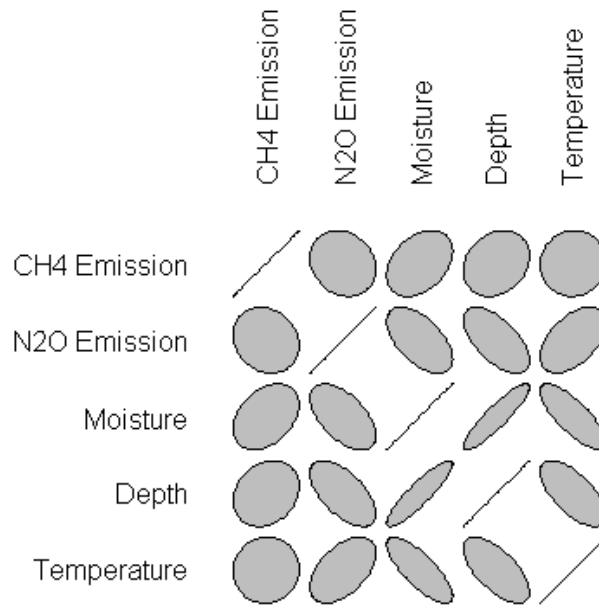


Figure 3.6. Correlation between measured southern feedlot variables. The more linear an ellipse appears, the greater the correlation, with slope representing the sign of the correlation.

Several of the stronger correlation relationships between emissions and pen characteristics at the northern feedlot have previously been observed in soil systems (Fig. 3.5). For example, N₂O emission relationships with moisture and temperature are key parameters of the Water and Nitrogen Management Model (WNMM) model (Xu et al., 1998; Li et al., 2007).

In other cases, published relationships were not evident, or were reversed. For example, a positive relationship of N₂O emission with EC has previously been described (via osmotic potential; Low et al., 1997), while total denitrification (N₂O + N₂ emission) in soil has been found to maximise at near neutral pH, with an increased ratio of N₂O:N₂ emission in more acid conditions (Simek and Cooper, 2002; Simek et al., 2002). We found a negative relationship between N₂O emission and EC (correlation coefficient -0.32), and rising N₂O emission with pH to slightly alkaline conditions (correlation coefficient 0.49; Figs. 3.4 and 3.5).

However, attributing causality to these correlation relationships may lead to errors, as many of these parameters are strongly related to each other. For example, pH was strongly related to moisture content in our study (Fig. 3.5). A long history of observations has suggested a strong relationship between water logging and soil pH (e.g. Metwally, 1978; Ohlsson, 1979). While pH is known to influence N₂O emission in many studies (though in a contrary direction to the relationship observed here; Simek and Cooper, 2002), the strong influence of moisture content (Figs. 3.6 and 3.7; Xu et al., 1998, Dalal et al., 2003), and permeability-limited oxygen supply on N₂O emission is undeniable (Groffman and Tiedje, 1991; de Klein and Van Logtestijn, 1996; Dobbie and Smith, 2001a). In the case of the two feedlots studied here, higher moisture contents are associated with decreased emissions, despite the associated decrease in pH, possibly as a result of decreased oxygen diffusion and supply. Other relationships in the northern feedlot data are probably also related to oxygen availability. There is a negative relationship between N₂O emission and organic carbon content (OC; correlation coefficient, -0.43) and similarly with VS (correlation coefficient, -0.35), which may be related to oxygen consumption during decay processes decreasing opportunities of nitrogen oxidation (Fig 5). Organic carbon is a required microbial substrate for nitrous oxide emissions (Swerts et al., 1996; Gillam et al., 2008); however, it did not appear to control N₂O emission at this feedlot. Presumably this was because the substrate was always in

abundance. Bulk density was also confounded by correlations. Bulk density is strongly related to N_2O emission, but also with moisture content. We observed that manure tends to expand as the water content increases.

Our observations suggest that some of the limiting relationships observed in soils do not limit N_2O emission from the pen manure. For example, it is widely recognised that a supply of mineral N is required for nitrous oxide emission to occur and greater nitrate availability can be related to greater N_2O emission as a proportion of total denitrification (Swerts et al., 1996; Ball et al., 1997; Dalal et al., 2003). Additionally, greenhouse gas inventory calculations often use total masses of N multiplied by an emission factor to estimate manure emissions (e.g. IPCC, 2006; National Greenhouse Gas Inventory Committee, 2007). It is evident that emission from the pen surface of the northern feedlot was not related to the total N contained in the manure, or the mass of total N on the pen surface, and was not strongly correlated with nitrate concentration or mass (Figs. 3.4 and 3.5). Attempting to separate other stronger relationships did not strengthen relationships with N forms. For example the residuals of an exponential curve fitted to the N_2O emission versus moisture content relationship were also uncorrelated with N-form concentrations or total N-form masses (correlation not significant; $P > 0.18$).

Presumably limitations related to other factors are reached before N content limitations. This is an important observation, due to the N-mass approach of many standard emission estimation protocols (e.g. IPCC, 2006; Department of the Environment, 2014). We speculate that the lack of a relationship with total N could be influenced by poor oxygen permeability of the heavily compacted pen manure – where oxygen availability limits N_2O emission rather than N supply. This is a target for further research.

Strong correlation relationships between CH_4 emission rate and parameters other than those discussed above for the two feedlots were largely lacking. One exception is a moderately strong relationship between northern feedlot methane emission and manure depth (correlation coefficient, 0.60; Figs. 3.5 and 3.6). This may reflect an effect of depth on the development of completely anaerobic conditions, or the effect of the manure mass enclosed by the chamber on total CH_4 emissions.

3.4.3 Estimating annual emissions

Given the pen area and occupancy (northern feedlot, 3000 m², 134 head; southern feedlot, 3016 m², 206 head; time-averaged basis), the emission measurements amount to about 0.35 and 0.002 kg N_2O head⁻¹ year⁻¹ (northern and southern feedlots). Standard inventory calculations produce much larger estimates of emission: 2.6 (stockpile plus pen manure emissions; Environment, 2013) and 3.0 kg N_2O head⁻¹ year⁻¹ (IPCC, 2006). However, the measured emissions are larger than the lower temperature emissions observed by Boadi et al. (2004; about 0.06 N_2O head⁻¹ year⁻¹, determined at < 0.4 °C). Observed emissions from dairy “open lots” of about 3.7 kg N_2O head⁻¹ year⁻¹, were also collected under a different production system and in a different region (Idaho, USA; Leytem et al., 2011) to those we investigated. Direct comparison of our field measurements to the laboratory study of Miller and Berry (2005) is not possible due to the likely mixing ratio of manure and soil at the southern and northern feedlots (pen manures were approximately 40% soil based on VS) and the presented detection limits of Miller and Berry (2005) at similar mixing ratios.

When averaged, the CH_4 emission data equates to about 0.273 and 2.11 kg CH_4 head⁻¹ year⁻¹ (northern and southern feedlots).

Using Australian GHG Inventory values gives an emission rate of 1.24 kg CH_4 head⁻¹ year⁻¹ and 4.14 kg CH_4 head⁻¹ year⁻¹ for the southern and northern feedlots (the southern feedlot's climate is classified as ‘temperate’ whereas the northern feedlot's climate is ‘warm’; Environment, 2014). The use of ‘warm’ factors produces an estimate that substantially

exceeds our measurements. By comparison, using the most recent Intergovernmental Panel on Climate Change parameters (where both feedlots' climate would be regarded as 'temperate') gives a CH₄ emission rate of 1.9 kg head⁻¹ year⁻¹ (IPCC, 2006).

Few field data are available for comparison. Boadi et al. (2004) observed much greater emissions (about 23 kg CH₄ head⁻¹ year⁻¹) under low-temperature conditions (< 0.4 °C) in Canada, based on three measurement periods and six small chambers (0.1 m radius). The mean of collected emission values are as representative of annual emissions as the conditions at the time of sampling are representative of yearly conditions. This can be assessed by comparison of the temperature and manure moisture during chamber deployments with those logged throughout the year.

In terms of moisture, this assessment is reliant on the reliability of soil moisture probe data as an indicator of manure moisture. This was the case. A strong relationship between site manure moisture and the soil moisture probe data was evident (overall R² = 72 %, *P* < 0.0001). This relationship is comparable to that developed between the moisture contents of two sets of manure cores (sites 1 and 3, Fig. 3.1; R² = 76 %, *P* < 0.0001).

These northern feedlot data revealed a distribution of moisture contents that overlapped strongly with the data collected from the moisture probes (Fig. 3.7). However, it appears the probability distributions of the data may differ (Kolmogorov-Smirnov Test, *P* < 0.05; gamma distributions fitted; mean, moisture probe data, 41.0 % moisture; mean, cores during emission measurements, 0.34 % moisture; Fig. 3.7). For the temperature data the distribution of pen temperatures during chamber measurements differed somewhat from the probe data (Kolmogorov-Smirnov Test, *P* < 0.05; mean, IR probe data, 21.0 °C; mean, chamber measurement temperatures, 24.5 °C; Fig. 3.8), though they largely overlapped.

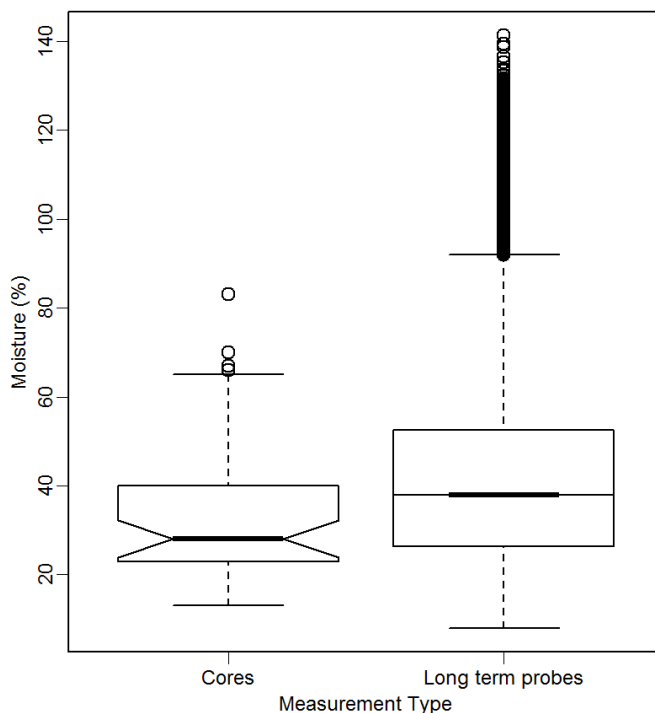


Figure 3.7. Manure moisture contents collected during emission measurement (cores) and those collected over 22 months using soil moisture probes. A notch in the side of the core box and whisker plot centres on the median value; however, the corresponding notch about the median of the probe data is too small to be seen. The differences in the ranges of the notches about the median values (very small on the probe data) suggest that median values probably differ (Leytem et al., 2011).

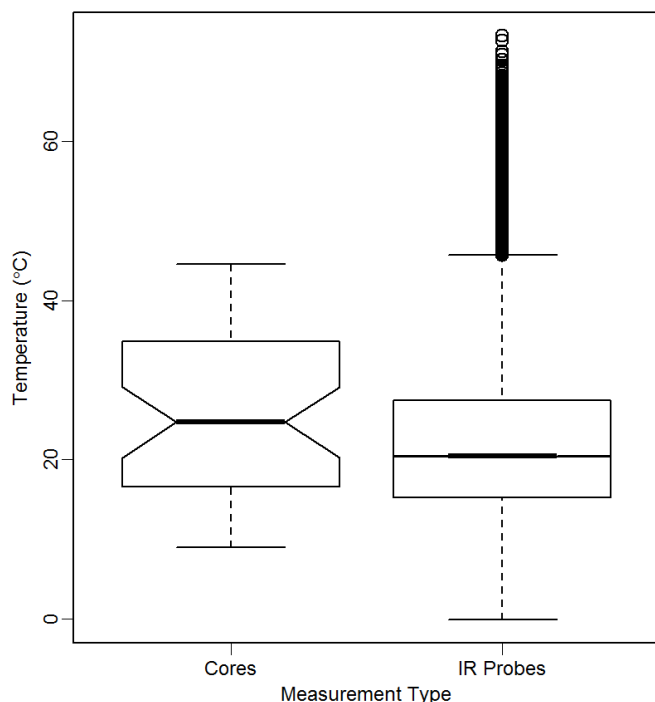


Figure 3.8. Manure temperatures collected during emission measurement (cores) and those collected over 22 months using soil moisture probes. A notch in the side of the core box and whisker plot centres on the median value; however, the corresponding notch about the median of the probe data is too small to be seen. Notches on the box plots indicate the likely range of median values (very small on the probe data).

Comparable data for the southern feedlot were not collected. Measurements were conducted in two concentrated periods (February and July 2011), and it is possible that the full range of conditions may not have been represented. However, mean annual temperatures for the area range from 15 to 18 °C (Bureau of Meteorology, 2014), close to the measurement average air temperature of 18°C. For the air temperature data from the area, the distribution of air temperatures during chamber measurements differed somewhat from the annual data (Kolmogorov-Smirnov Test, $P < 0.05$).

Calibrated, process-based models have the potential to allow further generalisation from the findings of this study. This type of modelling is the subject of further investigation.

3.4.4 Emissions from bare pen soils

In the course of conducting the pen manure emission measurements, a limited number of measurements were collected from bare soil in a recently cleaned pen. These measurements suggest that N_2O emissions from these soils at this location ($1.34 \pm 0.53 \mu\text{g N}_2\text{O s}^{-1} \text{m}^{-2}$) were higher than most emissions from the manures themselves ($1.01 \pm 1.43 \mu\text{g N}_2\text{O s}^{-1} \text{m}^{-2}$), despite the moisture content at the site being much lower ($15 \pm 3\%$ dry basis gravimetric) than the optimum for emissions (around 85 %, Chapter 5). This is almost certainly related to the very high nitrate concentrations measured in this soil ($378 \pm 27 \text{ mg NO}_3^- \text{-N kg}$). At higher moisture contents (in the range 82 to 95% for this soil; Chapter 5) emission fluxes from this soil likely exceed all the emission fluxes measured from the pen manure.

Additional measurements of emissions from the soil and infrastructure areas of the feedlot are required to allow the contribution of these sources to be adequately quantified.

3.5 Conclusion

Though IPCC inventory calculation protocols rely on relationships based on masses of N in the manure, strong relationships between masses and concentrations of either NO_3^- or total N with N_2O emission were not evident.

Mean measured pen N_2O emissions were revealed to be $0.496 \mu\text{g m}^{-2} \text{s}^{-1}$ (upper and lower 0.292 to $0.800 \mu\text{g m}^{-2} \text{s}^{-1}$) and $0.00469 \mu\text{g m}^{-2} \text{s}^{-1}$ (0.00132 to $0.0128 \mu\text{g m}^{-2} \text{s}^{-1}$) for the northern and southern feedlots (range indicates 95 % confidence interval), values which are substantially less than IPCC inventory estimates (IPCC, 2006). Mean measured emission of CH_4 was $0.273 \mu\text{g m}^{-2} \text{s}^{-1}$ (0.189 to $0.385 \mu\text{g m}^{-2} \text{s}^{-1}$) and $4.55 \mu\text{g m}^{-2} \text{s}^{-1}$ (2.99 to $6.72 \mu\text{g m}^{-2} \text{s}^{-1}$) for the northern and southern feedlots. For the southern feedlot, these values are less than some inventory protocol-calculated values and greater than others for these types of emissions. However, at the northern feedlot, the CH_4 emissions observed were less than 14 % of those predicted by a range of inventory calculation techniques.

Nitrous oxide emission increased as density, pH, temperature, and manure mass increased. Negative relationships were evident for both moisture and OC with N_2O emission. However, there were correlations between some of these parameters that could confound their predictive potential (e.g. between manure mass and manure bulk density).

The frequency distributions of both the 22-month moisture and temperature data overlapped the corresponding distributions from the emission measurements. However, probability distribution tests applied to temperature and moisture data collected over a 22-month period at the northern feedlot suggest that the mean emission values collected may differ from actual emissions at the site. Unbiased estimates of emissions may be drawn from the data sets via modelling, which is the subject of further research.

At higher moisture contents emission fluxes from bare soil in vacant pens may exceed emission fluxes measured from the pen manure. Additional measurements of emissions from the soil and infrastructure areas of the feedlot would be required to quantify these emissions.

4 From control factors to an emission protocol (based on shorten and Redding, in Press)

P. Shorten^b, M.R. Redding^a, R.L. Lewis^a, O. Smith^a (^aDAF; ^bAgResearch New Zealand)

4.1 Summary

More accurate, but comparably simple inventory calculations are required to calculate N₂O and CH₄ emissions from pen manure. Ideally these calculation protocols would be representative of Australian conditions, and be responsive to the effect of management practices. This study used the data sets developed from the previous chapter's measurements to explore the potential for a relatively simple, but management- responsive and region- specific, emission prediction protocol from pen manure. The calculation approach developed was successfully region-specific. However, key control factors that were expected (based on the current inventory approaches) to have a strong influence – namely total nitrogen content and total mass of manure – did not control emission.

We found that much of the variability in emission of nitrous oxide and methane in an existing data set were accounted for by modelling interactions of two readily measured manure parameters (e.g. moisture content and temperature). Emission was more related to the area of manure -covered pens than the total mass of manure or the manure N content. Management that results in altered manure covered area, or altered moisture contents relative to the peak emission moisture range, will alter emissions.

We found that the peak N₂O emission in manure occurred for a moisture fraction of 0.20 as opposed to 0.59 in soil. This may result from the anaerobic conditions occurring at lower moisture contents in pen manure than occurs in soils. We also developed and validated a physical process-based model of the effect of air temperature, solar radiation and time of day on manure temperature.

A physical process-based model was also formulated to characterise the effect of rainfall, evapo-transpiration and drainage on manure moisture.

Methane emissions at the northern feedlot were predicted to be 0.40 kg CH₄ head⁻¹ year⁻¹, substantially less than the standard protocol calculated values for manure emission: 4.14 and 1.9 kg CH₄ head⁻¹ year⁻¹ (Australian and IPCC inventories). Nitrous oxide emissions at the northern feedlot were predicted to be 0.31 kg N₂O head⁻¹ year⁻¹. Standard inventory calculation approaches produce larger estimates of emission: 2.6 and 3.0 kg N₂O head⁻¹ year⁻¹. These differences could be partly related to regional conditions and climates; however, the inventory calculation protocols are reliant on a relationship between emission magnitude and total excreted N that was not supported by our study.

In order to ensure that this study effectively impacts Australian inventory protocols these results have been submitted to a major international journal, and the manuscript is now in its first review (Shorten and Redding, In Press).

4.2 Introduction

This paper attempts to allow more general conclusions from the field N₂O and CH₄ emissions measurements collected from pen surface manure in a beef feedlot (Redding et al., 2015). The preceding study successfully isolated manure N₂O and CH₄ emissions *in situ* (excluding enteric emissions), providing the first isolated measurements of pen manure N₂O and CH₄ emissions under Australian-comparable conditions. Measurements of N₂O and CH₄

emitted from the manure and pen surface were previously largely lacking from the literature except for low-temperature conditions ($< 10\text{ }^{\circ}\text{C}$) (Boadi et al., 2004) or other production systems (Leytem et al., 2011).

Given a body of reliable field pen-manure emission values, a further valuable step becomes possible: development of an understanding of factors that control manure-sourced emissions. Such an understanding is required to use emission data to develop appropriate emission mitigation strategies. An understanding of N_2O emission processes in soils is already well supported by a wide range of mechanistic models (the status of N_2O -emission modelling progress is reviewed by Butterbach-Bahl et al., 2013). Some of these models are complex, seeking to represent many interactions (Giltrap et al., 2008). Others seek to represent a critical subset of the process interactions. The WNMM Model (Water and Nitrogen Management Model) (Li et al., 2007) successfully adopts a significantly mechanistic basis (Xu et al., 1998), but avoids complexity.

Fewer models have been developed specifically to represent manure system N_2O or CH_4 emissions (Rigolot et al., 2010; Li et al., 2012). In other cases, soil emission models have been applied or adapted to manure or effluent systems. For example, during the development of WNMM (Li et al., 2007), the model was validated against piggery effluent applications to soil, performing well (correlation coefficients 0.92, 0.90, and 0.88, for 144, 95, and $48\text{ kg of N ha}^{-1}$).

Given the background of an appropriate data set from our previous study (Redding et al., 2015) we sought to investigate two hypotheses: 1) much of the variability in emission of nitrous oxide and methane from a commercial pen is well accounted for by modelling interactions of readily measured manure and climate parameters (e.g. moisture content and temperature); and 2) these models will allow estimation of annual emissions from the sites that will be consistent with conventional calculations (IPCC, 2006). Having conducted this study, however, our final assessment suggests some caveats to the accepted calculation approach for our study sites.

4.3 Materials and methods

4.3.1 Modelling data set

A full description of the modelling data set is available in Redding et al. (2015). Measurements were conducted at Australian feedlots at two contrasting sites. The Queensland (northern) feedlot was characterised by summer-dominated rainfall of 634 mm annually, and an annual average temperature of 25°C . A total of 44 emission measurements were collected from four locations within a single pen using a large chamber of a design demonstrated to produce comparable N_2O and CH_4 emission values to those collected using the open-air backward Lagrangian stochastic technique (the chamber encloses an area of 20 m^2) (Redding et al., 2013). The pen locations were selected to be representative of the range of manure depths, moistures, and feed wastage content (influenced by proximity to the feed bunkers). One of the sites was located within the area that received partial or full shade from approximately 10:00 to 14:00 each day.

The southern feedlot (New South Wales) was characterised by average annual rainfall of 530 mm with more rain falling in the spring-summer months than autumn-winter months. Average annual temperature is 22°C . All 54 measurements were conducted within the same pen, from one of three zones representative of the total pen area.

The northern feedlot data set includes manure moisture (directly measured for each emission measurement, and 22 months of data determined from a mathematical relationship between manure moisture and adjacent soil moisture measured via frequency domain

reflectometry), manure temperature (22 months of continuous data), manure depth, manure density, total N content, NO_3^- concentration, volatile solids (V_S), and pH (and a range of other parameters not referred to in the current modelling study).

Instrumentation at the southern feedlot was restricted to the period during chamber measurements, and was more limited. This modelling study refers to the manure temperature and moisture content and publicly available air temperature, rainfall and evapotranspiration data (Bureau of Meteorology, 2014).

4.3.2 Emission process modelling

Nitrous oxide emission processes were investigated in the pen manure via application of an existing soil process-based model (Water and Nitrogen Management Model; WNMM) (Li et al., 2007), selecting suitable parameters to better represent the manure system.

Xu et al.'s (1998) WNMM nitrous oxide emission algorithm provides a mathematical framework for the emission processes. The nitrification rate (q_N ; $\mu\text{g s}^{-1} \text{m}^{-2}$) is based on the following equation:

$$q_N = k_N f_T f_W, \quad [1]$$

where k_N is a nitrification rate constant under optimal conditions, f_T is a temperature stress function (ranging from 0–1), and f_W is a water stress function (ranging from 0–1) representing the effects of water stress via a relationship with the water filled pore space (W).

The nitrification N_2O emission rate ($\mu\text{g s}^{-1} \text{m}^{-2}$) is:

$$q_{NN_2O} = q_N \alpha_N f_T f_W, \quad [2]$$

where the fraction α_N represents the maximum loss of N_2O from the nitrification process. The wet period denitrification rate ($\mu\text{g s}^{-1} \text{m}^{-2}$) is represented by:

$$q_w = k_D [\text{NO}_3] f_T, \quad [3]$$

where k_D is the first-order rate coefficient for denitrification, and is determined by soil organic matter content, soil drainage, tillage applied, presence of manure, climate, the occurrence of pans and $[\text{NO}_3]$ is the nitrate content of the surface soil. The corresponding equation for dry period denitrification is:

$$q_d = k_D [\text{NO}_3] f_T f'_w, \quad [4]$$

where f'_w is a water stress function for anaerobic processes (ranging from 0–1).

Partitioning of the total denitrification into N_2 , NO , and N_2O is achieved empirically through calibration coefficients. The wet period N_2O emission rate is:

$$q_{wDN_2O} = \alpha_w q_w, \quad [5]$$

where α_w (ranging from 0–1) represents the proportion of wet period denitrification products emitted as N_2O multiplied by the proportion of wet days. The dry period N_2O emission rate is:

$$q_{dDN_2O} = \alpha_d q_d (1 - f'_w), \quad [6]$$

where α_d (ranging from 0–1) represents the proportion of dry period denitrification products emitted as N_2O multiplied by the proportion of dry days. The total rate of N_2O emission ($\mu g\ s^{-1}\ m^{-2}$) is therefore described by:

$$q_{N_2O} = k_N \alpha_N (f_T f_W)^2 + k_D \alpha_w [NO_3] f_T + \alpha_d k_D [NO_3] f_T f'_w (1 - f'_w) \quad [7]$$

If the dry period denitrification is ignored then the model dependence on the rate of N_2O emission on temperature, water filled pore space and $[NO_3]$ is shown in Fig. 4.1. The functions f_T , f_W , and f'_w are determined empirically from fits to nitrous oxide emission in soil (Shaffer et al., 1991) (Fig. 4.1, d and e). These equations are:

$$f_T(T) = 1.68 \times 10^9 (\exp(-13.0/[1.99 \times 10^{-3}(34.53 - |34.53 - T| + 273)]))$$

$$f_W(W) = \begin{cases} 0.0075W, & W \leq 20 \\ -0.253 + 0.0218(W - 20) + 0.0203 \times 20, & 20 < W < 59 \\ 40.0 \exp(-0.0625W), & W \geq 59 \end{cases} \quad [8]$$

$$f'_w(W) = 0.0304 \exp(0.0815W)/(1.0529),$$

where T is temperature ($^{\circ}C$) and W is % water-filled pore space.

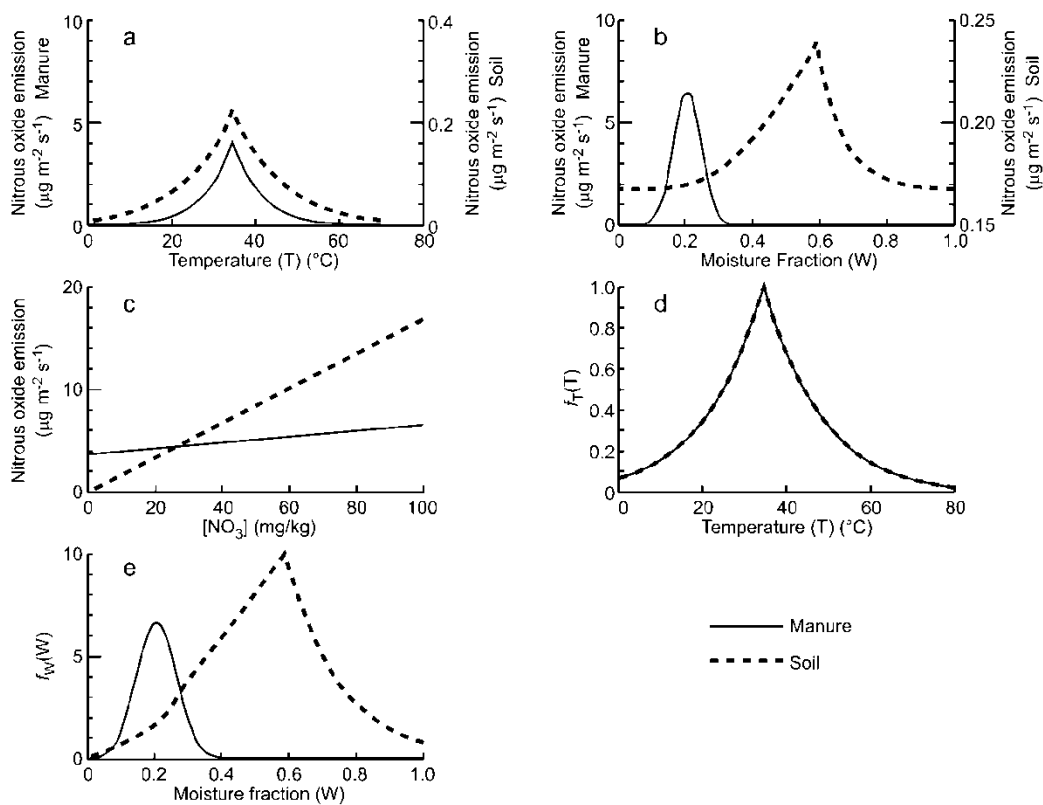


Figure 4.1. The relationships controlling soil N_2O emission, as described by the original WNMM model, and the modified model more suitable for manure.

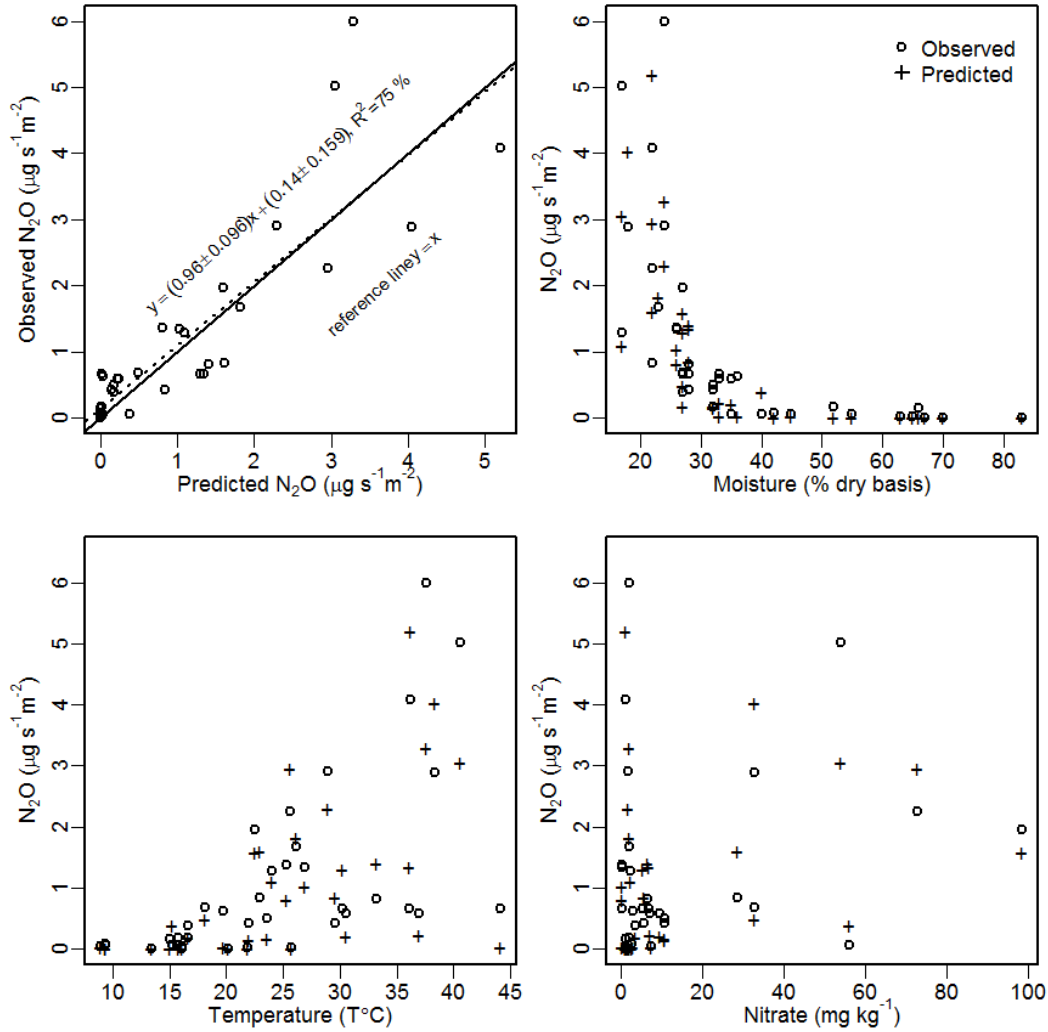


Fig. Figure 4.2. The fit of the proposed N_2O model (Eq. [9]) to the northern feedlot field data, with panels representing observed versus predicted N_2O emission, and N_2O emission versus each of the key model parameters (dry basis moisture, temperature, and nitrate content).

If dry period denitrification is ignored then the total rate of N_2O emission ($\mu\text{g s}^{-1} \text{m}^{-2}$) can be described by a modification of Eq. [8]:

$$q_{N_2O} = \alpha_1 (f_T f_W)^2 + \alpha_2 [\text{NO}_3] f_T, \quad [9]$$

where α_1 , α_2 represent the rates of loss due to nitrification and denitrification respectively and the functions f_T and f_W are:

$$\begin{aligned} f_T(T) &= 1.68 \times 10^9 (\exp(-13.0 / [1.99 \times 10^{-3} (34.53 - |34.53 - T| + 273)])) \\ f_W(W) &= N(W; \mu_W, \sigma_w^2), \end{aligned} \quad [10]$$

where W is the gravimetric moisture fraction and $N(W; \mu_W, \sigma_w^2)$ is the normal distribution with mean μ_W and variance σ_w^2 . A simplified model, with no requirement for $[\text{NO}_3]$ was also examined:

$$q_{N_2O} = \alpha_1 (f_T f_W)^2 + \alpha_2 f_T. \quad [11]$$

A prototype methane emission model was also constructed to represent the field observations collected. We assumed that the rate of methane emission is dependent on temperature (T) (van Hulzen et al., 1999), moisture fraction (W) (van Hulzen et al., 1999; Li, 2000), pH (Wang et al., 1993) and the fraction of volatile solids (V_S) (Sommer et al., 2004b). The total rate of methane emission ($\mu\text{g s}^{-1} \text{m}^{-2}$) can be described by

$$q_{CH_4} = \alpha_1 f_T(T) f_W(W) f_{pH}(pH) \times V_S, \quad [12]$$

where α_1 is the rate of emission and the functions f_T , f_W and f_{pH} are:

$$\begin{aligned} f_T(T) &= \exp(-|T - \mu_T| / \sigma_T) \\ f_W(W) &= N(W; \mu_W, \sigma_w^2) \\ f_{pH}(pH) &= (pH - pH_{\min}) H(pH - pH_{\min}), \end{aligned} \quad [13]$$

where T is temperature, μ_T is the optimal temperature for methane emission, σ_T determines the effect of temperature on the methane emission rate, pH_{\min} is the minimum pH required for methanogenesis, W is the moisture fraction, $N(W; \mu_W, \sigma_w^2)$ is the normal distribution with mean μ_W and variance σ_w^2 and $H(z)$ is the Heaviside switch function ($H(z) = 1$ if $z > 0$ and $H(z) = 0$ if $z \leq 0$). A simplified model was also investigated:

$$q_{CH_4} = \alpha_1 f_T(T) f_W(W). \quad [14]$$

Emissions were estimated for the 22-month period of pen temperature and moisture measurements (30-minute data). Nitrate concentrations were measured during chamber emission measurements. For N_2O emissions at the northern feedlot, a set of estimates of NO_3^- concentration to match the frequency of the pen manure temperature was required. This was obtained through the observed relationship between NO_3^- concentration and manure moisture content, where individual estimates of NO_3^- concentration were simulated from a gamma probability distribution (rgamma function in R, R Development Core Team, 2014):

$$\begin{aligned} &\Gamma([NO_3^-]; \alpha, \beta) \\ \alpha &= \frac{\overline{[NO_3^-]}^2}{\text{var}[NO_3^-]} \\ \beta &= \frac{\overline{[NO_3^-]}}{\text{var}[NO_3^-]}, \end{aligned} \quad [15]$$

where $\overline{[NO_3^-]}$ is a 5-value running mean of measured nitrate concentration versus moisture content, and $\text{var}[NO_3^-]$ is likewise a running variance.

4.3.3 Temperature process modelling

The transfer of heat in manure determines the temperature within the manure and consequently the rate of N_2O emission in the manure layer near its surface. Here we

develop a physical process-based model to characterise the temperature differences between air, the surface of manure, the interior of the manure and the base of the manure. This model can be used to predict internal manure temperature based on readily available climate data: air temperature, solar radiation and time of day.

The temperature of the manure is determined by air temperature, pad/soil temperature, solar radiation, manure physical characteristics and heat production by microbes within the manure. The thermal diffusion of heat in manure can be described by the diffusion equation for temperature (T) ($^{\circ}\text{C}$) (Farlow, 1993):

$$\begin{aligned}\frac{\partial T(z,t)}{\partial t} &= \frac{1}{c(z)\rho(z)} \frac{\partial}{\partial z} \left(k(z) \frac{\partial T(z,t)}{\partial z} \right) + s(z,t) \\ \frac{\partial T(z=L,t)}{\partial z} &= -\frac{h}{k(L)} (T(L,t) - T_{air}(t)) + b_{solar}(t) \\ T(z,t=0) &= T_0(z)\end{aligned}\quad [16]$$

where ρ is the density of the manure/soil, c is the thermal capacity of the manure/soil (which is moisture dependent), h is the heat exchange coefficient for manure/air, L is the depth of manure, k is the thermal conductivity of manure/soil, $s(z,t)$ is the rate of heat production by microbes within the manure, $T_{air}(t)$ is the air temperature at time t , $T_0(z)$ is the initial manure temperature, z is the distance between the pad/soil interface and the point of prediction within the manure, and $b_{solar}(t)$ is the rate of solar irradiance at the manure surface at time t (that is dependent on factors such as manure colour). Generic half-sine and sine functions are used to describe solar irradiance ($^{\circ}\text{C mm}^{-1}$) and air temperature ($^{\circ}\text{C}$):

$$\begin{aligned}b_{solar}(t) &= 100 \times \sin(2\pi(t-360)/1440) H(t-360) H(1080-t) \\ T_{air}(t) &= \frac{1}{2} (T_{air,max} + T_{air,min}) + \frac{1}{2} (T_{air,max} - T_{air,min}) \sin(2\pi(t-360)/1440)\end{aligned}\quad [17]$$

where t denotes time (mins), $T_{air,max}$ is the maximum daily temperature, $T_{air,min}$ is the minimum daily temperature and $H(z)$ is the Heaviside switch function ($H(z) = 1$ if $z > 0$ and $H(z) = 0$ if $z \leq 0$). The conversion of measured radiation, Radn (MJ m^{-2}), to the maximum rate of solar irradiance at the manure surface, $b_{solar,max}$ ($^{\circ}\text{C mm}^{-1}$), was $4.0 \times \text{Radn}$ (i.e., $b_{solar,max} = 4.0 \times \text{Radn}$ ($^{\circ}\text{C mm}^{-1}$)). Partial differential equations (Eq. 16,17) were solved using pdepe in MATLAB.

The process-based manure temperature model was validated using the measured relationship between air temperature and manure interior temperature at a distance 5 mm from the manure surface. Measurements were made between 8:30 am and 3:30 pm (hourly changes in air temperature were not recorded).

4.3.4 Moisture process modelling

The transfer of water in manure determines the moisture within the manure and consequently the rate of N_2O emission in the manure layer near the manure surface. Here we develop a physical process-based model to characterise the effect of rainfall, evapo-transpiration and drainage on manure moisture. This model can be used to predict internal manure moisture based on readily available climate data. The dynamic change in manure water content can be described by the water balance model

$$\frac{dW(t)}{dt} = a_R R(t) - a_E E(t) \times W - k_S f(W) \quad [18]$$

$$f(W) = W^{1/2} \left(1 - \left(1 - W^{1/m} \right)^m \right)^2$$

where W is the manure water content, t is time (days), $R(t)$ is the rate of rainfall at time t (mm day⁻¹), $E(t)$ is the rate of evapotranspiration at time t (mm day⁻¹), the effect of evapotranspiration on the change in manure water content is assumed to be proportional to manure water content, $f(W)$ describes the dependence of conductivity on water content (Roose and Fowler, 2004; Shorten and Pleasants, 2007), a_R is the manure water capacity (mm⁻¹), a_E is the rate of decrease in water content due to evapotranspiration (mm⁻¹), k_S is the saturated manure conductivity (day⁻¹), and $m = 0.5$ is the water flow parameter. Differential equations (Eq. 18) were solved using the stiff system solver ode15s in MATLAB.

4.3.5 Statistics

Several approaches were employed to assist with modelling and model parameter estimation. In particular, non-linear partial/differential equations were employed for model development, while non-linear optimisation methods were employed for parameter estimation. Models were fitted to the data (nitrous oxide or methane emission rates) using linear and nonlinear regression (Bates and Watts, 2007). Model residuals were analysed for homoscedasticity and normality. We assumed that the variances of the deviations in measurements within response variables were constant. Markov Chain Monte Carlo techniques (Gilks et al., 1996a) were used to determine the standard errors in the model parameters. Model fit was assessed using the correlation, slope and intercept between the predicted and observed emission rates (Pineiro et al., 2008). Pearson product moment correlation coefficient and Kendall's tau were used to describe the correlation of the predicted and observed emission rates. A generalized linear model was used to test for quadratic relationships between time of day and manure temperature. Calculations were completed using MATLAB and R (The Mathworks Inc., 2012; R Development Core Team, 2014).

4.4 Results and discussion

4.4.1 Emission modelling

Pen manure pore space, bulk density, and structure change rapidly with moisture content and treading, rendering water filled pore space (WFPS) values difficult to define in this context. The moisture content versus emission relationship we developed used gravimetric moisture content as an alternative to WFPS. The manure bulk density and moisture data collected indicated that manure N₂O emission halted at moisture contents at the lower end of the range measured. This is in contrast with the soil observations used to develop WNMM, where emissions tend to occur under wet conditions (compare Fig. 4.1). This may be the result of development of anaerobic conditions at lower moisture contents in pen manure than occurs in soils.

The model (Eq. [9]) represented nitrous oxide emission data from field manure reasonably well (Fig. 4.2; R² = 0.75; Table 4.1). Limited cross validation was possible with the data collected from the southern feedlot, though NO₃⁻ data for these manures were not available. The significant fit of Eq. [11] to the data for both feedlots (Table 4.1, Fig. 4.3) suggests that similar relationships between N₂O emission and both temperature and moisture content is likely, with emission peaking at both feedlots at similar moisture (μ_w) and temperature.

For this data set, relationships between N₂O emissions and N-forms (total mass or concentration) were not strong (Redding et al., 2015). For the northern feedlot, the residuals of the application of the simplified model (Eq. [11]) are not significantly related to total N, NO₃⁻, or the total masses of these two quantities enclosed by the chamber (Kendall's τ , $P > 0.5$).

The fit of the prototype model (Eq. [12]) to the methane data was less satisfactory than for the N₂O model, though significant (Fig. 4.4; Table 4.1; Eq. [12]). Peak CH₄ emission from this model occurs at high moisture content (114 % dry basis) and a temperature of 34.4°C. This is consistent with an optimum temperature for methanogenesis of between 30 and 40°C in soil (Le Mer and Roger, 2001). Wet or saturated moisture promotes development of anaerobic conditions, promoting methanogenesis, and inhibiting aerobic consumption of methane (Chadwick et al., 2000; White et al., 2008). The prototype model suggests that the minimum pH for methane emission is 6.53, consistent with maximum methane formation in the neutral to slightly alkaline range in anaerobic soils (Wang et al., 1993). An attempt to fit this model to the southern feedlot data using northern feedlot parameters and non-linear regression to fit missing parameters (V_s and pH) resulted in a fairly poor fit ($P < 0.1$).

Table 4.1. Summary of fitted models for N₂O and CH₄ emission at the northern and southern feedlots.

Site:	Northern	Northern	Southern
N₂O Models	Eq. [9]	Eq. [11]	Eq. [11]
α_1 ($\mu\text{g s}^{-1} \text{m}^{-2}$)	0.154±0.015	0.178±0.0189	0.106±0.007
α_2 ($\mu\text{g s}^{-1} \text{m}^{-2}$)	0.0292±0.036	0.6±0.0889	0.0967±0.0064
μ_w (moisture fraction)	0.206±0.003	0.196±0.0033	0.234±0.005
σ_w (moisture fraction)	0.0596±0.0028	0.064±0.0032	0.138±0.004
Peak Temperature (°C)	34.5	34.5	34.5
Observed vs. Predicted			
R ²	0.73	0.72	0.47
Kendall's τ	0.75	0.70	0.31
P <	3x10 ⁻¹¹	4 x 10 ⁻¹¹	2x10 ⁻⁷
Slope	0.94±0.1	0.98±0.1	1±0.16
Intercept ($\mu\text{g s}^{-1} \text{m}^{-2}$)	0.58±0.66	0.19±0.60	-0.005±0.11
CH₄ Models	Eq. [12]	Eq. [14]	Eq. [14]
α_1 ($\mu\text{g s}^{-1} \text{m}^{-2}$)	6.38±0.33	1.54±0.77	870±63
μ_w (moisture fraction)	1.14±0.1	0.79±0.23	2.2±0.07
σ_w (moisture fraction)	0.46±0.06	0.54±0.15	0.6±0.03
μ_T (°C)	34.4±1.4	36.1±0.37	34.7±0.6
σ_T (°C)	27.7±13.1	13.7±1.3	6.6±0.3
pH_{min}	6.53±0.08		
Observed vs. Predicted			
R ²	0.3025	0.14	0.1936
Kendall's τ	0.48	0.3	0.16
P <	0.002	0.04	0.1
Slope	0.87±0.25	0.81±0.38	0.73±0.22
Intercept ($\mu\text{g s}^{-1} \text{m}^{-2}$)	0.25±0.39	0.29±0.58	13.5±6.5

However, the temperature associated with peak emission was similar to that identified for the northern feedlot (μ_T), and saturated conditions tended to promote maximal CH_4 emission (μ_W).

The simplified methane model (Eq. [14]) did not represent the data well (Table 4.1), though the fit for the northern feedlot was significant ($P < 0.05$).

Further development and validation is required for the N_2O and CH_4 models to extend them beyond application to the northern feedlot. The lack of full parameter sets and the considerably different conditions and emission ranges present challenges using the southern data set for validation purposes.

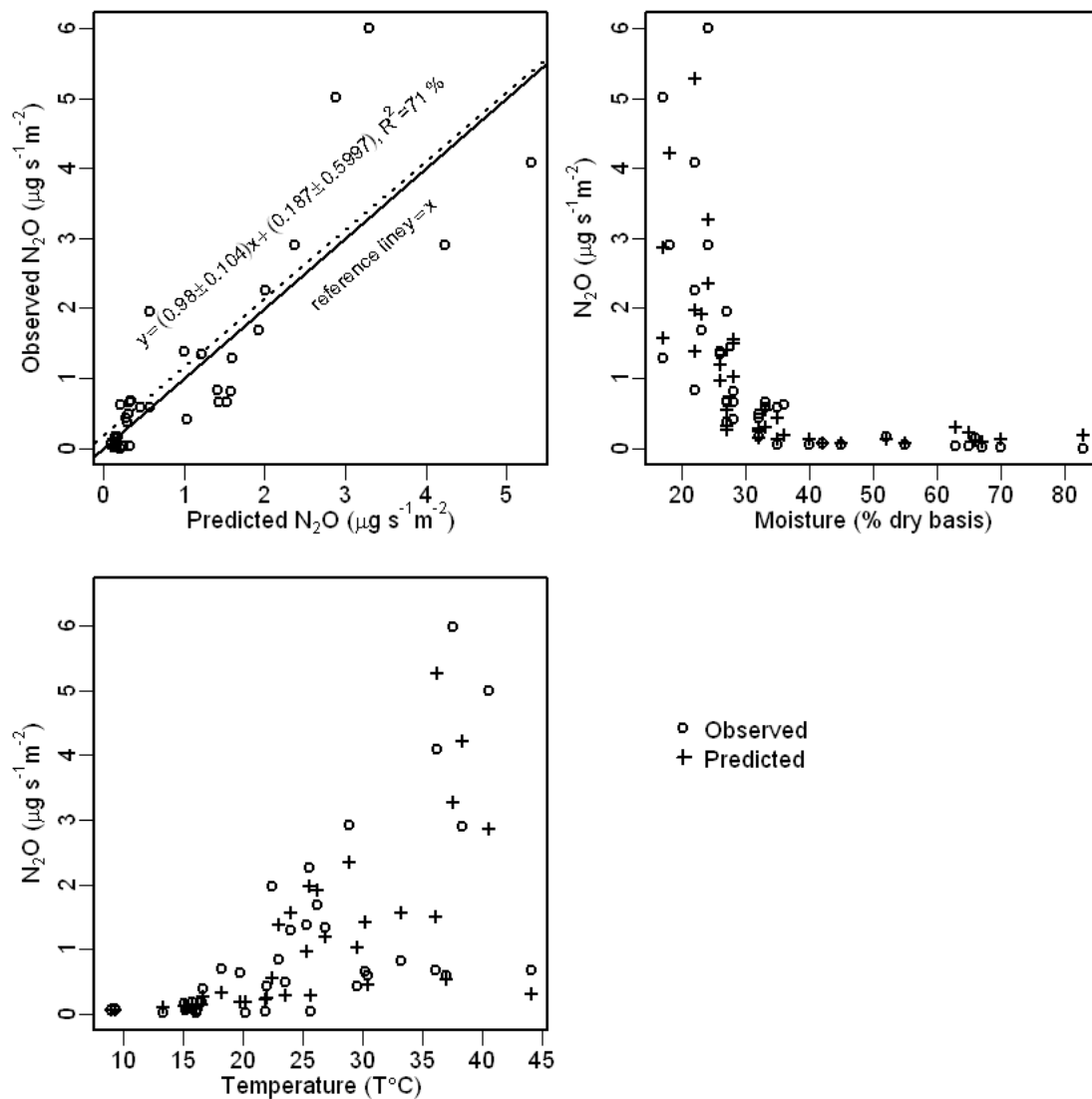


Figure 4.3. The fit of the simplified N_2O model (Eq. [11]) to the northern feedlot field data, with panels representing observed versus predicted N_2O emission, and N_2O emission versus each of the key model parameters (dry basis moisture, temperature).

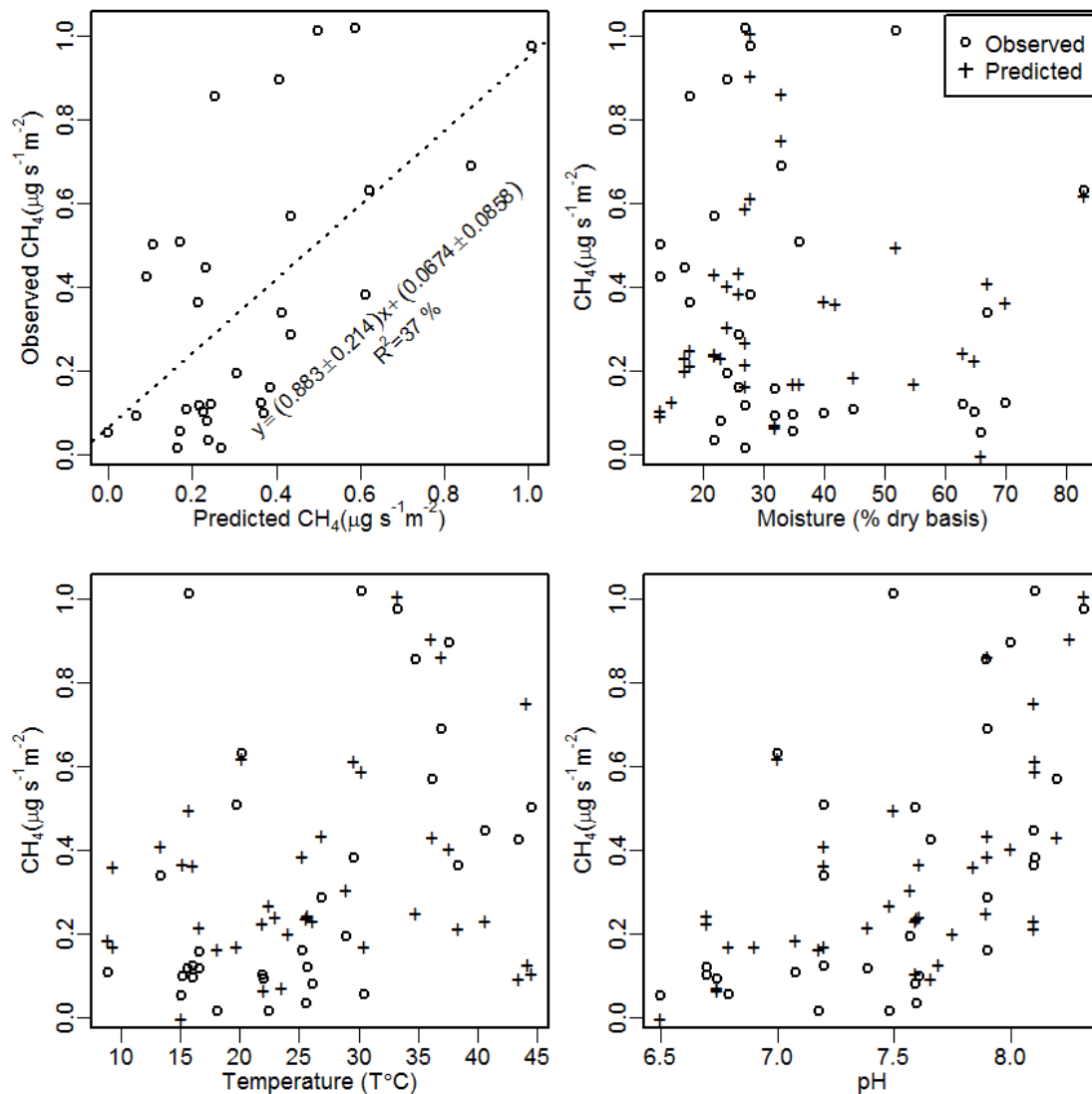


Figure 4.4. The weak fit of the prototype CH₄ model to the field data (Eq. [12]), with panels representing observed versus predicted CH₄ emission, and CH₄ emission versus each of the key model parameters (dry basis moisture, temperature and pH).

4.4.2 Manure temperature modelling

As manure temperature is one of the inputs to the emission models (Eqs. [9-14]), a method of calculating this parameter from more readily available parameters would be a considerable advantage. Observations suggest that peak manure surface and base temperature occurs at 12 noon, with a significant quadratic relationship between time of day and both manure surface temperature ($P < 0.001$) and manure base temperature ($P < 0.05$). The highest temperatures occur at the surface, though the surface and base temperatures are strongly related ($P < 0.01$). Surface temperature is significantly greater than air temperature ($+12\text{ °C} \pm 3.3\text{ °C}$; $P < 0.01$).

Bulk density, an input to the proposed temperature model (Eq. [16-17]), ranges from 250 to 1100 kg m⁻³ for beef cattle manure, with thermal conductivity ranging from 0.05 to 6.0 W m⁻¹ °C⁻¹, and the thermal capacity ranges from 1.4 to 3.88 kJ kg⁻¹ °C⁻¹. A model simulation was

based on these parameters and selected temperature relationships ($\rho = 1000 \text{ kg m}^{-3}$, $c = 2.59 \text{ kJ kg}^{-1} \text{ }^\circ\text{C}^{-1}$, $k = 0.136 \text{ W m}^{-1} \text{ }^\circ\text{C}^{-1}$, $h = 1000 \text{ W m}^{-2} \text{ }^\circ\text{C}^{-1}$, $L = 70 \text{ mm}$, $T_0 = 20 \text{ }^\circ\text{C}$, $T_{\text{air,max}} = 35 \text{ }^\circ\text{C}$, $T_{\text{air,min}} = 10 \text{ }^\circ\text{C}$, $s = 0 \text{ }^\circ\text{C min}^{-1}$, $b_{\text{solar,max}} = 100 \text{ }^\circ\text{C mm}^{-1}$; time as day fractions, with midnight as 0).

The manure temperature is closely linked to air temperature ($R^2 = 0.74$). Manure interior temperature is also significantly greater than air temperature ($6.3 \text{ }^\circ\text{C} \pm 1 \text{ }^\circ\text{C}$, $P = 0.01$). The model-simulated relationship between air temperature and internal manure temperature between 8:30 am and 3:30 pm is based on the daily changes in air temperature and solar radiation. The model characterises the difference between manure interior temperature and air temperature at $30 \text{ }^\circ\text{C}$ (4 to $9 \text{ }^\circ\text{C}$ depending on time of day). The model also predicts that the relationship between air temperature and interior temperature is greater in the afternoon than the morning ($4 \text{ }^\circ\text{C}$ at an air temperature of $30 \text{ }^\circ\text{C}$).

It appears that the model may provide a reasonable, mechanistic basis to predict manure temperature from readily available air temperature data for inputs to the emissions models. Subsequent evaluation at other sites would be valuable.

The temperature modelling also provided information addressing several important questions. By comparing emission data and manure characteristics it is evident that there is no significant effect of manure depth independent of temperature on the rate of nitrous oxide emission ($P > 0.2$; Redding et al., 2015). This is consistent with no significant relationship between total mass of manure N and the total rate of N_2O emission. This suggests that the N_2O emission process is localised to the surface layer of manure, a possibility that is supported by the temperature modelling. Indeed, temperature modelling suggests that the soil under the manure is not the major contributor of N_2O emission. An increase in the internal manure temperature 5 mm from the manure surface from $20 \text{ }^\circ\text{C}$ to $35 \text{ }^\circ\text{C}$ is associated with an increase in temperature at the base of the manure from $20 \text{ }^\circ\text{C}$ to $25 \text{ }^\circ\text{C}$. Based on the Xu et al. (1998) soil model, an increase of soil temperature from $20 \text{ }^\circ\text{C}$ to $25 \text{ }^\circ\text{C}$ would increase N_2O emission by approximately 50 %. However, the N_2O emission rate increases approximately 500 % when the internal manure temperature 5 mm from the manure surface increases from $20 \text{ }^\circ\text{C}$ to $35 \text{ }^\circ\text{C}$. This suggests that the soil under the manure contributes at most 10 % of the N_2O emission from manure on soil.

4.4.3 Manure moisture modelling

Another key parameter of the emission models is manure moisture content (Eq. [18]). Since manure moisture content varies throughout the year, with location, and weather a method to estimate this parameter from more readily available parameters is required to allow the emission models to be widely applied. Fitting the moisture model (Eq. 18) to the 2012 data (first 10 time points in Fig. 4.5; 212 data points) indicated a good relationship to observations ($R^2 = 0.95$) using the optimal parameters: $a_R = 0.0080 \pm 0.0008 \text{ mm}^{-1}$, $a_E = 0.0037 \pm 0.0005 \text{ mm}^{-1}$, and $k_S = 4.15 \pm 0.43 \text{ day}^{-1}$. Rainfall and evapotranspiration data were obtained from interpolated Bureau of Meteorology daily records (Bureau of Meteorology, 2014). The northern feedlot data from 2013 provided one of the validation sets for the moisture model, with adequate results ($R^2 = 0.31$), where the water content peaks coincide with rainfall events.

Soil moisture probe data provided an additional, more detailed development and validation set for the period 14/03/2012 to 17/01/2014 (Redding et al., 2015). Fitting the moisture model (Eq. 18) to the 2012 data suggested that the optimal model parameters are $a_R = 0.0061 \pm 0.0005 \text{ mm}^{-1}$, $a_E = 0.0034 \pm 0.0004 \text{ mm}^{-1}$, and $k_S = 2.22 \pm 0.23 \text{ day}^{-1}$ (Fig. 4.5B). Using the corresponding soil moisture probe data from 2013 as a validation data set indicated that the model provides a good description of the changes in soil water content (R^2

= 0.64). The estimated model drainage parameter (k_s) was also significantly lower in soil than in manure ($P < 0.01$).

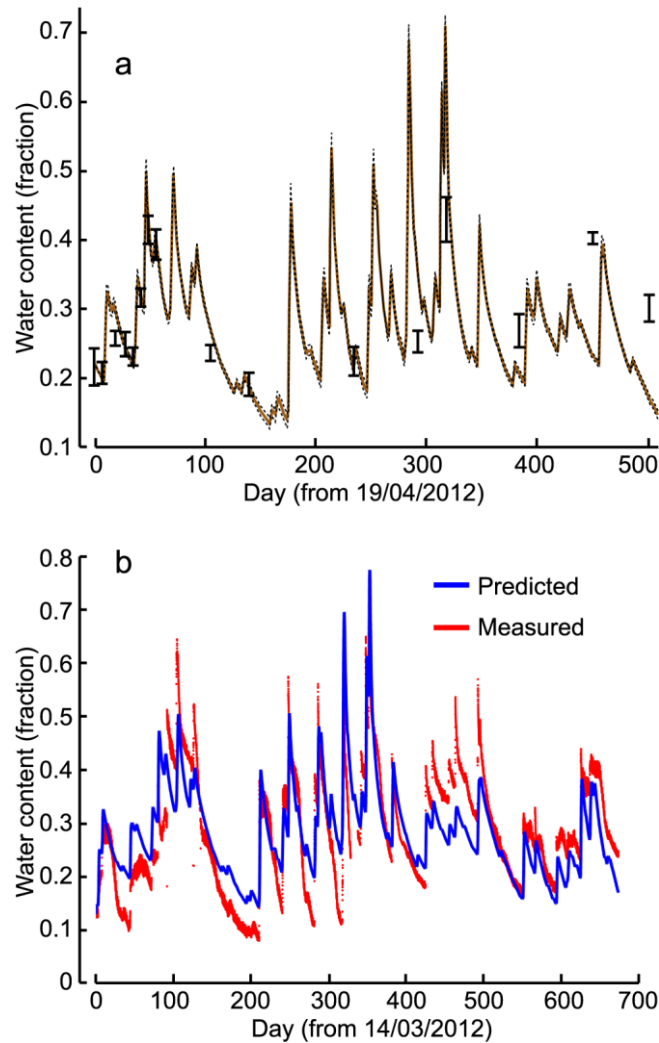


Figure 4.5. A) The measured and predicted change in manure water content at the northern feedlot in 2012/2013. B) The measured and predicted change in soil water content at the northern feedlot from 14/03/2012 to 17/01/2014.

4.4.4 Model prediction at the southern feedlot

The models for moisture, temperature, N_2O emission and CH_4 emission were validated using measurements from the southern feedlot. The models were used to predict the manure moisture and temperature at the southern feedlot using the northern feedlot parameters and southern feedlot climate data from interpolated Bureau of Meteorology daily records (rainfall, evapotranspiration and radiation). Predicted moisture and temperature were then used to predict CH_4 and N_2O emissions at the southern feedlot (Eq. 11, 12). Manure pH was assumed to be 7.53 and $V_s = 45\%$ (based on average measurements from the northern feedlot). The predicted and measured manure temperature (5 mm from surface) at the southern feedlot ($R^2 = 0.71$; $P < 0.001$) demonstrates that the model provides a good description of the daily and annual changes in manure temperature. The predicted and measured N_2O emission from manure at the southern feedlot is shown in Fig. 4.5B ($R^2 = 0.14$; $P < 0.02$). The slope (0.67 ± 0.28) and intercept ($-0.11 \pm 0.10 \mu g s^{-1} m^{-2}$) between the

predicted and measured N_2O emission are not significantly different from one and zero respectively. Although the correlation between predicted and measured CH_4 emission was significant ($R^2 = 0.24$; $P < 0.01$), the measured CH_4 emissions at the southern feedlot are approximately ten times greater than predicted CH_4 emissions. This may reflect higher pen cleaning frequency at the southern feedlot than the northern feedlot (resulting in higher V_S than assumed). However, this also demonstrates that a site-specific calibration for CH_4 is required, and that further testing of the models at other sites is required.

4.4.5 Estimated annual emissions

The more complex N_2O model (Eq. [9]) in conjunction with 22 months of pen temperature measurements and the manure NO_3^- concentration estimates were used to estimate annual emissions for the northern feedlot. Based on Eq.'s [9 and 15] estimated N_2O emissions over 22 months for the four sites were $0.43, 0.62, 0.38,$ and $0.30 \mu\text{g m}^{-2} \text{s}^{-1}$ (sites 1 to 4; Fig. 4.2), values which are comparable with the mean measured emission values ($0.496 \mu\text{g N}_2\text{O m}^{-2} \text{s}^{-1}$; 95 % confidence interval, 0.292 to $0.800 \mu\text{g m}^{-2} \text{s}^{-1}$; Redding et al., 2015). Assuming that the four sites are representative of approximately equal proportions of the pen, and given the pen area and occupancy (3000 m^2 ; 134 head on a time-averaged basis), this amounts to about $0.31 \text{ kg N}_2\text{O head}^{-1} \text{ year}^{-1}$. Standard inventory calculation approaches produce much larger estimates of emission: 2.6 (stockpile plus pen manure; Department of Environment, 2013) and $3.0 \text{ kg N}_2\text{O head}^{-1} \text{ year}^{-1}$ (IPCC, 2006). These differences could be partly related to regional conditions and climates. However, the inventory calculation protocols are reliant on a relationship between emission magnitude and total excreted N.

In contrast, it is evident that emission from the pen of the northern feedlot was not related to the total N contained in the manure, or the mass of total N on the pen surface (Redding et al., 2015). As expected (Fig. 4.1), these emissions are larger than the much lower temperature emissions observed by Boadi et al. (2004; about $0.06 \text{ N}_2\text{O head}^{-1} \text{ year}^{-1}$, determined at $< 0.4 \text{ }^\circ\text{C}$). Observed emissions from dairy "open lots" of about $3.7 \text{ kg N}_2\text{O head}^{-1} \text{ year}^{-1}$, were collected under a different production system and in a different region (Idaho, USA; Leytem et al., 2011) to those we investigated.

The prototype CH_4 emission model (Eq. [12]) was less strong than the N_2O emission relationship, and was dependent on the existence of pH data throughout the simulation period. Both manure V_S and pH are required to complete estimates with this model, and since neither strong relationships nor data were available for these parameters, mean values from the northern site were used in the calculations (pH, 7.6, V_S 45 %). Estimated time-averaged CH_4 emissions over 22 months for the four sites were $0.45, 0.42, 0.66,$ and $0.71 \mu\text{g m}^{-2} \text{s}^{-1}$ (sites 1 to 4; Fig. 4.4), values which are comparable with the mean measured emission values (0.273 ; 95 % confidence interval, 0.189 to $0.385 \mu\text{g m}^{-2} \text{s}^{-1}$; Redding et al. 2015). When averaged, this equates to about $0.40 \text{ kg CH}_4 \text{ head}^{-1} \text{ year}^{-1}$, substantially less than the standard protocol calculated values for manure emission: 1.24 and 4.14 (southern and northern feedlot estimates) (Environment, 2014) and $1.9 \text{ kg CH}_4 \text{ head}^{-1} \text{ year}^{-1}$ (IPCC, 2006). Boadi et al. (2004) observed much greater emissions (about $23 \text{ kg CH}_4 \text{ head}^{-1} \text{ year}^{-1}$) under low-temperature conditions ($< 0.4 \text{ }^\circ\text{C}$) in Canada, based on three measurement periods and six small chambers (0.1 m radius).

In the absence of southern feedlot temperature and manure moisture data, N_2O and CH_4 emission values were estimated using the temperature and moisture models parameterised at the northern feedlot in conjunction with publicly available interpolated climate data (Wang et al., 2013). It must be noted, however, that: a) the temperature and moisture models have not been validated for the southern feedlot; b) the parameters a_R , a_E , and k_S are those estimated from the northern feedlot. The corresponding predicted average annual N_2O emission was $0.38 \mu\text{g m}^{-2} \text{s}^{-1}$, while predicted average annual CH_4 emission was $0.63 \mu\text{g m}^{-2}$

s^{-1} , which are both comparable to predictions from the northern feedlot. A site-specific calibration of the model would need to produce much higher emission estimates to match the observed CH_4 emissions at the southern site.

4.4.6 Implications

The adapted model developed lends itself to region-specific estimation of emissions under Australian conditions, by using the moisture, temperature and emission components. The research team assisted FSA Consulting to prepare a regionalised tabulation of results using this model in a report commissioned by the Federal Department of Environment (Wiedemann, 2014).

4.5 Conclusion

We developed process-based models of N_2O and CH_4 emissions from pen surface manure in a beef feedlot. We found that much of the variability in emission of nitrous oxide and methane from a commercial pen is well accounted for by modelling interactions of readily measured manure parameters (e.g. manure moisture content and manure temperature). The models were also applied to measurements conducted at a second feedlot. The manure bulk density and moisture data collected indicated that manure N_2O emission halted as moisture contents rose from the lower end of the range measured. This is in contrast with the soil observations, where emissions tend to occur under wet conditions.

We also developed a physical, process-based model to characterise the effect of air temperature on manure temperature. This model can be used to predict internal manure temperature based on air temperature, solar radiation and time of day. A simple model based on readily available climate data also adequately characterised the effect of rainfall, evapo-transpiration and drainage on manure moisture.

N_2O emissions at the northern feedlot are predicted to be $0.31 \text{ kg } N_2O \text{ head}^{-1} \text{ year}^{-1}$. Standard inventory calculation approaches produce much larger estimates of emission: 2.6 (stockpile plus pen manure; Department of Environment, 2013) and $3.0 \text{ kg } N_2O \text{ head}^{-1} \text{ year}^{-1}$ (IPCC, 2006). CH_4 emissions at the northern feedlot are predicted to be $0.40 \text{ kg } CH_4 \text{ head}^{-1} \text{ year}^{-1}$, substantially less than the standard protocol calculated values for manure emission: 4.14 (Department of Environment, 2013) and $1.9 \text{ kg } CH_4 \text{ head}^{-1} \text{ year}^{-1}$ (IPCC, 2006). These differences could be partly related to regional conditions and climates. However, the inventory calculation protocols are reliant on a relationship between emission magnitude and total excreted N – a relationship that is not supported by the data set.

5 Processes controlling emission of nitrous oxide suggest a flaw in the current inventory approach (Redding et al., review)

M.R. Redding^a, P. Shorten^b, C. Pratt^a, R.L. Lewis^a, J.Hill^a, O. Smith^a

^aDAF, ^bAgResearch New Zealand

5.1 Summary

Cattle ingest nitrogen in feed and excrete urea in urine. This urea is rapidly converted to ammonia and dissolved ammonium in the environment. Accordingly, feedlots are major sources of ammonia, a large proportion of which is lost as a gas (volatilised).

In the landscape surrounding a feedlot volatilised ammonia may be re-deposited, increasing the fertility of soils, but also presenting a risk of subsequent conversion and loss as an indirect N₂O emission.

This study investigated the relationship between N₂O emissions, low -magnitude NH₄⁺ deposition (0 to 30 kg N ha⁻¹), and soil moisture content in two soils using in-vessel incubations. Emissions from a clay soil peaked (< 0.002 µg N [g soil]⁻¹ min⁻¹) from 85 to 93 % WFPS (water filled pore space; in this case very close to saturation with water), increasing to a plateau as remaining mineral-N increased. Peak N₂O emissions for a sandy soil were much lower (< 5 x 10⁻⁵ µg N [g soil]⁻¹ min⁻¹) and occurred at about 60 % WFPS (much dryer than was observed for the clay soil), with an indistinct relationship with increasing resident mineral N due to the low rate of nitrification in that soil.

A process-based mathematical model was well suited to the clay soil data where all mineral-N was assumed to be nitrified (R² = 90%). This function was not well suited to the sandy soil where nitrification was much less complete. An equation representing mineral-N pool conversions (NO₃⁻ and NH₄⁺) was proposed based on time, pool concentrations, moisture relationships, and soil rate constants (preliminary testing only).

A threshold for mineral-N was observed: emission of N₂O did not occur from the clay soil for mineral-N < 70 mg (kg of soil)⁻¹. Our results showed that soil N availability controls indirect N₂O emissions. This outcome challenges the IPCC approach which predicts indirect emissions from atmospheric N deposition. Our management-responsive clay soil emission model suggests a range of scenarios that would result in decreased emission, potentially providing an incentive for improved management.

5.2 Introduction

Ammonia-N is volatilised from a wide range of human production systems and activities including animal production (intensive and extensive), sewage treatment, and manure or inorganic fertiliser application to land. Ammonia, although not itself a greenhouse gas (GHG), has the potential to form nitrous oxide (N₂O). Ammonia volatilisation sources are therefore recognised in GHG inventory calculation protocols (IPCC, 2006). Ultimately, much of the volatilised ammonia is assumed to be deposited from the atmosphere onto land and ocean surfaces. Data suggest that some of this deposition can be relatively close to the source. For example, ammonia volatilisation from cattle feed yards results in adjacent nitrogen deposition, sometimes peaking within 75 m of the source (Todd et al., 2008b). However, it appears that most of the volatilised ammonia (90%) is advected away from the source. In one study only 10 % was deposited (dry deposition) within 4 km of the source

(Staebler et al., 2009). This estimate was similar to those of a previous study, where 3 to 10 % of volatilised ammonia from a poultry shed was observed to be deposited within 300 m of the source (Fowler et al., 1998).

The factor for secondary N₂O emissions from deposited ammonia employed by the IPCC, 0.01 [kg N₂O-N][kg NH₃-N volatilized]⁻¹ (IPCC, 2006), was based on a limited range of northern hemisphere studies. Two key studies involved the measurement of N₂O emission from forest soils in Germany (Butterbach-Bahl et al., 1997; Brumme et al., 1999), another included a literature review and calculations based on Netherlands-specific scenarios (Denier van der Gon and Bleeker, 2005). Within the inventory guidelines (IPCC, 2006) there is recognition that low deposition rates lead to low indirect emissions rates (based on measurements from low ammonia depositions in Canada; Corre et al., 1999), and a lower emission factor may be appropriate. The accuracy of this approach for varied agricultural systems in other locations is unknown, and all of the cited studies assumed ammonia deposition rates based on literature values (Pratt et al., 2014). However, actual measurement of ammonia deposition rates suggests that these rates exhibit large spatial variability. This variability may be dependent on the proximity to land uses that are strong volatilisation sources e.g. industrial processes, intensive livestock production, and sewage treatment (IPCC, 2006).

However, deposition rate is unlikely to be the only controlling influence on these indirect N₂O emissions. A wide range of geochemical factors are known to influence the microbial communities ultimately responsible for N₂O emission from soils. These include soil moisture, temperature (Dobbie and Smith, 2001a), oxygen supply, decomposable organic matter content, pH, and salinity (as reviewed by Dalal et al., 2003).

There is an unfilled niche for a systematic investigation of the influence of low-magnitude ammonia deposition (rates that reflect common ammonia deposition of volatilised NH₄⁺-N in agricultural landscapes) and soil moisture conditions on N₂O emission intensity. This investigation seeks to fill this niche through the collection of high-resolution, laboratory-based data that demonstrates the interrelationship between moisture content, ammonia deposition, and their combined effect on N₂O emission for two soils. Subsequently these data are compared to field collected data. Our hypothesis is that the described influence of ammonia deposition rate (IPCC, 2006), and moisture content (Linn and Doran, 1984; Bouwman, 1998) on N₂O emission forms a continuous relationship that can readily be characterised by an equation. The hypothesised equation, based on a previously published model (Xu et al., 1998), relates N₂O emission to ammonia deposition and moisture content (via a stress function, ranging from 0-1). Our studies also revealed several management approaches relating to ammonia deposition or fertiliser use that will likely decrease indirect N₂O emissions.

5.3 Materials and methods

5.3.1 Soil samples

Two soils representative of the surface 0.01 m of the profile were selected for the study, both from the Darling Downs of Queensland, but of very different character. The sandy soil was collected from the A horizon of a Natrustalf (Soil Survey Staff, 1998), and is classified as a Grey Sodosol soil in the Australian Soil Classification (Isbell, 2002). A self-mulching expanding clay soil, typical of the highly productive broad acre cropping areas of the Darling Downs was also collected. This soil was classified as a Vertisol (Soil Survey Staff, 1998) and a Black Vertisol using the Australian Soil Classification (Isbell, 2002; note the different spellings used by the different classification systems).

Soil samples were sieved to pass a 2 mm mesh, and retained in the field moist condition.

The following analytical techniques as set out in Rayment and Lyons (2011) were applied to the two soil samples collected: pH in 1:5 soil:water suspension (Method 4A1); electrical conductivity (EC; Method 3A1); 2 M KCl extractable ammonium-N (NH_4^+ -N) and nitrite+nitrate-N by steam distillation ($\text{NO}_3^- + \text{NO}_2^-$ -N; Method 7A1); total N and total C by Dumas high temperature oxidation (Method 7A5 and 6B2b); organic carbon (OC) content by the method attributed to Walkley and Black (1934; Method 6A1); cation exchange capacity via alcoholic 1 M ammonium chloride (Method 15C1); particle size analysis of the soil samples was carried out using the hydrometer method described by Gee and Bauder (1986); moisture content was determined at 105°C and reported on dry basis. in Gee and Bauder (1986); moisture content was determined at 105 °C and reported on dry basis.

Surface soil (0.01m) bulk density was estimated from repacked bulk density. Saturated water content was determined by slowly immersing a 500 ml Buchner funnel filled with the soil in distilled water, until the water level was coincident with the surface of the soil. The soil remained immersed for 8 hours before the moisture content was determined based on the final weight less dry weight of the soil and Buchner funnel. This method allowed the clay soil to expand in response to the presence of water, allowing an estimate of 100 % water filled pore space (WFPS).

5.3.2 Gas sampling and analysis apparatus

Two analysers were employed to obtain gas concentration data: a prototype FTIR closed path analyser (subsequently commercialised as a Spectronus FTIR Analyser) and a Cavity Ring Down Spectrophotometer (Picarro model 2130) allowed on-line analysis for CO_2 and N_2O (one analysis minute⁻¹) and NH_3 (30 second average values delivered every half second).

Sample gas was supplied to these analysers at a flow rate of 2.5 l min⁻¹ (all flow rates and gas volumes standardised to 101.325 kPa and 25°C °C), via an automated gas flow manifold and a vacuum pump (12 V KNF diaphragm vacuum pump; www.knf.com). This flow manifold (Fig. 5.1) was constructed to deliver gas samples sequentially from 32 vessels, by opening and closing inlet and outlet valves (a total of 64 SMC solenoid valves; www.smcusa.com). The 64 solenoid valves were controlled by a single board computer (Technologies Systems Embedded Arm TS4200-8160; www.embeddedarm.com) using four 8-relay boards (Technologies Systems TS-Relay8). Gas flow was controlled by mass flow controller (Alicat MC series 10 litre capacity; www.alicat.com) with flow rate set by the single board computer via serial communications (RS232 interface).

The valve sequencing and MFC flow control were accomplished via python programming (Python Software Foundation, 2014), based on timing (correction via network time protocol) and serial communications from Spectronus's valve control (RS485 protocol).

A supply of sweep gas was connected in common to all 32 inlet valves (Fig. 5.1). For our experiments, ambient air was drawn through a 21 l mixing drum to the sweep gas inlet.

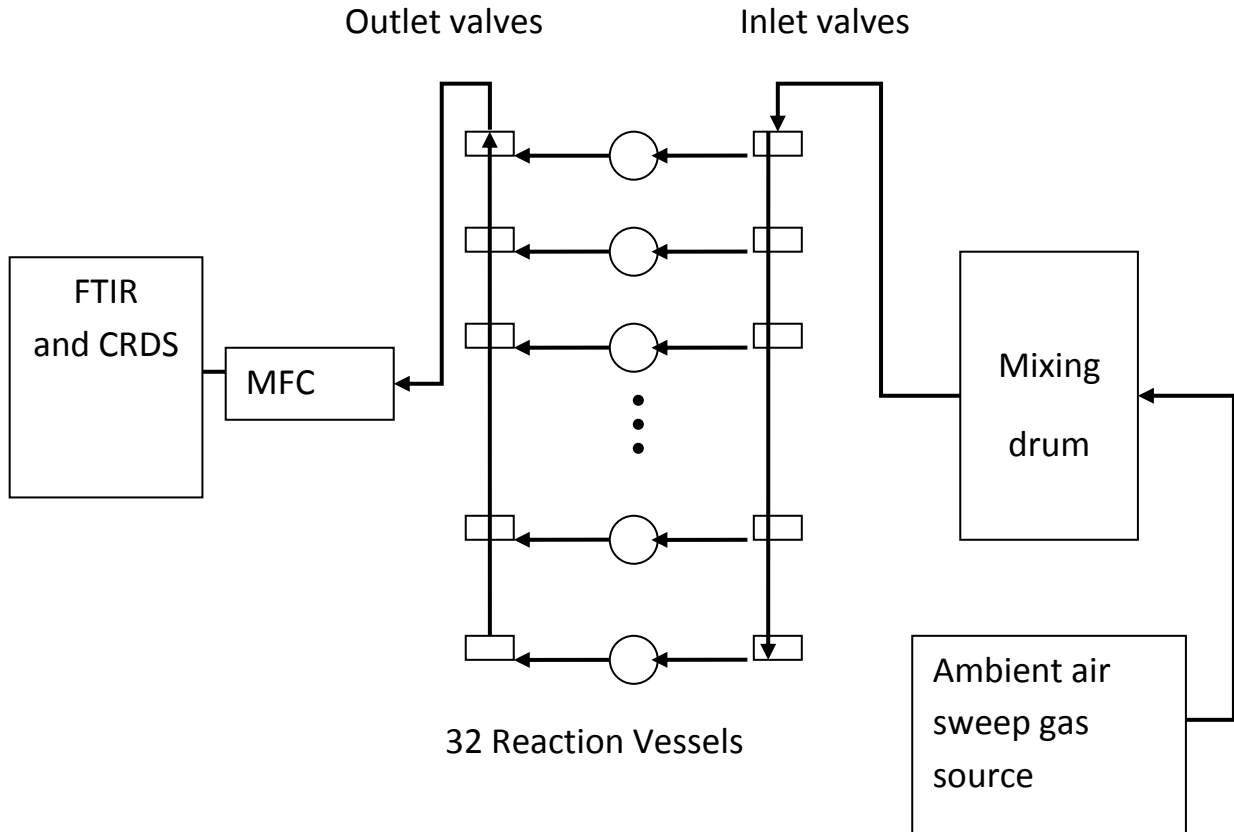


Figure 5.1. Gas sampling and analysis layout. The system consists of a common sweep gas source (in this case ambient air), an array of inlet solenoid valves, reaction vessels, and outlet solenoid valves (32 of each), leading to a Fourier Transform Infrared Spectrophotometer (FTIR) and a Cavity Ring Down Spectrophotometer (CRDS). Flow rates (via mass flow controller; MFC) and switching are controlled by a single board computer (Redding, In Review).

5.3.3 Experimental design

In summary the treatment for each soil represented a wide range of NH_4^+ deposition rates, using two starting moisture contents. These were allowed to subsequently pass through a drying cycle providing emission measurements corresponding to a wide range of moisture contents (20 to 100 % WFPS) and mineral N contents.

Treatments were selected to be representative of from 0 to 30 kg of NH_4^+ -N deposited ha^{-1} (assuming deposited N is retained in a soil depth of 0.01 m), with particular attention to collecting high-resolution data at lower application rates. In practice this involved applications of 0, and 0.000169 to 0.0202 g N NH_4^+ -N rising in a geometric series. These treatments, in the form of ammonium chloride solution, were applied to 64 g of the clay soil and 84 g of the sandy soil (based on bulk density of the surface of the self-mulching vertosol of 0.95 kg l^{-1} ; and 1.24 kg l^{-1} for the sandy sodosol soil) in 92 mm diameter cylindrical reaction vessels. Solution concentrations were formulated such that additions raised the WFPS of the soils to the targeted water contents (65 and 100 % WFPS; 0 kg of NH_4^+ -N ha^{-1} plus 14 deposition levels for 100 % WFPS treatments, 0 kg of NH_4^+ -N ha^{-1} plus 15 deposition levels for the 65 % WFPS treatments). Each soil was examined in separate experiments, with one reaction vessel remaining empty to provide a blank (31 vessels with treated soil + blank).

Room temperature was controlled to $25 \pm 2^\circ\text{C}$, and bottle mass was monitored to assess the moisture content of each vessel every second day. Valve sequencing was set to allow sweep gas through each vessel for 10 minutes, followed immediately by 10 minutes of flow through the blank (640 minute cycle), with flow set to $3.0 \text{ l minute}^{-1}$. The measurement cycle was commenced a day before treatments and soils were added to the vessels, and continued for a sufficient period for drying processes to allow emission measurements to be collected from saturated to air-dry soil conditions (37 days for the clay soil, 25 days for the sandy soil).

5.3.4 Emission modelling

Nitrous oxide emission processes were investigated in soil via modification of an existing soil process-based model (Water and Nitrogen Management Model; WNMM) (Xu et al., 1998; Li et al., 2007), selecting suitable parameters to better represent the system.

Following Xu et al. (1998), with the temperature term removed, the total rate of N_2O emission ($\mu\text{g} [\text{g soil}]^{-1} \text{ min}^{-1}$) can be described by:

$$q_{\text{N}_2\text{O}} = k_D f_W(W), \quad [1]$$

where k_D is the first-order emission coefficient and is determined by soil organic matter content, soil drainage, tillage applied, presence of manure, climate, the occurrence of pans and $f_W(W)$ is a water stress function (ranging from 0-1) representing the effects of water stress via a relationship with the fraction of water filled pore space (W). Our function $f_W(W)$ is:

$$f_W(W; \mu_W, \alpha, \beta) = N(W; \mu_W, \alpha, \beta) / N(0; 0, \alpha, \beta),$$

$$N(W; \mu_W, \alpha, \beta) = \frac{\beta}{2\alpha\Gamma(1/\beta)} \exp\left(-\left(\frac{|W - \mu_W|}{\alpha}\right)^\beta\right), \quad [2]$$

where W is the WFPS (as a fraction) and $N(W; \mu_W, \alpha, \beta)$ is the generalised normal distribution with mean μ_W and variance $\sigma_w^2 = \alpha^2\Gamma(3/\beta)/\Gamma(1/\beta)$, where Γ is the gamma function (α, β are the scale/shape parameters respectively). This equation also ensures that $f_W(W; \mu_W, \alpha, \beta) = 1$ when $W = \mu_W$. Note that when $\beta = 2$, Eq. [2 line 2] reduces to the normal distribution. The moisture fraction for peak emission is μ_W .

The effect of soil nitrate on the total rate of N_2O emission ($\mu\text{g} [\text{g soil}]^{-1} \text{ min}^{-1}$) can be described by

$$q_{\text{N}_2\text{O}} = k_D f_W(W) [\text{NO}_3], \quad [3]$$

where $[\text{NO}_3]$ is the nitrate content of the surface soil ($\mu\text{g} [\text{g soil}]^{-1}$). An incremental development of this model (Eq. [3]) allows a nitrate-dependent effect on the fraction of water filled pore space for peak emission (μ_W), α, β and the threshold effect of $[\text{NO}_3]$ on the N_2O emission rate to be described:

$$q_{\text{N}_2\text{O}} = k_D f_W(W; \mu_W - c_1 E, \alpha + c_2 E, \beta + c_3 E) \frac{[\text{NO}_3]^M}{[\text{NO}_3]^M + K^M},$$

$$E = \frac{k_D [\text{NO}_3]^M}{[\text{NO}_3]^M + K^M}, \quad [4]$$

where k_D determines the maximum N_2O emission rate, μ_w is the fraction of water filled pore space for peak emission at low $[NO_3]$, α is the scale parameter for low $[NO_3]$, β is the shape parameter for low $[NO_3]$, c_1, c_2, c_3 describe the effect of $[NO_3]$ on the fraction of water filled pore space for peak emission, the scale parameter and the shape parameter respectively, K is the $[NO_3]$ for half-maximal N_2O emission and M determines the threshold effect of $[NO_3]$ on N_2O emission.

A model that incorporated both nitrification and N_2O emission was also developed to investigate the role of nitrification on emission and to characterise soils based on their emission potential. Mineral N was partitioned into pools of ammonium (A) and nitrate (N). The two pool model is described by the coupled ordinary equations:

$$\begin{aligned} \frac{dA}{dt} &= B\delta(t-t_0) - k_N A - g(t), & A(t=0) &= A_0 \\ \frac{dN}{dt} &= k_N A - k_D f_w(W)N, & N(t=0) &= N_0 \end{aligned} \quad [5]$$

where k_N is the rate of nitrification (day^{-1}), B is the concentration ($\mu\text{g} [\text{g soil}]^{-1}$) of added mineral N at time t_0 (day), $\delta(t)$ is the Dirac delta function, W is the fraction of water filled pore space, k_D is the first-order emission rate coefficient (day^{-1}), $f_w(W)$ is a water stress function (Eq. 2), $g(t)$ is the measured rate of ammonia volatilization, A_0 is the initial soil ammonium concentration ($\mu\text{g} [\text{g soil}]^{-1}$) and N_0 is the initial soil nitrate concentration ($\mu\text{g} [\text{g soil}]^{-1}$).

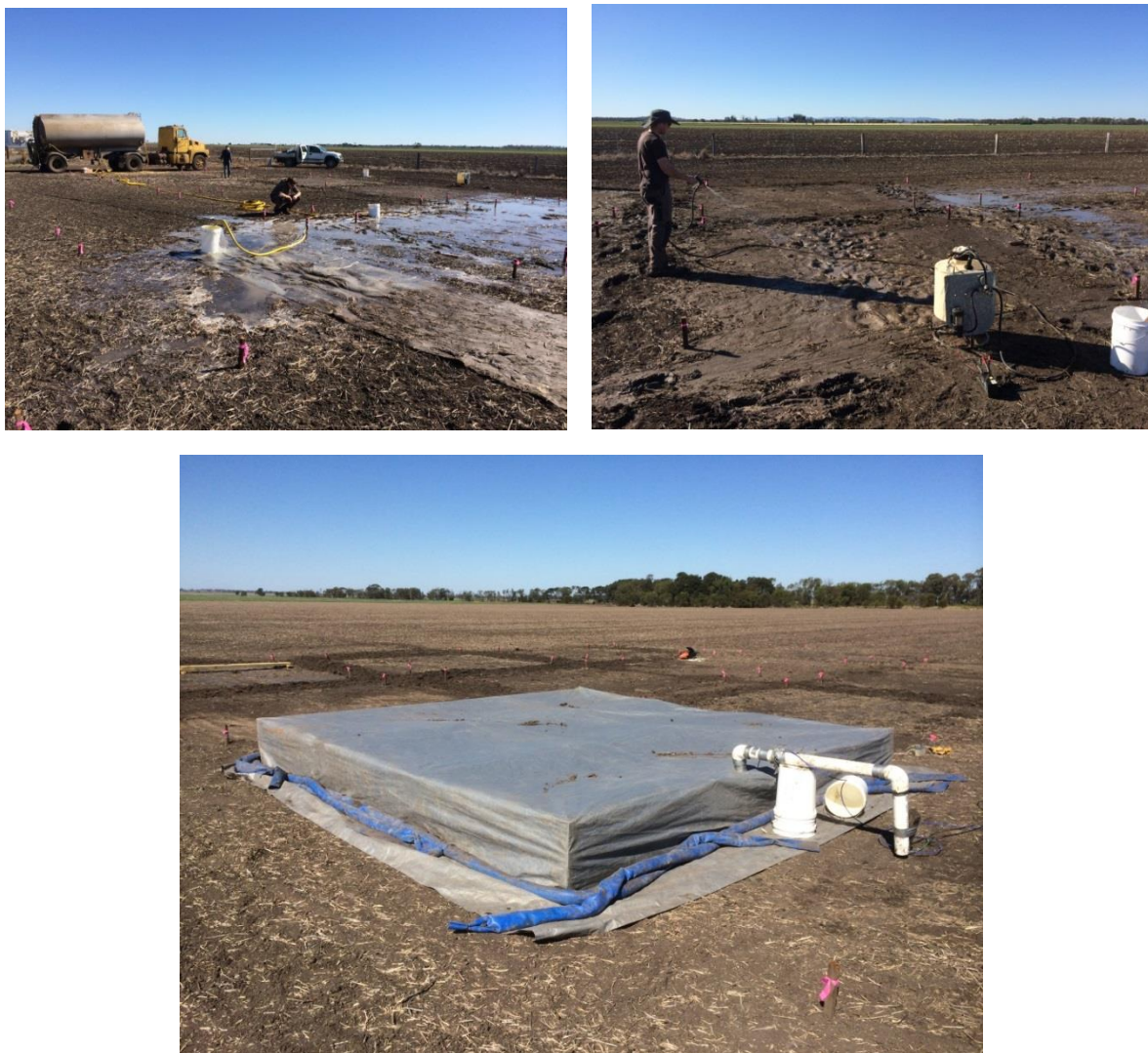


Figure 5.2. Field trial to investigate the relevance of the laboratory-based model.

5.3.5 Field validation

In order to test the performance of this model, a field trial was conducted involving 14 plots (4.3 x 4.3 m; Fig 5.2) with variable applications of water and nitrate (as potassium nitrate; treatment layout Table 5.1). An area was pegged out to provide a matrix of these plots (4 x 4) on the same soil type as the vertisol used for the development of the emission model. Treatments were allocated randomly (14) with two spare plots.

Water was pumped from a tanker, with 1200 L applied to the plots targeting 100 % WFPS, while 600 L was intended for plots targeting 65 % WFPS. Applications of water at the higher rate were made in separate 600 L additions. All final additions to plots were made on the same day, followed by treatment applications of N via spray pack (20 Litre solutions containing the treatment amount of KNO_3).

Emission measurements were conducted using a very large fabric-covered chamber previously validated to produce comparable emission estimates to the open air bLS technique (Redding et al., 2013), with one to two measurements per plot (plots 3, 5, and 16 only). Immediately after each chamber measurement, 12 soil cores (20 mm diameter, 0 to 75 mm depth interval) were collected. Each was analysed for moisture content, KCl extractable nitrate+nitrite-N, and KCl extractable NH_4^+ -N, (Rayment and Lyons, 2011).

In addition, four profile pits were also sampled per plot after emission measurements were completed to delineate the vertical distribution of water, added N, and soil characteristics. Samples were collected (0.3 x 0.3 m pit) from 0 to 5 mm, 5 to 15 mm, 15 mm to 35 mm, 35 to 55 mm. These samples were analysed as described for the cores, with the addition of pH, EC, and OC.

The distribution of moisture and NO_3^- -N down the profile was determined from the distribution of moisture determined from the profile sampling and the 75 mm core data. In addition the probability distribution of moisture contents was determined from the core data. These probability distributions provided the WFPS inputs to predict emission (Eq. [4], this chapter) for each plot. The predicted emissions were then compared to those measured using the chamber. In order to account for the divergence of the measurement conditions from 25°C, a temperature stress function (value 0 to 1) was applied to the data (Shaffer et al., 1991; Shorten and Redding, In Press; Shaffer et al., 1991):

$$f_T(T) = 1.68 \times 10^9 (\exp(-13.0 / [1.99 \times 10^{-3} (34.53 - |34.53 - T| + 273)])) , \quad [6]$$

Table 5.1. Treatment layout for field validation of the clay soil model. Water filled pore space (WFPS) values were targets only – and difficult to precisely achieve.

Plot	Treatment	Nitrate application kg N ha ⁻¹	WFPS
1	1	0	100%
10	1	0	100%
12	1	0	100%
16	2	0.25	100%
3	3	1	100%
2	4	4	100%
6	5	8	100%
11	6	16	100%
5	7	32	100%
9	8	0	65%
8	8	0	65%
15	8	0	65%
13	9	8	65%
14	10	32	65%

5.3.6 Statistics

Cumulative emission curves and parameter relationships for the collected data were fitted by non-linear regression (nls procedure in R, R Development Core Team, 2014). Surface splines and spline curves were fitted via loess techniques, each using R (nls procedure in R R Development Core Team, 2014). Models were fit to the nitrous oxide emission data using linear and nonlinear regression (Bates and Watts, 2007). Model residuals were analysed for homoscedasticity and normality. We assumed that the variances of the deviations in measurements within response variables were constant. Markov Chain Monte Carlo was used to determine the standard errors in the model parameters (Gilks et al., 1996b). Model fit was assessed using the correlation, slope and intercept between the predicted and observed emission rate (Pineiro et al., 2008). Pearson product moment correlation coefficient and Kendall's tau were used to describe the correlation between predicted and observed emission. Calculations were performed in R and MATLAB (The Mathworks Inc., 2012; R Development Core Team, 2014).

5.4 Results and discussion

In our study, resident treatment-N was approximated by treatment-N less the emission of $\text{NH}_3\text{-N}$ and $\text{N}_2\text{O-N}$. The losses of NH_3 from the treated samples ranged from a small to substantial proportion of the treatment additions (0.4 to 15 % for the high clay vertosol; 0.2 to 20 % for the coarse textured sodosol soil; contrasting characteristics of the two soils, Table 5.2). Mono nitrogen oxide (NO_x) losses were not measured during the trial, however default inventory values suggest that volatilisation of $\text{NH}_3\text{-N} + \text{NO}_x\text{-N}$ from synthetic fertiliser application ranges from 0.03 to 0.3 of the total N applied (Intergovernmental Panel on Climate Change, 2006). Other studies indicate that the magnitude of NO-N losses are of the same order of magnitude as $\text{N}_2\text{O-N}$ emissions (Sanz-Cobena et al., 2012; Abalos et al., 2013), and are likely small relative to losses observed due to ammonia volatilisation (Stehfest and Bouwman, 2006; Yang et al., 2010).

Cumulate emission curves and parameter relationships for the collected data were fitted by non-linear regression (nls procedure in R, R Development Core Team, 2014). Surface splines and spline curves were fitted via loess techniques, each using R (nls procedure in R R Development Core Team, 2014). Models were fit to the nitrous oxide emission data using linear and nonlinear regression (Bates and Watts, 2007). Model residuals were analysed for homoscedasticity and normality. We assumed that the variances of the deviations in measurements within response variables were constant. Markov Chain Monte Carlo was used to determine the standard errors in the model parameters (Gilks et al., 1996b). Model fit was assessed using the correlation, slope and intercept between the predicted and observed emission rate (Pineiro et al., 2008). Pearson product moment correlation coefficient and Kendall's tau were used to describe the correlation between predicted and observed emission. Calculations were performed in R and MATLAB (The Mathworks Inc., 2012; R Development Core Team, 2014).

Table 5.2. Soil characteristics

		The clay soil			The sandy soil		
pH		7.9	±	0.0	6.0	±	0.1
EC	dS m ⁻¹	0.21	±	0.00	0.03	±	0.00
NH ₄ -N	mg kg ⁻¹	2.33	±	0.25	0.81	±	0.08
NO ₃ -N	mg kg ⁻¹	33.86	±	0.47	2.43	±	0.32
Dumas N	%	0.114	±	0.008	0.03	±	0.00
Dumas C	%	1.17	±	0.01	0.22	±	0.05
Total Org C	%	1.29	±	0.04		-	
Sand	%	47.0	±	1.0	93.3	±	0.6
Silt	%	14.0	±	0.0	3.0	±	0.0
Clay	%	38.7	±	0.6	6.0	±	0.0
CEC	cmol kg ⁻¹	31.3	±	0.6	1.0	±	0.0

Emission values contributed a detailed three dimensional landscape representing N_2O emission's dependence on WFPS and mineral-N (Figs. 5.2 and 5.3). Emissions from the clay soil tended to peak from 85 to 93 % WFPS, increasing as mineral-N increased. Emissions of N_2O from the sandy soil peaked at a lower WFPS (about 60%). This relationship is consistent with observations regarding emission dependence on water filled pore space, which confirmed that emissions peak at relatively high moisture contents (Dobbie and Smith, 2001b; Dalal et al., 2003). For the clay soil, nitrification was almost complete at the end of the trial and N was dominantly in the form of NO_3^- (mean 95 %, range 50 to 100%). The results for the clay soil (Fig. 5.2) are consistent with the understanding

that N_2O emission requires a source of mineral-N, and this emission becomes more prevalent compared to N_2 emission with a greater supply of NO_3^- (Swerts et al., 1996; Ball et al., 1997; Dalal et al., 2003.Figures 5.3 and 5.4).

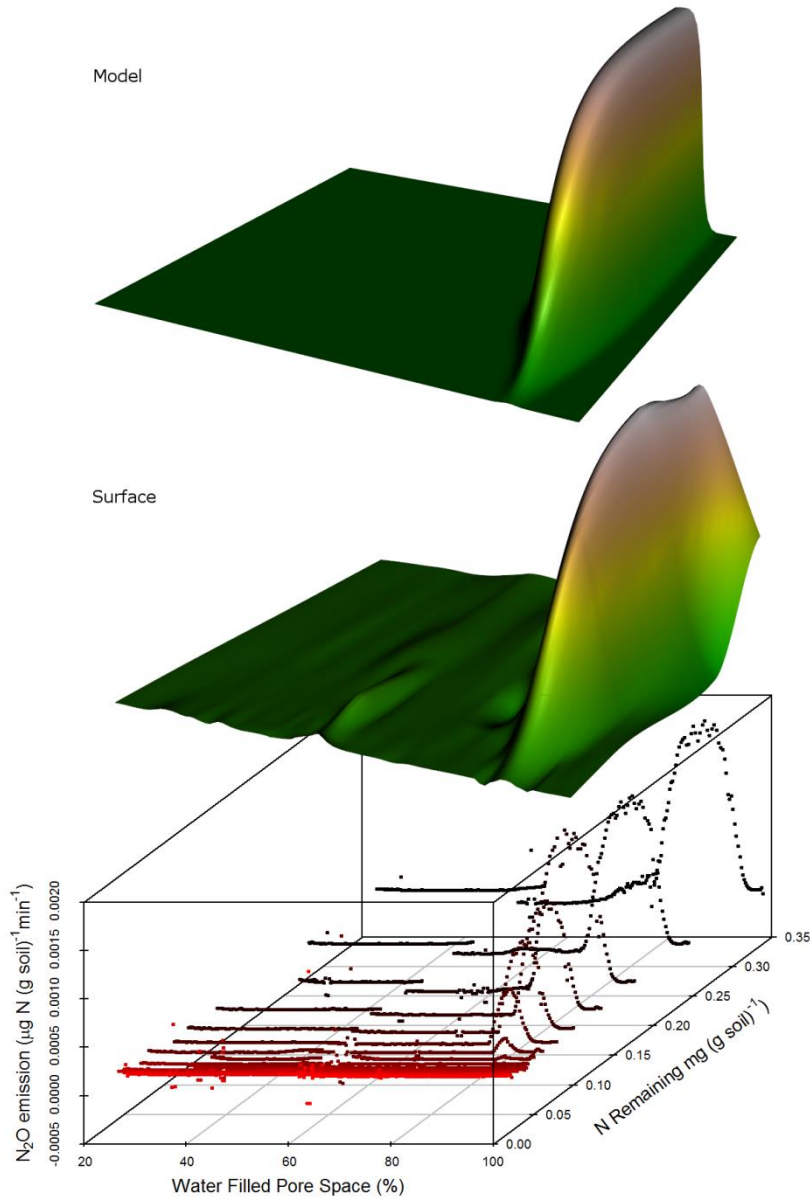


Figure 5.3. Measured relationship between soil moisture (WFPS), mineral-N, and N_2O emission for the clay soil. A smoothed surface (loess smoothing) is superimposed to assist visualisation, in addition to the Eq [4] fit (model predicted values). Closer values (lower remaining N) are more red (Redding, In Review).

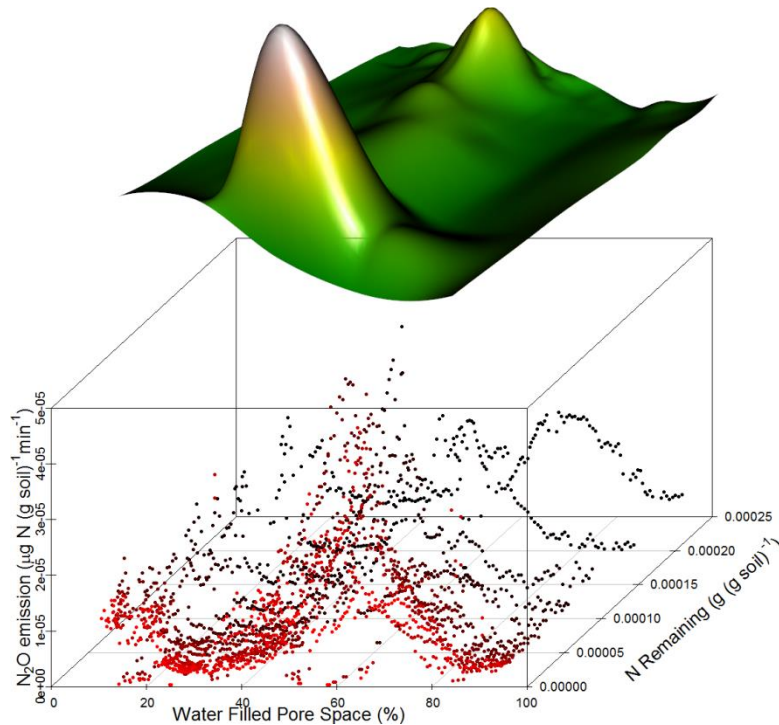


Figure 5.4. Measured relationship between soil moisture (WFPS), mineral-N, and N₂O emission for the sandy soil, illustrating much lower emissions than observed from the clay soil. A surface plot based on loess smoothing is superimposed to assist visualisation. Closer values (lower remaining N) are more red (Redding, In Review).

In contrast to the clay soil, there is no strong relationship between mineral-N addition (or resident mineral-N) and N₂O emission for the sandy soil. Unlike the clay soil, simulated deposition of NH₄⁺ resulted in little nitrification in the sandy sodosol soil. For the sandy sodosol soil 40 to almost 100% of the resident mineral-N persisted as NH₄⁺, and there was a strong relationship between added NH₄⁺-N and final NH₄⁺-N ($R^2 = 0.96$). Suppression of nitrification has previously been partly attributed to high ammonia concentrations (Anthonisen et al., 1976), and this in turn may have contributed to the low N₂O emissions from this soil (compare emission scales, Figs. 5.2 and 5.3). (Anthonisen et al., 1976), and this in turn may have contributed to the low N₂O emissions from this soil (compare emission scales, Figs. 5.4 and 5.5). The sandy soil is also lacking in organic carbon (Table 5.1), and may well be an environment that will not support extensive microbial activity. Emissions from the sandy sodosol soil (Fig. 5.4) are only a few percent of those from the clay soil, requiring analytical resolutions that were much closer to the limits of the FTIR instrument. It appeared that NH₄⁺ added to the sandy soil was unrelated to the final NO₃⁻ concentration ($P < 0.95$).

5.4.1 Toward an indirect emission factor algorithm

It was evident during application of Eq [1] and [2] that a good fit could only be achieved with this model by using a variable value of the emission coefficient (k_D , Eq. [1]), dependent on the moisture fraction for peak emission (μ_w), the scale parameter (α) and the shape parameter (β ; linear relationships, $P < 0.01$). In particular, it was apparent (Fig. 5.3) that a model that quantified the relationships between peak emissions and WFPS, and the effect of nitrate concentration on the magnitude of peaks may better suit the data. Equation [4] has both of these characteristics, and conforms reasonably closely to the observed emission threshold related to N remaining in the clay soil, where it is assumed that soil mineral N was retained entirely as NO₃⁻ (Figs. 5.3 and 5.5). The relationship between measured and

model-predicted N_2O emission from the clay soil is strong (Eq. [4]; $R^2=0.90$, $P<0.001$; Figs. 5.5 and 5.6). In this case, the estimated model parameters are $k_D = 0.00154 \pm 0.00018 \mu\text{g (g soil)}^{-1} \text{min}^{-1}$, $\mu_W = 0.896 \pm 0.016$, $\alpha = 0.0137 \pm 0.0062$, $\beta = 2.11 \pm 0.68$, $c_1 = 0.0313 \pm 0.0182$, $c_2 = 0.0434 \pm 0.0170$, $c_3 = 1.64 \pm 1.41$, $K = 1.11 \times 10^{-4} \pm 0.14 \times 10^{-4} \mu\text{g (g soil)}^{-1}$, and $M = 4.13 \pm 0.98$. Though Eq [4] does not conform closely to the observed NO_3^- -N concentration threshold for N_2O emission (Fig. 5.6), the statistical fit further confirms that this threshold is statistically significant (M is significantly greater than 1; $P < 0.01$).

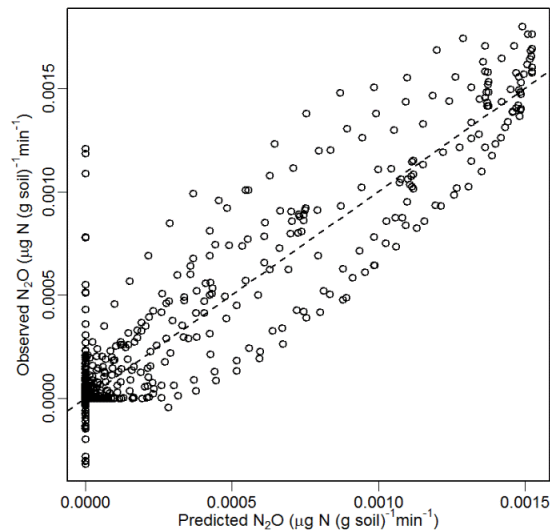


Figure 5.5. Relationship between measured and model-predicted N_2O emission (Eq. [4]) from the clay soil ($R^2 = 0.90$; Redding, In Review).

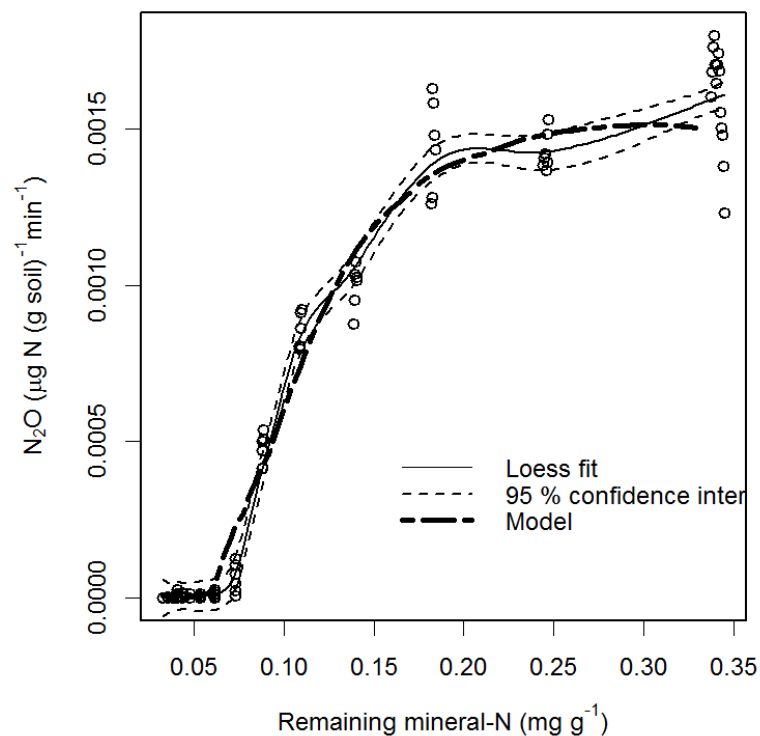


Figure 5.6. A Loess spline fitted to follow the peak values of the clay soil data (Fig. 5.3; peak $\text{WFPS} \pm 1\%$), illustrating that emissions do not significantly rise until $> 0.07 \text{ mg resident}$

mineral-N g^{-1} . The spline (span 0.3) is bracketed by lines representing the upper and lower confidence interval of the mean (95 %). The model (Eq [4]) has also been plotted (Redding, In Review).

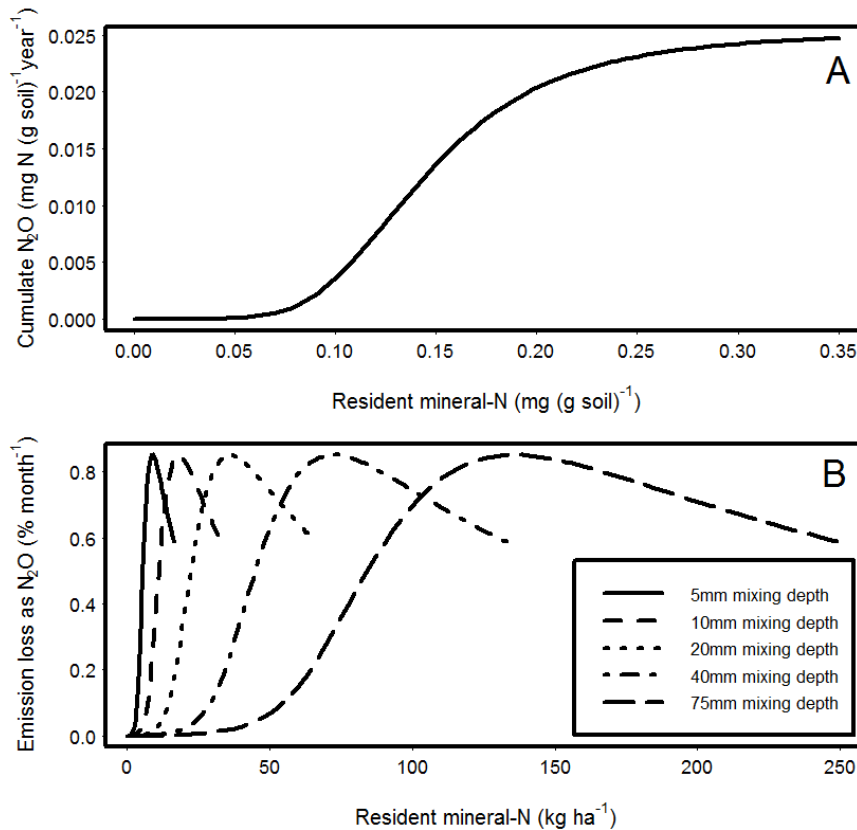


Figure 5.7. Maintaining lower surplus mineral-N in the soil decreases N₂O emissions (Redding, In Review). Application of Eq [4] to 12 months of clay soil moisture data collected from the field, for a range of resident mineral N values (panel A). This relationship is then applied to a range of hypothetical resident mineral-N scenarios and for different depths of homogenous mixing (panel B).

Nitrate-N concentrations in the clay soil were strongly dependent on the NH₄⁺-N treatment rate, and nitrification appeared almost complete. A WNMM-based model (Xu et al., 1998; Li et al., 2007) was therefore a sound choice. In contrast, oxidation of NH₄⁺-N to NO₃⁻-N in the sandy soil was much less complete, and Eq [4], provided unsatisfactory fits, probably because it assumed added (and pre-existing) mineral N was converted to NO₃⁻. Introducing a component to predict the degree of nitrification of mineral-N at a given point in time is perhaps the next step in producing a more generally applicable extension of Eq. [4]. Kendall's tau values for the relationship between N₂O emission and NO₃⁻ concentrations under peak emission conditions (WFPS 55 to 65 %) for the sandy soil suggested that emissions were significantly related to the final NO₃⁻ concentrations (tau 0.23, $P < 0.001$).

Though NO₃⁻-N concentrations were measured before treatment and at the completion of the experiment, progressive concentrations are not available. These initial and final data, however, provide an opportunity for a preliminary evaluation of the relationship proposed to predict NO₃⁻-N concentration (Eq. [5]). The model was fit to the combined 31 treatments for each soil. The estimated model parameters are $k_N = 0.91 \pm 0.26 \text{ day}^{-1}$, $k_D = 0.0084 \pm 0.0026 \text{ day}^{-1}$, $\mu_W = 0.875 \pm 0.008$, $\alpha = 0.054 \pm 0.012$, $\beta = 2.50 \pm 0.58$, $A_0 = 11.69 \pm 2.63 \mu\text{g (g soil)}^{-1}$ and $N_0 = 22.04 \pm 2.66 \mu\text{g (g soil)}^{-1}$ for the clay soil and $k_N = 0.00024 \pm$

$0.000048 \text{ day}^{-1}$, $k_D = 0.00019 \pm 0.000087 \text{ day}^{-1}$, $\mu_W = 0.63 \pm 0.02$, $\alpha = 0.22 \pm 0.05$, $\beta = 0.49 \pm 0.17$, $A_0 = 7.33 \pm 0.43 \mu\text{g (g soil)}^{-1}$ and $N_0 = 22.97 \pm 0.50 \mu\text{g (g soil)}^{-1}$ for the sandy soil. The rate of nitrification (k_N) is significantly greater in the clay soil than the sandy soil ($P < 0.001$) and the rate of N_2O emission (k_D) is 45 times greater in the clay soil than the sandy soil ($P < 0.01$). The moisture-dependent emission parameters (μ_W, α, β) are also significantly different between the clay soil and the sandy soil ($P < 0.01$).

Importantly, the relationships between predicted (Eq [5]) and observed NO_3^- -N concentrations at the end of the trial were strong for the clay soil ($R^2 = 87\%$, the clay soil) though less satisfactory for the sandy soil (fit not significant for the sandy soil, due to NO_3^- -N concentration being relatively close to zero). Final NH_4^+ concentrations were well predicted for the sandy soil ($R^2 = 98\%$, the sandy soil; fit not significant for the clay soil, due to NH_4^+ -N concentration being relatively close to zero). While these results are positive, further development of this model is required, preferably with incremental analyses of mineral-N species over time.

5.4.2 Clay soil field validation

Pre-existent nitrate concentrations at the site were extra-ordinarily high, and this had a detrimental effect on the experiment. However, a range of useful observations and associated conclusions were possible.

Emission data collected with the large chamber was quite strongly related to the predicted emission from the surface 5 mm layer using the laboratory model (predicted versus observed $R^2 = 62\%$; $P < 0.001$; Kendall's Tau = 0.67, $P < 0.001$). However, the emissions predicted from this layer were a small fraction of the emissions measured:

$$F_{obs} = F_{mod} \times (223 \pm 50) + 0.1 \pm 0.1, \quad [6]$$

where F_{obs} and F_{mod} are the observed and modelled emissions fluxes ($\mu\text{g N}_2\text{O-N m}^{-2} \text{ s}^{-1}$).

The relationships determined for the lower layers in the profile using both the layer nitrate concentration and moisture content as model inputs were not strong. However, assuming that the surface layer moisture content (0 to 5 mm depth) controlled oxygen entry into the profile produced a more convincing relationship where all studied profile layers were included (predicted versus observed $R^2 = 50\%$; $P < 0.001$; Kendall's Tau = 0.74, $P < 0.001$):

$$F_{obs} = F_{mod} \times (9.2 \pm 3.3) + 0.3 \pm 0.1 \quad [7]$$

Notably, the model estimates are still only a fraction of those observed. This, along with the behaviour of one outlier (removed from the data set, plot 6, Table 5.1) suggests that emission processes deeper in the profile ($> 75 \text{ mm}$) contribute significantly to emissions.

Applying the stress function for temperature resulted in a slightly worse fit for the surface 5 mm ($R^2 = 57\%$). This was probably as a result of a lack of a strong relationship between surface measured temperatures and the temperature within the soil profile where most of the N_2O was being formed.

We concluded that the laboratory model (eq. 6.4) is supported to some extent by the field data, with surface moisture contents controlling emissions. Emissions processes from deeper in the profile than studied are probably contributing very significantly to emissions.

Emissions from untreated soil were $0.42 \pm 0.43 \mu\text{g N}_2\text{O m}^{-2} \text{ s}^{-1}$ (6 replicates), where the surface 75 mm nitrate content was $77 \pm 22 \text{ mg NO}_3^- \text{-N [kg soil]}^{-1}$. These native emissions are relatively large compared to the maximal emissions collected (around 20% of the maximum emission measured in the trial). Scaling this result to the lower panel of Fig. 5.7, and assuming that the highest emission measured in the field corresponds to about 0.8 % of resident N month⁻¹, 20% of this emission would correspond to about 0.16 % of resident N month⁻¹. If deposited ammonia resides in the soil for one or two growing seasons, this would lead to losses of 0.48 to 0.96 % of resident N.

Our measurements suggest that emissions will likely be 0.48 to 4.8 % (using a 3 to 6 month period and maximal monthly emission of 0.8%).

Our data therefore suggests that the dry-land emission value of 0.3% of mineral-N (Environment, 2014) is not a suitable representation of deposition-related emissions from this site. However, it is equally clear that emissions are determined by profile mineral-N rather than mineral-N deposition rates.

5.4.3 Implications

Nitrous oxide emission from soil proceeds only during the process of nitrate or nitrite formation (nitrification emission) or following nitrification processes (denitrification, assimilatory nitrate reduction, and abiotic nitrate/nitrite reduction) (Dalal et al., 2003). The ammonia deposition simulated in our study aligns well with these findings: a sandy soil with little nitrate formation resulted in little emission, while a strongly nitrifying clay soil displayed strong emissions and a clear relationship between nitrate concentration and emission. Validation of a nitrification relationship (e.g. Eq [5]) would strengthen Eq [4]'s ability to predict the lower emissions from poorly nitrifying soils. However, using ammonia deposition as a surrogate for final nitrified mineral-N in Eq [4] is an effective representation of a worse-case scenario, in terms of emission losses.

Nitrous oxide emission from soil is also strongly related to soil moisture content. This is evident from published literature (Dobbie and Smith, 2001) and for both of the soils we studied.

Applying Eq [4] to the soil moisture data collected from the clay soil (Redding et al., 2015), moistures measured for 12 months at a depth of 75 mm using an in-soil moisture probe), enables prediction of emission factors for a range of resident mineral-N scenarios, conservatively assuming that all mineral-N occurs as NO_3^- and a temperature of 25°C (Fig 5.7). The calculations for this figure hinge on the assumptions that deposited mineral-N and moisture are distributed homogeneously to a specific depth (Fig. 5.7, panel B). While we are constrained by these caveats of the data set, it nonetheless provides a valuable example of how this type of model can be applied.

This exercise highlights the critical importance of the mixing depth of nitrate in the soil where Eq [4] is applied to calculate emissions from areas of land. While the profile distribution has been widely measured (e.g. Koehler et al., 2012), it is controlled by site-specific factors: management, climate, and variation with time and in space. Given a 75 mm homogeneous mixing depth of deposited $\text{NH}_4^+ \text{-N}$, the range of mineral-N concentrations modelled (Fig. 5.7, panel B) corresponds to 0 to 249 kg resident mineral-N ha⁻¹ (assuming soil upper cultivated layer bulk density is 950 kg ha⁻¹), with emission maximising as a proportion of resident mineral-N at around 130 kg ha⁻¹. Resident mineral-N of less than about 50 kg N ha⁻¹ would result in no significant indirect N₂O emission (the threshold effect; 70 mg [kg of soil]⁻¹, Figs. 5.6 and 5.7). A different scenario, with a mixing depth of 10 mm would result in emission maximising at a resident mineral-N concentration of about 20 kg ha⁻¹.

Human-influenced annual atmospheric N deposition values have been measured, finding that most of the NH_4^+ volatilised from these sources is likely to be advected away. In one study only 10 % was deposited (dry deposition) within 4 km of the source (Staebler et al., 2009). A preceding study found that as little as 3 to 10 % of volatilised ammonia from a poultry shed was deposited within 300 m of the source (Fowler et al., 1998). In these scenarios, the advected plume of dispersing NH_4^+ may be re-deposited to the wider landscape, which will include a mosaic of less fertile areas and more intensively managed agricultural land. This diluted deposition would result in emissions that may be largely dependent on the soil initial NO_3^- -N status rather than the deposition rate. Where deposition occurs to the clay soil resulting in resident mineral-N of less than 70 mg kg^{-1} , negligible N_2O emission will result (under the conditions investigated).

Close to the source, higher ammonia deposition rates are observed. Within 700 m of a poultry barn deposition of 42 to $68 \text{ kg N ha}^{-1} \text{ year}^{-1}$ has been observed (Berendse et al., 1988). Based on deposition traps sited immediately downwind of four beef feedlots (7 to 14 day measurements), deposition of 29 to $172 \text{ kg N ha}^{-1} \text{ year}^{-1}$ was observed (McGinn et al., 2003). Average deposition within 400 m of a feedlot, based on several aerial surveys, was estimated at equivalent to $254 \text{ kg N ha}^{-1} \text{ year}^{-1}$ (Staebler et al., 2009). In another feedlot study, deposition was < 49 within 550 m of beef feedlot boundary, maximising at 75 to $106 \text{ mg N m}^{-2} \text{ day}^{-1}$ (Todd et al., 2008b). Given that 90% of the volatilized NH_4^+ is advected away (and perhaps ultimately deposited over a much larger area), these values probably over-estimate the median deposition rates.

This model and our observations suggest a range of emission mitigation opportunities. Maintaining lower surplus mineral-N in the soil decreases N_2O emissions, and has potential to completely eliminate emissions below the threshold value for the clay soil ($70 \text{ mg [kg of soil]}^{-1}$). Plant uptake (including crops and managed pastures) would constantly act to decrease the mineral-N resident at any time, and may provide a viable and cost-effective tool to decrease emissions.

This discussion of scenarios is a simplification. Peak emission moisture conditions at this site are concentrated in the summer months. Also, where temperatures are substantially different, a temperature-dependent extension is required, or calibration for a specific temperature range. A raft of approaches are likely to be effective in this respect (e.g. Shaffer et al., 1991; Xu et al., 1998).

While based directly on experimental observations, these relationships are out of step with the inventory approach (IPCC, 2006). The inventory uses a linear emission factor multiplied by the magnitude of total N in the system for both direct and indirect emissions. Wider validation of the modelling approach described here (Eq [4]) may allow more rigorous, country-specific determination of the IPCC emission factors for both direct and indirect emissions.

The cumulative emission values (Fig. 5.7) maximise at greater than the default inventory estimate (1 % of deposited N emitted as N_2O , Intergovernmental Panel on Climate Change, 2006; 0.3 % of deposited N emitted as N_2O , Environment, 2014), while the lower range values are effectively zero. The combination of three assumptions leads to an outcome where emission would always be less than the default IPCC inventory estimate (actually < 1.02 % of deposited N emitted as N_2O , annually; Fig. 5.7). This would be the case where, firstly, deposition from the advected proportion of the volatilised ammonia occurs to the clay soil at cumulative concentrations less than the emission threshold ($70 \text{ mg [kg of soil]}^{-1}$). In combination with this, deposition in the proximal feedlot zone is assumed to be $< 10\%$ of the total volatilised. The final required assumption is that the soil of the proximal zone has characteristics that result in equivalent (or less) nitrification activity and emission potential than the clay soil.

Conversely, if more than 65 kg of N ha⁻¹ is resident in the surface 75 mm of soil for half the year emissions from these areas are unlikely to be less than 1.2 % given the prevailing moisture contents variation at this site (Fig. 5.7). This seems quite likely for locations with a productive cropping history. Indeed a single rainfall event could generate these losses.

An improved management-responsive approach to inventory estimation would achieve more than improved calculation accuracy. Such an approach may also provide an incentive for improved management. The model fitted here (Eq [4]) suggests that for a range of management scenarios and region-specific conditions emissions are likely to be larger or less than indicated by the inventory emission factor (1 % of deposited N emitted as N₂O, IPCC, 2006). This type of simple modelling approach could form the basis of a more region-specific and management responsive inventory protocol.

Our data also suggests that the dry-land N₂O emission value of 0.3% of mineral-N (Environment, 2014) is not a suitable representation of deposition-related emissions from this site.

5.5 Conclusion

Emission values contributed a detailed three-dimensional representation of the dependence of N₂O emissions on WFPS and mineral-N. Emissions from the vertisol clay soil peaked at less than 0.002 µg N [g soil]⁻¹ min⁻¹ when WFPS was 85 to 93%, increasing as resident mineral-N increased, up to a plateau. Emissions of N₂O from the sandy soil peaked at a lower value than the clay soil, less than 5 x 10⁻⁵ µg N [g soil]⁻¹ min⁻¹. Peak N₂O emissions occurred when WFPS was about 60%, with an indistinct relationship with resident mineral N. This difference was associated with strong conversion of added NH₄⁺ to NO₃⁻ in the clay soil, but poor conversion in the sandy soil.

A process-based, mathematical model incorporating a relationship involving soil NO₃⁻ (where all added NH₄⁺ was assumed to be nitrified) and a moisture stress function was well suited to the clay soil data (R² = 90%). This function was not well suited to the sandy soil, where nitrification was much less complete. Preliminary investigations of a relationship representing mineral-N pools (NO₃⁻ and NH₄⁺) was conducted but further investigation is required.

A “threshold effect” was observed in the vertisol (the clay soil) where resident mineral-N did not result in increased N₂O emissions until concentrations exceeded a threshold concentration (about 70 mg [kg of soil]⁻¹), indicating potential for managements that minimise N₂O emission. For example, via minimising additional fertiliser applications where ammonia deposition may satisfy crop needs. This may have applications for fertiliser management, beyond the implications considered here for ammonia deposition.

In a field validation exercise, model- predicted emissions were strongly related to field emissions, though the observations suggested that most of the emissions originated from below the profile depth investigated via soil sampling (0 to 75 mm).

The model (Eq [4]) fitted to the clay soil data suggests that in a range of scenarios emissions can be greater than or substantially less than indicated by the current inventory approach, under different regional and management conditions. This more management-responsive emission calculation approach could provide a more effective incentive for improved nutrient management.

6 The extent of ammonia volatilisation and deposition to the landscape (manuscript prepared for submission)

M.R. Redding^a, P. Shorten^b, R.L. Lewis^a, O. Smith^a, C. Pratt^a, J. Hill^a

^aDAF, ^bAgResearch New Zealand

6.1 Summary

At intensive livestock enterprises, excreted N is vulnerable to volatilisation, and subsequently may form a source of indirect nitrous oxide (N₂O) emissions. This study sought to continuously measure volatilisation and deposition of N at a beef feedlot over a 5-month period of time. Volatilisation measurements were conducted using a single, heated, air sampling inlet centrally located in a feedlot's pen area and analysis for ammonia (NH₃). Deposited mineral-N was determined via two transects of soil deposition traps with samples collected and re-deployed every two weeks. Total ammonia volatilised amounted to 210 tonnes of NH₃-N (110 g animal⁻¹ day⁻¹), suggesting that the inventory volatilisation factor (30% of excreted N) probably underestimates volatilisation in this case. Deposition within 600 m of the pen boundary represented only 1.7 to 3.2 % of volatilised NH₄⁺-N, between 3.6 to 6.7 Mg N. Beyond this distance deposition approached background rates.

Ammonia volatilization and subsequent indirect emission of nitrous oxide-N probably represents around 0.012 kg N₂O-N/(kg of N excreted). This estimate assumes 5% infrastructure area within 600 m of the feedlot with no effective N uptake by plants, 0.01 kg N₂O-N/(kg of N deposited on cultivated land), and 0.6 kg of NH₄⁺-N volatilised/(kg of N excreted)... Minimising the unproductive infrastructure areas at the edge of the feedlot in new feedlot designs, instituting good nutrient management practices and crop or pasture production on the feedlot boundary may effectively eliminate much of the indirect N₂O emission from this area. The decrease to overall emissions may be small.

Further from the feedlot, N deposition likely occurs at rates that are small relative to the nutrient requirements of the cultivated land that tends to surround Australian feedlots. The benefits of what is effectively a low-embodied-emission fertiliser application to these areas accrue to the landholder, while the emissions are attributed to the emitter.

6.2 Introduction

Volatilised ammonia has the potential to form nitrous oxide (N₂O), and though ammonia itself is not a greenhouse gas (GHG) it is recognised as an indirect source of GHG emissions in inventory calculation protocols (Intergovernmental Panel on Climate Change, 2006). A wide range of human production systems and activities are sources of volatilised ammonia including animal production (intensive and extensive), sewage treatment, and manure or inorganic fertiliser application to land.

About 65 % of atmospheric ammonia (NH₃) is derived from livestock manure that is exposed to air (National Research Council, 2002). When beef cattle are involved, much of this ammonia is derived via the hydrolysis of the urea in urine, the N form that makes up ≈50 % of the N excreted (Viets, 1970; Mosier et al., 1973).

Estimates of losses of excreted N via ammonia volatilisation vary widely. An early estimate suggested losses of about 50 % due to runoff, volatilisation, and denitrification before manure removal from the pen (Eghball and Power, 1994). A more recent measurement of NH₃ volatilisation from an Australian feedlot calculated that these losses amounted to about

60% of that excreted (Denmead et al., 2008), and in another study at the same location, greater than 90% (Loh et al., 2008a; both > 60% of dietary N).

Early studies of ammonia volatilisation from beef feedlots focussed on air concentrations of ammonia, observing the concentration profile from immediately adjacent beef feedlots to up to a kilometre distant (McGinn et al., 2003). There is also a limited body of data on fluxes of volatilisation from intensive livestock production systems. One study of a Texan beef feedlot found annual NH_3 volatilisation of around 19.3 kg NH_3 per animal on feed (39 days of measurement spread throughout 3 years)(Todd et al., 2008a). Measurement of volatilisation from a southern Alberta feedlot were around 89 kg head⁻¹ year⁻¹ (Staebler et al., 2009) or 53 kg head⁻¹ year⁻¹ (McGinn et al., 2007). A study involving backgrounding and finishing beef steers on varied diets at a Canadian feedlot observed ammonia volatilisation of 4.3 to 76.3 g N (steer-d)⁻¹ (annualised to 2 to 34 kg head⁻¹ year⁻¹)(Koenig et al., 2013).

Ultimately, much of the volatilised ammonia is assumed to be deposited from the atmosphere onto land and ocean surfaces. Two processes are commonly responsible: wet and dry deposition. Wet deposition occurs via in-cloud processes (rain clouds) or through wash out of the atmosphere via rain – and subsequent deposition to the land surface and the surfaces of plants. The relative importance of these processes appears clear (Krupa, 2003): wet deposition dominates where atmospheric concentrations are low, while dry deposition dominates where these concentrations are high, e.g. close to a major source of contamination.

Several published studies suggest that some of this deposition can be relatively close to the source, while much of the volatilised ammonia is advected away. As little as 10 % of volatilised ammonia was deposited (dry deposition) within 4 km of the source in one study (Staebler et al., 2009). A preceding study found that only 3 to 10 % of volatilised ammonia from a poultry shed was deposited within 300 m of the source (Fowler et al., 1998). In these scenarios, the advected, possibly dilute, plume of dispersing NH_4^+ may be re-deposited to the wider landscape.

However, close to the source, higher deposition rates have been observed. Within 0 to 700 m of various volatilisation sources, deposition rates of up to 254 kg N ha⁻¹ have been observed (Berendse et al., 1988; McGinn et al., 2003; Todd et al., 2008a; Staebler et al., 2009).

It is currently unclear how consistent the deposition and volatilisation flux estimates are, as simultaneous volatilisation flux measurement and deposition measurements are largely lacking in the literature. One of the studies summarised above used on-going ammonia volatilisation measurements via open path laser and three flights of an air-borne analyser through the plume to calculate estimates of both volatilisation fluxes and dry deposition (Staebler et al., 2009).

Our study differs from those others summarised here in that deposition and volatilisation are simultaneously measured for a moderately long, almost continuous period (continuous for 4 months, with an additional prior measurement period of 1 month). Additionally these deposition measurements are collected in a southern hemisphere (Queensland, Australia) environment not previously subject to study to our knowledge. Our hypothesis is that only a small proportion of volatilised NH_3 from a feedlot source is deposited in close proximity to its boundaries, and that volatilisation losses are in agreement with recent measurements (50 to 90+ % of excreted N) rather than the inventory estimate (30 % of excreted N; Intergovernmental Panel on Climate Change, 2006). We also describe the relationships between fluxes and deposition and several potential controlling factors (wind speed, temperature, rainfall, and manure moisture).

6.3 Materials and methods

6.3.1 Site selection

Measurements were at an Australian feedlot, located on the Darling Downs in Queensland. This location has an average, summer-dominated rainfall of 634 mm, and an annual average temperature of 25°C. Cattle on-feed were recorded daily for the study period (a short trial period from 1/2/2013 to 2/03/2013 and a longer campaign 12/02/2014 to 17/06/2014) by the operators and the data made available for the purposes of this study (average 12 779, minimum 10 201, maximum 15 373). The enterprise is sited on a uniform self-mulching expanding clay soil, typical of the highly productive broad acre cropping areas of the Darling Downs. This soil was classified as a Vertisol (Soil Survey Staff, 1998) and a Black Vertosol using the Australian Soil Classification (Isbell, 2002).

6.3.2 Site instrumentation and calculated manure condition

Instrumentation was largely located in a clear area between the pens themselves (Fig. 6.1), and within 60 m of the calculated centroid of the pen area. Wind data were monitored using a sonic anemometer (CSAT 3d, Campbell Scientific; <https://www.campbellsci.com.au/csats3>), air temperature logged from a shielded probe (HMP45 C, Vaisala; <http://www.vaisala.com>), and rainfall was recorded via a tipping bucket rain gauge (<http://odysseydatarecording.com/>). Additional data for the site were reported in two other studies conducted at the site over an overlapping period where manure emissions were measured and modelled (Redding et al., 2015; Shorten and Redding, In Press). This study also refers to publicly available air temperature, rainfall, humidity and evapo-transpiration data for the site (Bureau of Meteorology, 2014), using these data in conjunction with air temperatures and rainfall measured on-site to model manure moisture (Shorten and Redding, In Press).

6.3.3 Ammonia sampling and measurement

A filtered air sampling intake (Mykrolis cartridge filter, catalog number WGFG21KP3) was located at the height of the top of the pen rail within 60 m of the centroid of the total pen area (shaded portions Fig. 6.1). A stainless steel sample line led 10 m to the instrument enclosure. Nickel-chromium wire was coiled around the entire length of the stainless steel intake line, and the air stream temperature maintained at 60°C via a DC current flow and proportional integral differential controller (<http://novusautomation.co.uk/>) in order to decrease sorption of ammonia to the walls of the sampling tube. The intake tubes were insulated to prevent excessive heat-loss using domestic pipe lagging.

Sample air was drawn into the intake at a flow rate of 2.5 l min⁻¹ (flow rates controlled by Alicat MC series 10 litre capacity; www.alicat.com; gas volumes standardised to 101.325 kPa and 25°C), via a vacuum pump (12 V KNF diaphragm vacuum pump; www.knf.com).

Analyses for NH₃ were conducted using a Cavity Ring Down Spectrophotometer (Picarro model 2130) (30 second average values delivered every half second).

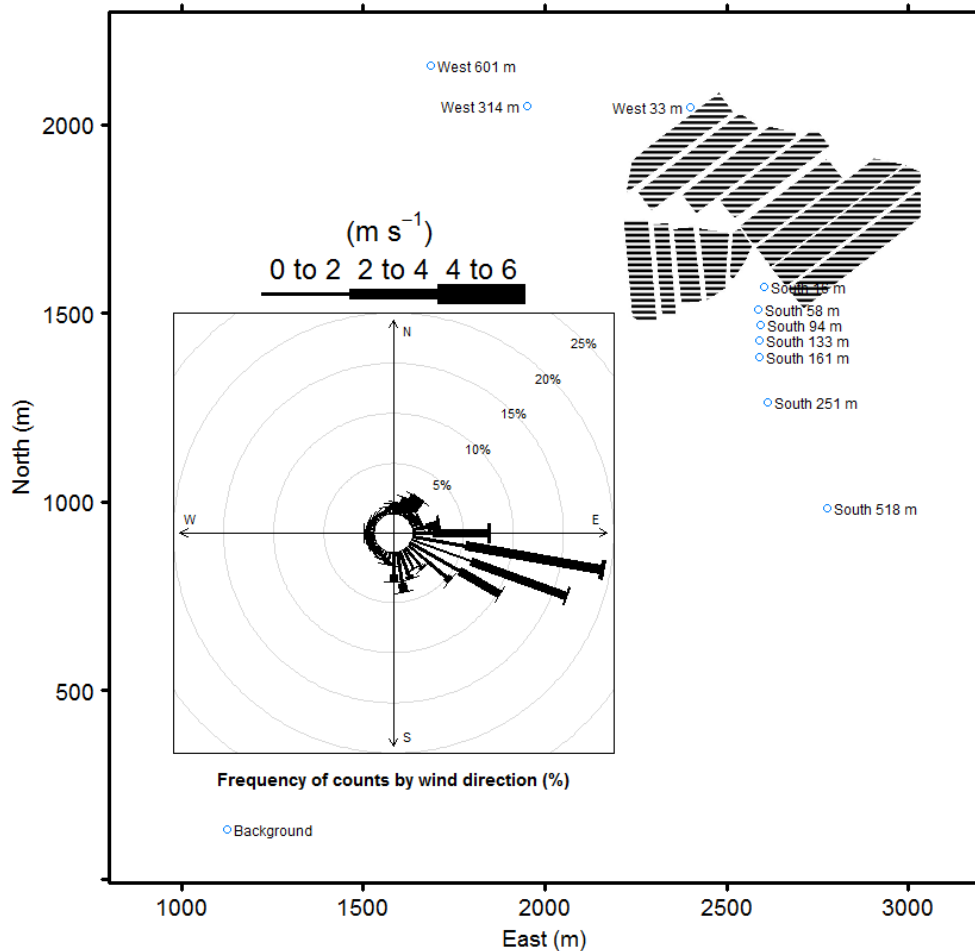


Figure 6.1. Feedlot site layout (outline) and the location of deposition traps, and the sampler intake. The sonic anemometer, temperature and rainfall monitoring equipment were located close to the anemometer, within 60 m of the centroid of the pen area. The windrose for the period is included as an inset.

The backward Lagrangian stochastic (bLs) technique was applied to determine the flux of ammonia from the site (Flesch and Wilson, 2005), using the data from the intake and the sonic anemometer in conjunction with the Windtrax model (Crenna et al., 2008). The model was applied to conduct micrometeorological flux calculations using the half-hourly gas analyses, half-hourly wind statistics, and the experimental layout.

Standard NH_3 gas releases of 4 concentrations (< 5, 1300, 14000, and 19 000 ppb; concentrations determined by instrument grade air and permeation tubes available) were used to determine what lag correction was required to account for tube transit time.

Standard rejection criteria (Flesch et al., 2005, 2007; Loh et al., 2008a) were applied: where the friction velocity (u^*) fell below 0.15 m s^{-1} , where the Obukhov length (L) was between +10 and -10 m, and where the estimated roughness height exceeded the sampler height. Data with inappropriate wind directions for the intake layout were removed from the data set, which generally removed Windtrax-calculated emission estimates with high standard deviations.

6.3.4 Deposition traps

Dry deposition was investigated using soil traps, using a method similar to that described previously (McGinn et al., 2003). Polypropylene lids with an internal 0.0478 m radius were used as a soil reservoir (affixed with glue to a ceramic tile to provide stability in the field).

A mass of 15 kg of soil from the surface 10 mm adjacent to the West 601 m transect site (Fig. 6.1) was collected. This soil was sieved to pass a 2-mm diameter aperture, but retained in a field moist state at room temperature in a well-aerated container.

During the continuous ammonia volatilisation monitoring period (about 5 months), 7 trap deployments (each of about 3 weeks) were conducted. A mass of 62 g (oven dry equivalent, but in the moist condition described) was deployed in each deposition trap, into the field. Two traps were placed at each of the west and south transect sites, an additional 3 at the background site, and a further sample placed in a jar in the laboratory and maintained at 25 °C for the duration of the deployment (Fig. 6.1). A sample of the soil deployed to the field was also retained in a sealed vial and analysed at the same time as the samples recovered from the field.

The location of deposition traps at the site (Fig. 6.1) was largely restricted by the normal operation of this feedlot enterprise, but were selected to allow representation of both the dominant wind direction, and a wind direction representative of a less common orientation.

At the end of each deployment, the soil samples were recovered from the deposition trap, and immediately bottled in the field. The samples were stored frozen in the laboratory until analysis via 2 M KCl extraction followed by colorimetric analysis (method 7C2, Rayment and Lyons, 2011) for NH_4^+ -N and $\text{NO}_3^- + \text{NO}_2^-$ - N. These values were summed to give a total mineral-N concentration of the material. The mineral-N sum less mineral-N concentration changes in the three background site deposition traps was used to calculate NH_3 -N deposition for the deployment period.

6.3.5 Emission modelling

Ammonia volatilisation processes were investigated via an existing process-based model (Sommer and Olesen, 2000; Sommer et al., 2003). The total flux of ammonia volatilisation ($\mu\text{g s}^{-1} \text{m}^{-2}$) is driven by the concentration gradient in NH_3 gas and can be described by

$$F_v = K(\text{NH}_{3,g} - \text{NH}_{3,a}), \quad [1]$$

where K is the transport coefficient (m s^{-1}), $\text{NH}_{3,g}$ is the concentration directly above the manure surface and $\text{NH}_{3,a}$ is the concentration in the atmosphere at a height that is not affected by manure emission. The transport coefficient K is a function of wind speed, manure surface roughness, and manure/air temperature. The transport coefficient is usually described by a series of resistances (via Ohm's Law)

$$K = \frac{1}{r_a + r_b + r_c}, \quad [2]$$

where r_a ($s\ m^{-1}$) is the resistance of the turbulent air layer above the manure, r_b is the resistance of the laminar boundary layer, and r_c is the resistance within the manure surface layer. The resistance of the turbulent air layer above the manure is

$$r_a(l) = \frac{\ln[l/z_0]}{ku_*} \zeta, \quad [3]$$

where l is the height of the internal boundary layer, z_0 is [what?], k is von Karman's constant (0.4), u_* is the friction velocity and ζ is the stability correction factor. The wind velocity at height z above the manure for neutral conditions is

$$u(z) = \frac{u_*}{k} \ln[z/z_0]. \quad [4]$$

The depth of the internal boundary layer was assumed to be 1% of the distance from the windward edge of the slurry-treated area (x ; the fetch) (Sommer et al., 2003)

$$l = 10^{-2} x. \quad [5]$$

The stability correction factor (ζ) is a function of the Richardson number (Ri)

$$Ri = \frac{gz(T_a - T_s)}{u(z)^2 T_a}, \quad [6]$$

where g is the standard acceleration due to gravity ($9.8\ m\ s^{-2}$), T_a is the air temperature and T_s is the manure temperature. The Richardson number expresses the importance of natural convection relative to the forced convection. The stability correction factor (ζ) is

$$\zeta = \begin{cases} (1 - Ri)^{-2}, & Ri \geq -0.1 \\ (1 - 16Ri)^{-0.75}, & Ri < -0.1 \end{cases}. \quad [7]$$

The resistance of the laminar boundary layer above the manure is

$$r_b = 6.2u_*^{-0.67}. \quad [8]$$

The resistance within the manure (r_c) accounts for the possibility that emission can occur within the manure and must be transported to the manure surface prior to release to the atmosphere. We allowed for a potential effect of manure relative to moisture content (θ) on the manure resistance according to a linear relationship ($r_c = \beta_1 + \beta_2(1 - \theta)$) (Sommer et al., 2000). Furthermore, because the NH_3 concentration directly above the manure surface is much greater than atmospheric NH_3 concentrations we assumed that $NH_{3,a} = 0$. For model fitting purposes the NH_3 emission was described by

$$F_v(\beta_0, \beta_1, \beta_2) = \frac{\beta_0 + \beta_3 C_1 + \beta_4 C_2}{r_a + r_b + \beta_1 + \beta_2(1 - \theta)}, \quad [9]$$

where C_2 is the total number of cattle in the feedlot, C_1 is the number of cattle in the pen closest to the intake location and β_3, β_4 are regression coefficients.

Publicly available air temperature, radiation, rainfall, humidity and evapo-transpiration data for the site (Bureau of Meteorology, 2014) were used with air temperatures and rainfall measured on-site to predict manure moisture and surface temperature (Shorten and Redding, In Press).

6.3.6 Deposition modelling

Ammonia deposition processes were investigated via an existing process-based model (Asman, 1998). The model for NH₃ gas concentration (g m⁻²) is described by

$$\frac{\partial C}{\partial t} + u(z) \frac{\partial C}{\partial x} = \frac{\partial}{\partial z} \left(K_H(z) \frac{\partial C}{\partial z} \right) + Q(x, z) - S(x, z), \quad [10]$$

where $C(x, z, t)$ is the crosswind NH₃ integrated concentration (g m⁻²), t is time (s), $u(z)$ is the wind velocity at height z (m) above the manure for neutral conditions (Eq. 4) (m s⁻¹), $K_H(z)$ is the eddy diffusivity (m² s⁻¹), Q denotes NH₃ emission (g m⁻² s⁻¹) and S denotes NH₃ deposition (g m⁻² s⁻¹). The eddy diffusivity is

$$K_H(z) = \frac{k u_* z}{\phi_H}, \quad [11]$$

where k is von Karman's constant (0.4), u_* is the friction velocity and $\phi_H = 1$ under neutral conditions (Brown et al., 1993). The NH₃ deposition flux is

$$F(x) = -V_e(x, z_r) C(x, z_r), \quad [12]$$

where z_r is the reference height (1 m) and the exchange velocity is

$$V_e(x, z_r) = \frac{1}{r_a(z_r) + r_b + r_c}, \quad [13]$$

where r_a (s m⁻¹) is the resistance of the turbulent air layer above the trap (Eq. 3), r_b is the resistance of the laminar boundary layer (Eq. 8), and $r_c = 30$ s m⁻¹ (Asman, 1998) is the surface resistance. The average air temperature is 23 °C and the average temperature difference between the manure and air is 5 °C. The total amount (g m⁻²) of NH₃ deposited over the time interval T (s) is

$$\alpha_0 F(x) f(x) T + \alpha_1 \theta, \quad [14]$$

where $f(x)$ is the fraction of time that the wind was travelling in the direction from the pen towards the trap, $F(x)$ is calculated from the steady state NH₃ gas concentration $C(x, z, t \rightarrow \infty)$ and α_0, α_1 are regression coefficients that allow for a potential effect of manure relative moisture content (θ) on the total NH₃ deposition.

6.3.7 Statistical analysis

Models were fit to the emission data using linear and nonlinear regression (Bates and Watts, 2007). Model residuals were analysed for normality and homoscedasticity. Variances of the deviations in measurements within response variables were assumed to be proportional to the measured emission. Markov Chain Monte Carlo was used to obtain the standard errors of the model parameters (Gilks et al., 1996). The model fit was assessed using the

correlation, slope and intercept between the predicted and measured emission (Pineiro et al., 2008). Pearson product moment correlation and Kendall's tau were used to describe the relationship between predicted and observed emission. Calculations were conducted in R and MATLAB (R Development Core Team, 2014; The Mathworks Inc., 2012). Ordinary differential equations were solved using the stiff system solver ode15s in MATLAB and partial differential equations were solved using finite difference schemes in MATLAB (Farlow, 1993).

Non-linear models were fitted by non-linear regression using R (nls procedure in R, R Development Core Team, 2014). Analysis of variance, summary statistics, and t-tests were also conducted using R. Probability distributions of deposition trap data were compared to probability distributions of background deposition trap data using the fitdist function of R's fitdistrplus package, and the Kolmogorov-Smirnov Test was applied to determine if sample distributions differed significantly. Boxplots were plotted with "notches" designed to represent an approximate confidence interval of the median value of the distribution (Leytem, et al., 2011) using R.

6.4 Results and discussion

During the measurement period, the dominant wind direction at the site was from East South East (Fig. 6.1). Mean wind speeds were around 1.6 m s^{-1} , and rainfall during the period was 204 mm. The average temperature for the study period was $24.0 \text{ }^{\circ}\text{C}$, close to the average annual temperature (25°C).

Measurements of NH_3 conducted at the background site well removed from the feedlot (1.8 km from the feedlot) and where wind directions did not originate from the feedlot, median NH_3 concentrations were about 7 ppb, within the range reported previously (4 - 10 ppb; Denmead et al., 2008a), and < 1% of the intercepted air concentrations at the air intake at the feedlot. With this contrast between the background and feedlot NH_3 concentration, there is little risk of error in background determination leading to significant errors in emission estimates.

6.4.1 Ammonia volatilisation

Total ammonia volatilised from the operation during the period amounted to 210 tonnes of $\text{NH}_3\text{-N}$ during the study period (Table 6.1). While the inventory calculations assume that only 30% of excreted N becomes volatilised (Intergovernmental Panel on Climate Change, 2006; Environment, 2014), it is apparent that a higher proportion of volatilisation may be appropriate in this case – as supported by previous measurements of volatilisation (Denmead et al., 2008a; Loh et al., 2008a). Mean volatilisation during the 5-month period was equivalent to $110 \text{ g animal}^{-1} \text{ day}^{-1}$ (mean of half-hour measurements; lower and upper 95% confidence intervals were 16 and $289 \text{ g animal}^{-1} \text{ day}^{-1}$ for half-hour measurements). This value differs somewhat from Loh et al.'s (2008) two-week-long survey in Queensland under warmer conditions ($253 \text{ g animal}^{-1} \text{ day}^{-1}$), but is greater than the measurements from the same site for a two-week winter period ($46 \text{ g animal}^{-1} \text{ day}^{-1}$; Denmead et al., 2008a).

Table 6.1. Cumulative mineral-N data, both for deposition traps and total volatilisation from the feedlot (both measured and two inventory calculations). Two inventory estimates are included for comparison: the Australia inventory estimate (Environment, 2014), and the IPCC estimate (Intergovernmental Panel on Climate Change, 2006). The deposition entries represent an estimate of total deposition if the pattern represented by the transect were rotated around the entire boundary of the pen area.

Parameter	Flux $\mu\text{g N s}^{-1}\text{m}^{-2}$	Confidence Interval $\mu\text{g N s}^{-1}\text{m}^{-2}$	Cumulative Mg	Proportion of Measured %
Measured volatilisation	83.1	21.72 - 238	210	-
(Environment, 2014)	-	-	107	51
(Intergovernmental Panel on Climate Change, 2006)	-	-	78.4	37
Deposition west	0.25	0.003-2.00	6.7	3.2
Deposition south	0.211	0.009-1.19	3.6	1.7

As expected there was a strong diurnal pattern of volatilisation (Fig. 6.2), and also of temperature and wind friction velocity. Further investigation indicated that NH_3 volatilisation was related to friction velocity, roughness height, and temperature (Figs. 6.4 and 6.5). Given that friction velocity and roughness height are used in the bLs calculations to estimate emissions from NH_3 concentrations in air (Flesch et al., 2005), a relationship between volatilisation and these parameters is not surprising.

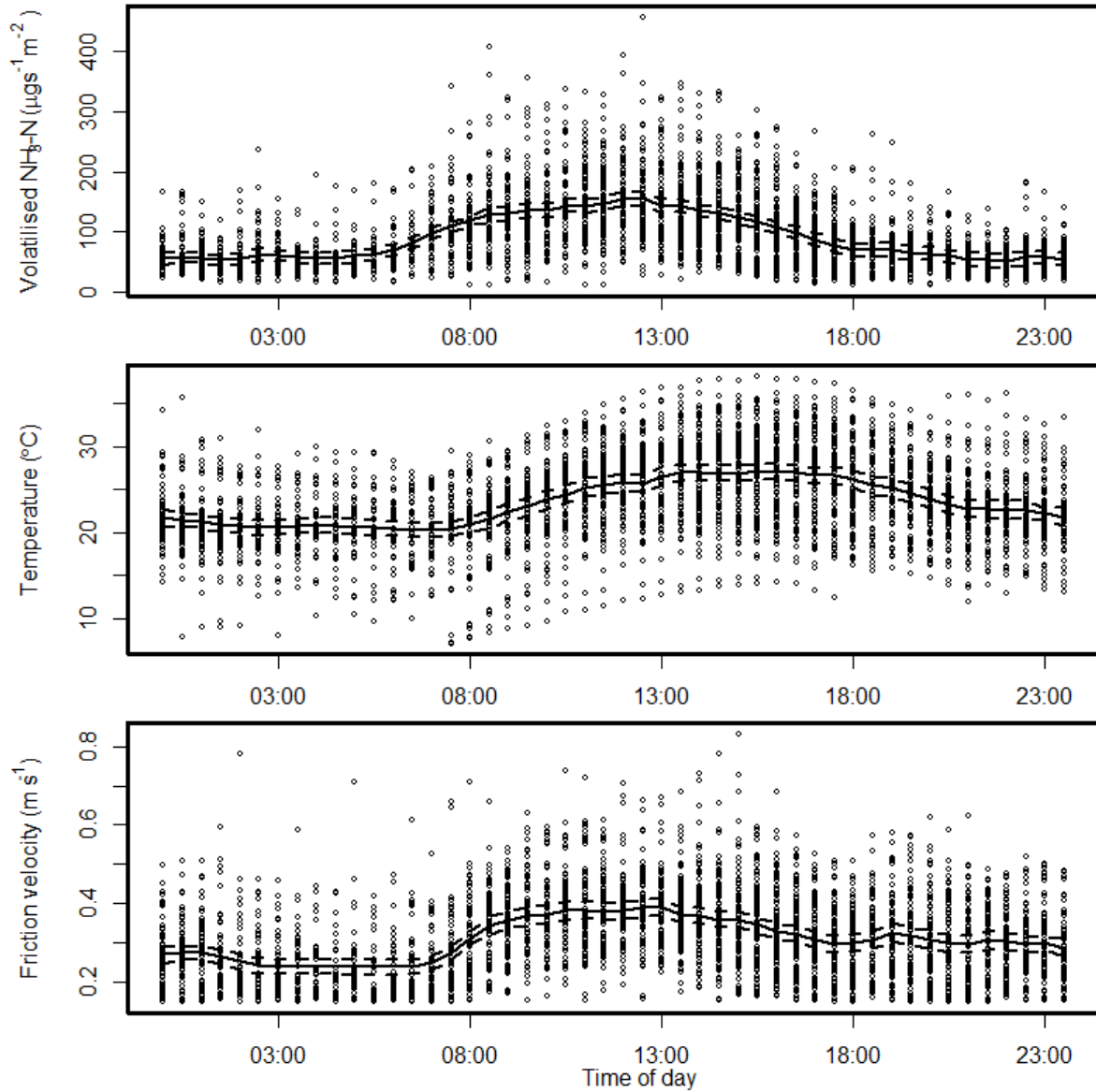


Figure 6.2. The diurnal pattern of volatilisation is accompanied by a diurnal pattern of temperature and friction velocity. The central line represents a loess spline through the data (span 0.1) while the dotted upper and lower lines represent 2 times the standard error of the mean.

Significant, but weak, correlations were observed between total ammonia volatilisation per second from the feedlot and temperature (0.16 Kendall's tau; Figs. 6.3 and 6.4). A stronger relationship was observed between the difference in temperature between manure (at 5 mm depth) and air and NH_3 volatilisation ($R = 0.62$; 0.46 Kendall's tau; Fig. 6.5). None of the other correlation relationships investigated with volatilisation of NH_3 were significant (cattle numbers, modelled manure moisture, or daily change in manure moisture). More sophisticated modelling investigations were required to identify process relationships.

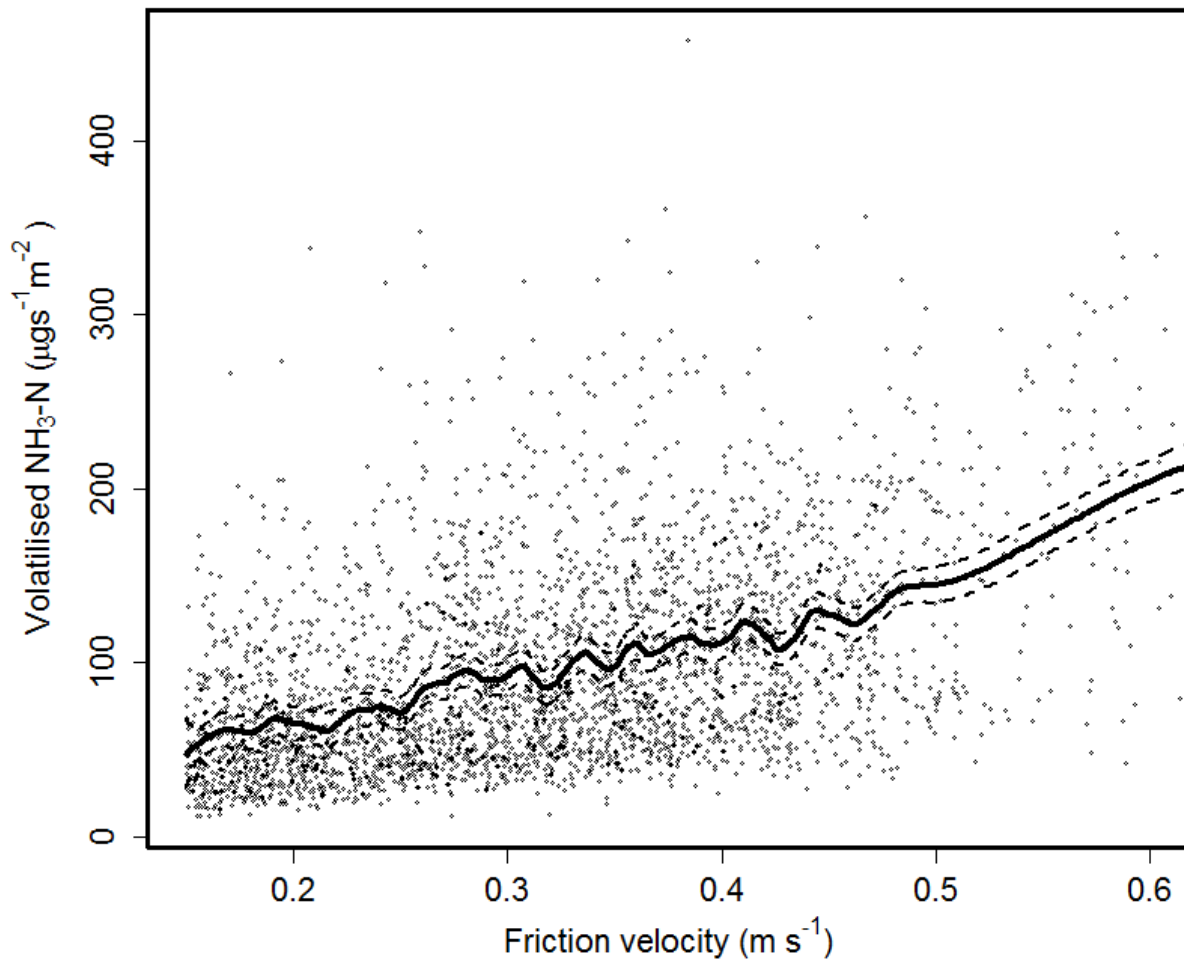


Figure 6.3. Ammonia volatilisation is related to the friction velocity. Given that friction velocity is used in bLs calculations to estimate emission, this is unsurprising.

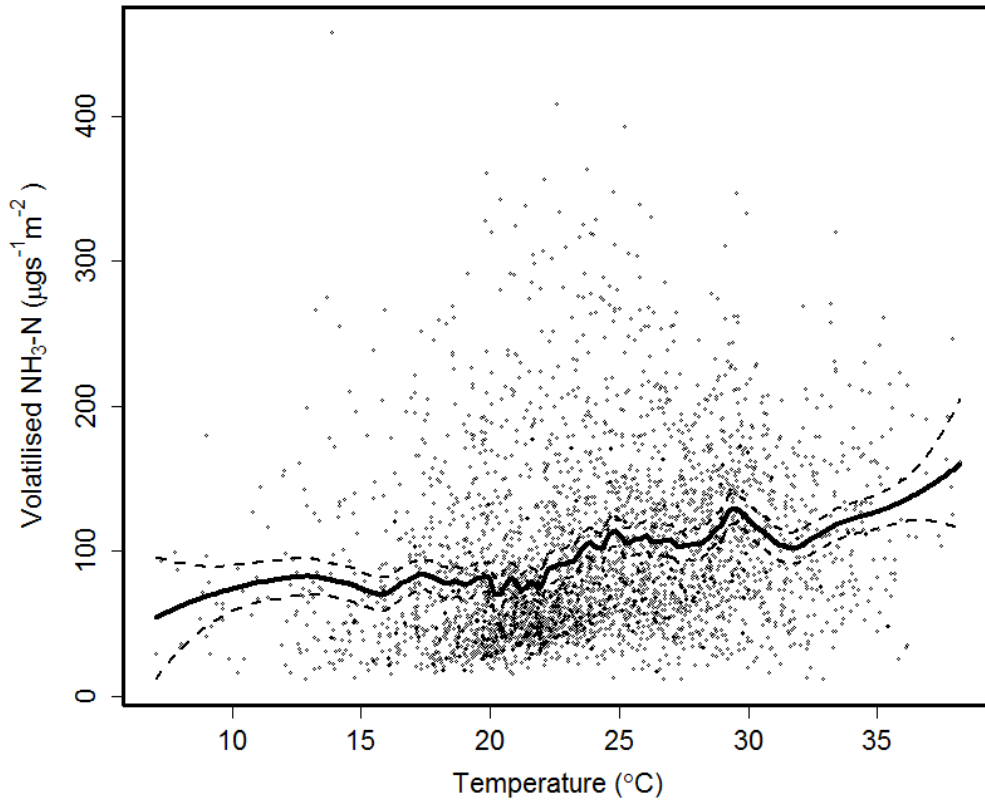


Figure 6.4. Ammonia volatilisation is related to the temperature. The central line represents a loess spline through the data (span 0.1) while the dotted upper and lower lines represent 2 times the standard error of the mean.

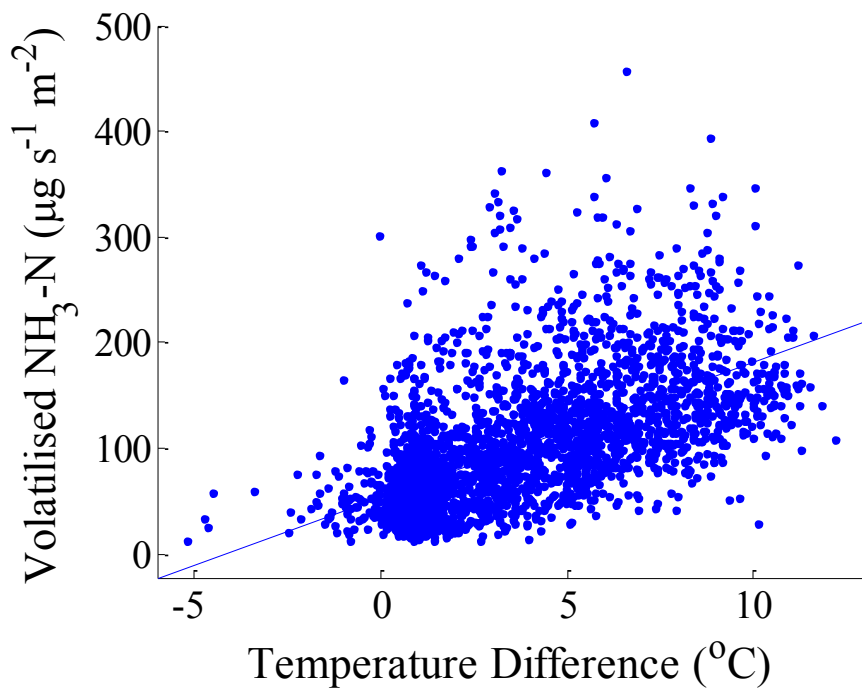


Fig 6.5. The effect of the difference in temperature between manure (at 5 mm depth) and air on NH₃ emission ($R^2 = 0.38$).

The feedlot layout used in bLS modelling (using Windtrax; Crenna et al., 2008) is very similar to that applied by other authors using a single sample intake (Denmead et al., 2008a). When using the bLS technique with this layout, more distant emission sources contribute far less to the emission estimate than the sources immediately adjacent to the sample intake. As noted previously (Denmead et al., 2008a), while there were ponds and manure piles at the western outer bound of the pen area (Fig. 6.1), these relatively distant and dominantly down-wind sources have little influence on the measured emissions as few of the simulated touchdowns were within these regions. Re-running the Windtrax model with a layout that included the pond area as part of the emission source had no significant effect on the emission flux ($P < 0.001$).

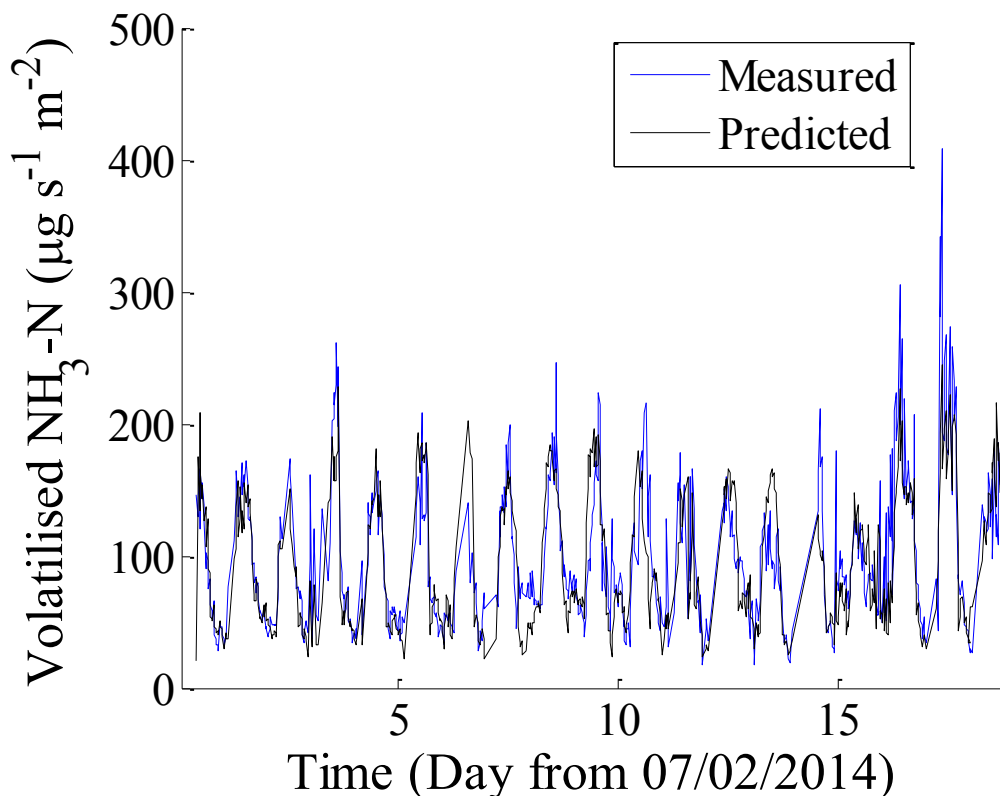


Figure 6.6. Relationship between the measured and predicted (Eq 1-9) NH₃ emission ($R^2 = 0.50$).

Volatilisation modelling successfully represented volatilisation from the site. The manure was assumed to have a density of 1000 kg m^{-3} . Publicly available data were also used to predict any missing on-site air temperatures with high correlation between predicted and measured on-site temperature ($R^2 = 0.82$).

We found that β_1, β_2 were not significant and therefore set $r_c = 0$, which suggests that the emission process is localized near the surface of the manure. This is also consistent with no significant effect of manure moisture on NH₃ emission. We also found that β_4 was not significant. We estimated that $\beta_0 = 924 \pm 35 \text{ } \mu\text{g m}^{-3}$, $\beta_3 = 5.76 \pm 0.17 \text{ } \mu\text{g m}^{-3} \text{ cattle}^{-1}$ and the model provides a good fit to the data ($R^2 = 0.53$; Fig. 6.6). A reduced model with no

cattle number effect ($\beta_3 = 0$) explained 50% of the measurement variance ($\beta_0 = 2127 \pm 19 \mu\text{g m}^{-3}$; $R^2 = 0.50$).

6.4.2 Nitrogen deposition

Cumulative deposition for the measurement period along the two transects amounts to 6.7 and 3.6 Mg N for the West and South transects, with deposition approaching background rates at their maximum distances from the pens (Figs. 6.7 and 6.8). Layout of the deposition trap transects was strongly dictated by feedlot infrastructure and operations of the feedlot and surrounding cropping areas. The west deposition transect was well aligned with the dominant wind direction (Fig. 6.1); however, only three locations were available along this transect (the transect consisted of only three traps). The detailed south transect was representative of a minor wind direction.

On this basis, it is likely that the West transect provides an upper estimate of deposition with evidence of around 3 % of volatilised ammonia being deposited within 601 m of the feedlot boundary. The lower limit suggested by the South transect is around 1.7 % of volatilised ammonia being deposited within 518 m of the pen boundary.

Consistently low median air concentrations at the background site relative to the pen air concentration (Fig. 6.1), irrespective of the wind direction (13 ppb at the background relative to a 240 to 4500 ppb range at the pen intake) suggests that the background site is appropriate to estimate native ammonia emissions in this landscape without influence from the feedlot.

For additional confidence, mineral-N analyses of the three deposition traps located at the background site were compared to the two traps at each the West 601 m or South 518 m, depending on dominant wind directions during the period, to ensure that measured background values were comparable to or lower than these sites.

The measured background deposition of ammonia plus soil N mineralisation was $0.0167 \pm 0.012 \text{ g N m}^{-1} \text{ day}^{-1}$ (mean \pm standard deviation). In reality, almost all of this mineral-N was attributable to soil mineralisation, rather than background deposition. Analysis of the vials of [word missing] retained in the laboratory at 25°C during each deposition trap deployment indicated average soil mineralisation of $0.0166 \pm 0.0088 \text{ g N m}^{-1} \text{ day}^{-1}$ (N deposition would therefore be equivalent to about $1 \text{ kg ha}^{-1} \text{ year}^{-1}$).

A review of NH_3 deposition rates indicated a range of bulk deposition from 9.2 to $16.8 \text{ kg ha}^{-1} \text{ year}^{-1}$, with deposition to plant canopies and grass surfaces of 19.6 to $95.6 \text{ kg ha}^{-1} \text{ year}^{-1}$ (Krupa, 2003). Such values are likely very location specific, and recent data from the United States indicate a much more restricted range of ammonium wet deposition not dissimilar to that estimated for our site (mean total N deposition for approximately 264 sites, 2012 was $3.2 \text{ kg N ha}^{-1} \text{ year}^{-1}$, with 95 % confidence interval of 0.2 to $7.3 \text{ kg N ha}^{-1} \text{ year}^{-1}$; <http://nadp.sws.uiuc.edu/ntn/annualmapsByYear.aspx>).

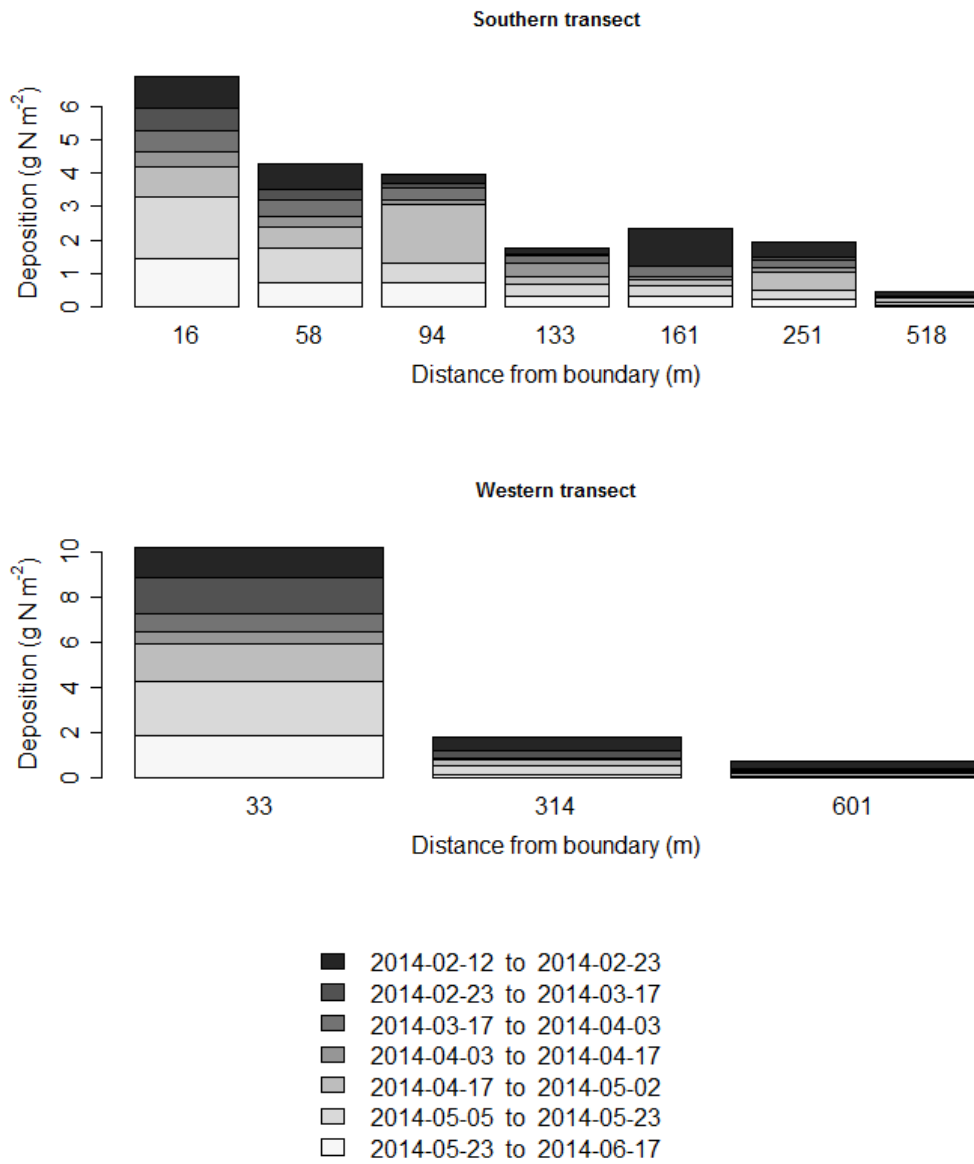


Figure 6.7. Data from the two transects of deposition traps.

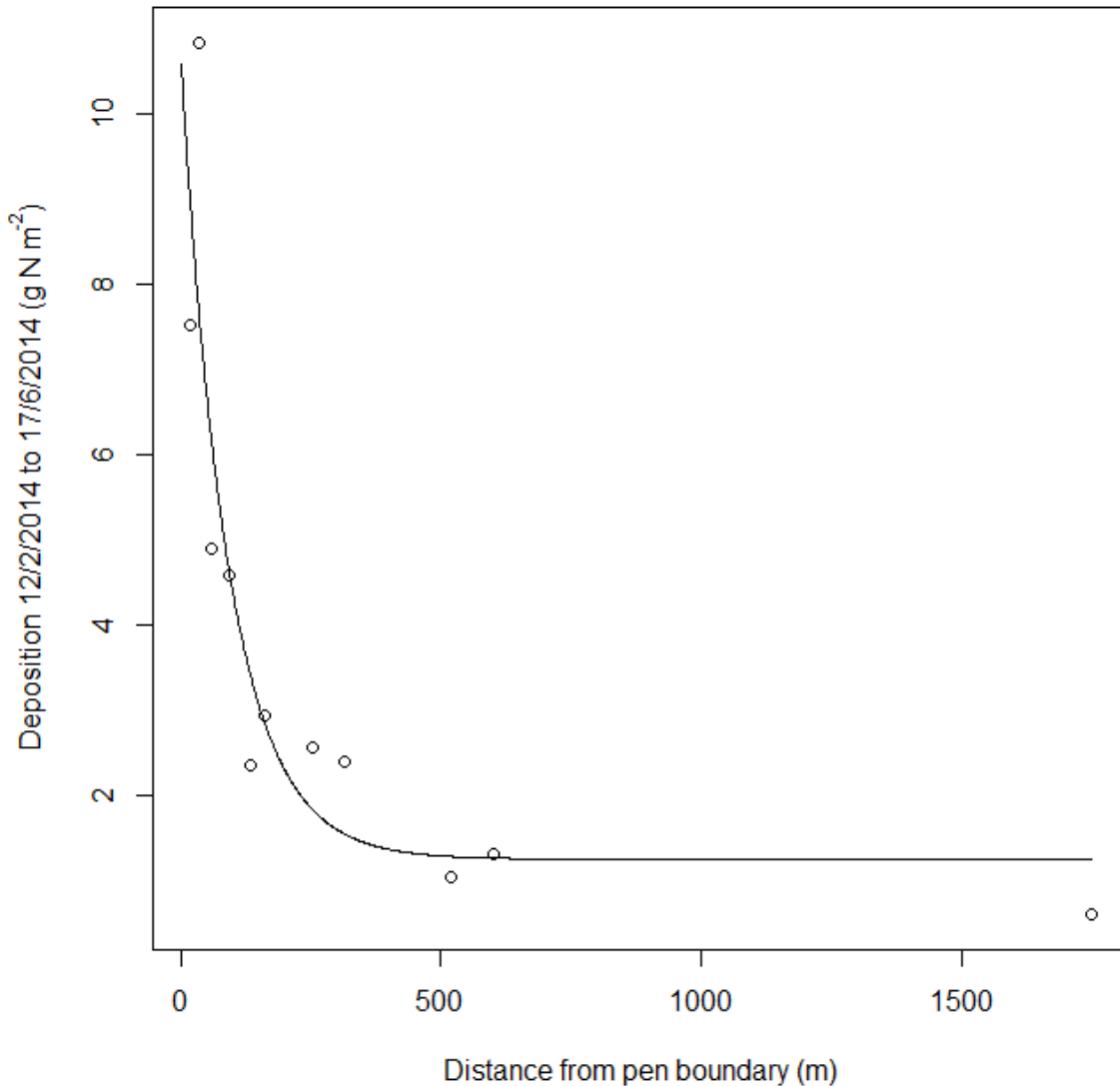


Figure 6.8. Fitting an exponential decay equation ($y = (9.34 \pm 1.73) * e^{\left(\frac{-x}{91 \pm 36}\right)} + 1.24 \pm 0.75$; $R^2 = 83\%$; parameter estimate \pm standard error) to the deposition data suggests that deposition has effectively returned to background levels ($1.24 \pm 0.75 \text{ g N m}^{-2}$ over a 125 day period; effectively not significantly different from 0 g N m^{-2}) within 600 m.

The average air temperature is 23 °C and the average temperature difference between the manure and air is 5 °C. Reasonable success was achieved in representing the observed behaviour with the deposition model. We observed no significant effect of manure moisture on total NH_3 deposition ($\alpha_1 = 0$). We estimated that $\alpha_0 = 2.2 \times 10^{-4} \pm 0.2 \times 10^{-4} \text{ m}^{-1}$, and the model provided a good fit to the data ($R^2 = 0.51$; Fig. 6.9).

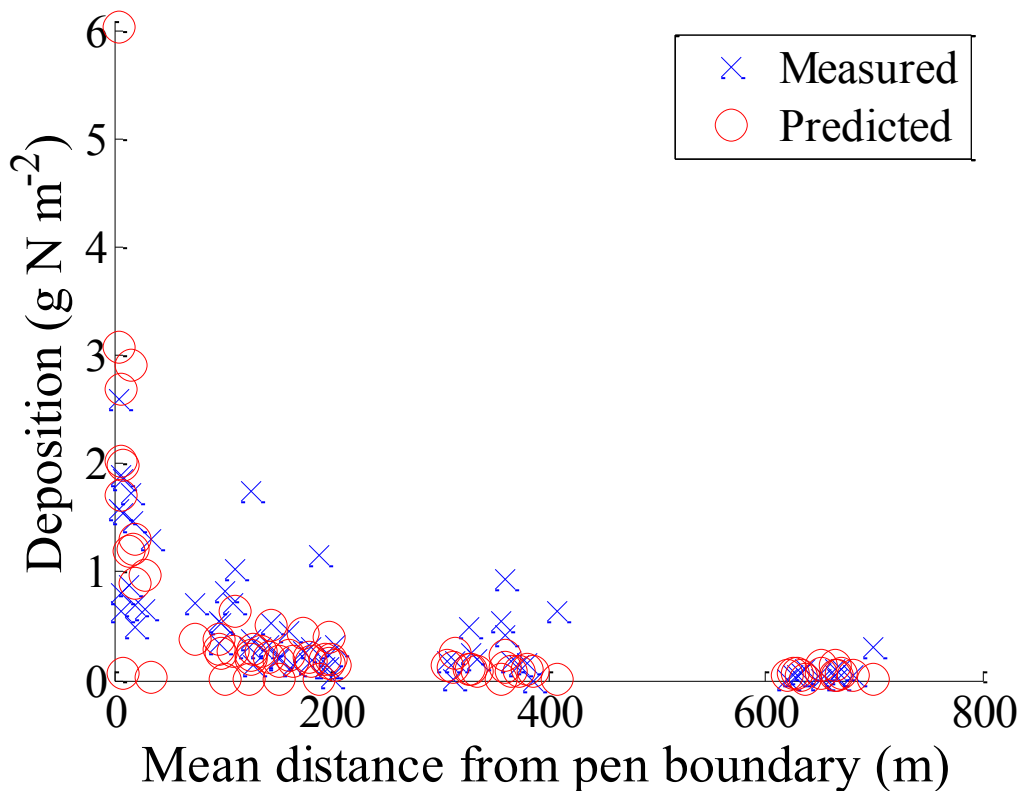


Figure 6.9. Relationship between the measured and predicted (Eq 10-14) NH_3 deposition as a function of mean distance from the pen boundary ($R^2 = 0.51$).

6.4.3 Implications

A detailed investigation of the soil from this site suggests that where mineral-N $< 70 \text{ mg (kg of soil)}^{-1}$, no significant N_2O emission occurs (Chapter 5). None of the deposition trap samples collected during 5 months from the South 518 m site and only one sample collected from West 601 exceeded $70 \text{ mg mineral-N (kg of soil)}^{-1}$. However, the depth of soil in the deposition traps (10 mm) may not have realistically represented the depth of interaction of deposited ammonia. In reality, ammonia may have been restricted to the upper few millimetres of the soil, leading to higher soil concentrations in that shallow zone.

However, several significant observations can be made. Firstly, little of the volatilised ammonia is deposited within 601 m of the feedlot ($< 3.7 \%$; Table 1). These deposition results are supported by the data of other authors collected from several locations, where the majority of volatilised N was observed to be advected away (measured $< 3.2 \%$ within 270 m of a poultry farm; Fowler et al., 1998; $< 10 \%$ within an 8 X 8 km square; Staebler et al., 2009). In this zone, application of an emission factor for indirect emissions (e.g. Intergovernmental Panel on Climate Change, 2006) is probably reasonably well supported by evidence. However, soil nutrient management approaches for efficient plant production may be able to greatly decrease indirect emissions, and a relatively simple, management-responsive calculation protocol for emissions has been developed (Chapter 5; manuscript submitted). Maximal recorded mineral-N deposition during the measurement period of 5 months (more than a single crop growth period) was approximately 100 kg N ha^{-1} , similar to a commercial fertiliser application rate.

Secondly, beyond 600 m from the pen boundaries, deposition fluxes appear to return to rates that are a relatively small proportion of seasonal crop or pasture requirements (close to background deposition). In our study, deposition in this external zone was probably $< 17 \text{ kg N ha}^{-1} \text{ year}^{-1}$ (based on background site deposition less the soil blank) and may actually not be significantly different from 0 kg N ha^{-1} (Fig. 6.6; fitting an exponential decay curve to the data). Using 17 kg N ha^{-1} as an upper limit, would require a depth of soil interaction of $< 8.7 \text{ mm}$ for deposited mineral-N for significant indirect N_2O emission to result (Chapter 5). These results are supported by a previous study that found that $> 500 \text{ m}$ from a feedlot, soil N remained at concentrations typical of the surrounding undisturbed shortgrass prairie (Todd et al., 2008b). However, field measurements at this site suggest that background fallow (but cultivated) soil mineral-N concentrations are close to the threshold for N_2O emission ($70 \text{ mg mineral-N (kg of soil)}^{-1}$; Chapter 5, field validation site, $77 \pm 22 \text{ mg mineral-N (kg of soil)}^{-1}$), indicating that deposition in these areas will result in N_2O emission.

The study site is located within a region of intensive grain production, on high-quality agricultural soils. This is the case for many intensive livestock enterprises where grain is an essential feedstock. It is likely that advected mineral-N is wet-deposited to this wider landscape, to soil where mineral-N concentrations are purposefully raised through fertiliser applications.

This wet deposition could be considered a manageable fertiliser application with low embodied transport and manufacturing emissions. Where re-deposition coincides with the nutrient uptake of any growing vegetation, these applications are unlikely to remain resident for long (e.g. Figs. 6.10 to 6.15) (plant growth curves estimated via a logistic curve and known production data; Hunt, 1982), meaning there would be little accumulation potential under these circumstances. It then becomes an issue of policy rather than science as to how these emissions are accounted; however, there is potential for further research to assist these decisions.

In the case of Staebler et al.'s (2009) feedlot, this means that emissions from 90% of volatilised N, or for our data a 96.3% of volatilised N, should be accounted in the inventory as standard fertiliser emissions, rather than a class of emissions apart, if:

- The feedlot is located in a cultivated agricultural setting (very likely).
- There is sufficient separation between volatilisation sources of ammonia.
- Surrounding agricultural land management conforms to prevailing nutrient management practice.

It is notable that the benefit from this “manageable fertiliser application with low embodied transport and manufacturing emissions” currently accrues to the third party land-holder, but the inventory imposition is applied to the originator.

Combining these results with those of Chapter 5, it is possible to make some estimates of the likely volatilisation and indirect emission contribution from the feedlot. It is clearly evident that the estimated volatilisation of excreted N applied in many inventories is incorrect (30 % ; Intergovernmental Panel on Climate Change, 2006; 40- 70 % is probably more appropriate based on a review; Pratt et al., 2014), with a more reasonable estimate being around 60% (based on our study).

Close to the feedlot, some areas are quite likely to have little effective nutrient uptake and removal. For example this would include areas around infrastructure, where surfaces are not impervious and banded. These areas may be grassed, but conventionally there will be little effective N removal via plant uptake. Accordingly, a build-up of mineral-N over time is likely, and emission will tend toward $(\text{N}_i + \text{N}_{\text{dep}}) * 0.053$. For these areas, emission of nitrous oxide is likely to continue until soil concentrations throughout the profile fall below the 70 mg nitrate-

N (kg of soil)⁻¹ threshold – through uptake or losses. Logically this could amount to a large proportion of the N deposited in these areas. Experimental data support this potential:

- Pen soil (with no covering manure) tended to have higher emissions (mean 1.34 $\mu\text{g N}_2\text{O s}^{-1} \text{m}^{-2}$) than pen area covered with manure (mean 1.01 $\mu\text{g N}_2\text{O s}^{-1} \text{m}^{-2}$). While this difference appears marginal, the moisture contents observed in these soils were entirely unfavourable for emission (around 21 % water filled pore space compared to Fig. 4.2), and nitrate concentrations were far higher (368 compared to 9 mg $\text{NO}_3^- \text{-N}$ [kg soil]⁻¹ (Chapter 2 data; four soil-only measurements collected).
- The field validation of the emission model (Chapter 4) indicated that N_2O emission originated from the surface to a significant depth in the soil profile (>> the 75 mm investigated). This suggests that $\text{NO}_3^- \text{-N}$ originating from deposition and leached into the profile may remain vulnerable to denitrification.
- One of the reasons University of Melbourne team's results for emission from the general pen area were substantially higher than those recorded by our very large chamber measurements (discussions re results with Prof Deli Chen) may be the inclusion of emissions from the infrastructure areas. This would include roads, roadsides, vacant areas, unoccupied and cleaned pens.

However, some proportion of deposited NH_4^+ may be emitted as N_2 or accumulate in organic forms. A small field study could readily clarify the accumulation and emission relationship.

It is important to minimise the contribution from this area of potentially ineffective removal, as emission from these areas is likely to be the greatest:

1. Feedlot layouts that minimise the proportion of the circumference that is not cultivated will produce lower indirect emissions from this proximal zone, assuming soil nitrogen is appropriately managed. At this feedlot site only about 25% of the pen boundary is not cultivated or occupied by ponds.
2. These proximal emissions could be further decreased via mowing and removing grass clippings, particularly close to the pen boundary.

While deposition rates close to the pen boundaries are around 290 kg N ha⁻¹ year⁻¹, at 250 m, this has fallen to about 58 kg N ha⁻¹ year⁻¹. Losses of deposited N at the study site due to deep drainage is likely to be negligible (Yee Yet and Silburn, 2003).

Taking this proximal deposition into account and assuming that, where deposition occurs to cultivated land, emissions are reflective of standard fertiliser emissions (0.01 of deposited N), a justifiable estimate of indirect emissions would be based on:

- 60 % of excreted N being volatilized.
- 3.2 % of this being deposited in the proximal zone, and about 5% of this being deposited where N uptake is not easily facilitated (based on area outside of the feedlot drainage area measured from an air photo). In these locations a large proportion may ultimately be lost via N_2O emission.
- The remainder is subject to emissions similar to those from the surrounding arable land. Currently the inventories estimate these indirect emissions as 1% or 0.3 % for dry land areas (Environment, 2014) though evidence for this value is slim (Pratt et al., 2014). For management systems that leave a year-round surplus of $\text{NO}_3^- \text{-N}$ in the soil, 1% or 0.3 % appears improbable. A year-round surplus of 200 mg $\text{NO}_3^- \text{-N}$ (kg of soil)⁻¹ for this high-quality agricultural soil could result in emission of as much as 10% as N_2O (Fig. 5.6). More careful nutrient management should be able to avoid the majority of this emission (e.g. Hulugalle, 2005). However, for the 75 mm depth cores collected from the fallow control plots in the field chamber measurements (Chapter 5), nitrate concentrations were 77 ± 22 mg $\text{NO}_3^- \text{-N}$ (kg of soil)⁻¹ (mean \pm standard deviation; compare to Fig. 5.6).

- Using the dryland N₂O emission value, proximal emissions will be less than $350 \times 0.6 \times 0.032 \times 0.05 \times (365/125) = 1$ tonnes of N. Using the 1% factor for the remainder, $(350 \times (365/125) \times 0.6 - 1) \times 0.003 = 2$ tonnes of N. So without modification of management, indirect emission at this site could be estimated as 3 tonnes of N₂O-N annually, about 0.46 % of volatilised N. The dry-land direct emission value may be an under-estimate of emissions on this soil where existing soil mineral N concentrations are as observed in the field (Chapter 5).
- Using the accepted N₂O emission factor, proximal emissions will be less than $350 \times 0.6 \times 0.032 \times 0.05 \times (365/125) = 1$ tonnes of N. Using the 1% factor for the remainder, $(350 \times (365/125) \times 0.6 - 1) \times 0.01 = 6$ tonnes of N. So without modification of management, indirect emission at this site could be estimated as 7 tonnes of N₂O-N annually, about 1.2 % of volatilised N.

Ammonia volatilization and subsequent indirect emission of nitrous oxide-N probably represents around 0.012 kg N₂O-N/(kg of N excreted). This estimate assumes 5% infrastructure area within 600 m of the feedlot with no effective N uptake by plants, 0.01 kg N₂O-N/(kg of N deposited on cultivated land), and 0.6 kg of NH₄⁺-N volatilised/(kg of N excreted).

A more detailed and accurate approach is possible, that can take into account improvements in management of this infrastructure area.

It is evident that annual emission from resident mineral-N in the clay soil investigated peaks at around 9 % (Fig. 5.7), with a threshold to emission of 70 mg mineral-N (kg of soil)⁻¹. The zone where this accumulation of deposited mineral-N attributable to the feedlot appeared in our research to be around 600 m from the pen boundary. Assuming that the maximal emission occurs for all of the deposited mineral-N (unlikely) emission for a given year may be estimated:

$$emission_{max} = \text{average total resident mineral N} \times 0.11 \quad [15]$$

However, we know that only a small proportion of volatilised-N is deposited close to the feedlot (< 3.7 % in our study), and it is likely that indirect emissions are not at this maximal rate (Fig 5.7):

$$emission_{close\ deposition} = \text{volatilised N} \times 0.053 \times 0.037 \quad [16]$$

To determine this more accurately for the feedlot, a soil profile survey around the feedlot would be required. We also know that volatilisation probably represents about 60% of excreted N, so considering only one year of volatilisation/deposition:

$$emission_{close\ deposition} = \text{excreted N} \times 0.6 \times 0.053 \times 0.037 \quad [17]$$

Accumulation and losses of deposited mineral-N will continue in this zone until the any deposited N is depleted. Including this consideration in our equation leads to:

$$\frac{d}{dt} emitted = const (-N_{uptake} - N_{loss} + N_i + N_{dep} - emitted) \quad [18]$$

where N_{uptake} , N_{loss} , N_{dep} , N_i are the plant extraction of N from the soil, N losses (leaching or volatilisation), N deposition, and initial mineral N (all as kg year^{-1}). The *const* is a constant term, which might be approximated by 0.053 (based on the mid-point of emission from Fig. 5.7).

The solution to this ordinary differential equation is:

$$emitted = -\%c e^{-const t} \left((N_{uptake} + N_{loss} - N_i - N_{dep}) \%c e^{const t} - \%c \right) \quad [19]$$

where an additional constant is introduced (%c). Assuming that emission at time zero is 0 kg N ($E_{proximal}$ represents emitted $\text{N}_2\text{O-N}$ from the area close to the feedlot):

$$E_{proximal} = ([N_{uptake} + N_{loss} - N_i - N_{dep}]e^{-0.053t} - [N_{uptake} + N_{loss} - N_i - N_{dep}]) \quad [20]$$

Given that a proportion of excreted N is volatilised (assumed to be 0.6), only a small proportion of this is deposited close to the feedlot (< 3.2 % in our study; amounting to 6700 kg; Table 1), and assuming that the existing factors for emission from the surrounding fertilised agricultural landscape are accurate (1 %; Environment, 2014), the equation for annual emission becomes:

$$E_{proximal} = ([N_{uptake} + N_{loss} - N_i - 6700]e^{-0.053t} - [N_{uptake} + N_{loss} - N_i - 6700]). \quad [21]$$

6.5 A mitigation management for indirect emissions

6.5.1 A small opportunity

It may be possible to improve management at some feedlots of the component of volatilised ammonia deposited proximal to the pens and ponds. Fortunately this area of high N deposition is a relatively small proportion of the total volatilisation. However, this advantage also means there is a limited impact for management of this area as a mitigation.

Staebler et al. (2009) observed that 90 % of the volatilisation emissions from a feedlot were advected away from the feedlot and re-deposition of this ammonia was not observed. We observed that about 3 % of volatilised ammonia was deposited within 520 m of the feedlot. It seems reasonable, however, that ultimately the balance of ammonia would be deposited (distal deposition), but only after significant dilution due to atmospheric turbulence and diffusion.

In the clay soil, distal deposition may occur at rates lower than the threshold for triggering N_2O emissions (Fig. 5.6), provided other major ammonia emission sources are not co-located and the soil is not fertilised. Since this is a valued agricultural soil, either or both of these caveats are likely.

This mitigation opportunity is relatively small. In the situation we studied only 3% of the total N volatilisation was deposited in this area. Additionally at the studied feedlot, about 95 % of the proximal area to 520 m from the pen and pond boundaries is already subject to cultivation and cropping, season permitting.

At other enterprises, the opportunity may well be larger, and there may be room for improvement by cropping or cutting pasture and accounting for N deposition in nutrient management in this proximal region.

6.5.2 Improved proximal nutrient management a small mitigation opportunity

Where re-deposition coincides with the nutrient uptake of any growing vegetation, these applications are unlikely to remain resident for long (e.g. Figs. 6.10 to 6.15)(plant growth curves estimated via a logistic curve and known production data; Hunt, 1982), meaning there would be little accumulation potential under these circumstances.

Crops and pastures established within several hundred metres downwind of a feedlot would therefore serve to decrease the secondary nitrous oxide emission potential.

Deposition rates close to and downwind of feedlots have been investigated in Texas at a 25 000 head facility (Todd et al., 2008b). Most of the mineral N deposition (based on soil nitrate and ammonia) appears to have occurred within 200 m of the feedlot. Peak N deposition appears to have occurred between 75 and 106 m from the feedlot, at a rate of $49 \text{ kg ha}^{-1} \text{ year}^{-1}$. In our study deposition directly at the boundary amounted to about $290 \text{ kg ha}^{-1} \text{ year}^{-1}$, but rapidly declined with distance from the boundary. Measurements at 58 m had halved that deposition rate (about $120 \text{ kg N ha}^{-1} \text{ year}^{-1}$).

This is not an excessive rate of application relative to the requirements of many broad-acre crops: e.g. summer sorghum (Fig. 6.10) and winter wheat (Fig. 6.12). Indeed the estimated uptake rates of these crops (determined from the derivative of the uptake curve) would readily accommodate or exceed the deposition rates observed at our site (Fig. 6.8) for most of their growing seasons. This would negate any N accumulation and prevent secondary emission losses attributable to air-fall N by ensuring it does not accumulate above the threshold N value.

It is clear that several types of management changes would significantly decrease or effectively eliminate secondary emissions from the proximal zone:

1. If this land area is commonly underutilised or fallow, growing a harvested crop here, while applying efficient nutrient practice, including accommodating the likely air-fall deposition.
2. If this is already a cropped area, decreasing fertiliser applications in this zone, allowing for a conservative amount of air-fall deposition.
3. If this area is currently under pasture, an approach that would decrease emissions would be to restrict stock access, and cut and remove pasture as dry matter production responds to N deposition.

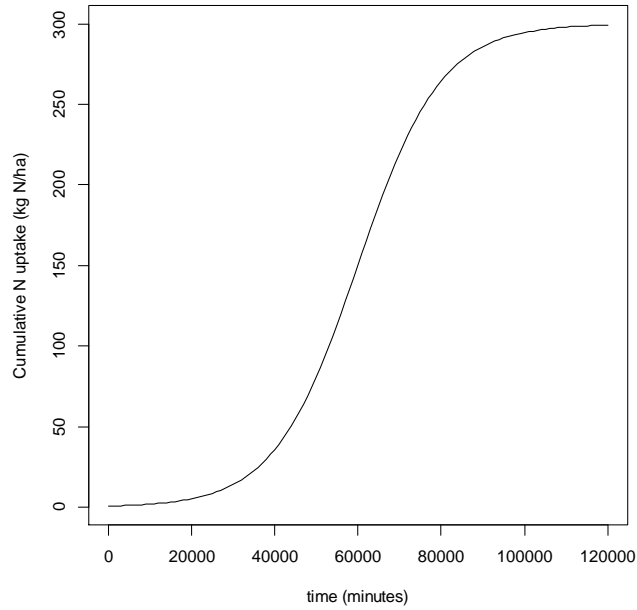


Figure 6.10. Sorghum growth curve estimated using a logistic relationship and assuming a final yield of 15 t ha⁻¹ developed over 12 weeks (120960 minutes).

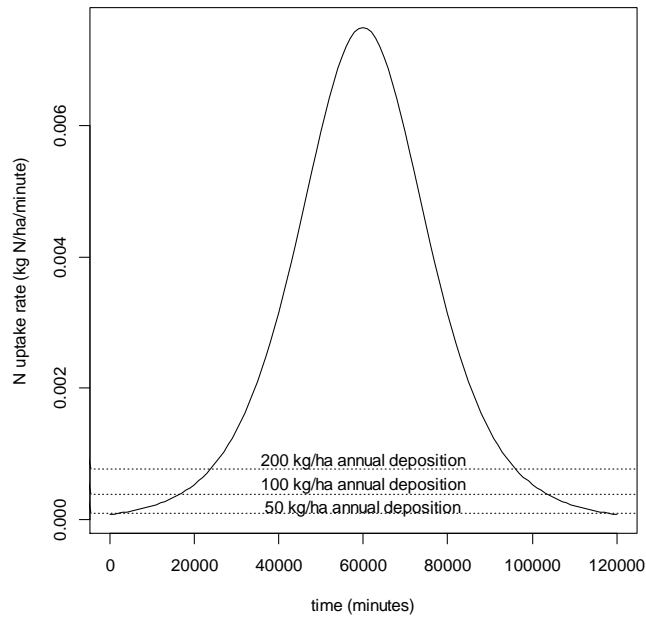


Figure 6.11. Uptake rate for the illustrated sorghum crop. Note that the air-fall ammonia application rates illustrated are relatively small relative to the N uptake rate.

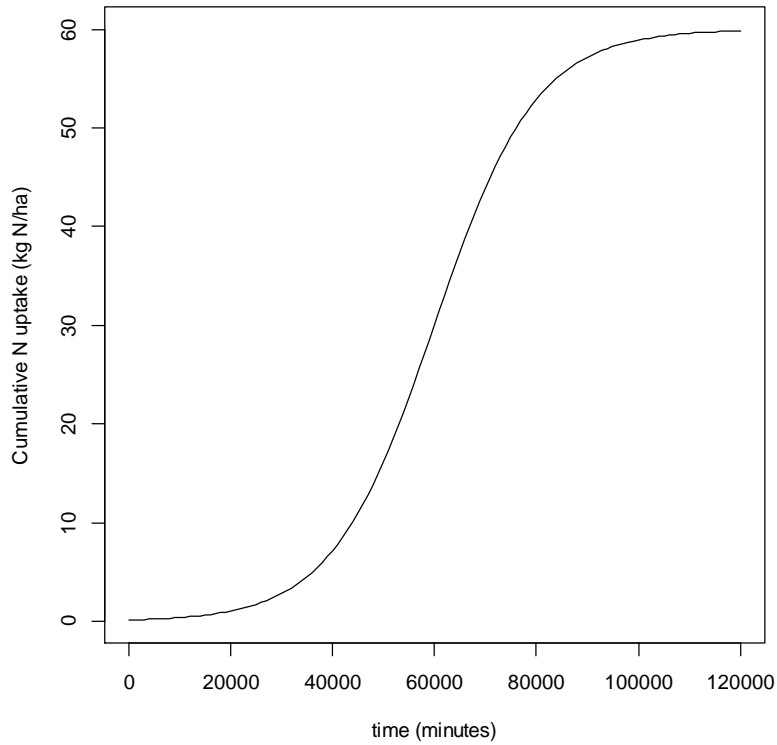


Figure 6.12. Dryland wheat growth curve estimated using a logistic relationship and assuming a final yield of 3 t ha⁻¹ developed over 12 weeks (120960 minutes).

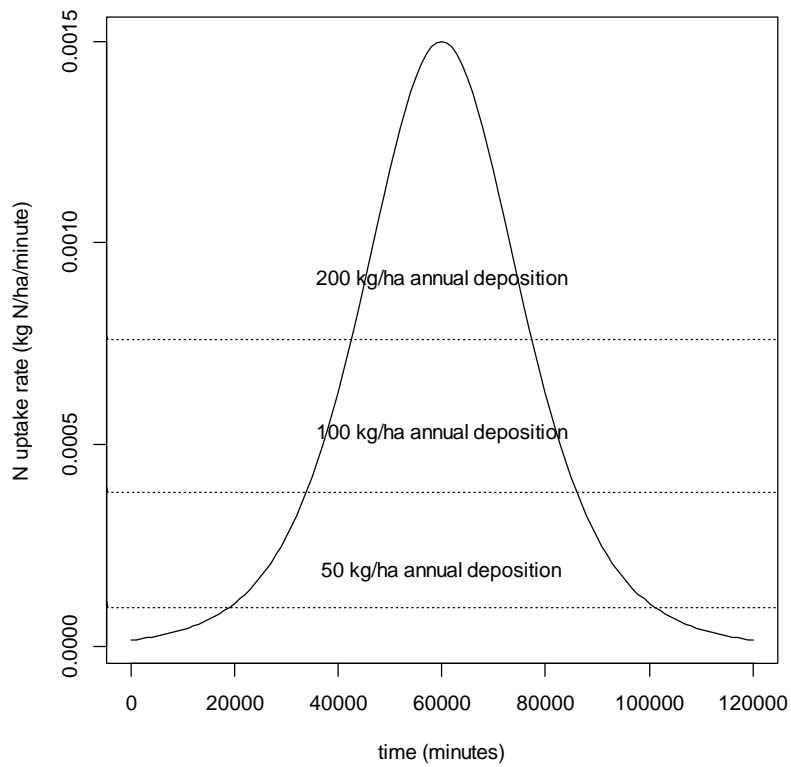


Figure 6.13. Uptake rate for the illustrated wheat crop.

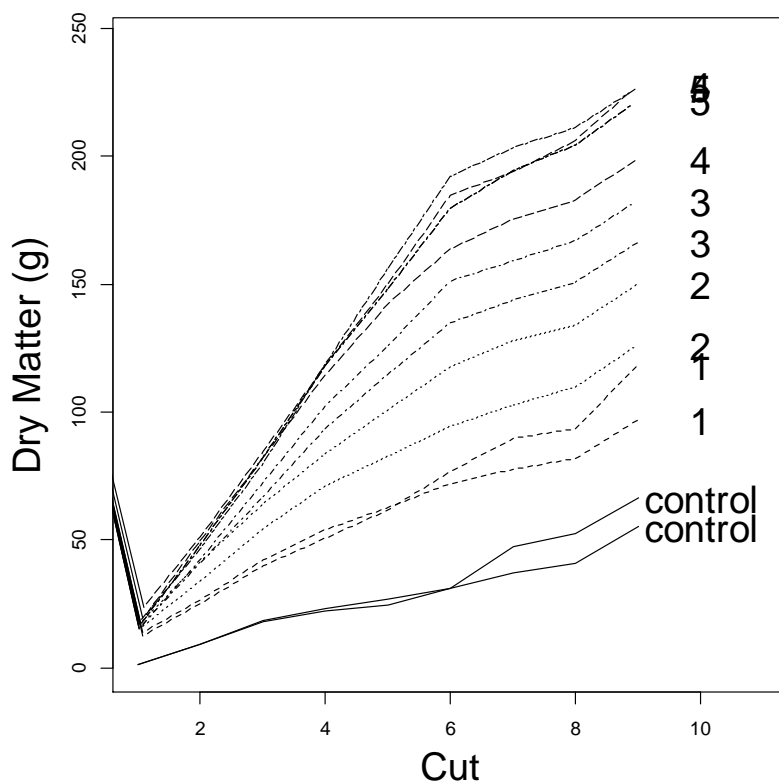


Figure 6.14. Dry matter production data from a pot trial with pasture. This example data illustrates the ability of pastures to continuously take up N where frequently cut and where conditions are not otherwise limiting. Numbers in the column to the right indicate fertiliser treatment rates.

In order to maximise the N_2O emission mitigation, the third option has some advantages over the other two. Firstly there is no ambiguity about the contribution of fertiliser practice to N_2O emissions. Secondly, given non-limiting conditions and cutting in response to dry matter production, uptake does not plateau (compare Fig. 6.14 to Figs. 6.10 and 6.12). Ideally these mitigation efforts could be prioritised and applied on the basis of local wind rose diagrams – rather than being applied 360° around the feedlot.

However, this kind of activity may not be justifiable relative to the size of the N_2O emission from the proximal zone relative to overall emission.

6.5.3 A potentially larger opportunity with a major caveat

Most N excreted to the pen surface appears to be volatilised as ammonia, leading to a significant indirect emission of N_2O (Fig. 8.6, Chapter 8). It is possible that N_2O emissions could be decreased by:

1. Decreasing volatilisation by modifications to pen conditions. This will retain more N in the pen manure, which is ideal for retaining fertiliser value.
2. Preventing subsequent emission from land-applied emissions from the increase in retained manure-N. Emissions from land-applied fertilisers can be quite significant, and in situations where emission is carbon limited (Chantigny et al., 2010) can lead to greater nitrous oxide emissions than inorganic N-fertiliser additions. For indirect emissions, emission can be considered an inorganic fertiliser application with no fuel consumption or embedded emissions, so the target may be a difficult one to match –

especially if the dry-land crop emission factor (0.003; Department of the Environment, 2013) applies to indirect emissions.

The scope of the current project did not include study of land application of manure, however, an associated study under the National Agricultural Manure Management Project conducted by the same team has developed evidence of a treatment that does decrease the N₂O emission potential of manure materials. This is the subject of on-going investigation.

A concurrent study (Deli Chen, University of Melbourne) is investigating the use of lignite to decrease volatilisation with some success. Decreased volatilisation in this case is probably largely due to the acid nature of most lignite materials. The very modest cation exchange capacity effect sometimes attributed to lignite (Schaaf et al., 2001; Stewart and Hossner, 2001; Qi et al., 2011; Uzinger et al., 2013), is usually measured at pH 7 or 8.5, and is probably is considerably less at the native pH of the lignite (due to variable charge effect of organic matter). Another possible mode of action, if the carbon contained in the lignite is not entirely resistant to breakdown, is microbial immobilisation of N. The University of Melbourne team is currently investigating the effect of lignite additions on field emissions in plot trials. If emissions related to land application are less than they would be for indirect emissions, there is scope to develop a Carbon Farming Initiative method.

If the University of Melbourne approaches are unsuccessful, there may well be scope for the DAF team to investigate the effectiveness of our NAMMP project technology in collaboration with University of Melbourne to enable the successful development of a Carbon Farming Initiative method.

6.6 Conclusion

Total ammonia volatilised from the operation during the period amounted to 210 tonnes of NH³-N during the study period (110 g animal⁻¹ day⁻¹). It is also apparent that the inventory volatilisation factor (30% of excreted N) underestimates volatilisation in this case.

Deposition within 600 m of the pen boundary is probably between 3.6 to 6.7 Mg N (1.7 to 3.2 % of volatilised NH₄⁺-N), with deposition approaching background rates at the maximum distances of the deposition traps from the pens (601 m for the West transect; 518 m for the South transect). Background deposition was measured at about 1 kg N ha⁻¹ year⁻¹.

Studies conducted within this project suggest that emission is dominantly controlled by the resident mineral-N in the soil, and by prevailing moisture content conditions. This weakens the position of having separate emission factors for direct and indirect emissions. Using this observation and observed deposition behaviour it is possible to supplement assumptions in the inventory and approach a more accurate emission factor. It appears that an indirect N₂O emission factor for this feedlot would more appropriately be 0.76 % rather than the value of 1 % currently recommended.

While it is possible to mitigate ammonia volatilisation from the pen, the successful development of a Carbon Farming Initiative method is dependent on also demonstrating that final manure application to land results in decreased emissions relative to the indirect N₂O emissions related to volatilisation.

7 Compacted stockpile and composting emissions (manuscript to be prepared)

M.R. Redding, J. Devereux, R.L. Lewis

7.1 Summary

Composting and stockpiling practices are a common part of the manure management systems of Australian feedlots. Surprisingly, the two studies described in this report are the first studies to measure feedlot manure emissions during composting and compacted stockpiles. Both studies were conducted at a scale equivalent to a small commercial operation, using common commercial techniques.

Composting emissions greatly exceed those from compacted stockpiling (54 x), largely due to the effect of aeration and turning on nitrous oxide emissions. This suggests that stockpiling is a mitigation practice relative to composting. Stockpiling is also beneficial with regard to nutrient retention, and maintaining the fertiliser value of the manure material. The flow-on effect of choosing to stockpile rather than compost is that the greater nutrient additions to soils may result at greater land application emissions.

The results suggest that the following changes to inventory values are warranted for temperate locations:

- A CH₄ conversion factor for compacted stockpiling of 0.14 % of initially excreted VS rather than the 4 % currently recommended (IPCC, 2006).
- A N₂O emission factor of 0.02% of initially excreted N rather than the current 0.5 % (IPCC, 2006).
- An NH₃ volatilisation factor of about 2 % of the initially excreted N contrasting with the current inventory value of 45 % (IPCC, 2006).
- A conservative CH₄ conversion factor for active windrow composting of 0.003 % of initial VS rather than the 1 % of initial VS currently recommended (IPCC, 2006).
- A N₂O emission factor of 1.4 % rather than the current 10 % for active windrow composting (IPCC, 2006)

7.2 Introduction

Stockpiling and composting of pen manure are relatively common practices in Australian feedlots. Manure from feedlots can be cleaned-out regularly (< 1 week) or as infrequently as < 6 months (Dantzman et al., 1983) and some subsequent form of temporary storage (stockpiling or composting) is likely to follow, depending on logistics, crop or pasture requirements, and the manure end-use. If manure is stockpiled or composted for a prolonged period, it could emit significant quantities of N₂O, NH₃ and CH₄ under suitable environmental conditions (Pratt et al., 2014).

In Australia, it is common practice to compact stockpiles to decrease the incidence of manure ignition through heat build-up. Compaction of manure stockpiles has demonstrated reductions in nitrous oxide and ammonia emissions (El Kader et al., 2007).

Unfortunately, little data on these practices is available. It may be a response to this lack of data that has led to emissions from stockpiled or composted manure being either unquantified or implicit in a more general pen manure emission estimate within the Australian GHG Inventory (Environment, 2014). Overseas studies exist measuring emissions from other manure storage systems (Petersen et al., 1998; Amon et al., 2001; Hao et al., 2001; Chadwick, 2005). Some studies are available that estimate greenhouse gas (GHG) emissions from Australian feedlot systems in the absence of field measurements. Estimates

based on theoretical mass balance studies indicate 20% of GHG emissions originate from solid storage and N₂O emissions from the stockpile and feedpad accounted for 80% of the greenhouse gas loss in CO₂ equivalents (Watts et al., 2012). A clear understanding of GHG sources is required to enable development of mitigation management strategies.

The studies described in this chapter seek to redress the lack of data globally, supplying local Australian data. This experimentally derived data are then used to calculate N₂O and CH₄ emission factors for pen manure compacted stockpile and compost practices. An ammonia volatilisation factor was also developed for compacted stockpiles. Determining the effects of these practices on greenhouse gas emissions will also enable the industry to identify any potential advantages or disadvantages of these, to some extent, elective practices.

7.3 Materials and methods

7.3.1 Location, stockpile, and composting

Stockpile monitoring was conducted on farming land 1750 m to the south west of the northern feedlot (Darling Downs, Queensland Australia, as described in Chapter 3).

Two manure stockpiles (windrows) were constructed from manure recently scraped from the feedlot pens (Fig. 7.1). Each stockpile consisted of 133.5 t of manure (wet mass) and measuring 47.5 meters long. The stockpiles were spaced 5.4m apart, and were compacted using a 6 t end loader. The stockpiles were retained in this condition for a period of 126 days, with continuous measurements from 20/6/13 to 12/7/13 and 15/10/13 to 29/10/13. Measurements were conducted during stockpile construction.

Similarly the composting windrows were constructed of recently scraped manure and spent woodchip collected from the handling runs (includes deposited manure) used to adjust the carbon:nitrogen ratio of the manure. Due to the volume of manure used and the lack of spacing between the intake manifolds at the site the initial blending was conducted on a pad located at the feedlot and then transported down to the measurement area. To form the piles 119.7 t of manure was combined with 39.6 t of woodchip and manure and mixed with an end loader. During this process 24 700 litres of water was added to increase the moisture content of the compost. This operation was completed by a commercial composting contractor. The moisture content was adjusted using a common practice in the composting sector, the “wet rag” moisture test, where a handful of compost is squeezed by hand and the moisture content is adjusted till the compost is moist like a wet rag but no moisture is lost when it is compressed. Compost windrows were spaced 5 m apart, were 5 m wide and 40 m long. Turning was accomplished using a skid loader, displacing several metres orthogonally to the long axis and then returning the pile to its original location. During this operation water was sprayed into the manure mix to replace moisture lost through evaporation. The compost pile was established 24/6/2014, turned on the 08/07/2014 and the 11/8/2014, with GHG emission measurements from 5/7/2014 to 14/8/2014. Emission measurement was not completed during compost windrow initial construction.

7.3.2 Windtrax layout, instrumentation and on-line analysis

Multiple inlets were configured in Windtrax to simulate line-averaging sensors matching the field positioned sample intakes, parallel to the windrows (Fig. 7.1). Methane and nitrous oxide were measure using a closed-cell fourier transform infrared spectra photometer (Spectronus FTIR). The intakes for the FTIR had 5 inlets positioned at a height of 1.75m spaced at 10m apart fabricated using ¼” internal diameter nylon line. To ensure even flow down the lines the multi-inlet manifold was constructed to an equal length design so the flow was distributed evenly between inlets. The manifolds were connected to two separate sealed

buckets to mix the incoming sample air and to provide sample integration (21 litre volume; air mixed internally using a computer fan). Air was continually drawn through the inlet manifolds using a vacuum pump (2 L min^{-1} , all air flows standardised to $25 \text{ }^\circ\text{C}$ and 1 atmosphere). Flow from the two inlets was alternately directed to the FTIR and the other to a vent when the line wasn't being sampled. The FTIR was set to measure each inlet for three 5-minute periods within each 30-minute averaging segment.

A similar design was used for ammonia measurements, though the five inlets were spaced 2m apart. The initial intake manifold was constructed of Teflon tube $\frac{1}{4}$ " internal dimension, each of 4 m length. This manifold was joined to $\frac{1}{4}$ " stainless steel line (swagelock) that ran back to a mobile laboratory located 30m north of the windrows. The Teflon manifold and stainless steel line were maintained at a temperature sufficient to raise the temperature of the sample air flow to $60 \text{ }^\circ\text{C}$. This was accomplished using resistive nichrome wire wrapped around the tube and connected to 24V power supplies, with temperature control via PID controllers and PT100 temperature probes positioned in the air stream at three points down the manifold. Air was drawn down the lines using 2 vacuum pumps (KNF 815 at 2 L min^{-1} ; controlled by Alicat MFC series mass flow controllers). An automated valve system (SMC solenoid valves controlled via Technologies TS-4200-8160 single board computer with python software) was used to alternate flow from the manifolds, alternately providing sample flow to an ammonia analyser (Picarro cavity ring-down spectrophotometer; <http://www.picarro.com/>) or to waste. Each intake flow was sampled for 3 five-minute periods within each 30 minute-time segment.

Windrow temperatures were monitored at six points using PT100 temperature probes mounted at the end of stainless steel tubes 1.2m long. These were positioned into the middle of each windrow's cross section, one at either end and one centrally located in each windrow after compaction. Bulk density of the compacted windrows was measured by collecting 6 undisturbed cores by hammering 75mm PVC tube vertically down through the pile. The cores were trimmed, the volume measured and the dry weight of the cores recorded. The windrows were sampled during construction by collecting grab samples (36 samples per replicate) as new material was deposited. This material was coned and quartered to obtain 3 replicate samples of the manure for chemical analysis. At the end of the monitoring period the piles were sampled by driving a 1.5 inch metal tube vertically through the pile. A total of 18 cores were collected with 6 cores being combined to form a replicate sample. Each replicate was coned and quartered down to a representative sample for chemical analysis. The manure samples were analysed for moisture, volatile solids (Greenberg et al., 1992), total N and C (Dumas technique), nitrate and ammonia (2 M KCl extract and steam distillation; Rayment and Lyons, 2010).

Meteorological data were collected using a 3D sonic anemometer (Campbell scientific Csat3D) located to the north of the windrows with wind statistics being collected continuously using a 30 minute averaging period.

7.4 Validation of ammonia measurements

While the closed-path approach to GHG emission measurement has been validated via tracer gas release (Redding et al., 2013), it was appropriate to conduct some validation of the ammonia technique where heated lines were used to convey the sample gas to a closed path analyser (in this case a Cavity Ring Down Spectrophotometer). A comparable approach to that employed for the compost and stockpile measurements was used to measure ammonia volatilisation from a volume of ammonium hydroxide solution ($20\text{g NH}_4\text{OH litre}^{-1}$).

The layout of intakes was essentially the same, though the western intake was repositioned with the intakes positioned 30cm above the ground with a 1.2m spacing, to better capture

the NH₃ plume coming from a 0.265 m diameter vessel holding 5.020 litres the reference solution. Emission and volatilisation measurements were conducted over a 3-day period.

Three aliquots of the source solution were analysed before and after the experiment, acidified to pH 2.0 then analysed for NH₄⁺ by steam distillation.

7.4.1 Data rejection criteria

Data collected were filtered according to accepted criteria to decrease the likelihood of unreliable results (Flesch, 1996; Loh et al., 2008b; McGinn et al., 2008). Periods were removed where the fraction of the emission source covered by touchdowns were < 0.30, -10 < stability lengths < 10 m, U* < 0.15, and Zo > 1.5 were rejected, leaving some gaps in the data. As is common with the bLS technique, data rejection based on standard criteria is often substantial (about 40% rejected in literature; Gao et al., 2009; Redding et al., 2013).

7.4.2 Statistics

Where substantial gaps in data were caused by data rejection, adjacent half-hourly (or hourly) figures were pooled to give adequate sample numbers (n > 5). An unbalanced analysis of variance was used to simultaneously estimate the 'day' effect (as these are likely to be different, due to meteorological conditions) and the 'time-of-day' effect. Due to the relatively sparse coverage on most days, the interaction was not considered. The standard deviations from the Windtrax model were analysed in parallel, using the same unbalanced analysis of variance. The residuals for all analyses proved to be approximately normal, so no transformation was required.

Table 7.1. Chemical composition of stockpiled manure and soil mixture at the start and end of trial.

		NH ₄ -N	NO ₃ -N	Dumas N	TKN	Total C	Org C	Al	Si	VS %
	pH	mg kg ⁻¹	mg kg ⁻¹	%	%	%	%	%	%	
Start	8.3 (0.04)	3561.4* (366.48)	107.9 (14.07)	2.93 (0.13)	2.84 (0.04)	27.91 (25.96)	26.77 (0.23)	1.76 (0.15)	13.5 (1.80)	0.59
End	8.3 (0.03)	6835.5* (53.43)	<LOQ	2.9 (0.07)	3.02 (0.07)	25.96 (0.57)	26.3 (0.6)	1.99 (0.27)	14.34 (1.51)	0.47

* Values significantly different at the 95% confidence level. Standard deviations of data stated below the mean.

<LOQ below lower limit of quantification.

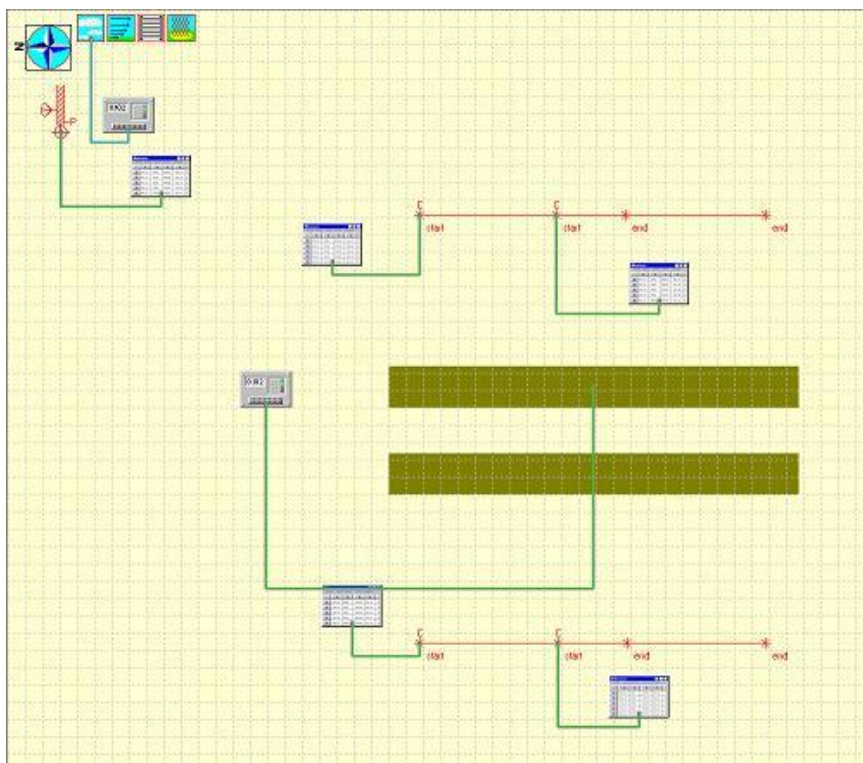


Figure 7.1. Windtrax layout with manure windrows running north to south with intakes located to the east and west of the windrows 3D sonic anemometer to the north east.

7.5 Results and discussion

Manure collected from feedlot pens contains a mixture of manure and the underlying soil and rock material on which the pen is constructed. By utilising the chemical properties of the base material of the soil compared to the stockpile manure it is possible to estimate the manure content of this material (Tables 1 and 3; initial manure for compost trial contained 1.5 ± 0.3 % Al and 9.4 ± 1.2 % Si; Pratt et al., 2015). Using this approach, it is estimated that the initial manure+soil mixture used to construct the stockpile contained about 69 % manure (of the 181.4 tonne dry mass, around 125 tonnes was manure). Likewise, for the compost pile it is estimated that around 63 % of the initial soil+manure mixture was manure (of the 78 tonne dry mass, about 49 tonnes was manure).

7.5.1 Stockpile measurements

7.5.1.1 Methane and nitrous oxide

While the first stockpile measurement campaign (20/6/13 to 12/7/13) was entirely successful, the subsequent measurements contained a long period of unexplained negative values and then a strong step change to high positive emissions. Since there was no corresponding change in the field situation at this time, these values were rejected as they probably represented an error in field practice, for example a substantial leak in the seal of one of the mixing drums. The following data analysis is therefore related to the measurements from 20/6/13 to 12/7/13.

The diurnal pattern of CH_4 and N_2O emissions is consistent with that reported by other researchers, where there is a peak in nitrous oxide emissions at midday (Figs 7.2 and 7.3; D Chen et al., 2009). While our pile temperature was very stable (average 37°C) the temperature was measured near the centre of the pile and the surface temperature of our

compacted piles may have varied diurnally. Pen emission data suggest that N₂O emissions peak at around 35 °C, which may have been more closely attained at the surface of the stockpile in the heat of the day (Redding et al, 2015).

The mean of the collected emission data represents an emission of 78.7±362 g of N₂O [tonne of manure]⁻¹ year⁻¹ (mean ± standard deviation; diurnal mean 85.7 g of N₂O [tonne of manure]⁻¹; Fig. 7.3, Table 7.1) and 544±2967 g of CH₄ [tonne of manure]⁻¹ year⁻¹ (mean ± standard deviation; diurnal mean 617 g of CH₄ [tonne of manure]⁻¹; Fig. 7.2, Table 7.1). No clear trends over time were evident with regard to CH₄ and N₂O emission, despite emission measurements commencing during construction of the stockpiles. This may partly be the result of the normal wide variability of the bLS method.

No published field-measured emissions from manure stockpiling exist (Pratt et al., 2014). The study described in this chapter is required to elucidate GHG emissions from stockpiled and composted beef feedlot manure in Australia. All subsequent comparisons here are based on other manure types.

The mean annual emission of CH₄ (Table 7.1) are at the lower range of the emission reported from other manure storage studies (range 620 - 43800g (t⁻¹.year⁻¹)) (Amon et al., 2001; Sommer, 2001; Chadwick, 2005; Yamulki, 2006; Moral et al., 2012). Methane production is highly dependent on temperature and only occurs under anaerobic conditions. Australian feedlot stockpiles are often compacted to create anaerobic conditions that reduce the chance of combustion. Very anaerobic conditions can result in high methane production from the stockpile (Amon et al., 2001). Our stockpiles were compacted (0.6 tonnes m⁻³), which should enhance anaerobic conditions in the pile and enhance methane emissions, but simultaneously decrease gas permeability out of the stockpile – potentially inhibiting emission (El Kader et al., 2007). The compacted stockpile temperatures measured from approximately the centre of the pile ranged from 28-40deg (30°C average) with a gradual rise over the study. Compaction may also serve to limit stockpile temperatures (Chadwick et al., 2011), potentially decreasing methane emission.

The reported effects of compaction on methane emissions in the literature are not entirely consistent. While Chadwick (2005) reported emission rates from compacted and covered stockpiles reaching values of approximately 120g.tonne⁻¹.d⁻¹, the emissions from two other storage periods were generally much lower: under 36g.tonne⁻¹.d⁻¹ and were apparently lower than the conventional stockpiles. Similarly while Sommer (2001) found much lower peak emission rates for compacted dairy manure (2.88g.Mg⁻¹.d⁻¹) the overall loss from the compacted treatment was higher than conventionally stored manure.

The source and age of the manure source stockpiled also probably served to decrease emissions. Before harvesting, feedlot pen manure has already accumulated on the pen surface for several months, and in this case has undergone mounding within the pen. This affords an opportunity for substantial decay prior to collection. Feedlot manures in stockpiles have lower biological methane potentials compared to fresh manure (Gopalan et al., 2013). This is in contrast to most farmyard manure studies which contain additional bedding materials such as straw which can increase methane production (Moller et al., 2008). In contrast, straw addition can reduce methane emissions, possibly due to increased aeration (Yamulki, 2006).

Annual emission of N₂O from the stockpile was estimated at 85.7 g [tonne of manure]⁻¹ year⁻¹. This is equivalent to an N loss of 0.320 g N₂O-N [kg initial N]⁻¹ over the 125.5 day period. It has previously been estimated that 27% of the initially excreted N in Australian feedlot systems is transported to manure stockpiles (Watts et al., 2012), while our volatilisation measurements from this feedlot suggest that about 60% of excreted N is likely volatilised as NH₃ (Chapter 6). These stockpile measurements would amount to losses of 0.09g N₂O-N per kg excreted N over the measurement period of 125.5 days. Other studies on compacted

stockpile have found a similar range. In a study comparing compacted and uncompacted manure (cattle deep litter; Sommer, 2001) reported emissions were comparable to those we observed: 109 - 328 g tonne⁻¹ year⁻¹. Our measurements are lower than those observed by Amon et al. (2001; dairy manure), who found N₂O emissions correspond to a range between 2.7 and 10.2 g N₂O–N per kg N excreted over a period of 80 days.

While the Australian inventory (Environment, 2014) does not separately account for manure stockpiles, the IPCC inventory does provide estimates for “solid storage” for cattle (IPCC, 2006). Given the initial VS measurements (Table 7.1), total mass of manures (126.7 tonnes), and emission observations, mass loss 40 to 120 days from deposition is likely to be around 35 % (Pratt et al., 2014), initial deposited VS is estimated at 175 tonnes.

Given the estimate of emission during the measurement period, and assuming that this emission continued throughout the stockpiling period, this amounts to 2.4 kg of CH₄ emissions over the stockpiling period. While this may over-estimate the actual emissions in this case, **we propose that a conservative emission factor for this manure management activity would be 0.14 % rather than the 4 % currently recommended (IPCC, 2006)** These values assume a value of 0.17 m³ [kg of VS excreted]⁻¹ for maximum methane producing capacity of this manure source, which is backed up by methane potential measurements conducted with this manure material (Pratt et al., 2014).

Similarly, it is also possible to estimate a nitrous oxide emission factor for the compacted stockpile management. Our volatilisation measurements from the entire feedlot (Chapter 6) suggests that the 5300 kg of N in the manure stockpile probably corresponds to about 13 000 kg of N excreted to the pen surface (60 % volatilisation from the pens). Assuming the observed rate of N₂O emission continued throughout the period of stockpile storage, about 27 kg of N may have been lost throughout the 125.5 days. **Using these measurements of an enterprise-scale Australian compacted stockpile management, we recommend an emission factor of 0.02% rather than the current 0.5 %.**

Table 7.2. Stockpile and composting emissions

	Mean Stockpile Emissions	
	g [tonne of manure] ⁻¹ year ⁻¹	kg CO ₂ -eq [tonne of manure] ⁻¹ year ⁻¹
CH ₄	617	15.5
N ₂ O	85.7	26.6
NH ₃	6209	-
Mean Composting Emissions		
CH ₄	15.6	0.39
N ₂ O	7429	2302

Table 7.3. Properties of compost and initial materials.

	VS	Total C	Organic C
		%	
Harvested pen manure	0.41	26.8 ± 3.2	25.4 ± 1.4
Initial wood chip	0.97	42	42
Initial mixed compost	0.58 ± 0.03	24.5 ± 0.1	22.2 ± 0.5
Compost sampled 08/07/14	0.49 ± 0.04	21.8	20.8
Compost sampled 11/08/14	0.41 ± 0.09	20.7	18.9
Compost final	0.45 ± 0.05	20.5	21.0

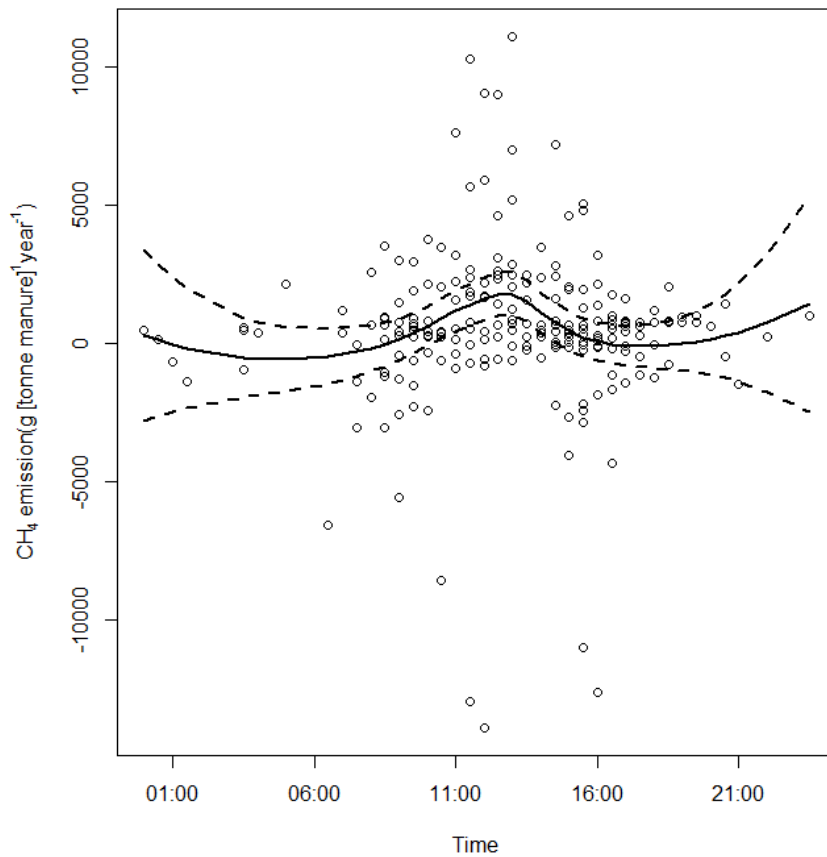


Figure 7.2. CH₄ diurnal emission pattern.

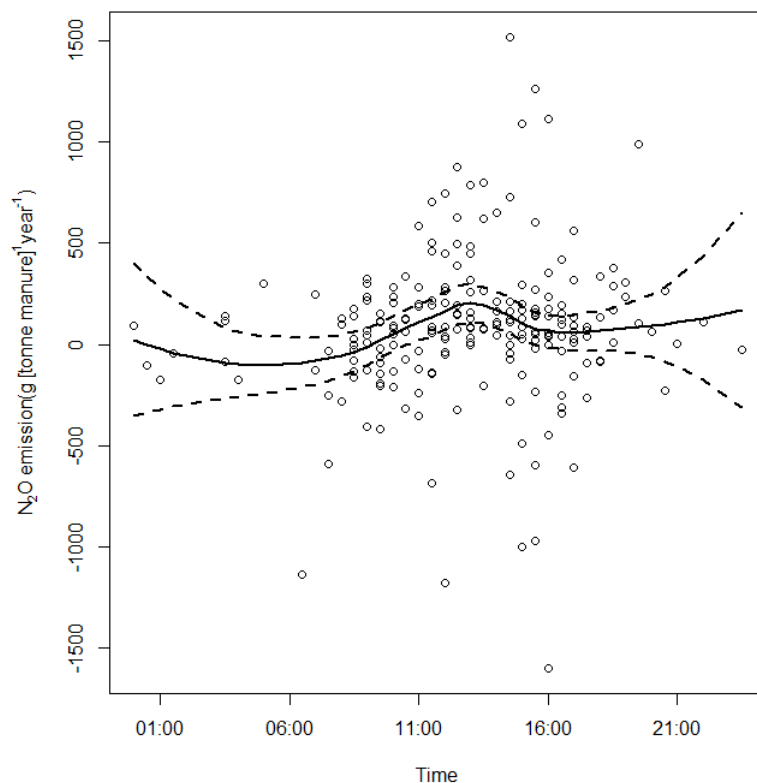


Figure 7.3. N₂O diurnal emission pattern.

7.5.1.2 Ammonia volatilisation

Ammonia emissions also peak around mid-day (Fig. 7.4), with mean volatilisation of 6137 ± 3552 g of NH₄ [tonne of manure]⁻¹ year⁻¹ (mean \pm standard deviation; diurnal mean 6209 g of NH₄ [tonne of manure]⁻¹ year⁻¹; Fig. 7.4, Table 7.1). Maximal volatilisation was around 21 000 g of NH₄ [tonne of manure]⁻¹ year⁻¹, though only for a short period (Fig. 7.5). These volatilisation rates are similar to the range published in other manure storage studies with maximum emission rates between approximately 5328 to 55 414 g of NH₄ [tonne of manure]⁻¹ year⁻¹ quickly dropping off to under 106 g of NH₄ [tonne of manure]⁻¹ year⁻¹ (Chadwick, 2005; El Kader et al., 2007). During the 125.5 days of the trial, volatilisation amounted to about 4% of the total N in the initial material, and a potential annual loss of around 12 %. In comparison to other published manure storage studies where cumulative loss of ammonia ranges from 0.3% to 4.5% of the total N, our measurements are similar.

Most studies indicate ammonia loss should occur rapidly within the first weeks of storage after which almost negligible emissions are expected (Moral et al., 2012). In comparison to the body of literature the mass of manure we used in the trial and period of experimentation were large and of a realistic commercial scale. In our case, ammonification was an on-going process (Table 7.1) within the stockpiles, leading to continued potential for ammonia volatilisation. As would be expected for compacted stockpiles, they appear to be strongly anaerobic, as evidenced by the lack of nitrate accumulation, and indeed the total elimination of nitrate via denitrification processes.

In a study between conventional and compacted and covered stockpiles Chadwick (2005) found compaction and covering could lower NH₃ emissions; however, rainfall suppressed emissions from the conventional stockpiles to similar levels as the covered piles in two of the three measured storage periods.

While the Australian inventory (Environment, 2014) does not provide separate account for manure stockpiles, the IPCC inventory does provide estimates for “solid storage” for cattle (IPCC, 2006). Our volatilisation measurements from the entire feedlot (Chapter 6) suggest that the 5300 kg of N in the manure stockpile probably corresponds to about 13 000 kg of N excreted to the pen surface (60 % volatilisation from the pens). We observed volatilisation of about 220 kg of this N within 125.5 days.

Our stockpile volatilisation measurements are close to the low end of the range of other authors, but are very much below the 10 to 65 % range included in inventory. These inventory volatilisation factors also include NO_x losses; however, these additional losses are likely to be a small fraction of the NH_3 volatilisation. Previous studies indicate that the magnitude of NO-N losses are of the same order of magnitude as $\text{N}_2\text{O-N}$ emissions (Sanz-Cobena et al., 2012; Abalos et al., 2013), and are likely small relative to losses observed due to ammonia volatilisation (Stehfest and Bouwman, 2006; Yang et al., 2010).

It appears that a volatilisation factor of about 2 % of the initially excreted N would appropriately represent the local Queensland conditions we observed. This contrasts strongly with the estimate published in the international inventory for solid storage of cattle manure (45 % of excreted N; IPCC, 2006).

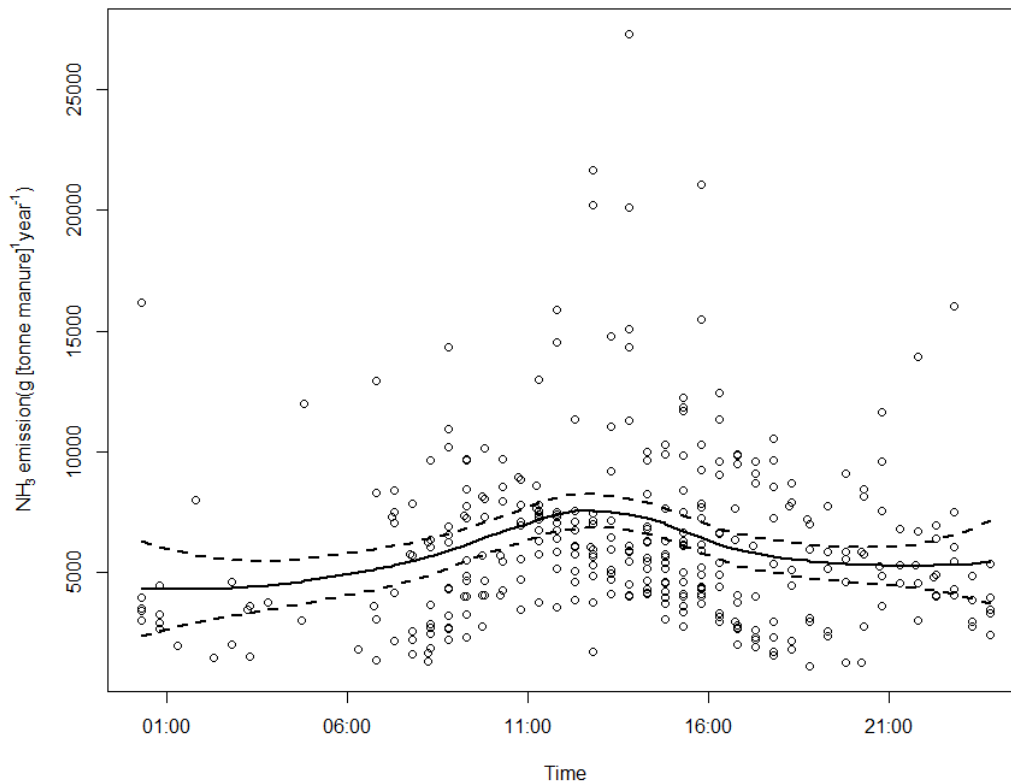


Figure 7.4. NH_3 diurnal emission pattern.

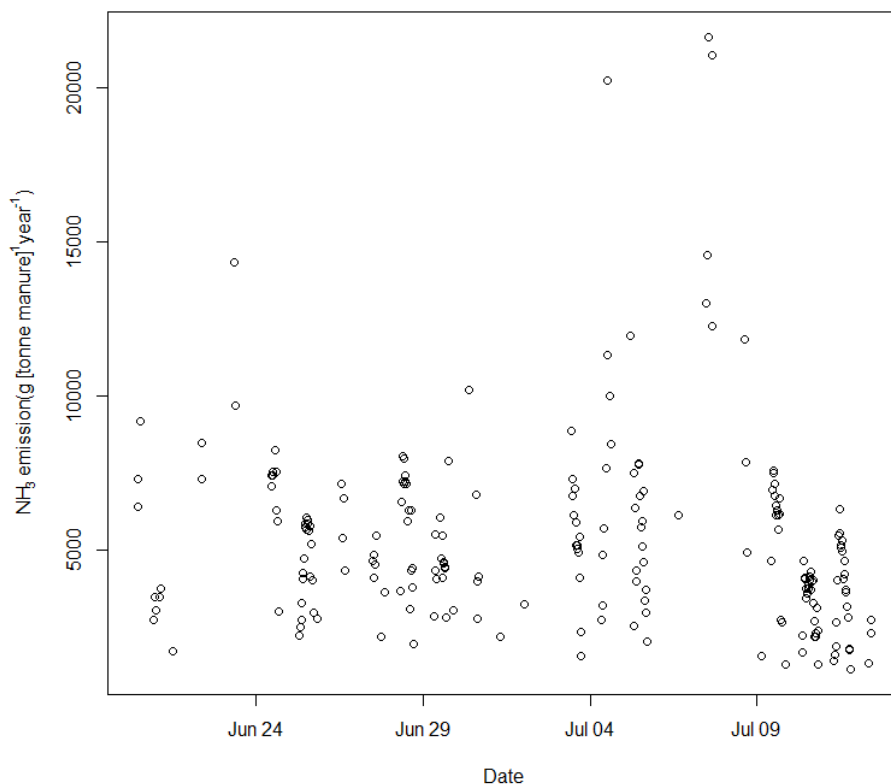


Figure 7.5. Progress of NH₃ volatilisation throughout the stockpile trial.

7.5.2 Compost emissions

The emission time series for CH₄ and N₂O indicate a fairly strong relationship with time, and the turning event during the measurement period (Figs. 7.6 and 7.7). This management responsive process, however, tended to obscure any diurnal pattern in emissions (Figs. 7.8 and 7.9).

A key finding is the comparison between compacted stockpile emission and composting emissions (Table 7.2), where greenhouse gas emissions attributable to composting greatly exceed those from compacted stockpiling, largely due to the effect of aeration and turning on nitrous oxide emissions.

As stated above, the Australian inventory (Environment, 2014) does not separately account for manure stockpiles, though the IPCC inventory does provide estimates for active and passive windrow composting (IPCC, 2006). Given the initial VS measurements (0.58 g g⁻¹), total mass of manures (49 tonnes), and observations that mass loss from this manure source 40 to 120 days from deposition is likely to be around 35 % (Pratt et al., 2014), initial deposited VS is estimated at 59 tonnes. Though the composting trial was limited (for logistic and project schedule reasons) to 51 days, commercial composting is quite likely to extend for around 12 weeks. Our 51-day emission measurements were therefore used to provide a conservative estimate of emissions over 84 days (84/51 x emission observed).

Using the estimate of emission during the measurement period (51 days; Table 7.2), and assuming that this emission continued throughout the composting period (typically 84 days), this amounts to 0.176 kg of CH₄ emissions over the composting period. While this may over-estimate the actual emissions in this case, **we propose that a conservative methane**

conversion factor for this manure management activity would be 0.003 % of initial VS rather than the 1 % of initial VS currently recommended for actively composted windrows (IPCC, 2006). These values assume a value of $0.17 \text{ m}^3 [\text{kg of VS excreted}]^{-1}$ for maximum methane producing capacity of this manure source.

Similarly, it is also possible to estimate a nitrous oxide emission factor for the composting procedure. Our volatilisation measurements from the entire feedlot (Chapter 6) suggest that the 1500 kg of N in the compost windrow probably corresponds to about 3741 kg of N excreted to the pen surface (60 % volatilisation from the pens). Assuming the observed rate of N_2O emission continued throughout the period of stockpile storage, about 32 kg of N may have been lost throughout the 51 days, and about 53 kg during a projected 84-day composting cycle. **Using these measurements of an enterprise-scale Australian composting operation, we recommend an emission factor of 1.4 % rather than the current 10 % for active windrow composting (IPCC, 2006).**

No comparable data are available on lot-fed beef manure composting. A study conducted on 100-day composting of beef manure (with or without distillers residue) indicated cumulative emission of 0.29 to 0.57 % of initial N as N_2O , and less than 0.4 % of the initial C in the manure as CH_4 (Hao et al., 2011). The emissions measured in our composting experiment exceeded these (around 2% of windrowed N). Szanto et al. (2007) found that nitrous oxide emissions from turned pig manure-straw compost piles emitted 2.5% of total N as nitrous oxide, while unturned piles were much worse, emitting 9.9% of total N as nitrous oxide. In another trial nitrous oxide was found to be the most significant GHG emission from a deep litter pig manure stockpile (78.4% of emissions CO_2 equivalent, Wolter et al., 2004), a finding that concurred with our own study (N_2O represented 99 % of CO_2 equivalent emissions; Table 7.2).

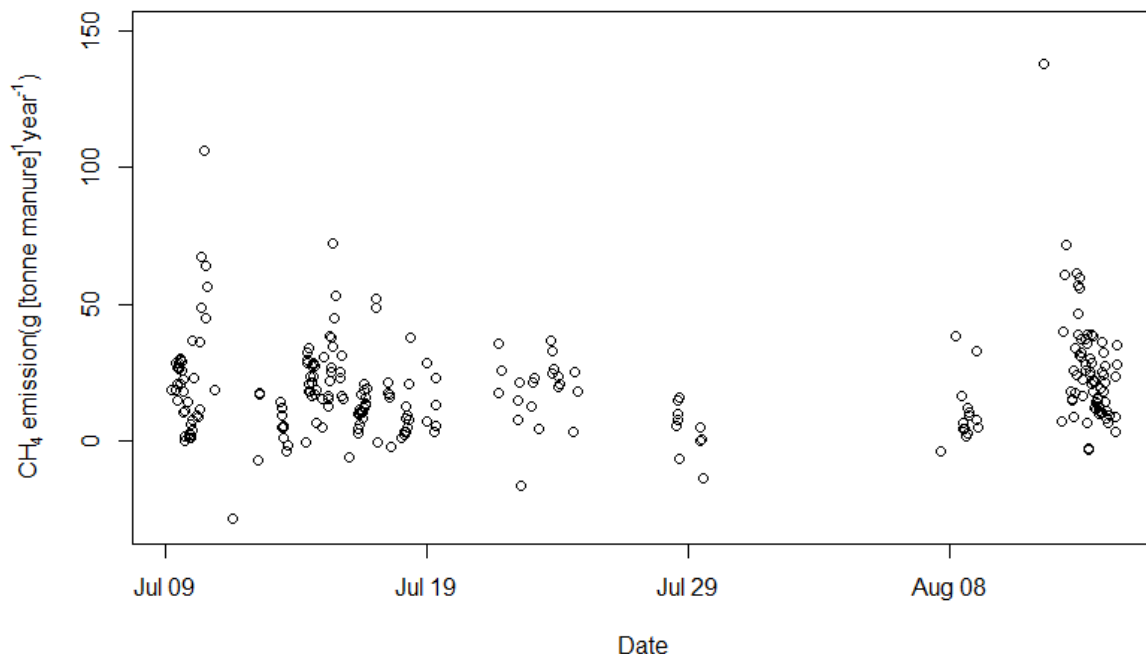


Figure 7.6. Methane emissions were strongly related to the occurrence of the turning events on the 8th of July and 11th of August.

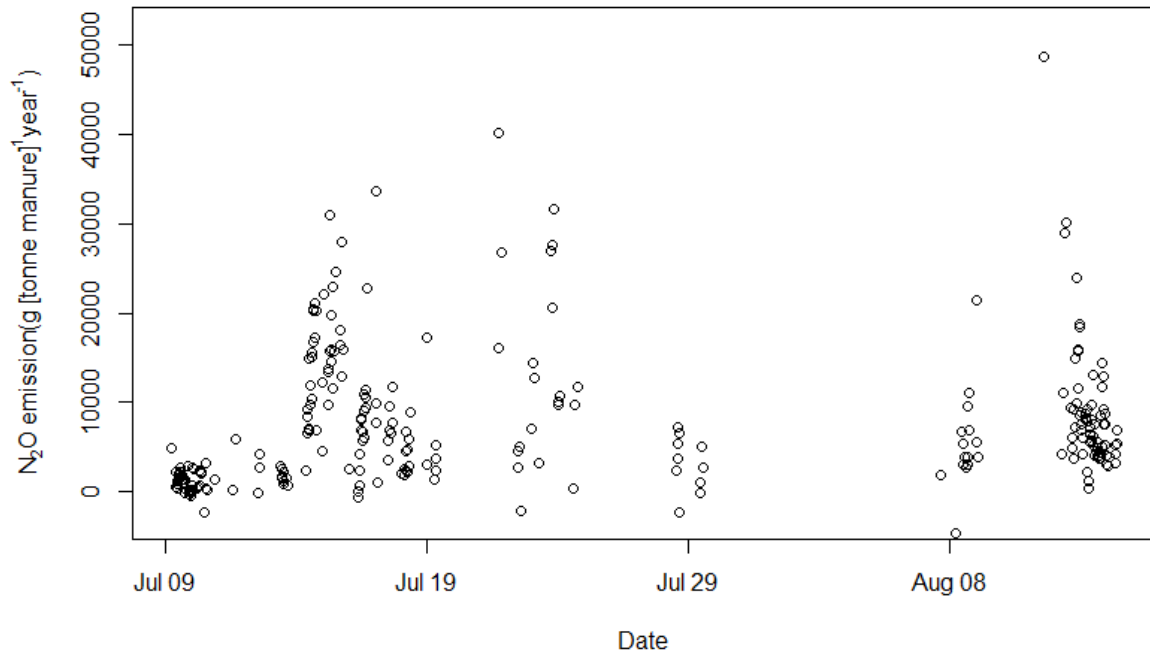


Figure 7.7. Nitrous oxide emissions were strongly related to the occurrence of the turning events on the 8th of July and 11th of August.

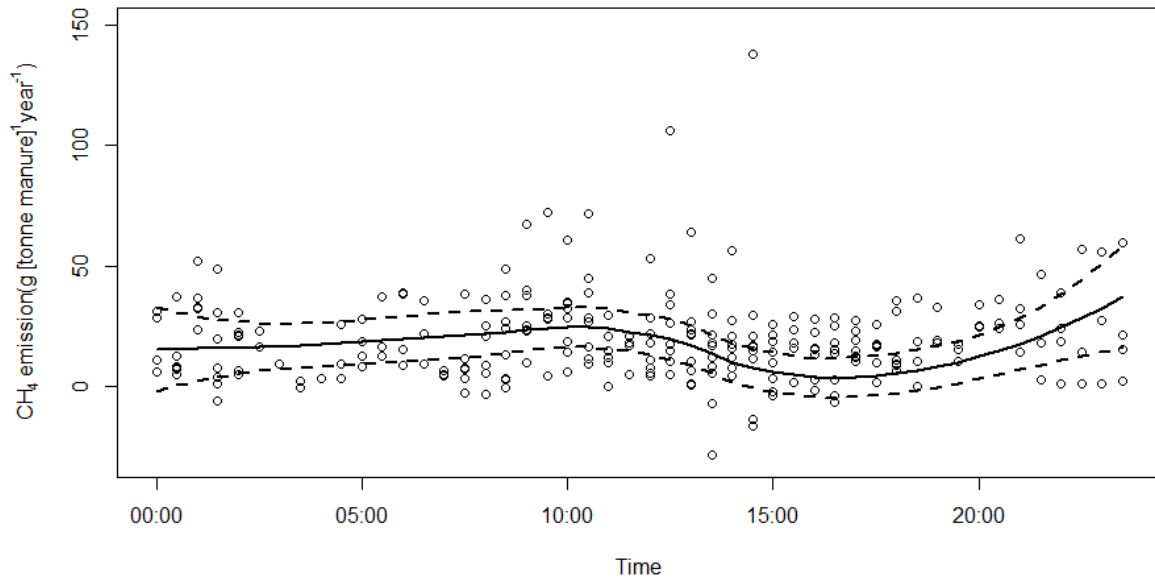


Figure 7.8. Clear diurnal patterns were not present for the composting CH₄ emission data.

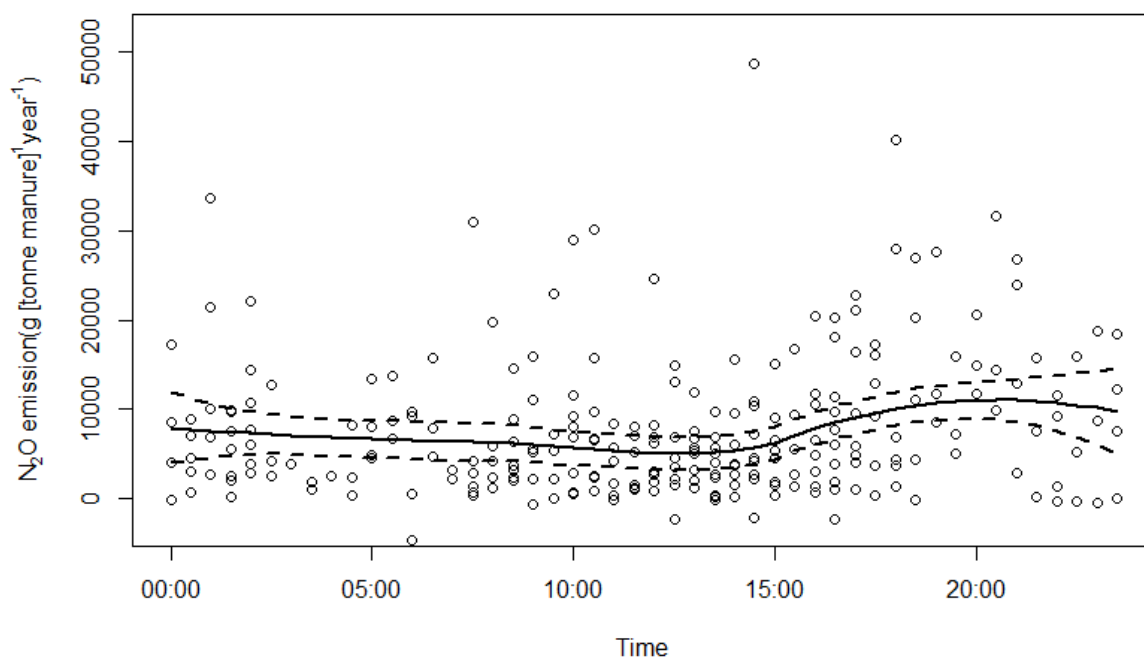


Figure 7.9. Clear diurnal patterns were not present for the composting N₂O emission data.

7.5.3 Mitigation options

A clear observation from the emission measurements is that composting emissions were far greater than those from the compacted stockpile. This was largely as a result of the high N₂O emissions from the compost windrows (54 x the emissions from the compacted stockpile; Table 7.2). Stockpiling is therefore a mitigation practice relative to composting, and provides less opportunity for N-value loss through ammonia volatilisation than actively turned composting. The flow-on effect of choosing to stockpile rather than compost is that the greater nutrient additions to soils may result in greater land application emissions.

Compost and stockpiled manure, however, are not equivalent products. Well composted manure is highly friable leading to ease of application, low odour, and physically stable, characteristics that are very different from those of stockpile manure. The markets and applications for these two materials are quite different.

7.6 Conclusion

The two studies described here are the first to measure feedlot manure emissions during composting and compacted stockpiles. The measurements were collected at a scale equivalent to a small commercial operation, using common commercial techniques.

Composting emissions greatly exceed those from compacted stockpiling, largely due to the effect of aeration and turning on nitrous oxide emissions. Switching from actively turned composting to compacted stockpile practices will result in lower emissions at that point in the manure management cycle. The additional N retained may result in greater emissions of N₂O at the point of land application.

From the results of the composting and compacted stockpiling measurements we are able to propose a range of conservative inventory parameters for temperate locations:

- A CH₄ conversion factor for compacted stockpiling of 0.14 % of initially excreted VS rather than the 4 % currently recommended (IPCC, 2006).
- A N₂O emission factor of 0.02% of initially excreted N rather than the current 0.5 % (IPCC, 2006).
- An NH₃ volatilisation factor of about 2 % of the initially excreted N contrasting with the current inventory value of 45 % (IPCC, 2006).
- A conservative CH₄ conversion factor for active windrow composting of 0.003 % of initial VS rather than the 1 % of initial VS currently recommended (IPCC, 2006).
- A N₂O emission factor of 1.4 % rather than the current 10 % for active windrow composting (IPCC, 2006).

8 Resource use and environmental impacts from grain finishing beef cattle in Australia feedlots: a gate-to-gate life cycle assessment (closely based on manuscript to be submitted)

Stephen Wiedemann¹, Rod Davis¹, Eugene McGahan¹, Caoilinn Murphy¹ and Matthew Redding²

¹FSA Consulting, PO Box 2175, Toowoomba Qld 4350, Email: stephen.wiedemann@fsaconsulting.net

² Agri-Science Queensland, Department of Agriculture and Fisheries, PO Box 102, Toowoomba Qld 4350

8.1 Summary

Grain finishing of cattle has become increasingly popular in Australia over the last thirty years; however the associated environmental impacts and resource use is a growing topic of interest that requires detailed analysis. This study used a gate-to-gate life cycle assessment (LCA) to investigate impacts of the grain finishing stage for cattle in seven feedlots in eastern Australia. Three market related feeding periods were investigated: short fed domestic market (55-80 days on feed), mid-fed export (108-164 days on feed) and long-fed export (>300 days on feed). Impacts were reported per kilogram of live weight gain. Mean fresh water consumption was found to vary from 171.9 to 510.1 L/kg live weight gain and mean stress weighted water use ranged from 100.9 to 193.2 WSI eq. L/kg live weight gain. Irrigation contributed 57-91% of total fresh water consumption across the market types. Due to the large range in irrigation water use at different feedlots, no association was found between consumption and productivity or market type. The mean fossil energy demand ranged from 16.6 to 34.5 MJ LHV/kg live weight gain and arable land occupation from 18.7 to 40.5 m²/kg live weight gain. Mean greenhouse gas emissions ranged from 4.0 to 7.8 kg CO₂-e/kg live weight gain (excluding land use and direct land use change emissions). Emissions were dominated by enteric methane and contributions from the production, transport and milling of feed inputs. Linear regression analysis showed that the feed conversion ratio was able to explain >86% of the variation in greenhouse gas intensity and energy demand.

Relative contributions to total manure management emissions (46 to 68 kg co₂ eq/ 100 kg live weight gain; northern and southern feedlots respectively; reverting to the 0.01 N₂O-N / kg N to land application and indirect emission factor; all units kg co₂ eq/ 100 kg live weight gain) given the assumptions were: pen and stockpile manure 22.5 and 10.2; indirect emission 27 and 4.5; pond 22.5 and 10.2; land application 6 and 4.4. Given the current inventory assumptions the corresponding manure management emission 146.7 and 183.4 kg co₂ eq/ 100 kg live weight gain, with the difference dominantly due to the revised emission estimates for the pen and stockpile made possible by this research project.

Current uncertainty around the appropriateness of the emission factors related to indirect nitrous oxide emission factors, and the emission factor associated with land application of manure are not likely to raise overall emission manure management emissions to the previous estimated values unless they are multiples higher than their current inventory value (0.01 N₂O-N / kg N).

A small additional study would likely resolve this uncertainty. Less conclusive data may also flow from several known concurrent research projects where this may be a peripheral observation.

8.2 Introduction

Grain finishing has become increasingly prevalent in Australia over the past three decades (Bindon and Jones, 2001) as a means of increasing cattle growth rates, allowing younger turnoff and potentially heavier finished weights. In Australia's variable climate, feedlots also have an important role finishing cattle in drought conditions when grass and forage supply is low. However, the impact of grain finishing on finite resources and environmental impacts is a topic of growing interest both in Australia and internationally, and this must be considered as part of a broader discussion on the advantages and costs of alternative beef finishing systems. Australian agriculture faces a number of environmental and resource issues. Agriculture generated 14.6% of Australia's total direct greenhouse gas (GHG) emissions in 2010 (Environment, 2014), with beef cattle contributing the largest proportion of these emissions. Agriculture also uses 65-70% of water extracted from the environment in Australia (ABS, 2006). Global resources of land suitable for agricultural production are also constrained and in Australia, cropping land represents <4% of land mass while the area of native and modified pastures is 56% of Australia's land mass (Lesslie and Mewett, 2013). Hence, the availability of arable land is a more acute concern than availability of non-arable rangelands. In the context of these constraints, agricultural systems must be assessed on their ability to produce food with minimum impacts in addition to other benefits. Life cycle assessment (LCA) is a tool particularly suited to multi-impact supply chain analysis and has been previously applied to Australian beef (Peters et al., 2010a; b; Eady et al., 2011; Ridoutt et al., 2012; Wiedemann et al., 2014a), wheat (Brock et al., 2013), pork (Wiedemann et al., 2010), poultry (Wiedemann and McGahan, 2011; Wiedemann et al., 2012) and lamb (Peters et al., 2010a; Wiedemann et al., 2014c) case studies. Wiedemann et al. (2014a) showed that water use and greenhouse gas emissions have declined in Australia over the past three decades, partly as a result of increased grain finishing. However, no study to date has provided a detailed analysis of resource use and environmental impacts of the grain finishing stage separately from the full supply chain. This is important, because the intensity of production and the inputs required are quite different during grain finishing compared to the breeding and backgrounding stages and independent analysis is required to understand impacts.

Grain finishing has a number of key differences from grass finishing; GHG emissions from enteric methane are lower (Dong et al., 2006) while emissions from manure management may be higher (Environment, 2014), though to date the Australian inventory has not based estimates of manure emissions on Australian research. Feedlot operations require the transport of feed inputs which are typically grown with inputs of fertiliser and machinery operations, increasing fossil fuel energy use and potentially greenhouse gas emissions. Fossil fuels are also important inputs for grain milling and feedlot operations, and have been quantified for Australian feedlots by Davis et al. (2010a; b). While detailed research on feedlot water use has been completed in Australia by Davis et al. (2010a) this did not include some aspects of the wider feedlot system, such as the production of feed inputs. Hence, a comprehensive understanding of water use for grain finishing has not been completed to date. One key advantage regarding resource use and environmental impacts proposed from grain finishing arises from the increase in growth rates, which can reduce impacts by lowering maintenance requirements relative to growth rate, via the dilution of maintenance effect (Johnson et al., 1996). This concept has been identified as a major factor contributing to the reduction of impacts throughout a supply chain where cattle are finished on grain with increased growth rates (Wiedemann et al., 2014a) though these authors found the reverse trend occurs with the intensity of fossil fuel use.

In order to understand the role of grain finishing in the full supply chain, a detailed understanding of the grain finishing system is required. The present study is the first to investigate impacts from beef grain finishing systems using a LCA approach. The study aimed to quantify impacts and identify hot-spots in the feedlot production system including all

elements of the supply chain associated with grain finishing, including production of feed and other inputs to the system, but excluding the beef cattle supply chain prior to feedlot entry (a gate to gate study).

8.3 Materials and methods

8.3.1 Goal and scope

This study reports a gate-to-gate life cycle assessment (LCA) of 7 beef feedlots in eastern Australia and is a companion study to Wiedemann et al. (2014b). The study investigated global warming (aggregated GHG emissions, including impacts from Land Use and direct Land Use Change – LU and dLUC), using Global Warming Potentials (GWPs) of 25 for methane and 298 for nitrous oxide (Solomon et al., 2007). Fossil fuel energy demand was assessed using the Fossil Fuel Depletion indicator (Frischknecht et al., 2007), measured in mega-joules (MJ) using lower heating values (LHV). Stress weighted water use was determined by multiplying the total fresh water consumption in each region with the appropriate water stress index (WSI) values from Pfister et al. (2009). The value was then divided by the global average WSI (0.602) and expressed as a water equivalent (H₂O-e) (Ridoutt and Pfister, 2010). Results from two life cycle inventory (LCI) methods were also assessed: fresh water consumption and land occupation. Results were presented using a functional unit (FU) of kilograms of live weight gain (kg LWG) in the grain finishing phase (gate-to-gate). This included all processes and inputs associated with grain finishing, including the impacts of producing the ration, but excluded the impact of producing the feeder cattle prior to feedlot entry.

8.3.2 Description of the case-study feedlots

The feedlots (FL) ranged in throughput from 6000-130,000 head of cattle annually, with a total mean throughput for the years 2007 and 2008 of 330,000, or ~15% of industry throughput for these years (ALFA and MLA 2007, 2008). Feedlots were located in the following regions: central Queensland (QLD – FL 1), southern QLD (FL 2, 3, 4), northern New South Wales (NSW – FL 5), southern NSW (FL 6) and Victoria (VIC – FL 7). Three market related feeding periods were investigated: short-fed domestic market (55-80 days on feed), mid-fed export (108-164 days on feed) and long-fed export (>300 days on feed).

8.3.3 Life cycle inventory

Detailed production data, livestock inventories and input data were collected from feedlot financial records, interviews and site visits (Davis et al., 2010a, 2010b). Production characteristics are provided in Table 8.1. Fossil fuel energy demand was determined from inventories of purchased fossil fuels and electricity use at the feedlot (Table 8.2, Table 8.4) and from impacts associated with commodity use. Transport records for livestock movements, purchased inputs and staff movements were determined from feedlot inventory data and were included in the analysis. Impacts associated with infrastructure, such as feedlot construction, were excluded based on the findings of a scoping study showing the contribution from these was <1% (unpublished data). Impacts associated with services such as communications, insurance and accounting, were modelled based on expenditure, using economic input-output data (Rebitzer et al., 2002).

Table 8.1 – Feedlot cattle production parameters for average market types

	Domestic Grain		Export grain		Export grain	
	Short fed		Mid fed		Long fed	
	mean	range	mean	range	mean	range
Entry Weight (kg LW)	347	327 - 370	421	392 - 463	441	n.a.
Days on feed (d)	69	55 - 80	125	108 - 164	346	n.a.
Average daily gain (kg/d)	1.8	1.7 - 1.9	1.8	1.7-2.0	1.0	n.a.
Feed conversion ratio (kg/kg)	5.3	4.7 - 5.8	6.0	5.4 - 6.5	10.4	n.a.
Exit Weight (kg LW)	469	438 - 502	652	594 - 730	784	n.a.
Mortality rate	0.8%	0.16%-1.65%	0.7%	0.40%-1.30%	2.1%	n.a.
Dry Matter Intake (DMI) (kg/hd/d)	9.2	8.7 - 9.7	10.9	10.2 - 12.1	10.3	n.a.
Number of feedlots (n)	5		4		1	n.a.

data were sourced from the Australian LCI database (Life Cycle Strategies, 2007) where available, or the European Ecoinvent (2.0) database (Frischknecht et al., 2005). Feed grain inventory data were reported in Wiedemann et al. (2010a) and Wiedemann and McGahan (2011)(Primary inventory data Tables 8.2 to 8.5).

Table 8.2– Feedlot purchased energy for general operations, reported per 1000 head days

	FL1	FL2	FL3	FL4	FL5	FL6	FL7
Electricity (kWh/1000 hd d)	19.55	58.37	63.84	84.73	17.01	19.84	68.83
Diesel (L/1000 hd d)	11.34	16.75	12.14	19.50	7.66	13.86	12.67
Gas (MJ/1000 hd d)	0.83	0.00	0.00	0.00	0.00	0.00	0.00
Petrol (L/1000 hd d)	0.72	0.81	8.16	9.65	11.03	11.76	6.90

Dry matter intake (DMI) was determined from records of feed delivery to the feed bunk at each feedlot. Feed delivery is weighed and recorded on an as-fed basis and was converted to DMI using recorded or calculated ration moisture contents. Feed intake and feed characteristics (Table 8.3) were used to model livestock greenhouse gas emissions using methods described below. Background data were sourced from the Australian LCI database (Life Cycle Strategies, 2007) where available, or the European Ecoinvent (2.0) database (Frischknecht et al., 2005). Feed grain inventory data were reported in Wiedemann et al. (2010a) and Wiedemann and McGahan (2011). Commodity data and energy use associated with ration production are provided in Table 8.3 and Table 8.4.

Table 8.3– Commodity purchases per tonne of ration for three market classes, averaged over two years

Ration component ^A	Short-fed Domestic	Mid-fed Export	Long-fed Export
Barley (10%)	75.7	94.7	136.7
Maize (8%)	68.7	0.0	0.0
Sorghum (10%)	313.2	289.4	157.3
Wheat (13%)	225.6	295.5	309.3
Canola (36%)	0.7	0.9	1.3
Cottonseed Meal (38%)	20.1	23.9	0.0
White fluffy cottonseed	61.8	63.4	0.0
Hay ^B	26.1	33.6	2.9
Straw ^C	10.6	3.2	89.0
Silage ^D	111.7	85.1	199.7
Cotton Hulls	4.3	17.2	0.0
Recycl Oil/Tallow	7.2	12.2	1.6
Molasses	25.1	21.9	71.2
Dry supplement	0.0	0.0	31.7
Wet supplement	51.2	58.7	0.0
Total (kg)	1,000	1,000	1,000

^A Protein content in brackets

^B Includes Lucerne, sorghum and wheat hay

^C includes corn, wheat, triticale and sorghum straw

^D Includes corn, sorghum, oaten and wheat silage

Table 8.4– Feed-milling energy and water inputs per tonne of ration delivered to the feed bunk

	FL1	FL2	FL3	FL4	FL5	FL6	FL7
Electricity (kwh/tonne ^A)	8.05	6.61	4.70	7.08	6.68	5.54	5.36
Diesel (L/tonne)	0.85	0.83	2.63	2.27	0.62	1.77	1.55
Gas (MJ/tonne)	180.65	128.90	0.00	0.00	163.91	163.21	191.59
Petrol (L/tonne)	0.00	0.00	0.00	0.00	0.03	0.00	0.00
Water (L/tonne)	138.89	130.61	189.36	42.44	194.29	80.46	197.27

^A Reported on an 'as fed' basis inclusive of moisture.

8.3.4 Fresh water consumption

The water use inventory was developed using measured water data described in Davis et al. (2010a); and modelling of dam water supply systems and dam supply efficiencies using methods outlined in Wiedemann et al. (2014b). Australian feedlots are designed to control drainage and overland flow around the feedlot site to restrict movement of manure nutrients to the environment (Skerman, 2000), thus restricting runoff to the environment compared to the reference site prior to feedlot construction. The change in runoff was included in the fresh water consumption inventory following guidance from the international standards organisation (ISO) by modelling long-term runoff from each feedlot based on the soil and vegetation properties of the reference site prior to feedlot construction. Runoff modelling was done using USDA-SCS KII curve numbers (USDA-SCS, 1972; USDA NRCS, 2007).

The water use inventory was developed using measured water data described in Davis et al. (2010a); and modelling of dam water supply systems and dam supply efficiencies using methods outlined in Wiedemann et al. (2014b). Details of the water supply system and system efficiency are provided in Table 8.5.

Australian feedlots are designed to control drainage and overland flow around the feedlot site to restrict movement of manure nutrients to the environment (Skerman 2000), thus restricting runoff to the environment compared to the reference site prior to feedlot construction. The change in runoff was included in the fresh water consumption inventory following guidance from ISO by modelling long-term runoff from each feedlot based on the soil and vegetation properties of the reference site prior to feedlot construction. Runoff modelling was done using USDA-SCS KII curve numbers (USDA-SCS 1972; USDA NRCS 2007). Data are shown in Table 8.6.

Irrigation water use associated with feed inputs was assessed both for ration inputs produced at feedlot farms, which was described as 'ration irrigation on-site, and irrigation associated with purchased commodities, described as 'ration irrigation off-site. A number of feedlots used irrigation on-site to produce hay or silage inputs. Irrigation water use was recorded from measured data collected from the feedlots, and was attributed to the cattle via the feed production system. Supply losses associated with on-site irrigation were also determined from farm water balances following methods described in Wiedemann et al. (2014b). Irrigation associated with purchased feed inputs was modelled using methods described in Wiedemann et al. (2014b).

Table 8.5– Land and water resources for seven feedlots in eastern Australia

	FL1	FL2	FL3	FL4	FL5	FL6	FL7
Location	QLD	QLD	QLD	QLD	NSW	NSW	VIC
Average annual rainfall (mm) ^A	555	582	624	662	526	857	430
Land use							
Feedlot area - non-arable (ha)	102.0	47.7	76.0	25.9	71.0	149.0	115.0
Feedlot water supply							
Dam (%)	100%	80%	25%	0%	0%	10%	0%
Bore (%)	0%	20%	75%	100%	2%	0%	100%
Creek (%)	0%	0%	0%	0%	0%	90%	0%
Reticulated (%)	0%	0%	0%	0%	98%	0%	0%
Dam efficiency factor	0.28	0.42	0.78	n.a.	n.a.	0.11	n.a.
Bore efficiency factor	n.a.	0.95	0.95	0.95	0.95	n.a.	0.95
Total water supply (ML)	221.3	305.9	157.0	15.2	293.1	319.5	261.7
Water stress index (WSI) (L/L)	0.855	0.021	0.021	0.021	0.815	0.021	0.815

^A Recorded for nearest major town

Table 8.6 – Runoff from reference land occupation attributed to feedlot cattle production

	FL1	FL2	FL3	FL4	FL5	FL6	FL7
Runoff from reference land occupation (ML/yr)	49.0	14.5	24.3	2.8	14.1	23.1	10.4
Runoff from feedlot controlled drainage area (ML/yr)	0.0	0.0	0.0	0.0	0.0	0.0	0.0
Fresh water consumption attributed to cattle production (L/hd finished)	1069.8	119.9	719.7	389.1	283.5	877.6	232.0

8.3.5 Land occupation

Land occupation was determined from records of the size of each facility and based on land occupation associated with purchased feed inputs. Land occupation was reported using three categories: arable land, non-arable land used for pasture and industrial land

occupation. Land occupation in background processes (classified predominantly as industrial land occupation) was included. These broad classifications provide an indication of the degree of disturbance associated with land occupation and the value of the land for alternative agricultural uses. Land occupation at each feedlot (Table 8.5) was verified using GIS software and aerial photography or satellite imagery. No characterisation factors were applied, and land occupation data were reported in square meter years ($m^2 \text{ yr}$).

8.3.6 Livestock and manure greenhouse gas emissions

Livestock and manure emissions were modelled using methods suited to Australian feedlot conditions. Our study uses the Australian National Greenhouse Gas Inventory (NGGI) preferred method to estimate enteric methane using the model of Moe and Tyrrell (1979). The NGGI applies manure emission methods from the international defaults established by the IPCC (1997) without Australian data. These methods are currently under review (P. Reyenga, Australian Federal Department of the Environment, pers. comm.). As noted by Redding et al. (2015), IPCC methods for important emission sources such as feed pad nitrous oxide are not substantiated by adequate field research and differ from both the mechanisms influencing emissions, and the intensity of emissions measured from Australian feedlots. In this paper we apply new methods for predicting manure emission sources based on Australian feedlot emission research, designated as method 1. Nitrous oxide and methane emissions from manure deposited to the feed pad were determined using data from Redding et al. (2015) and Shorten and Redding (In Press). Ammonia emissions, which contribute indirectly to soil emissions via the process of volatilisation and re-deposition, were determined from reported data reported by Redding et al. (submitted), Denmead et al. (2008b) and DEWR (2007). Our study uses the Australian National Greenhouse Gas Inventory (NGGI) preferred method to estimate enteric methane using the model of Moe and Tyrrell (1979). The NGGI applies manure emission methods from the international defaults established by the IPCC (1997) without Australian data. These methods are currently under review (P. Reyenga, Australian Federal Department of the Environment, pers. comm.). As noted by Redding et al. (2015), IPCC methods for important emission sources such as feed pad nitrous oxide are not substantiated by adequate field research and differ from both the mechanisms influencing emissions, and the intensity of emissions measured from Australian feedlots. In this paper we apply new methods for predicting manure emission sources based on Australian feedlot emission research, designated as method 1. Nitrous oxide and methane emissions from manure deposited to the feed pad were determined using data from Redding et al. (2015) and Shorten and Redding (In Press). Climate specific nitrous oxide emission factors based on emissions per m^2 of pen surface area occupied per animal were used for each feedlot region – see Table 8.7. Ammonia emissions, which contribute indirectly to soil emissions via the process of volatilisation and re-deposition, were determined from data reported by Redding et al. (In Review), Denmead et al. (2008) and DEWR (2007). Indirect N_2O emissions from the deposition of ammonia N to soils was determined based on recent Australian research by Redding et al. (In Review).

Measured deposition of ammonia-N was estimated at 3.2% of total ammonia-N emissions from the feedlot, with the remaining 96.8% advected and deposited at greater distances from the feedlot (Redding et al., In Review). Of the ammonia-N deposited locally, 5% was deposited in areas within the feedlot footprint, where ammonia-N emissions were assumed to be 100% of deposited N. Of the remaining locally deposited ammonia-N, this was deposited to crop land. Ammonia-N deposited to cropland was assumed to result in indirect emissions at a rate equivalent to emissions from N fertiliser on dryland crops (0.003 kg N_2O -N deposited – DCCEE, 2012), as was the ammonia advected away from the feedlot. The dryland crop factor differs from the application of the standard indirect inventory approach (Equation 4D3_5, page 307, DCCEE, 2012), where a 0.01 kg N_2O -N deposited is applied. However, conditions into which this inorganic N is deposited are more analogous to those of

the dry-land cropping conditions represented by the 0.003 kg N₂O-N applied factor than to the more general cropping conditions that the 0.01 kg N₂O-N applied factor represents.

Nitrous oxide and methane emissions from manure stockpiles were determined from Redding et al. (in preparation; Chapter 7), who studied emissions from Australian feedlot manure stockpiles and compost windrows. Emissions from nitrogen in manure and effluent applied to land were determined using the equivalent fertiliser emission factor of 0.003 kg N₂O-N per kilogram of nitrogen applied to soil (DCCEE, 2012). Emissions from nitrogen in manure and effluent applied to land was determined using the equivalent synthetic fertiliser emission factor of 0.003 kg N₂O-N per kilogram of nitrogen applied to soil diverging from the standard inventory calculation procedure (DCCEE, 2012).

A comparison analysis using manure management methods published by the Intergovernmental Panel on Climate Change (IPCC - Dong et al., 2006) was also conducted and is designated as method 2. Uncertainty estimates were made based on the IPCC (Dong et al., 2006) and uncertainty estimates from the original studies. Key emission factors and uncertainty data are described in Table 8.7 and Table 8.8.

Table 8.7 – GHG emission factors with uncertainty for modelling livestock emissions from feedlot cattle (Method 1)

Emission source	Emission and units	Key parameters / model	Assumed Uncertainty	Reference
Enteric fermentation	kg CH ₄ / head	3.406 + 0.510SR + 1.736H + 2.648C / F	SR: 0.23-0.79 H: 1.47-2.00 C: 2.46-2.83	DCCEE (2010) – from Moe and Tyrrell (1979)
Manure – from pen surface	MCF	2% (QLD) 1.5% (NSW, VIC)	± 50%	Dong et al. (2006) dry lot factors for 'warm' and 'temperate' regions
	N ₂ O / m ² d	0.039 (Nth QLD) 0.033 (Sth QLD) 0.012 (Nth NSW) 0.016 (Sth NSW) 0.005 (VIC)	Factor of 2	Redding <i>et al.</i> (In press) Shorten and Redding (submitted)
	NH ₃ -N / kg N excreted	0.6	± 50%	Watts <i>et al.</i> (2012), (Recent measurements, Redding pers. comm)
Manure – from storage	MCF	0.2%	± 50%	Redding pers. comm
	N ₂ O-N / kg N to storage	0.0004	Factor of 2	Redding pers. comm
	NH ₃ -N / kg N to storage	0.04	± 25%	Redding pers. comm

Emission source	Emission and units	Key parameters / model	Assumed Uncertainty	Reference
Effluent – from anaerobic storage	MCF	77% (QLD) 75% (NSW, VIC)	± 15%	Dong <i>et al.</i> (2006)
	NH ₃ -N / kg N to effluent pond	0.35	± 25%	Dong <i>et al.</i> (2006) and Watts <i>et al.</i> (2012)
Land application	N ₂ O-N / kg N to land application	0.003	0.002 - 0.01	Equivalent to crop factor from DCCEE (2013)
	NH ₃ -N / kg N to land application	0.2	0.18 - 0.22	Watts <i>et al.</i> (2012)
Indirect N ₂ O from NH ₃ -N losses	NH ₃ -N deposited within feedlot controlled drainage area (kg N ₂ O-N/kg NH ₃ -N) ^A	1.00		Redding <i>et al.</i> pers. comm
	NH ₃ -N deposited within 500m of feedlot (kg N ₂ O-N/kg NH ₃ -N) ^B	0.0528		Redding <i>et al.</i> pers. comm
	Advected NH ₃ (kg N ₂ O-N/kg NH ₃ -N) ^C	0.003	Factor of 2	Equivalent to crop factor from DCCEE (2013)

^A It assumed that 3.2% of NH₃ is deposited locally, and 5% of this has an EF of 1 (Redding *et al.* pers. comm)

^B The remainder of the locally deposited NH₃ uses an EF equivalent to the factor used for cropping soils

^C It assumed that 96.8% of NH₃ is advected away from the site

Table 8.8 – GHG emission factors with uncertainty for modelling livestock emissions from feedlot cattle (Method 2)

Emission source	Emission and units	Key parameters / model	Assumed Uncertainty	Reference
Enteric fermentation ^A	kg CH ₄ / head	(GE*Y _m *days on feed)/55.65	± 50%	Dong <i>et al.</i> (2006)
Manure – from pen surface and stockpile (solid storage factors) ^B	MCF	0.05 for mean temperature > 15°C 0.04 for mean temperature < 15°C	± 20%	Dong <i>et al.</i> (2006)
	kg N ₂ O-N / kg N excreted	0.025 ^C	Factor of 2	Dong <i>et al.</i> (2006)
Manure – from pen surface and stockpile (solid storage factors) ^B	kg NH ₃ -N / kg N excreted	0.45	0.1 – 0.65	Dong <i>et al.</i> (2006)
Effluent – from anaerobic storage	MCF	0.75 (FL 5) 0.71 (FL 6) 0.74 (FL 7) 0.79 (All other feedlots)	± 20%	Dong <i>et al.</i> (2006)
	kg NH ₃ -N / kg N to effluent pond	0.35	0.25 - 0.75	Dong <i>et al.</i> (2006) ^B
Land application	kg N ₂ O-N / kg N to land application	0.01	0.003 - 0.03	De Klein <i>et al.</i> (2006)
	kg NH ₃ -N / kg N to land application	0.2	0.05 - 0.5	De Klein <i>et al.</i> (2006)
Volatilisation of NH ₃ and re-deposition and loss as N ₂ O		0.01	0.002 - 0.05	De Klein <i>et al.</i> (2006)

^A GE = gross energy intake, MJ/head/d, Y_m = methane conversion factor, 0.03 for feedlot fed cattle, the factor 55.65 (MJ/kg CH₄) is the energy content of methane

^B Factors inclusive of the feed pad and stockpile

^C Factor combined to include the feed pad and stockpile.

8.3.7 Greenhouse gas emissions – feedlot operations and feed inputs

Greenhouse gas emissions associated with fossil fuel use at the feedlot were determined from the inventory of fossil fuel use in Davis et al. (2010b). Greenhouse gas emissions arising from grain or forage production were determined from the databases described. Previous grain studies reported in Wiedemann et al. (2010a) and Brock et al. (2013) have not included soil carbon losses associated with LU and dLUC. Methods used to estimate LU and dLUC emissions were adapted from Wiedemann et al. (2014c) and are detailed in the supplementary material. This analysis included assessment of emissions associated with LU as a result of cultivation for crop production, and dLUC as a result of the expansion of crop land in the eastern states of Australia. Total reported LU and dLUC emissions applied in the present study were 0.44, 0.51 and 0.67 t CO₂-e / ha.yr for NSW, southern NSW/Victoria, and Queensland respectively.

8.3.8 Handling co-production

The feedlot system produced beef and manure. Manure is sold as a fertiliser replacement and soil conditioner and has a very low value compared to beef. Co-production of manure was handled by system expansion taking into account the avoided fertiliser that would be required in the absence of feedlot manure, using the method described by Wiedemann et al. (2010b).

8.3.9 Data analysis

The study was modelled using SimaPro™ 7.3 (Pré-Consultants, 2012). Comparison between the short-fed and mid-fed market types was done using the t-test in R (R Development Core Team, 2014). Results from the single long-fed market type analysis are described qualitatively. Linear regression analysis was used to describe the influence of key production parameters and farm variables on GHG emissions and resources using R. An uncertainty assessment of modelled manure emissions was performed using Monte Carlo analysis in Simapro 7.3. One thousand iterations provided a 95% confidence interval for the results. A comparison of manure emissions was done using comparative Monte Carlo analysis in SimaPro 7.3 to remove the effect of shared uncertainty using methods described in Goedkoop et al. (2010).

8.4 Results

8.4.1 Fresh water consumption and stress weighted water use

Mean fresh water consumption was not significantly different between the short-fed and mid-fed market types (see Table 8.10) and varied widely from feedlot to feedlot in response to changes in irrigation water use. Fresh water consumption was lower from the long fed feedlot in response to lower on-site irrigation and the low use of specific water intensive ration commodities. Mean fresh water consumption was dominated by off-site irrigation water use and supply losses (combined) and on-site irrigation water use and supply losses (combined). Off-site irrigation contributed 35-57% of total fresh water consumption (see Figure 8.1), while on-site contributed 43-56% (Figure 8.1). For off-site irrigation, the single largest input was associated with cotton seed, which was a common feed input for the short-fed and mid-fed market types. Variation in irrigation water use was determined by two factors: the availability of on-site irrigation, which varied from feedlot to feedlot and was not associated with market type, and the use of specific commodities such as cotton seed, which varied between feedlots but was not strongly related to market type. No association was found between fresh water use and the productivity factors, feed conversion ratio (FCR) or average daily gain (ADG).

Mean stress weighted water use was not significantly different between the short-fed and mid-fed cattle (Table 8.10) and tended to be lower from the long-fed feedlot. Stress weighted water use was related to both the volume of water used and regional differences in the WSI.

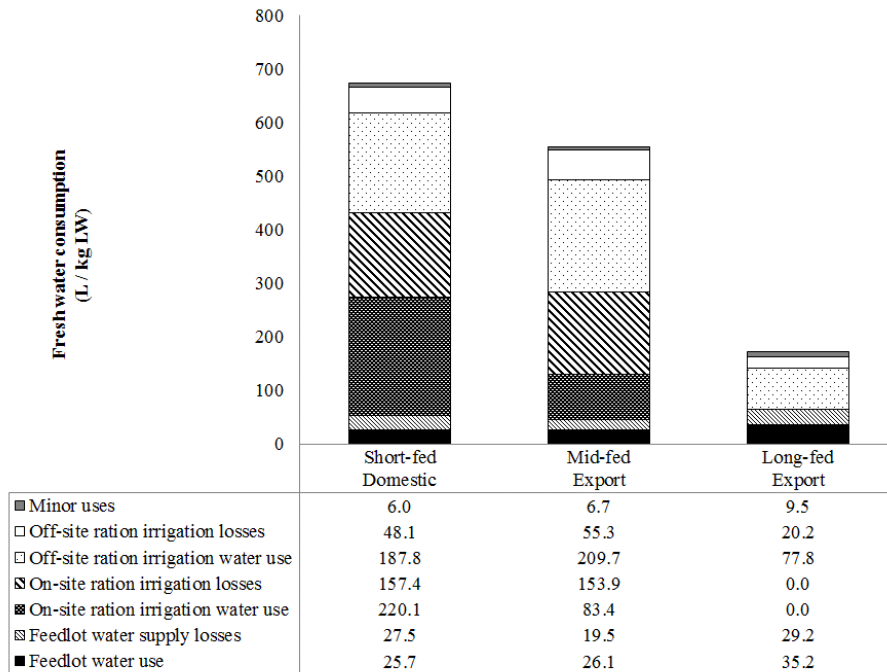


Figure 8.1 – Contribution to fresh water consumption per kg of LWG from domestic short-fed, and mid-fed and long-fed export feedlot steers.

8.4.2 Land Occupation

Mean arable land occupation was highest for the long-fed cattle, while the short-fed and mid-fed cattle were considerably lower (see Table 8.10/Figure 8.2).

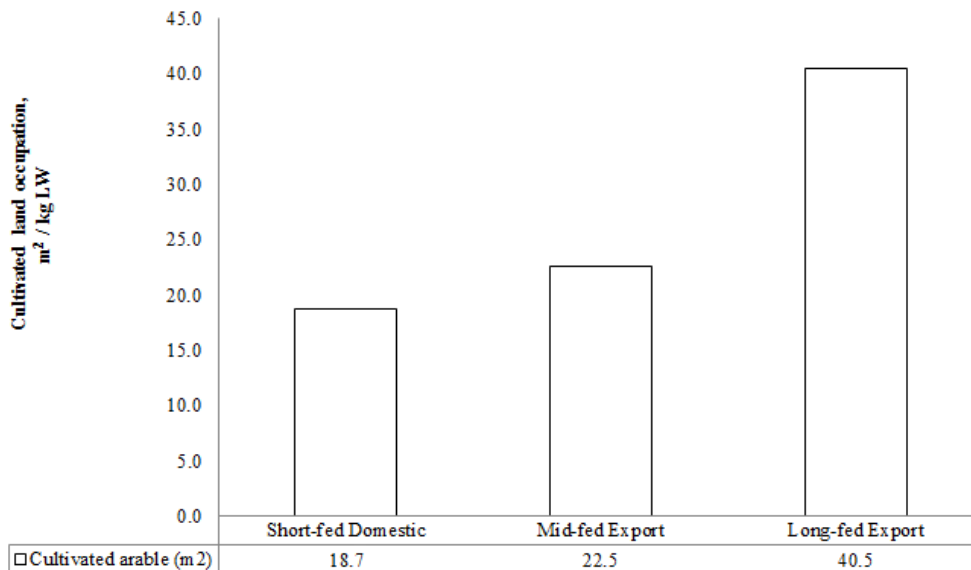


Figure 8.2 – Arable land occupation per kg of LWG from domestic short fed, and mid fed and long fed export feedlot steers.

8.4.3 Energy demand

Mean fossil fuel energy demand was significantly lower for the short-fed cattle than the mid-fed cattle. Energy demand was considerably higher in the long-fed market class (see Table 8.10/Figure 8.3). Feed production and milling were the largest contribution to energy demand. Among individual feedlots, energy demand varied by 43% between the lowest and highest values for the short-fed and mid-fed market classes. The linear regression of energy demand and feed conversion ratio showed that this parameter explained 0.86 of the variability ($P < 0.001$) according to the following equation:

$$\text{Energy Demand} = 3.34\text{FCR} - 0.83 \quad (R^2 = 0.86)$$

While the dataset precluded statistical comparison of the long-fed system to the shorter feeding periods, there was a strong trend towards lower impacts from the shorter feeding periods, supported by the regression analysis of impacts and feed conversion ratio.

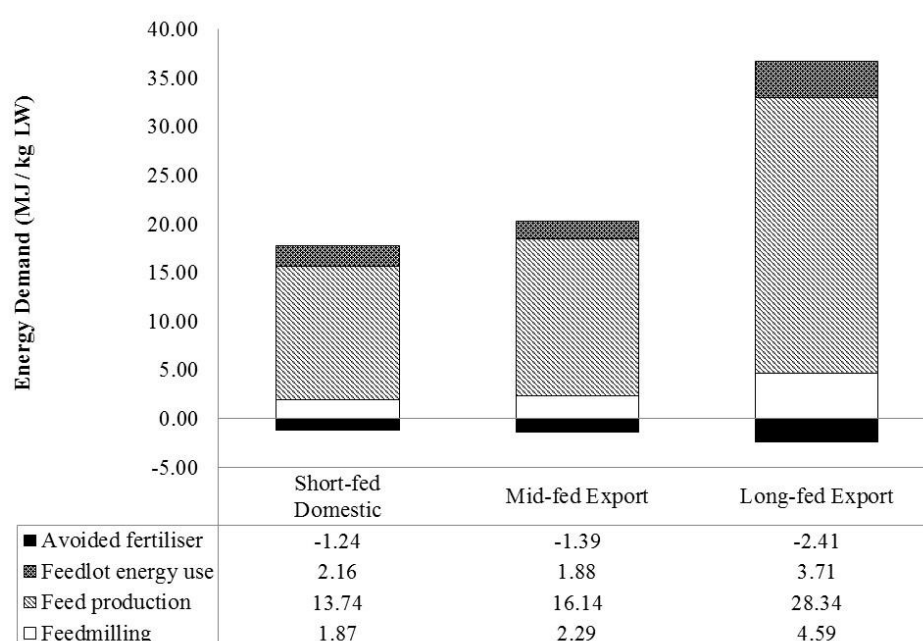


Figure 8.3 – Energy demand per kg of LWG from domestic short-fed, and mid-fed and long-fed export feedlot steers.

8.4.4 Greenhouse gas emissions – gate-to-gate

The mean estimated GHG intensity (excluding LU and dLUC) was 4-4.3 kg CO₂-e/kg LWG for the short-fed and mid-fed cattle with a 26% variation between the highest and lowest individual values. Emissions from short-fed and mid-fed cattle were significantly lower than for long-fed cattle. Mean emissions from LU and dLUC sources were 1.19, 1.32 and 1.8 kg CO₂-e/kg LWG for the short-fed, mid-fed and long-fed cattle respectively, with differences associated with feed conversion ratio and grain production region. The GHG contribution analysis showed mean contribution (excl. LU and dLUC) by gas type was similar across market classes. When analysed by gas type, 61% was contributed by methane, predominantly from enteric sources, 23% from carbon dioxide associated with fossil fuel use, and 15% from nitrous oxide associated with feedlot manure and soil emissions from crop production (Figure 8.4). When analysed by contributing source based on the mean of all feedlots, 33% of GHG impacts arose from ration production, transport and milling, 3% from

feedlot operations (excluding milling), 6% from manure emission sources, and 58% from livestock enteric methane.

The linear regression analysis showed the feed conversion ratio was able to explain 0.97 of the variation ($P < 0.001$) in GHG intensity. The regression model of GHG emissions intensity was:

$$\text{GHG} = 0.78\text{FCR} - 0.15 \quad (R^2 = 0.97)$$

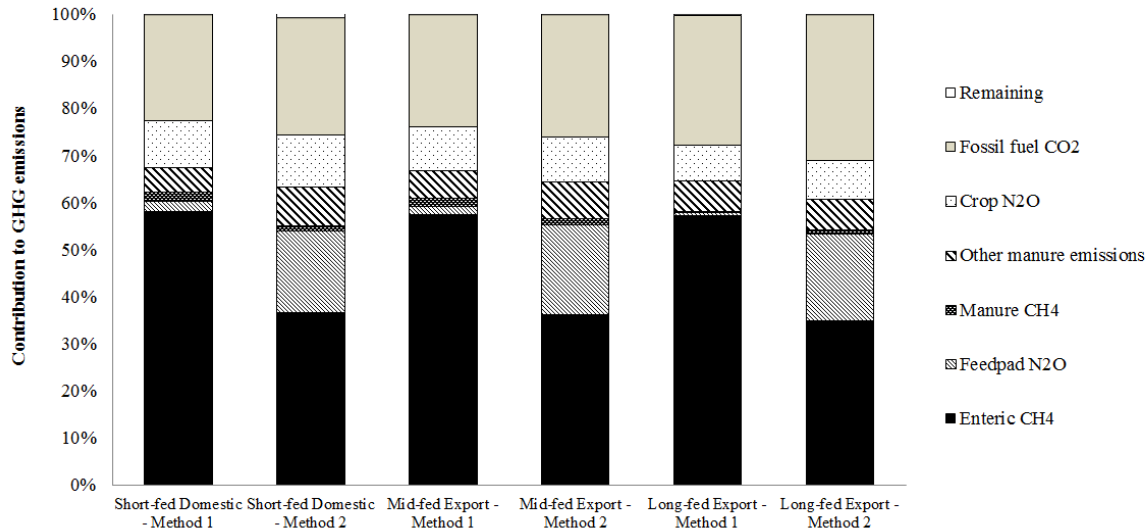


Figure 8.4 – Major sources of GHG per kg of LWG from domestic short fed, and mid fed and long fed export feedlot steers.

8.4.5 Greenhouse gas emissions – livestock and manure management sources

Livestock emissions dominate the emissions profile of grain-finished cattle. Modelling of these emission sources introduces uncertainty into the analysis associated with model inputs and the models or emission factors selected. Results from the comparison of the two methods, Australian inventory/measured data – method 1 and IPCC – method 2 are shown in Figure 8.4 to determine the sensitivity of results to the chosen methods. This comparison was done for two feedlots where GHG emission sampling took place (Redding et al., 2015). Estimated emissions together with mean results calculated using a Monte Carlo analysis of uncertainty are shown in Table 8.9. Calculated totals based on the emission factors reported in Table 8.7 and Table 8.8 were slightly lower than the mean results from the Monte Carlo analysis, because the uncertainty analysis applied skewed distributions for some factors such as nitrous oxide from land application of manure, and emissions of indirect nitrous oxide from ammonia volatilisation (see Table 8.8).

Table 8.9 – Mean livestock manure GHG emissions with uncertainty using two methods

	Northern Feedlot		Southern Feedlot	
	Method 1	Method 2	Method 1	Method 2
Manure Excretion	(kg / 100 kg LWG)			
Nitrogen	7.3	7.3	9.9	9.9
Volatile solids	124.4	124.4	92.7	92.7
Emission source	(kg CO ₂ -e / 100 kg LWG)			
Feed pad and stockpile nitrous oxide	14.0	86.0	5.3	115.9
Feed pad and stockpile methane	8.5	17.5	4.9	13.0
Indirect nitrous oxide (via NH ₃ -N)	10.8	19.1	14.5	25.7
Land application nitrous oxide	3.7	18.1	5.1	24.3
Pond methane	6.0	6.0	4.4	4.4
Total emissions	43.0	146.7	34.1	183.4
Mean emissions - uncertainty analysis	55.3 ± 11	168.0 ± 66	44.9 ± 11	212.0 ± 92

To analyse the sensitivity of the manure results in method 1 to alternative emission factors for indirect nitrous oxide (0.01 compared to 0.003) and land application of manure (0.01 compared to 0.003) scenarios were modelled using these factors. The result was an increase in estimated indirect nitrous oxide from 10.8 to 27.0 kg CO₂-e / 100 kg LWG for the northern feedlot, and an increase in land application nitrous oxide from 3.7 to 12.4 kg CO₂-e / 100 kg LWG. With both combined, total manure management emissions increased 69% to 61.2 kg / 100 kg LWG for the northern feedlot. While these increases appear to be substantial, the impact on total emissions from all sources (excl. LU and dLUC) showed a modest increase of 7% for the short fed and long fed market classes, and an 8% for the mid fed market class.

Table 8.10– Resource use and environmental impacts per kg of LWG from short-fed, and mid-fed and long-fed export feedlot steers

Number of farms	Market	Impact / Inventory Categories									
		Fossil energy (MJ LHV)		Fresh water consumption (L)		Water stress (WSI eq L)		Cultivated arable land (m ²)		Global Warming (excl LUC) (kg CO ₂ -e)	
		Mean	Range	Mean	Range	Mean	Range	Mean	Range	Mean	Range
5	Short-fed Domestic	16.5	15.5- 18.1	671.3	221.1 - 1246	193.2	17.9 - 484	18.7	17.2 - 20.9	4.0	3.7 - 4.5
4	Mid-fed Export	18.9	16.3 - 23.3	554.0	246.1 - 1087.3	191.8	19.1 - 510.1	22.5	18.4 - 28.7	4.3	4.1 – 5.0
1	Long-fed Export	34.2	n.a.	171.9	n.a.	100.9	n.a.	40.5	n.a.	7.9	n.a.

8.5 Discussion

The number of cattle finished on grain in Australia has increased substantially, to approximately 45% of young slaughter cattle in Australia over the past 30 years, with the net impact being lower GHG emissions across the Australian herd (Wiedemann et al., 2014a). This study is the first to provide a detailed analysis of the grain finishing component of the supply chain using a gate-to-gate LCA methodology. We found feed conversion ratio, a major productivity factor for the industry, to explain a high proportion of the variability in GHG emissions intensity, energy demand and arable land occupation but not fresh water consumption or stress weighted water use. A significant but lesser association was also found between average daily gain and resource use and emissions intensity (results not shown). Fresh water consumption and stress weighted water use were more heavily influenced by the use of irrigation for particular feed inputs and regional water stress than livestock productivity.

8.5.1 Resource use

Water is a critical input for livestock production. A detailed analysis of water use at Australian feedlots by Davis et al. (2010a) showed that water use within the feedlot complex is dominated by cattle drinking water, with smaller contributions from feed management, cattle washing and other minor uses. In the present study, we used this dataset but expanded the analysis to include supply losses and irrigation water use both on-site and off-site. The fresh water consumption results reported by Davis et al. (2010a) converted to a LWG basis ranged from 22.5-32 L/kg LWG, which represented only ~10% of the fresh water consumption when additional sources were included in the analysis (Figure 8.1).

We found irrigation to be the largest source of fresh water consumption, with mean contributions across the market types being between 57-91%. Specifically, large water flows were associated with the use of cotton seed and cotton seed meal which were used by the majority of feedlots, and irrigation of hay and silage on feedlot farms. This study found mean on-site irrigation to be 49% of total fresh water consumption across all feedlots and market types. Among individual feedlots the contribution ranged from zero to 898.8 L / kg LWG in response to local irrigation water availability. Cotton seed and cotton seed meal were common feed inputs (see Table 8.3) and alone accounted for 25-35% of total fresh water consumption for the short-fed and mid-fed market types. Because of the wide range in irrigation water use between feedlots, no association was found between fresh water consumption and productivity or market type.

Fossil fuel energy demand was dominated by feed production and milling rather than feedlot operations. When analysed separately, feed milling contributed 12% to overall energy demand while other feedlot operations contributed 11%. Within feedlot operations, milling and general feedlot operations are the only parts of the operation under the direct control of feedlot operators. However, because of the importance of upstream energy demand associated with the production of grain, productivity factors such as feed conversion ratio are a more significant influence on total fossil energy demand than direct factors. Total energy demand was considerably higher than reported by Davis et al. (2010b), who reported direct energy demand of 2.1-5.7 MJ for feedlot operations. This value excluded energy demand associated with feed production, and also excluded upstream impacts from the supply of energy, accounting for the higher reported energy demand in the present study.

Land occupation was dominated by feed production, while the feedlot itself was insignificant because of the very high density of livestock on relatively small land areas.

Within the LCA literature, previous Australian beef studies (Peters et al., 2010ab; Eady et al., 2011; Wiedemann et al., 2014b) have focussed on the whole production system including

breeding and finishing, making these studies not comparable to the gate-to-gate study reported here. However, the intensity of impacts from the feedlot stage compared to full supply chain results for grass finishing does provide insight into the relative efficiency of the grain finishing stage. In comparison with grass finishing (whole supply chain) results, beef production from NSW and QLD was found to use 117.9-332.4 L / kg LW (Wiedemann et al., 2014b) which was lower than the mean water use for grain finishing presented here. In the same study, mean energy demand was found to range from 5.6 – 8.4 MJ / kg LW which was less than half the energy intensity of grain finishing for the shorter feeding periods. This would suggest that grain finishing is likely to result in higher water and energy demand across the whole supply chain.

8.5.2 Greenhouse gas emissions

Greenhouse gas emissions from sources other than LU and dLUC were dominated by enteric methane and manure emissions, with smaller contributions of nitrous oxide from cropping and fossil fuel-related carbon dioxide (Figure 4). Emissions intensity was largely governed by productivity factors, which influenced both enteric methane, manure and feed related emissions. The significance of average daily gain on emissions intensity was shown by Hunter and Niethe (2009) and Wiedemann et al. (2014b) and was confirmed in the present study (results not shown), though stronger regression relationships were found to feed conversion ratio. Contributions from LU and dLUC sources were found to increase total GHG emissions by 28-31%. When these emission sources were included in the contribution analysis, feed production, transport and milling became the largest impact, ranging from 47% for the long-fed market to 50% for the mid-fed market.

8.5.3 Sensitivity to emission factors for GHG prediction

Emission intensity prediction is sensitive to specific emission methods. In the current study we applied factors developed in recent research on Australian feedlots, or applied estimation techniques that approximated results from measurement studies (method 1). Results from the comparison with method 2 (Dong et al., 2006) showed enteric methane predictions to be much higher using method 1 and manure nitrous oxide to be lower (Figure 8.4). Enteric methane emissions were higher using Australian methods were almost double the emissions predicted using the IPCC method. Predicted enteric methane emissions using Australian inventory method were compared to measured emissions by McGinn et al. (2008) at one Queensland feedlot. Based on ration and herd data collected over two years, predicted enteric methane emissions were 191 g per animal per day and manure emissions were 0.9 g (combined 191.9 g) using DCCEE (2012) methods. This value was 20% higher than the reported mean of 166 g CH₄ per animal per day reported by McGinn et al. (2008). In contrast, enteric methane emissions predicted using the IPCC method for this feedlot were 110 g per animal per day, or 34% below the reported mean emissions. While both results were within the confidence interval reported by McGinn et al. (2008) of 76-256 g, the former method provided a closer, more conservative estimate which is considered appropriate until further research is available to support a different estimation methodology.

In the current study we applied manure emission factors developed in recent research on Australian feedlots (method 1). Compared to the IPCC (method 2) the Australian manure emission factors resulted in much lower estimates of nitrous oxide (Table 8.9). Manure emissions were 6% of total emissions for method 1, and 26% of total emissions for method 2 when the latter was combined with the IPCC enteric methane factor of 3% GEI. IPCC defaults (method 2) identify nitrous oxide from the feed pad as the largest source of emissions from the manure management system. However, factors determined by the IPCC were not based on research that reflect Australian management conditions and greatly exceed measured pen nitrous oxide emissions (Redding et al., 2015). In contrast, Australian measured ammonia emissions (Redding, manuscript in preparation, discussed here in

Chapter 6; Denmead et al., 2000,2008b;) were higher than predicted using the IPCC method. Results from method 1 were also sensitive to the factors applied for indirect emissions via the ammonia volatilisation pathway, and the factor used for land application of manure. Changing these emission factors to IPCC values (0.01 kg N₂O-N / kg N deposited for both pathways) resulted in manure emissions increasing by 69% and overall emissions increasing by 7% for the average short fed and long fed market class, and 8% for the mid fed market class. Considering this, further research may be warranted to provide more robust emission factors from these loss pathways.

The overall consequence of applying local emission factors based on research was a considerable reduction in estimated manure management system emissions, resulting in proportionally higher enteric methane emissions and emissions from other sources such as feedlot operations (fossil fuel use) and crop production.

8.6 Conclusions

Grain finishing beef was found to result in relatively high energy demand and fresh water consumption, but low requirements for land occupation and modest GHG emissions per kilogram of LW gain in the feedlot. Impacts and resource use, with the exception of water, were largely explained by differences in feed conversion ratio within the dataset analysed. Application of local emission factors based on Australian feedlot research showed impacts from manure management were lower than estimated using international default methods, while enteric methane emissions were proportionally higher. These results suggest that feed grain production practices and enteric methane production are the dominant emission sources and should receive most focus when aiming to mitigate GHG emissions associated with grain finishing.

9 Identifying target soils for manure carbon sequestration (manuscript to be prepared)

M.R. Redding, R.L. Lewis, J. Devereux, O. Smith, C. Pratt, J. Hill

9.1 Summary

Recent advances in understanding the retention of carbon in soils suggests that some soils may have greater potential for retention of manure carbon than others. This study sought to answer the question as to whether site selection may be critically important in order to maximise the carbon sequestration potential of pen manure carbon. Moreover, we specifically sought to test whether the greatest carbon retention will be achieved with soils that have previously **lost** the most carbon. For this study we used soils that had undergone decades of cultivation as examples of carbon-degraded soils, comparing them with the adjacent soils that were retained at the site in “native” state (un-degraded, uncultivated, largely un-disturbed).

We found that site selection was very important with regard to maximising carbon retention. Unfortunately degraded sites did not consistently retain greater carbon. While this could conceivably indicate that the paired sites did not reliably represent the same initial soils, in practice this approach is not likely to bear fruit for manure end users with less resources at their disposal.

We also observed that halting natural carbon inputs to soils collected from native sites resulted in considerable carbon content decline. Much of the soil carbon at these sites appears to be in a steady state with on-going inputs.

Approximate retention of applied manure carbon ranged from 30 to 60 %, with significant differences between soils.

It is also known that some carbon additions to soils can result in destruction of pre-existent long term soil carbon. This detrimental effect is known as “priming”. Encouragingly, evidence of priming effects leading to destruction of pre-existent soil carbon was only evident in one of the 12 soils.

9.2 Introduction

Recent advances in defining the controls on carbon contents of soils (Wynn et al., 2006), the likely mechanisms of sequestration (von Lutzow et al., 2006), and the knowledge that degraded soils have the greatest capacity to sequester carbon due to the large difference between current carbon concentrations and the saturation limit (Stewart et al., 2008) suggest that some soils may have greater potential for retention of manure carbon than others.

The carbon contained in pen manure represents a very considerable carbon source. A recent review (von Lutzow et al., 2006) indicates that the following mechanisms each may act to increase carbon mean-residence times in soils:

- Selective preservation due to recalcitrance (through black carbon in soils, and possibly recalcitrance of humic polymers);
- Occlusion (trapping and surrounding) of organic matter (OM) by aggregates (particularly in the < 20 µm aggregate fraction);
- Through intercalation (inter-layering) in phyllosilicates (including clays);
- Through processes related to hydrophobicity (which may involve some of the other mechanisms mentioned here); and
- Via encapsulation in organic macromolecules.

- Surface interactions and complex formation with metal ions. Data suggest that such mechanisms include ligand exchange mechanisms in acid soils and soils rich in oxides; formation of polyvalent cation bridging in soils dominated by exchangeable Ca^{2+} or Al^{3+} ; and weak physical interactions (van der Waals forces); and through the formation of organo-metal complexes in acidic, calcareous, or heavy metal-contaminated soils.

The timescales of these carbon-protective mechanisms vary with soil mineralogy and pH. However, additions of beef manure directly to soils may not result in noticeable increases in sequestered carbon (Fontaine and Barot, 2005; Fontaine et al., 2007). It appears likely that each soil has a characteristic limit to carbon sequestration, determined by soil physicochemical characteristics and controlled by the capacity of several soil pools to store carbon (Stewart et al., 2007, 2008). An empirical method to calculate carbon content in relatively undisturbed soils (which may effectively be the saturation limit) has been proposed for Australian soils (Wynn et al., 2006). In Australian soils, there is a clear relationship between soil organic carbon (SOC) content, water availability, mean annual temperature, and soil texture (Wynn et al., 2006). It seems likely that this relationship is closely related to the soil carbon saturation concept, and developing a link between these factors may allow an index of carbon sequestration potential to be formulated.

Under some circumstances, additions of carbon to soil are also capable of resulting in destruction of a portion of the soil's old, long mean-residence organic matter. This can occur through a process referred to as priming (Fontaine et al., 2004, 2007; Fontaine and Barot, 2005; Fontaine and Carrere, 2008).

Under normal circumstances only a small proportion of C added to soils will be retained as long mean-residence carbon. Manure applications to a range of soil environments have resulted in 3 to 50% sequestration (Sommerfeldt et al., 1988; Webster and Goulding, 1989; Angers and N'Dayegamiye, 1991; Chang et al., 1991; Collins et al., 1992; Gupta et al., 1992; Yang et al., 2007; Johnson et al., 2007; Kaur et al., 2008; Fronning et al., 2008). Some of this variability might be explained in terms of there being an upper maximum limit to the capacity of each of the protective mechanisms in a soil (Hassink and Whitmore, 1997; Six et al., 2002ab; Stewart et al., 2007). As this limit is more closely approached, the rate of retention tends to decrease and the rate of decomposition increases. Many trials have not displayed this behaviour, but Stewart et al. (2007) argue that this reflects the narrow range of applications used in these trials, and application rates that do not approach the saturation limit.

Another concept of interest is the separate one of equilibrium. While saturation limits are most often considered to be reached via a rise in C content, Johnston et al.'s (2009) equilibria were reached via a fall in carbon content after carbon additions have ended. Johnston et al. (2009) noted that this carbon half-life, and possibly the equilibrium level, differs with varying additions of different carbon sources. The equilibrium level is also specific to the farming system, climate, and soil type — with clay soils having higher equilibrium levels than sandy soils.

Our study is related to the contention that site selection may be critically important in order to maximise the carbon sequestration potential of pen manure carbon. Our hypothesis is that the greatest efficiency will be achieved with soils further from C saturation. We were seeking to identify if degraded soils — soils displaying the greatest soil carbon decline — may be the best target for application of the manure carbon resource.

9.3 Materials and methods

Thirteen paired sites in south east and south west Queensland were proposed that allowed collection of soil from long-term cultivated areas, and an immediately adjacent area with no

cultivation history. The soils from these sites were then screened to determine suitability for inclusion in the incubation trial:

- Soil classification at the paired sites were conducted to ensure that the two sites had soils similar enough that they were likely initially the same. This included profile sampling via soil sampling rig and examination by a qualified pedologist.
- Site history was investigated to ensure that several decades of cultivation had been conducted.
- Bulk densities of both sites were determined for the surface 100 mm.

Of the likely suitable sites, 40 kg of soil were collected to a 25 mm depth, air dried, passed through a 2 mm aperture sieve and a range of soil analyses conducted to identify key soil characteristics (three replicates for each sample), including Dumas carbon, Organic carbon (Walkley and Black, 1934), carbon isotopes via mass spectrometer (δC^{13}), pH, mineral-N, and total N.

Two manure samples were collected for soil treatment: A 10 kg pen mound sample from the Northern feedlot; and a sample from a feeding trial at Brian Pastures Research Station. This provided a C3 grass species dominated manure sample (northern feedlot) and a C4 grass species dominated sample (Brian Pastures). This provided a sample naturally more depleted in C^{13} (C3 sample) and one tending to be less depleted (C4 sample).

Six soil pairs were selected based on:

1. An established carbon difference between the cultivated and native soil samples.
2. Strong contrast in isotopic carbon signature with either the C3 or the C4 manure.

Approximate water holding capacity was determined for each soil via hanging water column with a zero length water column (Dane and Hopmans, 2002).

For each paired site the following replicated 75 g (oven dry equivalent) samples (5) were incubated:

- Untreated cultivated soil
- Untreated native soil
- Cultivated soil treated with the most isotopically contrasting manure (C3 or C4) to provide carbon equivalent to 1.1 X (carbon contained in native soil - carbon contained in the cultivated soil). The manure treatment was introduced to the slightly moist soil sample and thoroughly mixed.
- Native soil treated with the same quantity of carbon as the treated cultivated soil.

Each sample was transferred to a 150 ml polycarbonate cylindrical vial. Soils were raised to container capacity moisture content via distilled water addition, and the vials (with a small hole drilled in their lid to allow gas exchange) placed in an incubator and maintained at 35 degrees. Incubation continued for the period from 19/08/2013 to 6/8/2014, and the moisture returned to field capacity every two weeks.

Four times throughout the incubation period, respiration emissions (CO_2 and CO_2 isotopologues) were measured using a Fourier Transform Infrared Spectrophotometer, and the automated sampling manifold described in Chapter 5, plumbed to the incubator.

At the completion of the trial, all samples were analysed for total C (TC), organic carbon (OC), δC^{13} (isotope ratio mass spectrometer), and total N (TN).

For the purposes of this analysis, isotope ratios were assumed to be constant in the bulk materials, and a simple mixing model applied (O'Brien et al., 2013):

$$\delta C^{13}_{\text{final}} = f \delta C^{13}_{\text{soil}} + (1-f) \delta C^{13}_{\text{manure}}, \quad [1]$$

where f is the fraction of initial soil carbon remaining, and the respective isotopic signatures are represented by the subscript. Another key assumption was that manure carbon was dominated by organic carbon.

Given the assumption of Eq [1] and minimal non-organic carbon, δC^{13} and OC data were plotted as the y- and x- axes of graphs. This allows the graphical (and regression-based) determination of preferential decay of carbon components. For example, where added manure-carbon is preferentially being respired, the x (OC) and y (δC^{13}) coordinates would trend with time from the manure amended soil coordinates directly toward the initial soil coordinates (x=soil OC and y = soil δC^{13}). Deviation from this decay path would represent a different behaviour.

Analysis of variance was conducted to determine the significance of differences between treatments using the Genstat software package (VSN International, 2012). Linear regressions were conducted using R (R Development Core Team, 2014).

9.4 Results and discussion

A wide range of sites were canvassed by telephone and visited to identify potential for inclusion in this trial. Thirteen sites were sampled, and only 6 appeared suitable for further investigation, based on proximity of cultivated and native sites (usually in uncleared areas or beneath long-established fencelines), reasonable similarity of soil classifications, and evidence of organic carbon decline (Table 9.1). Manures collected contained comparable carbon contents (C3 manure 41% total carbon and 39% OC; C4 manure 41% total carbon and 40% OC) but strongly contrasting isotopic signatures (δC^{13} C3, -24.5; C4, -13.8).

Table 9.1. Sites selected for the study based on similarity of soil classifications for the paired sites (classification according to Isbell, 2002), proximity, extended cultivation history, and an established contrast in organic carbon contents (%) between the cultivated and native sites.

Site	Cultivated	Native
Du	Black Dermosol (0.73)	Black Dermosol (3.46)
Eg	Grey Vertisol (0.35)	Grey Vertisol (0.69)
Lr	Ferrosol (1.76)	Ferrosol (3.68)
Pe	Grey Kurosol (1.2)	Grey Kurosol (2.9)
Wa	Grey Sodosol (0.34)	Grey Sodosol sandy layer (0.66)
We	Black vertisol (2.1)	Black vertisol (4.3)

Organic carbon analysis following incubation produced fairly inconsistent results. The different soils displayed the range of possible behaviours when treated with manure carbon (Table 9.2): no significant difference between cultivated and native sites (sites Pe, We, Lr; however at the $P < 0.1$, the picture is different); significantly greater retention of carbon following cultivation (site Du); significantly greater retention of carbon in the native condition (sites Wa and Eg).

While individual soils displayed a range of behaviour, the mean picture did not support the contention that soils from degraded sites have an unfilled capacity to protect carbon (Figs. 9.1 to 9.3; Table 9.2). This could also conceivably indicate that the paired sites in some cases did not represent the same initial soils, despite all the care taken. However, the practical message here is that given that the research team could not select degraded sites to reliably retain carbon, it seems that less rigorous approaches (e.g. in the context of manure end-use) would have little likelihood of success.

It is also evident that removing and incubating soil from the “undisturbed” native sites resulted in a net decrease in organic carbon content. When these soils are removed from their original environments, carbon inputs to the soil are curtailed, and more labile carbon in these soils is lost through respiration.

Approximate retention of applied manure carbon ranged from 30 to 60 %, with one exception probably related to moisture content determination error and the very small additions to this soil (Site Wa; Table 9.2). These recoveries may also be a product of the type of manure used to treat the soils. Manure derived from C4 grass feeding were used to treat the Lr, Wa, and Eg site soils, which is likely to result in decreased overall carbon retention in these soils relative to the sites treated with C3 derived material. The active pool of soil organic carbon derived from C4 plants is known to degrade at more than twice the rate of the total active pool of soil organic carbon (Wynn and Bird, 2007). This C4 treatment approach was unavoidable where the isotopic contrast was required to investigate soil carbon priming.

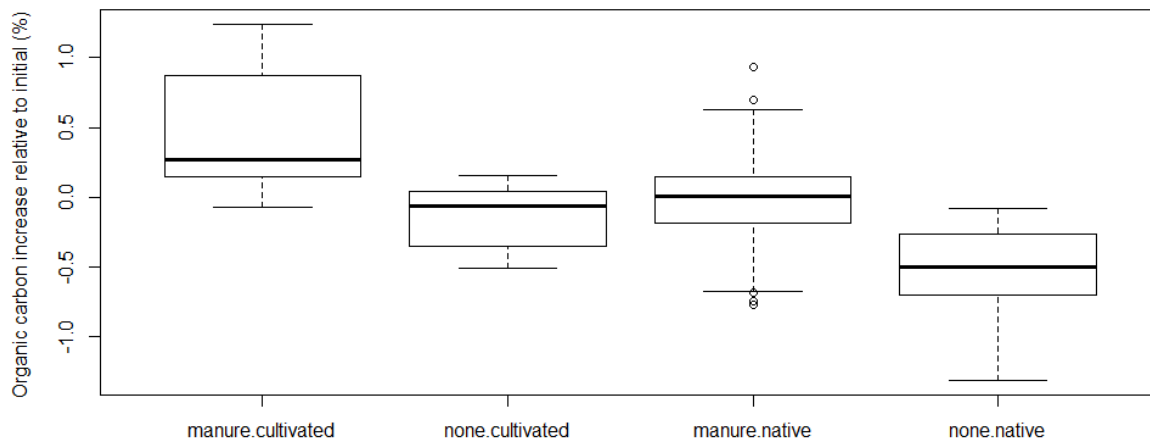


Figure 9.1. When final organic carbon contents are compared to the initial, each treatment versus history is significantly different ($P < 0.05$).

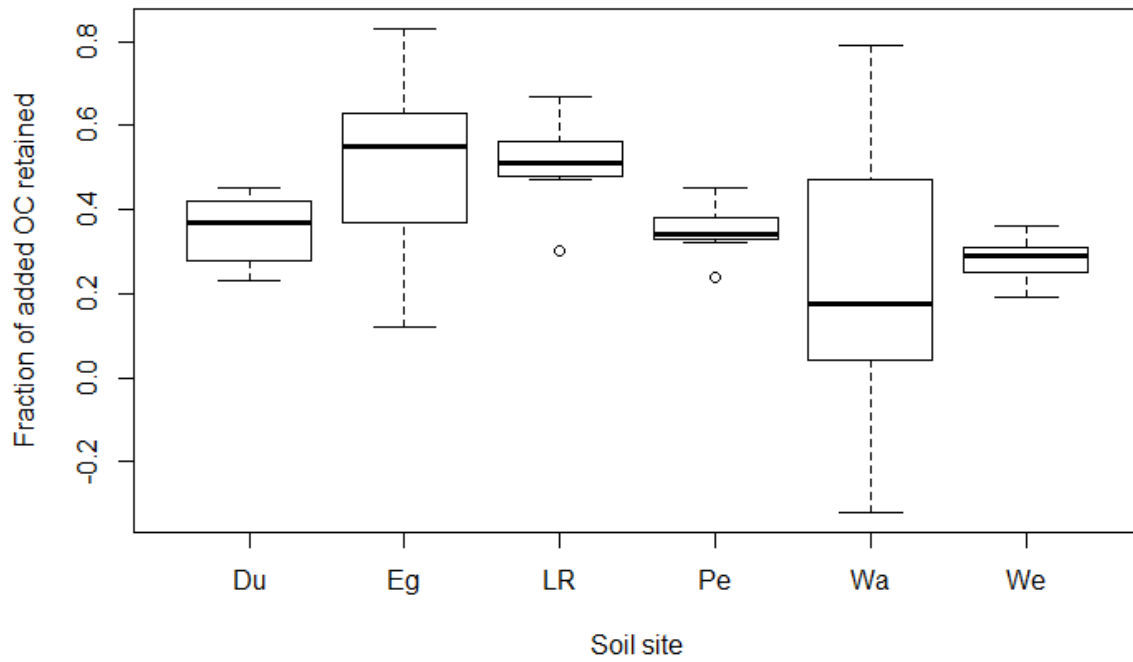


Figure 9.2. There is a clear effect of soil type on carbon retention (ANOVA, $P < 0.001$) – though predicting which soil is most suitable for manure application is a challenge.

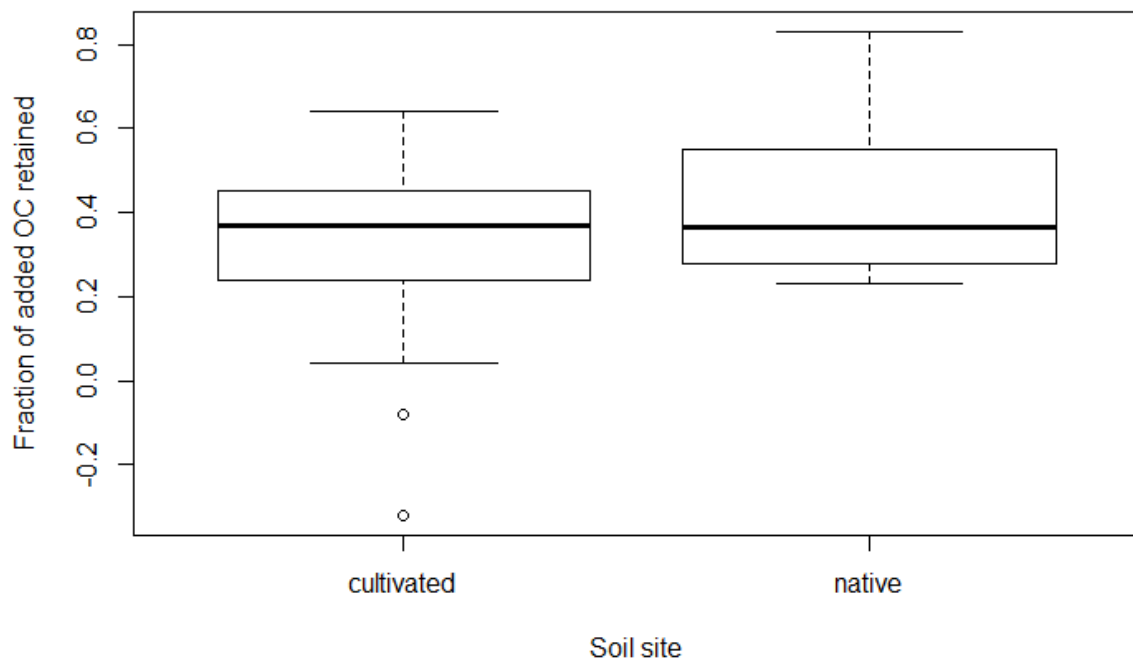


Figure 9.3. In individual soils long-term cultivation did allow greater carbon retention, but this observation could not be generalised.

Table 9.2. Comparing the effect of carbon decline due to cultivation for each soil reveals that any effect is not consistent across the soils.

Soil	Cultivated	Native	Cultivated	Native
	% OC Difference		Approx. % Retention	
Du	1.192	0.726*	40	30
Eg	0.142	0.210*	40	60
Lr	0.988	0.954	50	50
Pe	0.618	0.618	30	35
Wa	-0.010	0.132*	0	50
We	0.582	0.554	30	30

* significantly different, $P < 0.05$, ANOVA and LSD.

Soil carbon priming occurs where added organic matter “primes” or triggers decomposition of pre-existent (and possibly highly desirable long mean residence) soil carbon (Fontaine et al., 2004). This effect was investigated via the end member mixing model (Eq. [1]; Figs. 9.4 to 9.8). Using Eq [1], strong (Fontaine et al., 2004). This effect was investigated via the end member mixing model with results displayed here using the graphical technique described (Eq. [1]; Fig’s 9.4 to 9.8). In most cases the slope of the line through the initial manure treated soil coordinates to the final manure treated coordinates suggested that, as respiration continued and initial soil carbon contents approached, the signatures would likely match the initial soil δC^{13} (linear regression, $P < 0.05$). Strong isotopic evidence of priming was evident for several of the soils. These included both soils from the Du site (Fig 9.7) and both soils from the We site (figure 9.4), where the manure treated sample contained significantly less ($P < 0.05$) soil derived carbon than the incubated untreated soil.

The mean residence time of carbon in soils is important in any consideration of manure as a source of carbon for sequestration in soil. While it is not possible to directly measure carbon mean residence time in soil, we pursued the potential to use emerging analysis techniques to determine if the likely protective mechanisms for carbon in soil (von Lutzow et al., 2006) may be in evidence as an indicator of potential for long mean residence.

To this end, the research team sought access to new techniques to allow the nano-scale investigation of mineral associations of carbon compounds, and compound-specific analysis of persistence of carbon in soils. Despite on-going negotiations with synchrotron facilities in Australia and overseas no suitable technique has yet been located. The Australian Synchrotron (<http://www.synchrotron.org.au/>) appears to be severely limited with regard to soil analyses of this type due to a lack of appropriate beam lines. The Chicago Synchrotron (<https://www1.aps.anl.gov/>) has appropriate beam lines, though advice suggests that unrealistic carbon contents are required to allow this type of analysis ($> 10\%$ C). Contacts made at the Chicago facility may ultimately enable an appropriate collaboration associated with that facility. Initial analyses were conducted by Raman microscopy and FTIR-ATR via collaborative links with New Zealand (Massey University), promising results for the identification of stable carbon compounds.

It appears that appropriate techniques and instrumentation, while emerging, are not yet currently mature. We will continue to pursue these links with a view to applying these

technologies via our National Animal Manure Management Project to better understand how to utilise the manure carbon as a source of sequestered carbon.

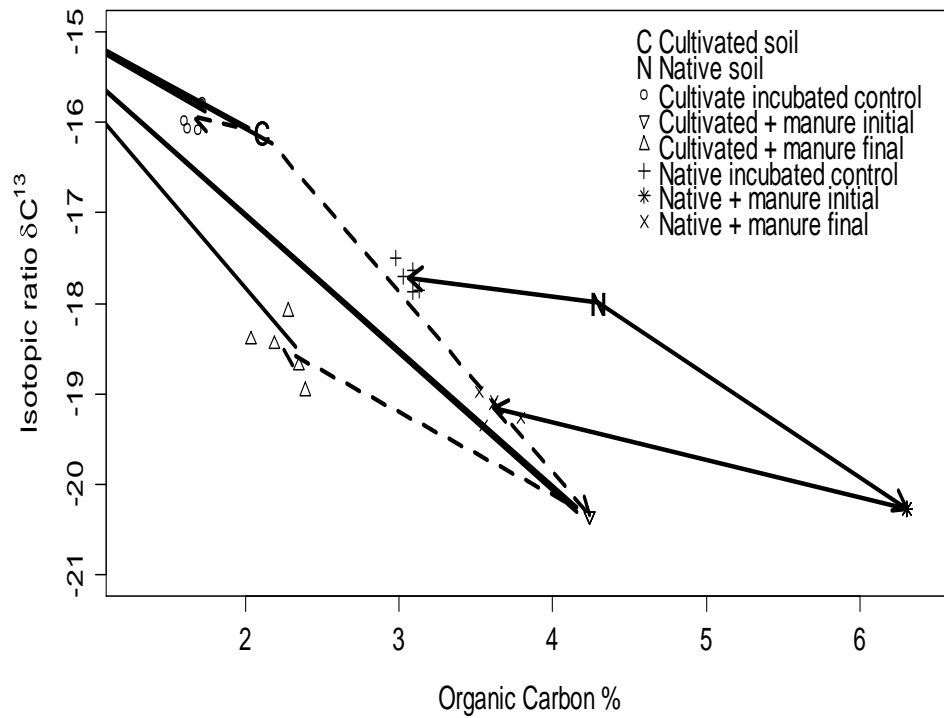


Figure 9.4. Site We isotopic ratios, before, at commencement, and the end of incubation. It is very clear that the isotopic signatures of the bulk materials are not constant throughout the trial. In this case the manure treatment was derived from C3-fed cattle.

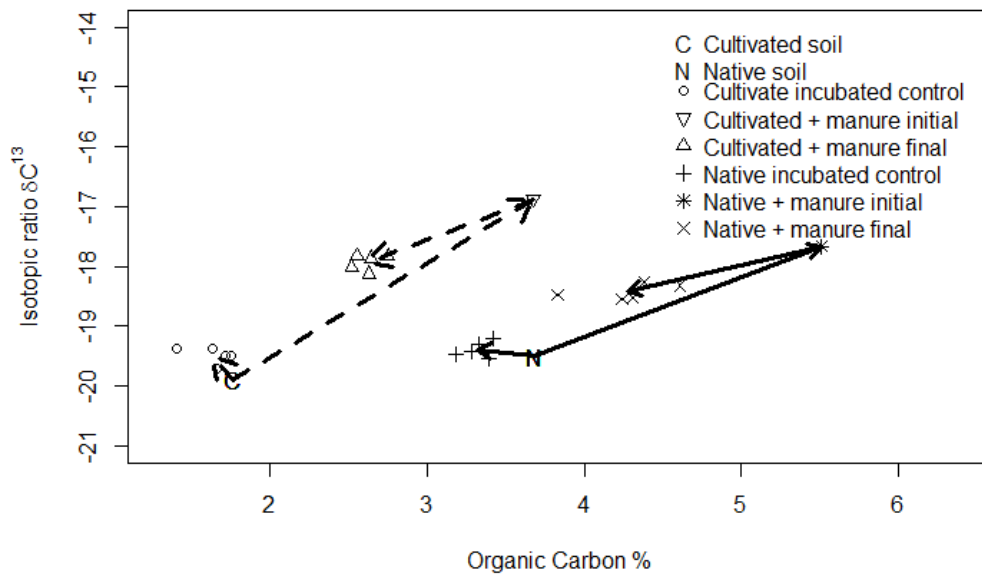


Figure 9.5. Site Lr isotopic ratios, before, at commencement, and the end of incubation. It is very clear that the isotopic signatures of the bulk materials are not constant throughout the trial. In this case the manure treatment was derived from C4-fed cattle.

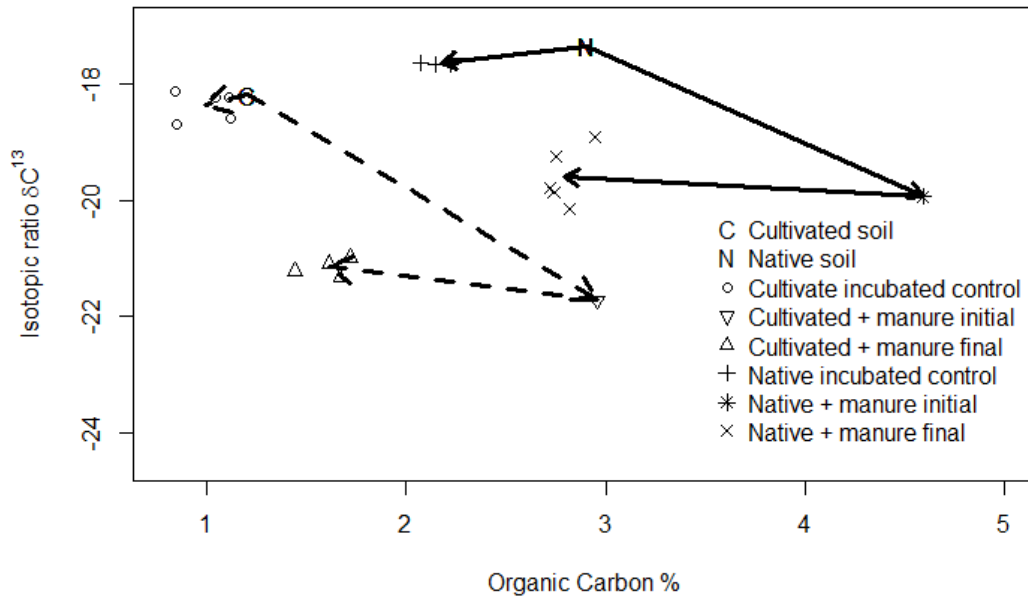


Figure 9.6. Site Pe isotopic ratios, before, at commencement, and the end of incubation. It is very clear that the isotopic signatures of the bulk materials are not constant throughout the trial. In this case the manure treatment was derived from C3-fed cattle.

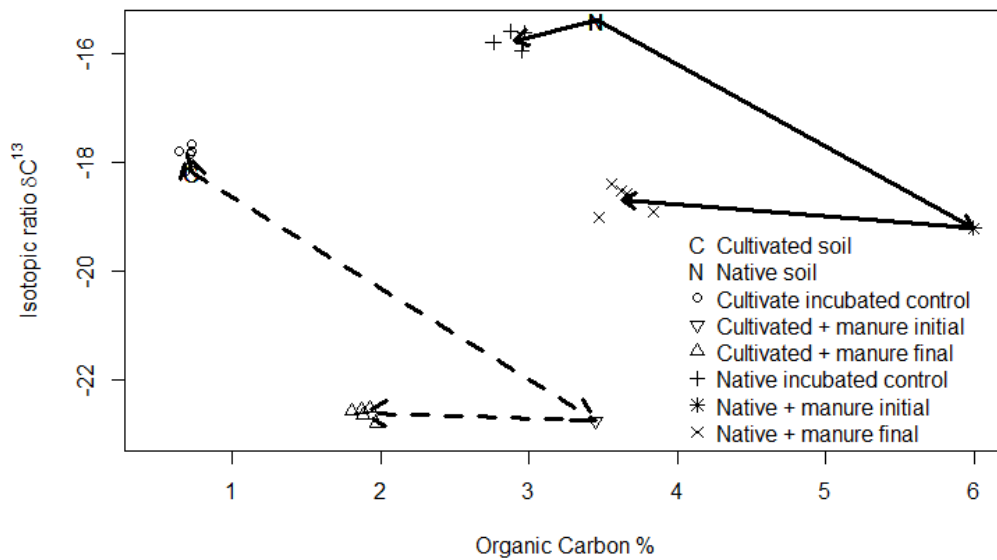


Figure 9.7. Site Du isotopic ratios, before, at commencement, and the end of incubation. In this case the manure treatment was derived from C3-fed cattle.

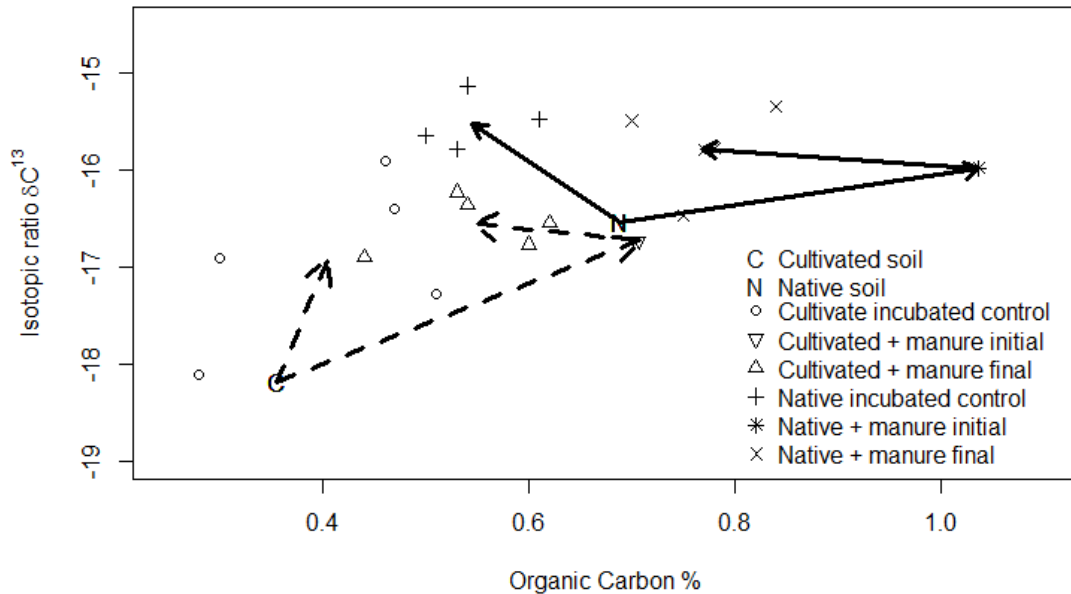


Figure 9.8. Site Eg isotopic ratios, before, at commencement, and the end of incubation. In this case the manure treatment was derived from C4 feed.

9.5 Conclusion

Degraded sites did not consistently retain greater carbon. This could conceivably indicate that the paired sites did not reliably represent the same initial soils. However, in practice attempting to select degraded sites for manure application is not likely to bear fruit for manure end users with less resources at their disposal than our research team.

Considerable carbon decline was noted in the incubated native soils, possibly to the halt in natural carbon additions with the collection of these soils. Much of the soil carbon at these sites appears to be in a steady state with on-going inputs.

Approximate retention of applied manure carbon ranged from 30 to 60 %, with significant differences between soils. Priming effects related to our manure carbon additions was observed in 4 of the 12 soils studied. This led to the destruction of pre-existent soil carbon was evident in 4 of the 12 soils, and suggests that in some cases manure carbon additions can be detrimental to soil carbon stocks. The reason why this occurred in some soils and not others needs to be understood to enable effective use of the carbon content of manures.

10 References

- Abalos, D., A. Sanz-Cobena, L. Garcia-Torres, J.W. van Groenigen, and A. Vallejo. 2013. Role of maize stover incorporation on nitrogen oxide emissions in a non-irrigated Mediterranean barley field. *PLANT SOIL* 364(1-2): 357–371.
- ABS. 2006. Water Use on Australian Farms 2005-06. Australian Bureau of Statistics, Canberra, Australia.
- ALFA, 2013. Key industry statistics. www.feedlots.com.au/images/Briefs/stats.pdf. Accessed 1/04/2015.
- ALFA, and MLA. 2007. National Accredited Feedlot Survey. October-December 2007. Australian Lot Feeders Association, Sydney.
- ALFA, and MLA. 2008. National Accredited Feedlot Survey. October-December 2008. Australian Lot Feeders Association, Sydney.
- Amon, B., T. Amon, J. Boxberger, and C. Alt. 2001. Emissions of NH₃, N₂O and CH₄ from dairy cows housed in a farmyard manure tying stall (housing, manure storage, manure spreading). *Nutr. Cycl. Agroecosystems* 60(1-3): 103–113.
- Angers, D.A., and A. N'Dayegamiye. 1991. Effects of manure application on carbon, nitrogen, and carbohydrate contents of a silt loam and its particle-size fractions. *Biol. Fertil. Soils* 11(1): 79–82.
- Anthonisen, A.C., R.C. Loehr, T.B.S. Prakasam, and E.G. Srinath. 1976. Inhibition of nitrification by ammonia and nitrous acid. *J. Water Pollut. Control Fed.* 48: 835–852.
- Asman, W.A.H. 1998. Factors influencing local dry deposition of gases with special reference to ammonia. *Atmos. Environ.* 32(3): 415–421.
- Ball, B.C., G.W. Horgan, H. Clayton, and J.P. Parker. 1997. Spatial variability of nitrous oxide fluxes and controlling soil and topographic properties. *J. Environ. Qual.* 26(5): 1399–1409.
- Bates, D.M., and D.G. Watts. 2007. Nonlinear regression analysis and its applications. John Wiley & Sons, New York.
- Baum, K.A., J.M. Ham, N.A. Brunsell, and P.I. Coyne. 2008. Surface boundary layer of cattle feedlots: Implications for air emissions measurement. *Agric. For. Meteorol.* 148(11): 1882–1893.
- Berendse, F., C. Laurijsen, and P. Okkerman. 1988. The acidifying effect of ammonia volatilized from farm-manure on forest soils. *Ecol. Bull.*: 136–138.
- Bindon, B., and N. Jones. 2001. Cattle supply, production systems and markets for Australian beef. *Aust. J. Exp. Agric.* 41(7): 861–877.
- Blackmer, A.M., and J.M. Bremner. 1976. Potential of soil as a sink for atmospheric nitrous oxide. *Geophys. Res. Lett.* 3(12): 739–742.
- Boadi, D.A., K.M. Wittenberg, S.L. Scott, D. Burton, K. Buckley, J.A. Small, and K.H. Ominski. 2004. Effect of low and high forage diet on enteric and manure pack greenhouse gas emissions from a feedlot. *Can. J. Anim. Sci.* 84(3): 445–453.

- Borhan, M.S., S.C. Capareda, S. Mukhtar, W.B. Faulkner, R. McGee, and C.B. Parnell. 2011. Greenhouse Gas Emissions from Ground Level Area Sources in Dairy and Cattle Feedyard Operations. *Atmosphere* 2(3): 303–329.
- Bouwman, A. 1998. Environmental science - Nitrogen oxides and tropical agriculture. *NATURE* 392(6679): 866–867.
- Bouwman, A.F., L.J.M. Boumans, and N.H. Batjes. 2002. Emissions of N₂O and NO from fertilized fields: Summary of available measurement data. *Glob. Biogeochem. Cycles* 16(4): 6/1–6/13.
- Brock, P.M., P. Graham, P. Madden, and D.J. Alcock. 2013. Greenhouse gas emissions profile for 1 kg of wool produced in the Yass Region, New South Wales: A Life Cycle Assessment approach. *Anim. Prod. Sci.* 53(6): 495–508.
- Brown, M.J., S.P. Arya, and W.H. Snyder. 1993. Vertical Dispersion from Surface and Elevated Releases: An Investigation of a Non-Gaussian Plume Model. *J. Appl. Meteorol.* 32(3): 490–505.
- Brumme, R., W. Borken, and S. Finke. 1999. Hierarchical control on nitrous oxide emission in forest ecosystems. *Glob. Biogeochem. Cycles* 13(4): 1137–1148.
- Bureau of Meteorology. 2014. Australian Bureau of Meteorology. Available at www.bom.gov.au.
- Butterbach-Bahl, K., E.M. Baggs, M. Dannenmann, R. Kiese, and S. Zechmeister-Boltenstern. 2013. Nitrous oxide emissions from soils: how well do we understand the processes and their controls? *Philos. Trans. R. Soc. B Biol. Sci.* 368(1621) Available at <http://www.ncbi.nlm.nih.gov/pmc/articles/PMC3682742/> (verified 20 November 2014).
- Butterbach-Bahl, K., R. Gasche, L. Breuer, and H. Papen. 1997. Fluxes of NO and N₂O from temperate forest soils: impact of forest type, N deposition and of liming on the NO and N₂O emissions. *Nutr. Cycl. Agroecosystems* 48(1-2): 79–90.
- Butterbach-Bahl, K., R. Kiese, and C.Y. Liu. 2011. Measurements of biosphere-atmosphere exchange of CH₄ in terrestrial ecosystems. p. 271–287. *In* Rosenzweig, A.C., Ragsdale, S.W. (eds.), *Methods in Enzymology: Methods in Methane Metabolism*, Vol 495, Pt B. Elsevier Academic Press Inc, San Diego.
- Canh, T.T., A.J.A. Aarnink, J.B. Schutte, A. Sutton, D.J. Langhout, and M.W.A. Verstegen. 1998. Dietary protein affects nitrogen excretion and ammonia emission from slurry of growing–finishing pigs. *Livest. Prod. Sci.* 56(3): 181–191.
- Chadwick, D.R. 2005. Emissions of ammonia, nitrous oxide and methane from cattle manure heaps: effect of compaction and covering. *Atmos. Environ.* 39(4): 787–799.
- Chadwick, D.R., B.F. Pain, and S.K.E. Brookman. 2000. Nitrous oxide and methane emissions following application of animal manures to grassland. *J. Environ. Qual.* 29: 277–287.
- Chadwick, D., S. Sommer, R. Thorman, D. Fangueiro, L. Cardenas, B. Amon, and T. Misselbrook. 2011. Manure management: Implications for greenhouse gas emissions. *Anim. Feed Sci. Technol.* 166–167(0): 514–531.
- Chambers, J.M., W.S. Cleveland, B. Kleiner, and P.A. Tukey. 1983. *Graphical Methods for Data Analysis*. Wadsworth & Brooks/Cole, Belmont, California.

- Chang, C., T.G. Sommerfeldt, and T. Entz. 1991. Soil Chemistry after Eleven Annual Applications of Cattle Feedlot Manure. *J. Env. Qual* 20(2): 475–480.
- Chantigny, M.H., P. Rochette, D.A. Angers, S. Bittman, K. Buckley, D. Massé, G. Bélanger, N. Eriksen-Hamel, and M.-O. Gasser. 2010. Soil Nitrous Oxide Emissions Following Band-Incorporation of Fertilizer Nitrogen and Swine Manure. *J. Environ. Qual.* 39(5): 1545–53.
- Chapuis-Lardy, L., N. Wrage, A. Metay, J.-L. Chotte, and M. Bernoux. 2007. Soils, a sink for N₂O? A review. *Glob. Change Biol.* 13(1): 1–17.
- Chung, M.L., A.N. Shilton, B. Guieysse, and C. Pratt. 2013. Questioning the Accuracy of Greenhouse Gas Accounting from Agricultural Waste: A Case Study. *J. Env. Qual* 42(3): 654–659.
- Collins, H.P., P.E. Rasmussen, and C.L. Douglas Jr. 1992. Crop rotation and residue management effects on soil carbon and microbial dynamics. *Soil Sci. Soc. Am. J.* 56(3): 783–788.
- Conen, F., and K.A. Smith. 1998. A re-examination of closed flux chamber methods for the measurement of trace gas emissions from soils to the atmosphere. *Eur. J. Soil Sci.* 49(4): 701–707.
- Conover, W.J., and R.L. Iman. 1981. Rank transformations as a bridge between parametric and non-parametric statistics. *Am. Stat.* 35(3): 124–129.
- Corre, M.D., D.J. Pennock, C.V. Kessel, and D. Kirkelliott. 1999. Estimation of annual nitrous oxide emissions from a transitional grassland-forest region in Saskatchewan, Canada. *Biogeochemistry* 44(1): 29–49.
- Cottle, D.J., J.V. Nolan, and S.G. Wiedemann. 2011. Ruminant enteric methane mitigation: a review. *Anim. Prod. Sci.* 51(6): 491–514.
- Crenna, B.P., T.K. Flesch, and J.D. Wilson. 2008. Windtrax 2.0.8.1. Thunder Beach Scientific, Alberta, Canada.
- Dalal, R.C., W.J. Wang, G.P. Robertson, and W.J. Parton. 2003. Nitrous oxide emission from Australian agricultural lands and mitigation options: a review. *Aust. J. Soil Res.* 41(2): 165–195.
- Dane, J.H., and J.W. Hopmans. 2002. Water retention and storage. p. 671–738. *In* Hopmans, J.W., Topp, G.C. (eds.), *Methods of Soil Analysis. Part 4. Physical Methods.* Soil Science Society Book Series. Agronomy Society of America, Madison, WI.
- Dantzman, C.L., M.F. Richter, and F.G. Martin. 1983. Chemical Elements in Soils Under Cattle Pens. *J. Env. Qual* 12(2): 164–168.
- Davis, R., S. Wiedemann, and P. Watts. 2010a. Quantifying the water and energy usage of individual activities within Australian feedlots -Part A report: Water usage at Australian feedlots 2007-2009. Meat & Livestock Australia Limited, North Sydney, NSW.
- Davis, R., S. Wiedemann, and P. Watts. 2010b. Quantifying the water and energy usage of individual activities within Australian feedlots -Part B report: Energy usage at Australian feedlots 2007-2009. Meat & Livestock Australia Limited, North Sydney, NSW.
- DCCEE. 2012. National Inventory Report 2010, Volume 1. The Australian Government Submission to the United Nations Framework Convention on Climate Change. Department of Climate Change and Energy Efficiency, Canberra, Australia.

- D Chen, M.B., OT Denmead, DWT Griffith, J Hill, ZM Loh, SM McGinn, S Muir, T Naylor, F Phillips and D Rowell. 2009. Greenhouse gas emissions from Australian beef cattle feedlots. NORTH SYDNEY NSW 2059.
- Denier van der Gon, H., and A. Bleeker. 2005. Indirect N₂O emission due to atmospheric N deposition for the Netherlands. *Atmos. Environ.* 39(32): 5827–5838.
- Denmead, O.T. 1979. Chamber systems for measuring nitrous oxide emission from soils in the field. *Soil Sci. Soc. Am. J.* 43(1): 89–95.
- Denmead, O.T. 1983. Micrometeorological methods for measuring gaseous losses of nitrogen in the field. p. 133–158. *In* Freney, J.R., Simpson, A.J. (eds.), *Gaseous Loss of Nitrogen from Plant-Soil Systems*. Martinus Nijhoff/Dr. W. Junk Publishers, The Hague, Netherlands.
- Denmead, O.T. 2008. Approaches to measuring fluxes of methane and nitrous oxide between landscapes and the atmosphere. *Plant Soil* 309(1-2): 5–24.
- Denmead, O.T., D. Chen, D.W.T. Griffith, Z.M. Loh, M. Bai, and T. Naylor. 2008. Emissions of the indirect greenhouse gases NH₃ and NO_x from Australian beef cattle feedlots. *Aust. J. Exp. Agric.* 48(1-2): 213–218.
- Department of the Environment. 2014. National Inventory Report 2012. Available at <http://www.environment.gov.au/climate-change/greenhouse-gas-measurement/publications/national-inventory-report-2012> (verified 15 September 2014).
- DEWR. 2007. Emission Estimation Technique Manual for Intensive Livestock - Beef Cattle, Version 3.1. Department of the Environment and Water Resources, Australian Government, Canberra, ACT.
- Dobbie, K.E., and K.A. Smith. 2001a. The effects of temperature, water-filled pore space and land use on N₂O emissions from an imperfectly drained gleysol. *Eur. J. Soil Sci.* 52(4): 667–673.
- Dobbie, K.E., and K.A. Smith. 2001b. The effects of temperature, water-filled pore space and land use on N₂O emissions from an imperfectly drained gleysol. *Eur. J. Soil Sci.* 52(4): 667–673.
- Dong, H., J. Mangino, T.A. McAllister, J. Hatfield, D.E. Johnson, K.R. Lassey, M. Aparecida de Lima, A. Romanovskaya, D. Bartram, D.J. Gibb, and J.H.J. Martin. 2006. Emissions from Livestock and Manure Management. *In* Eggleston, S., Buendia, L., Miwa, K., Ngara, T., Tanabe, K. (eds.), *IPCC Guidelines for National Greenhouse Gas Inventories*. Institute for Global Environmental Strategies, IGES, Japan.
- Eady, S., J. Viner, and J. MacDonnell. 2011. On-farm greenhouse gas emissions and water use: case studies in the Queensland beef industry. *Anim. Prod. Sci.* 51(8): 667–681.
- Eckard, R.J., C. Grainger, and C.A.M. de Klein. 2010. Options for the abatement of methane and nitrous oxide from ruminant production: A review. *Livest. Sci.* 130(1–3): 47–56.
- Eghball, B., and J. Power. 1994. Beef-Cattle Feedlot Manure Management. *J. Soil Water Conserv.* 49(2): 113–122.
- El Kader, N.A., P. Robin, J.M. Paillat, and P. Leterme. 2007. Turning, compacting and the addition of water as factors affecting gaseous emissions in farm manure composting. *Bioresour. Technol.* 98(14): 2619–2628.

- Farlow, S.J. 1993. Partial Differential Equations for Scientists and Engineers - Knovel.
Available at
https://app.knovel.com/web/toc.v/cid:kpPDESE002/viewerType:toc/root_slug:partial-differential/url_slug:partial-differential/ (verified 21 November 2014).
- Flesch, T.K. 1996. The footprint for flux measurements, from backward Lagrangian stochastic models. *Bound.-Layer Meteorol.* 78(3-4): 399–404.
- Flesch, T.K., and J.D. Wilson. 2005. Estimating trace emissions with a Backward Lagrangian Stochastic Technique. p. 513–531. *In* Viney, M.K., Hatfield, J.L., Baker, J.M. (eds.), *Micrometeorology in agricultural systems*. American Society of Agronomy, Inc., Madison, Wisconsin, U.S.A.
- Flesch, T.K., J.D. Wilson, L.A. Harper, and B.P. Crenna. 2005. Estimating gas emissions from a farm with an inverse-dispersion technique. *Atmos. Environ.* 39(27): 4863–4874.
- Flesch, T.K., J.D. Wilson, L.A. Harper, B.P. Crenna, and R.R. Sharpe. 2004. Deducing ground-to-air emissions from observed trace gas concentrations: A field trial. *J. Appl. Meteorol.* 43(3): 487–502.
- Flesch, T.K., J.D. Wilson, L.A. Harper, R.W. Todd, and N.A. Cole. 2007. Determining ammonia emissions from a cattle feedlot with an inverse dispersion technique. *Agric. For. Meteorol.* 144(1-2): 139–155.
- Flesch, T.K., J.D. Wilson, and E. Yee. 1995. Backward-time lagrangian stochastic dispersion models and their application to estimate gaseous emissions. *J. Appl. Meteorol.* 34(6): 1320–1332.
- Fontaine, S., G. Bardoux, L. Abbadie, and A. Mariotti. 2004. Carbon input to soil may decrease soil carbon content. *Ecol. Lett.* 7(4): 314–320.
- Fontaine, S., and S. Barot. 2005. Size and functional diversity of microbe populations control plant persistence and long-term soil carbon accumulation. *Ecol. Lett.* 8(10): 1075–1087.
- Fontaine, S., S. Barot, P. Barre, N. Bdioui, B. Mary, and C. Rumpel. 2007. Stability of organic carbon in deep soil layers controlled by fresh carbon supply. *Nature* 450(7167): 277–U10.
- Fontaine, S., and P. Carrere. 2008. Why carbon storage is more stable in the deep stratum of the ground. *Biofutur* (286): 54–56.
- Fowler, D., C. Pitcairn, M. Sutton, C. Flechard, B. Loubet, M. Coyle, and R. Munro. 1998. The mass budget of atmospheric ammonia in woodland within 1 km of livestock buildings. *Environ. Pollut.* 102(1): 343–348.
- Frischknecht, R., N. Jungbluth, H. Althaus, C. Bauer, G. Doka, R. Dones, R. Hischier, S. Hellweg, S. Humbert, and T. Köllner. 2007. Implementation of life cycle impact assessment methods. Swiss Centre for Life Cycle Inventories, Dübendorf, Switzerland.
- Fronning, B.E., K.D. Thelen, and D.H. Min. 2008. Use of Manure, Compost, and Cover Crops to Supplant Crop Residue Carbon in Corn Stover Removed Cropping Systems. *Agron. J.* 100(6): 1703–1710.
- Galle, B., L. Klemetsson, and D.W.T. Griffith. 1994. Application of a Fourier transform IR system for measurements of N₂O fluxes using micrometeorological methods, an ultralarge chamber system, and conventional field chambers. *J. Geophys. Res.* 99(D8): 16575–16583.

- Gao, Z.L., M. Mauder, R.L. Desjardins, T.K. Flesch, and R.P. van Haarlem. 2009. Assessment of the backward Lagrangian Stochastic dispersion technique for continuous measurements of CH₄ emissions. *Agric. For. Meteorol.* 149(9): 1516–1523.
- Gee, G.W., and J.W. Bauder. 1986. Particle-size analysis. p. 383–411. *In* Klute, A. (ed.), *Methods of soil analysis. Part 1- Physical and mineralogical methods.* American Society of Agronomy, Madison, Wisconsin.
- Gilks, W.R., A. Richardson, and D.J. Spiegelhalter. 1996. *Markov chain Monte Carlo in practice.* Chapman & Hall, London.
- Gillam, K.M., B.J. Zebarth, and D.L. Burton. 2008. Nitrous oxide emissions from denitrification and the partitioning of gaseous losses as affected by nitrate and carbon addition and soil aeration. *Can. J. Soil Sci.* 88(2): 133–143.
- Giltrap, D., S. Saggar, C.S. Li, and H. Wilde. 2008. Using the NZ-DNDC model to estimate agricultural N₂O emissions in the Manawatu-Wanganui region. *Plant Soil* 309(1-2): 191–209.
- Goedkoop, M., A. DeSchreyver, M. Oele, S. Durksz, and D. deRoest. 2010. *Introduction to LCA with Simapro 7.* PRé Consultants, Netherlands.
- Gopalan, P., P.D. Jensen, and D.J. Batstone. 2013. Biochemical Methane Potential of Beef Feedlot Manure: Impact of Manure Age and Storage. *J. Environ. Qual.* 42(4): 1205–1212.
- Greenberg, A., L. Clesceri, and A. Eaton. 1992. *Standard methods for the examination of water and wastewater.* 18th ed. American Public Health Association, Baltimore, Maryland.
- Griffith, D.W.T., N.M. Deutscher, C.G.R. Caldow, G. Kettlewell, M. Riggerbach, and S. Hammer. 2012. A Fourier transform infrared trace gas analyser for atmospheric applications. *Atmospheric Meas. Tech.* 5: 2481–2498.
- Groffman, P.M., and J.M. Tiedje. 1991. Relationships between denitrification, CO₂ production and air-filled porosity in soils of different texture and drainage. *Soil Biol. Biochem.* 23(3): 299–302.
- Gupta, A.P., R.P. Narwal, R.S. Antil, and S. Dev. 1992. Sustaining soil fertility with organic-C, N, P, and K by using farmyard manure and fertilizer-N in a semiarid zone: A long-term study. *Arid Land Res. Manag.* 6(3): 243 – 251.
- van Haarlem, R.P., R.L. Desjardins, Z. Gao, T.K. Flesch, and X. Li. 2008. Methane and ammonia emissions from a beef feedlot in western Canada for a twelve-day period in the fall. *Can. J. Anim. Sci.* 88(4): 641–649.
- Hammer, S., D.W.T. Griffith, G. Konrad, S. Vardag, C. Caldow, and I. Levin. 2012. Assessment of a multi-species in-situ FTIR for precise atmospheric greenhouse gas observations. *Atmospheric Meas. Tech. Discuss.* 5: 3645–3692.
- Hao, X., M. Benke, F.J. Larney, and T.A. McAllister. 2011. Greenhouse gas emissions when composting manure from cattle fed wheat dried distillers' grains with solubles. *Nutr. Cycl. Agroecosystems* 89(1): 105–114.
- Hao, X., C. Chang, F.J. Larney, and G.R. Travis. 2001. Greenhouse Gas Emissions during Cattle Feedlot Manure Composting. *J. Env. Qual* 30(2): 376–386.

- Harper, L.A., O.T. Denmead, J.R. Freney, and F.M. Byers. 1999. Direct measurements of methane emissions from grazing and feedlot cattle. *J. Anim. Sci.* 77(6): 1392–1401.
- Harper, L.A., T.K. Flesch, K.H. Weaver, and J.D. Wilson. 2010. The Effect of Biofuel Production on Swine Farm Methane and Ammonia Emissions. *J. Environ. Qual.* 39(6): 1984–92.
- Hassink, J., and A.P. Whitmore. 1997. A model of the physical protection of organic matter in soils. *Soil Sci. Soc. Am. J.* 61(1): 131–139.
- Hayes, E.T., A.B.G. Leek, T.P. Curran, V.A. Dodd, O.T. Carton, V.E. Beattie, and J.V. O’Doherty. 2004. The influence of diet crude protein level on odour and ammonia emissions from finishing pig houses. *Bioresour. Technol.* 91(3): 309–315.
- Hill, J. 2012. Recalculate Pork Industry Emissions Inventory. Massey University, New Zealand.
- Hulugalle, N.R. 2005. Recovering Leached N by Sowing Wheat After Irrigated Cotton in a Vertisol. *J. Sustain. Agric.* 27(2): 39–51.
- van Hulzen, J.B., R. Segers, P.M. van Bodegom, and P.A. Leffelaar. 1999. Temperature effects on soil methane production: an explanation for observed variability. *Soil Biol. Biochem.* 31(14): 1919–1929.
- Hunt, R. 1982. *Plant growth curves: the functional approach to plant growth analysis.* Arnold, London.
- Hunter, R.A., and G.E. Niethé. 2009. Efficiency of feed utilisation and methane emission for various cattle breeding and finishing systems. p. 75–79.
- Hutchings, N.J., S.G. Sommer, J.M. Andersen, and W.A.H. Asman. 2001. A detailed ammonia emission inventory for Denmark. *Atmos. Environ.* 35(11): 1959–1968.
- Hutchinson, G.L., and G.P. Livingston. 2001. Vents and seals in non-steady-state chambers used for measuring gas exchange between soil and the atmosphere. *Eur. J. Soil Sci.* 52(4): 675–682.
- Hutchinson, G.L., and A.R. Mosier. 1981. Improved Soil Cover Method for Field Measurement of Nitrous Oxide Fluxes. *Soil Sci Soc Am J* 45(2): 311–316.
- Intergovernmental Panel on Climate Change. 2006. IPCC - Task Force on National Greenhouse Gas Inventories. Available at <http://www.ipcc-nggip.iges.or.jp/public/2006gl/vol4.html> (verified 22 April 2014).
- IPCC. 1997. IPCC Guidelines for National Greenhouse Gas Inventories, Greenhouse Gas Inventory Reference Manual Volume 3. Meteorological Office, IPCC/OECD/IEA, Bracknell, UK.
- IPCC. 2006. Emissions from livestock and manure management. IPCC guidelines for national greenhouse gas inventories. Vol. 4. Kanegawa, Japan.
- Isbell, R. 2002. *The Australian Soil Classification.* Csiro Publishing.
- Johnson, J.M.F., A.J. Franzluebbers, S.L. Weyers, and D.C. Reicosky. 2007. Agricultural opportunities to mitigate greenhouse gas emissions. *Environ. Pollut.* 150(1): 107–124.
- Johnson, D.E., G.M. Ward, and J.J. Ramsey. 1996. *Nutrient Management of Food Animals to Enhance and Protect the Environment.* CRC Press LLC, USA.

- Johnston, A.E., P.R. Poulton, and K. Coleman. 2009. SOIL ORGANIC MATTER: ITS IMPORTANCE IN SUSTAINABLE AGRICULTURE AND CARBON DIOXIDE FLUXES. p. 1–57. *In* *Advances in Agronomy*, Vol 101.
- Kaur, T., B.S. Brar, and N.S. Dhillon. 2008. Soil organic matter dynamics as affected by long-term use of organic and inorganic fertilizers under maize-wheat cropping system. *Nutr. Cycl. Agroecosystems* 81(1): 59–69.
- de Klein, C.A.M., and R.S.P. Van Logtestijn. 1996. Denitrification in grassland soils in The Netherlands in relation to irrigation, N-application rate, soil water content and soil temperature. *Soil Biol. Biochem.* 28(2): 231–237.
- de Klein, C.A.M., R.R. Sherlock, K.C. Cameron, and T.J. van der Weerden. 2001. Nitrous oxide emissions from agricultural soils in New Zealand - a review of current knowledge and directions for future research. *J. R. Soc. N. Z.* 31(3): 543–574.
- de Klein, C.A.M., L.C. Smith, and R.M. Monaghan. 2006. Restricted autumn grazing to reduce nitrous oxide emissions from dairy pastures in Southland, New Zealand. *Agric. Ecosyst. Environ.* 112(2-3): 192–199.
- Frischknecht, R, Jungbluth, N, Althaus, H-J, Doka, G, Dones, R, Heck, T, Hellweg, S, Hischer, R, Nemecek, T, Rebitzer, G, Spielmann, M (2005) The ecoinvent Database: Overview and Methodological Framework *International Journal of Life Cycle Assessment* **10**, 3-9
- Koehler, B., M.D. Corre, K. Steger, R. Well, E. Zehe, J.P. Sueta, and E. Veldkamp. 2012. An in-depth look into a tropical lowland forest soil: nitrogen-addition effects on the contents of N₂O, CO₂ and CH₄ and N₂O isotopic signatures down to 2-m depth. *Biogeochemistry* 111(1-3): 695–713.
- Healy, R.W., R.G. Striegl, T.F. Russell, G.L. Hutchinson and G.P. Livingston. 1996. Numerical evaluation of static-chamber measurements of soil-atmosphere gas exchange: Identification of physical processes. *Soil Science Society of America Journal* 60: 740-747.
- Koenig, K.M., S.M. McGinn, and K.A. Beauchemin. 2013. Ammonia emissions and performance of backgrounding and finishing beef feedlot cattle fed barley-based diets varying in dietary crude protein concentration and rumen degradability^{1,2}. *J. Anim. Sci.* 91(5): 2278–94.
- Krupa, S.V. 2003. Effects of atmospheric ammonia (NH₃) on terrestrial vegetation: a review. *Environ. Pollut.* 124(2): 179–221.
- Külling, D.R., H. Menzi, F. Sutter, P. Lischer, and M. Kreuzer. 2003. Ammonia, nitrous oxide and methane emissions from differently stored dairy manure derived from grass- and hay-based rations. *Nutr. Cycl. Agroecosystems* 65: 13–22.
- Lesslie, R., and J. Mewett. 2013. Land use and management: the Australian context. Australian Bureau of Agricultural and Resource Economics and Sciences (ABARES).
- Le Mer, J., and P. Roger. 2001. Production, oxidation, emission and consumption of methane by soils: A review. *Eur. J. Soil Biol.* 37: 25-50.
- Leytem, A.B., R.S. Dungan, D.L. Bjorneberg, and A.C. Koehn. 2011. Emissions of Ammonia, Methane, Carbon Dioxide, and Nitrous Oxide from Dairy Cattle Housing and Manure Management Systems. *J. Environ. Qual.* 40(5): 1383–94.

- Li, C.S. 2000. Modeling trace gas emissions from agricultural ecosystems. *Nutr. Cycl. Agroecosystems* 58(1-3): 259–276.
- Life Cycle Strategies (2007) 'Australian Unit Process LCI Library and Methods.' Available at <http://www.lifecycles.com.au/#!australasian-database/cbm5> [Accessed 28 April 2014]
- Linn, D.M., and J.W. Doran. 1984. Effect of Water-Filled Pore Space on Carbon Dioxide and Nitrous Oxide Production in Tilled and Nontilled Soils¹. *Soil Sci. Soc. Am. J.* 48(6): 1267.
- Li, C.S., W. Salas, R.H. Zhang, C. Krauter, A. Rotz, and F. Mitloehner. 2012. Manure-DNDC: a biogeochemical process model for quantifying greenhouse gas and ammonia emissions from livestock manure systems. *Nutr. Cycl. Agroecosystems* 93(2): 163–200.
- Li, Y., R. White, D. Chen, J. Zhang, B. Li, Y. Zhang, Y. Huang, and R. Edis. 2007. A spatially referenced water and nitrogen management model (WNMM) for (irrigated) intensive cropping systems in the North China Plain. *Ecol. Model.* 203(3–4): 395–423.
- Loh, Z., D. Chen, M. Bai, T. Naylor, D. Griffith, J. Hill, T. Denmead, S. McGinn, and R. Edis. 2008a. Measurement of greenhouse gas emissions from Australian feedlot beef production using open-path spectroscopy and atmospheric dispersion modelling. *Aust. J. Exp. Agric.* 48(2): 244–247.
- Low, A.P., J.M. Stark, and L.M. Dudley. 1997. Effects of Soil Osmotic Potential on Nitrification, Ammonification, N-assimilation, and Nitrous Oxide Production: *Soil Sci.* 162(1): 16–27.
- von Lutzow, M., I. Kogel-Knabner, K. Ekschmitt, E. Matzner, G. Guggenberger, B. Marschner, and H. Flessa. 2006. Stabilization of organic matter in temperate soils: mechanisms and their relevance under different soil conditions - a review. *Eur. J. Soil Sci.* 57(4): 426–445.
- McBain, M.C., and R.L. Desjardins. 2005. The evaluation of a backward Lagrangian stochastic (bLS) model to estimate greenhouse gas emissions from agricultural sources using a synthetic tracer source. *Agric. For. Meteorol.* 135(1-4): 61–72.
- McGinn, S.M., D. Chen, Z. Loh, J. Hill, K.A. Beauchemin, and O.T. Denmead. 2008. Methane emissions from feedlot cattle in Australia and Canada. *Aust. J. Exp. Agric.* 48(2): 183–185.
- McGinn, S.M., T.K. Flesch, B.P. Crenna, K.A. Beauchemin, and T. Coates. 2007. Quantifying ammonia emissions from a cattle feedlot using a dispersion model. *J. Environ. Qual.* 36(6): 1585–1590.
- McGinn, S.M., T.K. Flesch, L.A. Harper, and K.A. Beauchemin. 2006. An Approach for Measuring Methane Emissions from Whole Farms. *J. Environ. Qual.* 35(1): 14–20.
- McGinn, S.M., H.H. Janzen, and T. Coates. 2003. Atmospheric Ammonia, Volatile Fatty Acids, and Other Odorants near Beef Feedlots. *J. Environ. Qual.* 32(4): 1173.
- The Mathworks Inc. 2012. Matlab. The MathWorks Inc., Natick, Massachusetts.
- Metwally, A.I. 1978. Chemical changes in soils accompanying waterlogging.
- Meyer, C.P., I.E. Galbally, Y.P. Wang, I.A. Weeks, I. Jamie, and D.W.T. Griffith. 2001. Two automatic chamber techniques for measuring soil-atmosphere exchanges of trace gases and results of their use in the OASIS field experiment. CSIRO Atmospheric Research, Aspendale, Australia.

- Miller, D.N., and E.D. Berry. 2005. Cattle Feedlot Soil Moisture and Manure Content: I. Impacts on Greenhouse Gases, Odor Compounds, Nitrogen Losses, and Dust. *J. Env. Qual* 34(2): 644–655.
- MLA. 2013. MLA Cattle. Available at <http://www.mla.com.au/About-the-red-meat-industry/Industry-overview/Cattle>.
- Moe, P.W., and H.F. Tyrrell. 1979. Methane production in dairy cows. *J. Dairy Sci.* 62(10): 1583–1586.
- Moller, K., W. Stinner, A. Deuker, and G. Leithold. 2008. Effects of different manuring systems with and without biogas digestion on nitrogen cycle and crop yield in mixed organic dairy farming systems. *Nutr. Cycl. Agroecosystems* 82(3): 209–232.
- Monaghan, R.M., L.C. Smith, and C.A.M. de Klein. 2013. The effectiveness of the nitrification inhibitor dicyandiamide (DCD) in reducing nitrate leaching and nitrous oxide emissions from a grazed winter forage crop in southern New Zealand. *Agric. Ecosyst. Environ.* 175: 29–38.
- Montes, F., R. Meinen, C. Dell, A. Rotz, A.N. Hristov, J. Oh, G. Waghorn, P.J. Gerber, B. Henderson, H.P. Makkar, and J. Dijkstra. 2013. Mitigation of methane and nitrous oxide emissions from animal operations: II. A review of manure management mitigation options. *J. Anim. Sci.* Available at <http://europemc.org/abstract/MED/24045493>.
- Moral, R., M.A. Bustamante, D.R. Chadwick, V. Camp, and T.H. Misselbrook. 2012. N and C transformations in stored cattle farmyard manure, including direct estimates of N₂ emission. *Resour. Conserv. Recycl.* 63(0): 35–42.
- Mosier, A.R., C.E. Andre, and F.G. Viets. 1973. Identification of aliphatic amines volatilized from cattle feedyard. *Environ. Sci. Technol.* 7(7): 642–644.
- Muir, S.K., D. Chen, D. Rowell, and J. Hill. 2011. Development and validation of a biophysical model of enteric methane emissions from Australian beef feedlots. p. 412–420. *In* Sauvart, D., Milgen, J., Faverdin, P., Friggens, N. (eds.), *Modelling nutrient digestion and utilisation in farm animals*. Wageningen Academic Publishers.
- National Greenhouse Gas Inventory Committee. 2007. *Agriculture*. Department of Climate Change, Australian Government, Canberra.
- National Research Council. 2002. *The scientific basis for estimating air emissions from animal feeding operations*. National Academy Press, Washington, D.C.
- O'Brien, S.L., J.D. Jastrow, K.J. McFarlane, T.P. Guilderson, and M.A. Gonzalez-Meler. 2013. Decadal cycling within long-lived carbon pools revealed by dual isotopic analysis of mineral-associated soil organic matter. *Biogeochemistry* 112(1-3): 111–125.
- Ohlsson, T. 1979. Redox reactions in soils. Sequence of redox reactions in a waterlogged soil. *Nord. Hydrol.* 10(2/3): 89–98.
- Patra, A. 2012. Enteric methane mitigation technologies for ruminant livestock: a synthesis of current research and future directions. *Environ. Monit. Assess.* 184(4): 1929–1952.
- Pattey, E., M.K. Trzcinski, and R.L. Desjardins. 2005. Quantifying the reduction of greenhouse gas emissions as a result of composting dairy and beef cattle manure. *Nutr. Cycl. Agroecosystems* 72(2): 173–187.
- Petersen, S.O., A.M. Lind, and S.G. Sommer. 1998. Nitrogen and organic matter losses during storage of cattle and pig manure. *J. Agric. Sci.* 130: 69–79.

- Peters, G.M., H.V. Rowley, S.G. Wiedemann, R.W. Tucker, M.D. Short, and M.S. Schulz. 2010a. Red meat production in Australia: Life cycle assessment and comparison with overseas studies. *Environ. Sci. Technol.* 44(4): 1327–1332.
- Peters, G.M., S.G. Wiedemann, H.V. Rowley, and R.W. Tucker. 2010b. Accounting for water use in Australian red meat production. *Int. J. Life Cycle Assess.* 15(3): 311–320.
- Pfister, S., A. Koehler, and S. Hellweg. 2009. Assessing the Environmental Impacts of Freshwater Consumption in LCA. *Environ. Sci. Technol.* 43(11): 4098–4104.
- Pineiro, G., S. Perelman, J.P. Guerschman, and J.M. Paruelo. 2008. How to evaluate models: Observed vs. predicted or predicted vs. observed? *Ecol. Model.* 216: 316–322.
- Pratt, C., M.R. Redding, and J. Hill. 2015. A promising and simple method to quantify soil/manure mixing on beef feedlot pens. *J. Anim. Prod. Sci.*
- Pratt, C., M.R. Redding, J. Hill, A. Shilton, M. Chung, and B. Guieysse. 2014. Good science for good policy: targeting agricultural manure greenhouse gas emissions. *Anim. Prod. Sci.* Available at <http://dx.doi.org/10.1071/AN13504> (verified 1 April 2015).
- Pré-Consultants. 2012. SimaPro 7.3 Software. Amersfoot, Netherlands.
- Qi, Y., A.F.A. Hoadley, A.L. Chaffee, and G. Garnier. 2011. Characterisation of lignite as an industrial adsorbent. *Fuel* 90(4): 1567–1574.
- Rahman, S., M.S. Borhan, and K. Swanson. 2013. Greenhouse gas emissions from beef cattle pen surfaces in North Dakota. *Environ. Technol.* 34(10): 1239–1246.
- Rayment, G.E., and D.J. Lyons. 2010. *Soil Chemical Methods - Australasia*.
- Rayment, G.E., and D.J. Lyons. 2011. *Soil Chemical Methods: Australasia*. Csiro Publishing.
- R Development Core Team. 2014. *R: a language and environment for statistical computing*. R Foundation for statistical computing, Vienna, Austria.
- Rebitzer, G., Y. Loerincik, and O. Jolliet. 2002. Input-output life cycle assessment: from theory to applications 16th discussion forum on life cycle assessment Lausanne, April 10, 2002. *Int. J. Life Cycle Assess.* 7(3): 174–176.
- Redding, M.R. 2011. Bentonites and layered double hydroxides can decrease nutrient losses from spent poultry litter. *Appl. Clay Sci.* 52(1-2): 20–26.
- Redding, M.R. 2013. Bentonite can decrease ammonia volatilisation losses from poultry litter: laboratory studies. *Animal production science* 53(10): 1115–1118.
- Redding, M., J. Devereux, F. Phillips, R. Lewis, T. Naylor, T. Kearton, J. Hill, and S. Wiedemann. 2015. Field measurement of beef pen manure CH₄ and N₂O emissions reveal surprising emission control factors. *Journal of Environmental Quality*. Accepted for publication, and on-line: doi:10.2134/jeq2014.04.0159.
- Redding, M.R., R. Lewis, J. Waller, F. Phillips, and D. Griffith. 2013. Large-Chamber Methane and Nitrous Oxide Measurements Are Comparable to the Backward Lagrangian Stochastic Method. *J. Environ. Qual.* 42(6): 1643–1651.
- Redding, M.R., P.R. Shorten, Lewis, R., C. Pratt, and J. Hill. In Review. Soil N availability, rather than N deposition, controls indirect N₂O emission. *PLoS ONE*. In Review.

- Ridoutt, B.G., and S. Pfister. 2010. A revised approach to water footprinting to make transparent the impacts of consumption and production on global freshwater scarcity. *Glob. Environ. Change* 20(1): 113–120.
- Ridoutt, B.G., P. Sanguansri, M. Freer, and G.S. Harper. 2012. Water footprint of livestock: comparison of six geographically defined beef production systems. *Int. J. Life Cycle Assess.* 17(2): 165–175.
- Rigolot, C., S. Espagnol, P. Robin, M. Hassouna, F. Beline, J.M. Paillat, and J.Y. Dourmad. 2010. Modelling of manure production by pigs and NH₃, N₂O and CH₄ emissions. Part II: effect of animal housing, manure storage and treatment practices. *Animal* 4(8): 1413–1424.
- Rochette, P., and N.S. Eriksen-Hamel. 2008. Chamber measurements of soil nitrous oxide flux: Are absolute values reliable? *Soil Sci. Soc. Am. J.* 72(2): 331–342.
- Roose, T., and A.C. Fowler. 2004. A mathematical model for water and nutrient uptake by plant root systems. *J. Theor. Biol.* 228(2): 173–184.
- Rotz, C.A. 2004. Management to reduce nitrogen losses in animal production. *J. Anim. Sci.* 82(13 suppl): E119–E137.
- Saggar, S., N.S. Bolan, R. Bhandral, C.B. Hedley, and J. Luo. 2004. A review of emissions of methane, ammonia, and nitrous oxide from animal excreta deposition and farm effluent application in grazed pastures. *N. Z. J. Agric. Res.* 47(4): 513–544.
- Sanz-Cobena, A., L. Sanchez-Martin, L. Garcia-Torres, and A. Vallejo. 2012. Gaseous emissions of N₂O and NO and NO₃⁻ leaching from urea applied with urease and nitrification inhibitors to a maize (*Zea mays*) crop. *Agric. Ecosyst. Environ.* 149: 64–73.
- Sanz, A., T. Misselbrook, M.J. Sanz, and A. Vallejo. 2010. Use of an inverse dispersion technique for estimating ammonia emission from surface-applied slurry. *Atmos. Environ.* 44(7): 999–1002.
- Schaaf, W., C. Neumann, and R.F. Hüttl. 2001. Short Communication Actual cation exchange capacity in lignite containing pyritic mine soils. *J. Plant Nutr. Soil Sci.* 164(1): 77–78.
- Shaffer, M.J., A.D. Halvorson, and F.J. Pierce. 1991. Nitrate Leaching and Economic Analysis Package (NLEAP): Model Description and Application. *Manag. Nitrogen Groundw. Qual. Farm Profitab.* [accesspublicati\(managingnitroge\)](#): 285–322.
- Shorten, P.R., and A.B. Pleasants. 2007. A stochastic model of urinary nitrogen and water flow in grassland soil in New Zealand. *Agric. Ecosyst. Environ.* 120(2–4): 145–152.
- Shorten, P., and M. Redding. In Press. Models fitted to manure emissions contrast with inventory estimates. *J. Environ. Qual.*
- Shorten, P., and M. Redding. Models fitted to manure emissions contrast with inventory. *J. Environ. Qual.* Submitted for publication 30/5/2014: 32.
- Simek, M., and J.E. Cooper. 2002. The influence of soil pH on denitrification: progress towards the understanding of this interaction over the last 50 years. *Eur. J. Soil Sci.* 53: 345–354.
- Simek, M., L. Jisova, and D.W. Hopkins. 2002. What is the so-called optimum pH for denitrification in soil. *Soil Biol. Biochem.* 34: 1227–1234.

- Six, J., R.T. Conant, E.A. Paul, and K. Paustian. 2002a. Stabilization mechanisms of soil organic matter: Implications for C-saturation of soils. *Plant Soil* 241(2): 155–176.
- Six, J., C. Feller, K. Denef, S.M. Ogle, J.C.D. Sa, and A. Albrecht. 2002b. Soil organic matter, biota and aggregation in temperate and tropical soils - Effects of no-tillage. p. 755–775.
- Skerman, A. 2000. Reference manual for the establishment and operation of beef cattle feedlots in Queensland. DPI Publications, Brisbane.
- Soil Survey Staff. 1998. Keys to soil taxonomy. 8th ed. United States Department of Agriculture, Natural Resource Conservation Service, Washington, D.C.
- Solomon, S., D. Qin, M. Manning, R.B. Alley, T. Berntsen, N.L. Bindoff, A. Chen, A. Chidthaisong, J.M. Gregory, G.C. Hegerl, M. Heimann, B. Hewitson, B. Hoskins, f Joos, J. Juozel, V. Kattsov, U. Lohmann, T. Matsuno, M. Molina, N. Nicholls, J. Overpeck, G. Raga, V. Ramaswamy, J. Ren, R. Somerville, T.F. Stocker, P. Whetten, R.A. Wood, and D. Wratt. 2007. Technical Summary. *In* Solomon, S., Qin, D., Manning, M., Chen, Z., Marquis, M., Averyt, K.B., Tignor, M., Miller, H.L. (eds.), *Climate Change 2007: The Physical Science Basis. Contribution of Working Group I to the Fourth Assessment Report of the Intergovernmental Panel on Climate Change*. Cambridge University Press, United Kingdom and New York, USA.
- Sommer, S.G. 2001. Effect of composting on nutrient loss and nitrogen availability of cattle deep litter. *Eur. J. Agron.* 14(2): 123–133.
- Sommerfeldt, T.G., C. Chang, and T. Entz. 1988. Long-term annual manure applications increase soil organic matter and nitrogen, and decrease carbon to nitrogen ratio. *Soil Sci. Soc. Am. J.* 52(6): 1668–1672.
- Sommer, S.G., S. Générmont, P. Cellier, N.J. Hutchings, J.E. Olesen, and T. Morvan. 2003. Processes controlling ammonia emission from livestock slurry in the field. *Eur. J. Agron.* 19(4): 465–486.
- Sommer, S.G., S.M. McGinn, X. Hao, and F.J. Larney. 2004a. Techniques for measuring gas emissions from a composting stockpile of cattle manure. *Atmos. Environ.* 38(28): 4643–4652.
- Sommer, S.G., and J.E. Olesen. 2000. Modelling ammonia volatilization from animal slurry applied with trail hoses to cereals. *Atmos. Environ.* 34(15): 2361–2372.
- Sommer, S.G., S.O. Petersen, and H.B. Moller. 2004b. Algorithms for calculating methane and nitrous oxide emissions from manure management. *Nutr. Cycl. Agroecosystems* 69(2): 143–154.
- Sommer, S.G., S.O. Petersen, and H.T. Sogaard. 2000. Greenhouse gas emission from stored livestock slurry. *J. Environ. Qual.* 29(3): 744–751.
- Staebler, R.M., S.M. McGinn, B.P. Crenna, T.K. Flesch, K.L. Hayden, and S. Li. 2009. Three-dimensional characterization of the ammonia plume from a beef cattle feedlot. *Atmos. Environ.* 43(38): 6091–6099.
- Stehfest, E., and L. Bouwman. 2006. N₂O and NO emission from agricultural fields and soils under natural vegetation: summarizing available measurement data and modeling of global annual emissions. *Nutr. Cycl. Agroecosystems* 74(3): 207–228.
- Stewart, W.M., and L.R. Hossner. 2001. Factors affecting the ratio of cation exchange capacity to clay content in lignite overburden. *J. Environ. Qual.* 30(4): 1143–9.

- Stewart, C., K. Paustian, R. Conant, A. Plante, and J. Six. 2007. Soil carbon saturation: concept, evidence and evaluation. *Biogeochemistry* 86(1): 19–31.
- Stewart, C.E., A.F. Plante, K. Paustian, R.T. Conant, and J. Six. 2008. Soil carbon saturation: Linking concept and measurable carbon pools. *Soil Sci. Soc. Am. J.* 72(2): 379–392.
- Swerts, M., R. Merckx, and K. Vlassak. 1996. Influence of carbon availability on the production of NO, N₂O, N₂, and CO₂ by soil cores during anaerobic incubation. *Plant Soil* 181: 145–151.
- Szanto, G.L., H.M. Hamelers, W.H. Rulkens, and A.H.M. Veeken. 2007. NH₃, N₂O and CH₄ emissions during passively aerated composting of straw-rich pig manure. *Bioresour. Technol.* 98(14): 2659–2670.
- Todd, R.W., N.A. Cole, R.N. Clark, T.K. Flesch, L.A. Harper, and B.H. Baek. 2008a. Ammonia emissions from a beef cattle feedyard on the southern High Plains. *Atmos. Environ.* 42(28): 6797–6805.
- Todd, R.W., N.A. Cole, R.N. Clark, W.C. Rice, and W.X. Guo. 2008b. Soil nitrogen distribution and deposition on shortgrass prairie adjacent to a beef cattle feedyard. *Biol. Fertil. Soils* 44(8): 1099–1102.
- USDA NRCS. 2007. Part 630 - Hydrology. *In* National engineering handbook. U.S. Department of Agriculture, Natural Resources Conservation Service, Washington, DC.
- USDA-SCS. 1972. Section 4 - Hydrology. *In* National Engineering Handbook. US Department of Agriculture, Washington D.C.
- Uzinger, N., M. Rékási, E. Draskovits, and A. Anton. 2013. Stabilization of Cr, Pb, and Zn in Soil Using Lignite. *Soil Sediment Contam. Int. J.* 23(3): 270–286.
- Varel, V.H., J.A. Nienaber, and H.C. Freetly. 1999. Conservation of nitrogen in cattle feedlot waste with urease inhibitors. *J. Anim. Sci.* 77(5): 1162–8.
- Viets, F.G. 1970.p. 11–16. *In* Bozeman, Montana.
- VSN International. 2012. GenStat for Windows 15th Edition. VSN International, Hemel Hempstead, UK.
- Walkley, A., and I. Black. 1934. An examination of the Degtjareff method for determining soil organic matter and a proposed modification of the chromic acid titration method. *Soil Sci.* 37: 29–38.
- Wang, Z.P., R.D. Delaune, P.H. Masscheleyn, and W.H. Patrick. 1993. Soil redox and pH effects on methane production in a flooded rice soil. *Soil Sci. Soc. Am. J.* 57(2): 382–385.
- Wang, W., W.Q. Liu, T.S. Zhang, and M.Y. Ren. 2013. Evaluation of backward Lagrangian stochastic (bLS) model to estimate gas emissions from complex sources based on numerical simulations. *Atmos. Environ.* 67: 211-218.
doi:10.1016/j.atmosenv.2012.10.064.
- Watts, P., E. McGahan, S.L. Bonner, and S. Wiedemann. 2012. Feedlot Mass Balance and Greenhouse Gas Emissions - A Literature Review. Meat & Livestock Australia, Sydney, Australia.

- Webster, C.P., and K.W.T. Goulding. 1989. Influence of soil carbon content on denitrification from fallow land during autumn. *J. Sci. Food Agric.* 49(2): 131–142.
- White, J.R., R.D. Shannon, J.F. Weltzin, J. Pastor, and S.D. Bridgham. 2008. Effects of soil warming and drying on methane cycling in a northern peatland mesocosm study. *J. Geophys. Res.: Biogeosci.* 113. doi:G00a0610.1029/2007jg000609.
- Wiedemann, S.G. 2014. REgionalised estimates of nitrous oxide emission from pen manures. FSA Consulting.
- Wiedemann, S., B. Henry, E. McGahan, T. Grant, C. Murphy, and G. Niethé. 2014a. Resource use and greenhouse gas intensity of Australian beef production: 1981 to 2010. *Agric. Syst. Press.*
- Wiedemann, S.G., and E.J. McGahan. 2011. Environmental assessment of an egg production supply chain using life cycle assessment. Australian Egg Corporation Limited, Sydney, Australia.
- Wiedemann, S., E. McGahan, S. Grist, and T. Grant. 2010a. Environmental assessment of two pork supply chains using life cycle assessment. Rural Industries Research and Development Corporation, Barton, ACT.
- Wiedemann, S, McGahan, E, Murphy, C, Yan, M (2014b) Resource use and environmental impacts from beef production in eastern Australia investigated using life cycle assessment. *Journal of Animal Production Science, In press*
- Wiedemann, S., E. McGahan, C. Murphy, and M. Yan. 2014b. Resource use and environmental impacts from beef production in eastern Australia investigated using life cycle assessment. *J. Anim. Prod. Sci. Press.*
- Wiedemann, S., E. McGahan, and G. Poad. 2012. Using Life Cycle Assessment to Quantify the Environmental Impact of Chicken Meat Production. Rural Industries Research and Development Corporation., Barton, ACT.
- Wiedemann, S.G., M.-J. Yan, and C.M. Murphy. 2014c. Resource use and environmental impacts from Australian export lamb production: a life cycle assessment. *J. Anim. Prod. Sci. Press.*
- Wilson, J.D., T.K. Flesch, and L.A. Harper. 2001. Micro-meteorological methods for estimating surface exchange with a disturbed windflow. *Agric. For. Meteorol.* 107(3): 207–225.
- Wolter, M., S. Prayitno, and F. Schuchardt. 2004. Greenhouse gas emission during storage of pig manure on a pilot scale. *Bioresour. Technol.* 95(3): 235–244.
- Wynn, J.G., and M.I. Bird. 2007. C₄-derived soil organic carbon decomposes faster than its C₃ counterpart in mixed C₃/C₄ soils. *Glob. Change Biol.* 13(10): 2206–2217.
- Wynn, J.G., M.I. Bird, L. Vellen, E. Grand-Clement, J. Carter, and S.L. Berry. 2006. Continental-scale measurement of the soil organic carbon pool with climatic, edaphic, and biotic controls. *Glob. Biogeochem. Cycles* 20(1) Available at ://000235362300001.
- Xu, C., M.J. Shaffer, and Al-kaisi M. 1998. Simulating the impact of management practices on nitrous oxide emissions. *Soil Sci. Soc. Am. J.* 62(3): 736–742.
- Yamulki, S. 2006. Effect of straw addition on nitrous oxide and methane emissions from stored farmyard manures. *Agric. Ecosyst. Environ.* 112(2-3): 140–145.

- Yang, S.M., S.S. Malhi, F.M. Li, D.R. Suo, M.G. Xu, P. Wang, G.J. Xiao, Y. Jia, T.W. Guo, and J.G. Wang. 2007. Long-term effects of manure and fertilization on soil organic matter and quality parameters of a calcareous soil in NW China. *J. Plant Nutr. Soil Sci.-Z. Pflanzenernahrung Bodenkd.* 170(2): 234–243.
- Yang, R., C. Ti, F. Li, M. Deng, and X. Yan. 2010. Assessment of N₂O, NO_x and NH₃ emissions from a typical rural catchment in Eastern China. *SOIL Sci. PLANT Nutr.* 56(1): 86–94.
- Yee Yet, J.S., and Silburn, D.M. 2003. Deep drainage estimates under a range of land uses in the Queensland Murray-Darling Basin using water balance modelling. Department of Natural Resources and Mines, Coorparoo, Queensland.